Identification of volatile organic compounds from *Eucalyptus* detected by *Gonipterus scutellatus* (Gyllenhal) females

by

Marc Clement Bouwer

Submitted in partial fulfillment for the degree

Master of Science (Chemistry)

in the

Faculty of Natural and Agricultural Sciences

University of Pretoria

Pretoria

May 2010

Declaration of Authorship

I, MARC CLEMENT BOUWER, declare that this dissertation, which I hereby submit for the degree Masters in Science at the University of Pretoria, is my own work and has not previously been submitted by me for a degree at this or any other tertiary institution.

Signed: _____

Date: _____

"None of our men are "experts." We have most unfortunately found it necessary to get rid of a man as soon as he thinks himself an expert–because no one ever considers himself an expert if he really knows his job. A man who knows a job sees so much more to be done than he has done, that he is always pressing forward and never gives up an instant of thought to how good and how efficient he is. Thinking always ahead, thinking always of trying to do more, brings a state of mind in which nothing is impossible. The moment one gets to the "expert" state of mind a great number of things become impossible."

Henry Ford

UNIVERSITY OF PRETORIA

Abstract

Faculty of Natural and Agricultural Sciences
Department of Chemistry

Master of Science in Chemistry

by Marc Clement Bouwer

This thesis concerns the development of semiochemical identification expertise and methodology at the University of Pretoria. The *Eucalyptus* snout beetle *Gonipterus scutellatus* was used as a model insect in developing these methods, firstly because it is a known pest in the *Eucalyptus* forestry industry of South Africa. Secondly, nothing is known about its chemical ecology and lastly, it is a relatively large insect that is easily worked on. Three main techniques were used namely: Electroantennography (EAG), Gas Chromatography Electroantennography Detection (GC-EAD) and Gas Chromatography Mass Spectrometry (GC-MS). EAG was used to differentiate and identify certain *Eucalyptus* species that were expected to contain compounds that may function as either kairomones or allomones for *G. scutellatus*. The EAG process revealed that *G. scutellatus* responds more intensely to damaged *Eucalyptus* leaves as compared to undamaged leaves. The crushed foliage of the known hosts *Eucalyptus globulus* and *E. viminalis* gave larger responses than the crushed foliage from a known non-host *E. citriodora*. We sampled the volatiles from the crushed foliage of these three species and tentatively identified sixteen compounds from the *E. globulus* volatile profile that was antennally active for *G. scutellatus* females. The presence of these volatiles were subsequently investigated for *E. viminalis* and *E. citriodora*. The green leaf volatiles, (Z)-3 hexenyl acetate, (Z)-3-hexen-1-ol and (E)-2-hexenal and aromatic compounds, 2-phenylethanol, benzyl acetate and ethylphenylacetate often gave larger responses than the terpenes such as α-pinene, β-pinene and camphene. Crushed *E. globulus* leaves contained 2-phenyl ethanol, benzyl acetate, ethylphenylacetate, eucalyptol, α-pinene, (Z)-3 hexenyl acetate, (Z)-3-hexen-1-ol and (E)-2-hexenal that were antennally active. The *E. viminalis* profile had very little 2-phenylethanol and virtually no benzyl acetate. The *E. citriodora* volatile profile contained very little (Z)-3-hexen-1-ol, (E)-2-hexenal, 2-phenylethanol, benzyl acetate and ethylphenylacetate. These compounds may influence the host selection behaviour of *G. scutellatus* females. These volatiles can be tested in a behavioural bioassay in order to determine their effect on the *Eucalyptus* snout beetle *G. scutellatus*.

Acknowledgements

I would like to thank the following people that have been involved in this project. Without them it would definitely not have been possible.

Firstly to Yevette Naudé, Ryan Nadel and Niel Malan. You have always been there to answer questions and help with matters that I myself could not do.

Secondly to my supervisors Prof Egmont Rohwer, Prof Bernard Slippers and Prof Mike Wingfield. Your continual motivation and advice has been essential especially in interpreting difficult results and writing correctly.

Lastly to the funding bodies: The Tree Protection Co-operative Programme (TPCP) and the Forestry Agricultural Biotechnology Institute (FABI).

A special thanks goes to all the FABI people because their positive attitude sets a stage that creates success.

Contents

List of Figures

List of Tables

Abbreviations

DC	**D**irect **C**urrent
EAG	**E**lectro**A**ntenno**G**raphy
GC-FID	**G**ass **C**romatography **F**lame **I**onization **D**etector
GC-FID-EAD	**G**ass **C**romatography **F**lame **I**onization **D**etector **E**lectro**A**ntennography **D**etector
GC-MS	**G**ass **C**romatography **M**ass **S**pectrometry
GLV	**G**reen **L**eaf **V**olatiles
VCC	**V**olatile **C**ollection **C**hamber
VOC	**V**olatile **O**rganic **C**ompounds

Symbols

A	term describing variability in flow path for a compound in a column
A_a	adsorbed molecule
A_m	Molecule A in the mobile phase
A_s	Molecule A in the stationary phase
A_g	Molecule A in gas phase
B	term describing diffusion coefficients for a compound in a column
C	term describing mass transfer rate in Van Deemter equation
H	plate height
K	distribution constant
K_a	distribution constant of a less retained compound than compound b
K_b	distribution constant of a more retained compound than compound a
k	adsorption coefficient
k_a	adsorption coefficient of a less retained compound than b
k_b	adsorption coefficient of a more retained compound than a
KI_a	Kovats index of n-alkane eluting before n-alkane b
KI_b	Kovats index of n-alkane eluting after n-alkane a
KI_x	Kovats index of an unknown compound
m_{max}	maximum mass of analyte on adsorbent
m/z	mass to charge ratio
N	number of theoretical plates
R	resolution
SN	separation number
σ	standard deviation
σ^2	variance
t_m	retention time of an unretained compound

t_r	retention time of a compound
tr_a	retention time of a less retained n-alkane than t_b
tr_b	retention time of a more retained n-alkane than t_a
tr_x	retention time of an unknown compound
V_m	volume of mobile phase
V_s	volume of stationary phase
W	width of peak at base
$W_{1/2}$	width of peak at half height
α	selectivity
μ	average linear rate of migration of the mobile phase in a column
υ	average linear rate of migration of a compound in a column
[ ]	concentration

Dedicated to my mother and father for their endless support and encouragement during my M.Sc. studies.

Chapter 1

The potential role of *Eucalyptus* volatiles in host detection by *Gonipterus scutellatus*

1.1 Introduction

The Eucalyptus snout beetle, *Gonipterus scutellatus* (Coleoptera, Curculionidae) originates from South East Australia and Tasmania where *Eucalyptus* trees grow endemically (Clarke *et al.*, 1998; Tooke, 1953). Here damage caused by *G. scutellatus* is isolated and the beetle is relatively rare (Tooke, 1953). This is not the case in countries where *Eucalyptus* trees have been introduced for plantation purposes. In these countries *Eucalyptus* trees are often grown in monocultures and *G. scutellatus* numbers are able to escalate rapidly, leading to significant damage due to adult and larval feeding (Hanks *et al.*, 2000; Tooke, 1953).

Bio-control with the egg parasitoid wasp (*Anaphes nitens*) is often the best method for controlling *G. scutellatus*. *A. nitens* was successfully introduced from Australia into most of the countries affected by this pest (Loch, 2006). In the majority of these cases it reduces *G. scutellatus* populations to below economically significant levels. Exceptions occur in some areas especially when the environment interferes with *A. nitens* life cycle, for example in areas with particularly cold winters (Loch and Floyd, 2001; Rivera and Carbone, 2000). Nevertheless, the overall efficiency of this egg parasitoid makes it one of the best examples of biological control in forestry (Hanks *et al.*, 2000; Lanfranco and Dungey, 2001; Rivera *et al.*, 1999).

Gonipterus scutellatus females are known to oviposit on selected foliage of susceptible *Eucalyptus* species and larvae and adults are able to only feed on *Eucalyptus* trees (Rivera and Carbone, 2000; Tooke, 1953). This makes *G. scutellatus* quite specific with regards to its host selection. The mechanism by which *G. scutellatus* selects these *Eucalyptus* host trees is largely unknown. Furthermore, the exact identities of preferred host tree species within the *Eucalyptus* genus is also unclear.

This review focuses on *G. scutellatus* as a pest in South Africa and other parts of the world and also specifically compares *Eucalyptus* hosts reported in different countries. It briefly describes the *G. scutellatus* life cycle, behaviour and control, but more specifically considers the possible involvement of semiochemicals in host choice. For this purpose, the host detection strategies by flying insects and diversity of *Eucalyptus* trees and volatiles is also considered.

1.2 The *Eucalyptus* snout beetle, *Gonipterus scutellatus*

1.2.1 Distribution of *Gonipterus scutellatus*

Gonipterus scutellatus has been spread to nearly all the continents through the activities of man. These include Europe, Asia, Africa, Oceania, North and South America (European and protection Organization (EPPO), 2005). Many countries have reported tremendous losses due to *G. scutellatus* including South Africa (Mally, 1924), New Zealand (Clark, 1932), Mauritius (Williams *et al.*, 1951), USA (Hanks *et al.*, 2000), Spain (Rivera and Carbone, 2000), Chile (Lanfranco and Dungey, 2001), South Western Australia (Loch and Floyd, 2001; Cunningham *et al.*, 2005) and France (Malausa *et al.*, 2008).

1.2.2 *Gonipterus scutellatus* in its native range of Tasmania

Gonipterus scutellatus mainly occurs in the dry sclerophyll *Eucalyptus* forests of the eastern half of Tasmania (Clarke *et al.*, 1998). *Eucalyptus* trees grow in mixed forests here and *G. scutellatus* concequintly has a much larger variety of *Eucalyptus* trees to choose from compared to countries where Eucalypts are grown in monocultures. The behavior of *G. scutellatus* in the native forests of Tasmania is different to its behavior in introduced environments (Clarke *et al.*, 1998).

In Tasmania *G. scutellatus* oviposition mostly occurs on peppermints (*E. pulchella, E. tenuiramis* and *E. amygdalina*) rather than on gums (*E. globulus, E. viminalis, E. ovata*

and *E. obliqua*) (Clarke *et al.*, 1998) (Table 1.1). This evidence contradicts reports from South Africa (Mally, 1924) and such observations have led to the conclusion that *G. scutellatus* is possibly forced to choose hosts other than the preferred hosts outside its native range (Clarke *et al.*, 1998).

Large differences in the number of eggs found on *E. globulus* and *E. pulchella* have been reported in Tasmania (Clarke *et al.*, 1998) with the majority of eggs found on the more abundant *E. pulchella* trees. Tree height was suspected to have an effect on the oviposition preference by *G. scutellatus*, but this was proven to be an insignificant factor (Clarke *et al.*, 1998). Other authors have reported that leaf shape is an insignificant factor relating to oviposition by *G. scutellatus* and that hybrid trees (*E. amygdalia*×*E. risdonii*) may be selected for oviposition above the individual pure breeds (Dungey and Potts, 2003).

TABLE 1.1: Host specificity of *G. scutellatus* according to the different authors.

Date	Authors	Country	*Eucalyptus* sp.
1924	Mally	South Africa	*E. viminalis, E. punctata, E. globulus*
1932	Clark	New Zealand	*E. globulus*
1940	Williams, Moutia & Hermelin	Mauritius	*E. kirtoniana, E. rubusta, E. tereticornis*
1955	Tooke	South Africa	*E. viminalis, E. globulus, E. maideni*
1986	Richardson & Meakins	South Africa	*E. scoparia, E. viminalis, E. punctata*
1995	Hanks et al.	California(USA)	*E. globulus*
1998	Clarke et al.	Tasmania	*E. pulchella E. tenuiramis, E. amygdalina*
2000	Rivera & Carbone	Spain	*E. globulus, E. longifolia, E grandis*
2001	Lanfranco & Dungey	Chile	*E. globulus, E. camaldulensis, E viminalis*
2001	Loch	South-western Australia	*E. globulus*
2005	Cunningham, Floyd & Weir	South-western Australia	*E. globulus, E. marginata*

1.2.3 *Gonipterus scutellatus* in non-native ranges

1.2.3.1 *Gonipterus scutellatus* and its hosts in South Africa

Gonipterus scutellatus was first noticed in South Africa in November 1916, and was recognized as most likely introduced from Australia (Tooke, 1953). Interestingly, *G.*

scutellatus was thought to have entered the country via the Cape Town harbor on a ship carrying crates of apples from Australia (Tooke, 1953). It subsequently caused major damage in the *Eucalyptus* plantations and was able to rapidly spread throughout South Africa (Tooke, 1953). The beetle then posed a significant threat to the entire *Eucalyptus* industry in South Africa (Tooke, 1953; Poynton, 1979).

Damage due to *G. scutellatus* seldom resulted in the death of trees, but rather stunted growth that caused malformations in the timber which lowered the quality of the wood. *Eucalyptus viminalis* trees that suffered prolonged damage were known to die, while *E. globulus* was severely damaged in early infestations (Mally, 1924; Tooke, 1953). Richardson and Meakins (1984) were able to show that repeated attack by *G. scutellatus* damaged trees and that these trees were shorter than trees that were not invested. Damage caused by the pest resulted in a recommendation to stop planting *E. viminalis* and *E. globulus* in South Africa (Richardson and Meakins, 1984). More recently damage has been confined to areas where biological control fails after colder winters in the highlands of South Africa near Lesotho (Richardson and Meakins, 1984).

With regards to host specificity, Mally (1924) ranked the most susceptible eucalypts as *E. viminalis, E. punctata* and *E. globulus*. According to Tooke (1953) *Eucalyptus viminalis*, *E. globulus* and *E. maideni* were the species having highest susceptibility, and of these *E. viminalis* was the preferred species. A case is mentioned by Tooke (1953) where an *E. viminalis* tree was singled out by the insect in the presence of other less palatable eucalypts. The mature foliage of *E. globulus* was noticed to be preferred to the juvenile leaves and stands often showed no damage until the mature leaves emerged. Tooke (1953) also listed many other eucalypts based on their susceptibility to *G. scutellatus*, but these were not as heavily damaged as *E. viminalis* and *E. globulus*.

Richardson and Meakins (1984) attempted to elucidate the host preference of *G. scutellatus* by studying it at two sites in Lesotho (Leshoboro and Tsikoane). Some species of eucalypts (*E. radiata, E. blaxlandii, E. elata, E. oreades* and *E. robertsonii*) were totally resistant to infestation and other species (*E. viminalis* and *E. dalrympleana*) showed varying degrees of resistance within different provenances. Here, the narrow leaved eucalypts were observed as being most susceptible and *E. scoparia* was shown to be more susceptible than *E. viminalis* (Table 1.1). Today, *G. scutellatus* is often found on *E. smithii, E. camaldulensis, E. grandis*×*camaldulensis* clones, *E. scoparia, E. viminalis, E. dunii* and *E. nitens* in South Africa (Hurley, Personal communication).

1.2.3.2 *Gonipterus scutellatus* and its hosts in countries other than South Africa

In New Zealand *G. scutellatus* was first recorded in 1890 in Wellington (Withers, 2001). According to Clark (1932), narrow leaved eucalypts such as *E. linearis* and *E. amygdalina* were rarely attacked and *G. scutellatus* rather fed on *E. globulus, E. viminalis, E. radiata, E. gunnii* and *E. macarthuri* (Table 1.1). *Gonipterus scutellatus* was a major pest in New Zealand before the introduction of *A. nitens* in 1927 (Clark, 1932; Withers, 2001).

Gonipterus scutellatus was found in *E. globulus* plantations in NW Spain in 1991 (Rivera and Carbone, 2000). Here tree species were found to have a significant effect on larval survival rate and *E. obliqua* was shown to be the least suitable for larval development (Rivera and Carbone, 2000). Adult females, however, showed no significant difference in the number of offspring they produced after feeding on the different *Eucalyptus* species as larvae (Rivera and Carbone, 2000). It was observed that *G. scutellatus* preferred *E. globulus, E. longifolia, E. grandis* and *E. propinqua* in the field (Table 1.1).

Gonipterus scutellatus also occurs in South America where it causes significant damage in countries such as Chile. The insect has four generations per year in that country which allows its populations to increase rapidly. The insect mainly defoliates *E. globulus, E. camaldulensis* and *E. viminalis* (Lanfranco and Dungey, 2001) (Table 1.1). Bio-control is successful in this region with *A. nitens* parasitism rates as high as 98 % one year after its initial release in 1998 (Lanfranco and Dungey, 2001).

Gonipterus scutellatus is regarded as an introduced species in South-Western Australia (Loch and Floyd, 2001). Here, the pest was found to be the most abundant species in *E. globulus* plantations (Loch, 2006) (Table 1.1). Biological control fails in this region due to a single generation of *G. scutellatus* and the unavailability of egg capsules for approximately six months of the year (Loch, 2008). Another factor that may contribute to the unsuccessful control by *A. nitens* in this area is the unavailability of new foliage during dry seasons, which cause lower numbers of egg capsules during these times (Loch, 2008). Damage caused by *G. scutellatus* may be exacerbated by the monoculture effect in this region (Loch, 2008). It was also observed that *G. scutellatus* preferred mature foliage above the juvenile foliage of *E. globulus*.

Gonipterus scutellatus has been reported in California where it was found on *E. globulus, E. viminalis and E. tereticornis*, which are the most abundant *Eucalyptus* trees in this region (Hanks *et al.*, 2000) (Table 1.1). Biological control with *A. nitens* is currently being employed in this region and is being monitored (Hanks *et al.*, 2000).

1.3 Identification, behavior and life cycle of *Gonipterus scutellatus*

Young *G. scutellatus* beetles are bright rusty red in colour. This colour does not last long and fades as the beetles age to a brownish grey. These beetles have a fairly well defined X-shaped mark on the hard top wings and a white mark often forming a median prothoracic stripe extending to the head. Females are usually larger than males and outnumber them in a 3 to 2 ratio (Tooke, 1953). The larvae are black and have yellow markings and are usually coated in green slime. The larvae also produce tendrils of black excrement, which appears as a "tail" which is carried around on its back Hanks *et al.* (2000). Males and females are distinguishable by examining their penultimate sternites. Males have a straight posterior margin covered by fine hairs that do not mask the dark colour of the sternite (Carbone and Rivera, 1998). Females have a rounded edge to the posterior border of their last sternite which is densely covered by hairs of equal diameter (Carbone and Rivera, 1998).

FIGURE 1.1: A young *G. scutellatus* female on a *Eucalyptus smithii* twig in a laboratory cage.

Adult insects are able to fly and usually take flight when temperatures exceed 26 °C (Tooke, 1953). Winds can easily carry them across treeless areas (Mally, 1924). These

beetles have the peculiar behavior of falling to the ground when their tree is disturbed (Mally, 1924). On the ground they tightly grip twigs and leaves and are very difficult to find. This behaviour may facilitate dispersal from nurseries (Tooke, 1953).

Adult *G. scutellatus* females fly and locate suitable host trees and usually lay their egg capsules on the top side of young leaves (Tooke, 1953). The egg capsules are brownish to black in colour and ±3 mm in diameter and contain 10 to 16 eggs (Mally, 1924). After 2 to 3 weeks, larvae emerge from these capsules by eating through the leaf on which they were laid (Mally, 1924). The young larvae feed mainly on mesophyll and epidermis layers of young foliage and adult larvae may consume the whole leaf (Tooke, 1953). The feeding behaviour of the larvae results in a characteristic snail trail like pattern on the leaf (Mally, 1924; Tooke, 1953). After 4 to 8 weeks and 4 instars (Tooke, 1953) the larvae reach a length of approximately 1.5 cm (Mally, 1924). The larvae drop to the ground and form a pupa in the soil. Two to three months later, the adult beetles emerge and start feeding on foliage of selected *Eucalyptus* species (Tooke, 1953). Males perform clear courtship behavior and copulation usually lasts for 7 hours, but may last for up to 55 hours (Carbone and Rivera, 1998). Beetles often seek refuge under bark and leaves during colder months and go into a state of hibernation during winter (Tooke, 1953). Few if any eggs are laid during hibernation (Tooke, 1953). Depending on conditions, one single female may be able to lay eggs for 2 to 3 months in South Africa and 2 to 3 life cycles may occur per year (Mally, 1924).

1.4 Control of *Gonipterus scutellatus*

1.4.1 Biological control of *G. scutellatus*

In 1926, Tooke (1953) discovered the egg parasitoid *Anaphes nitens* at Penola in Australia. This wasp lays its eggs inside the *G. scutellatus* egg mass and its larvae feed on the eggs. The wasp was introduced into South Africa in 1926 and has proven to be very successful in reducing *G. scutellatus* population levels (Tooke, 1953). This subsequently led to the introduction of the parasitoid from South Africa into many of the other affected countries.

Anaphes nitens is a particularly successful parasitoid because the egg capsules of *G. scutellatus* are easily accessible by the parasitoid which rapidly disperses due to its flight capabilities (Tooke, 1953; Hanks *et al.*, 2000). *A. nitens* almost always kills nearly all eggs within the *G. scutellatus* egg capsules (Hanks *et al.*, 2000) and the parasitoid has a short life cycle (<33 weeks in warm areas) (Tooke, 1953).

The success of *A. nitens* in South Africa is limited to areas with similar climate to its place of origin in Penola, Australia (Tooke, 1953). At Penola, *G. scutellatus* continues to breed during winter that allows the parasitoid to proliferate throughout the year (Tooke, 1953). These conditions are similar to the winter rainfall regions of South Africa (Tooke, 1953). Summer rainfall areas of high altitude (above 1219 meters) are the areas where bio-control often fails in Spring (Tooke, 1953). This is due to hibernation of *G. scutellatus* and unavailability of egg capsules during colder winter months (May to October). After winter, the beetles emerge and bio-control fails to controll their populations due to low *A. nitens* numbers (Tooke, 1953). This was also observed in high lying areas such as Leshoboro and Tsikoane in Lesotho (Richardson and Meakins, 1984).

Biological control has also been known to fail in other countries where *G. scutellatus* eggs are unavailable to *A. nitens* for extended periods of time (Loch, 2008). In North Western Spain, the initial release of *A. nitens* reduced the numbers of *G. scutellatus* to such low levels that the parasite itself suffered due to this so called super parasitism (Rivera *et al.*, 1999; Carbone and Rivera, 2003). The *G. scutellatus* population recovered and parasitism rates were then observed to be below acceptable levels (Rivera *et al.*, 1999). The failure of biological control in North Western Spain was ascribed to fluctuations in predator/prey populations (Rivera *et al.*, 1999).

1.4.2 Control of *G. scutellatus* using pesticides and biopesticides

Insecticides sutch as azadirachtin, flufenoxuron and ethofenprox have been considered for the control of *G. scutellatus* in some areas (Carbone and Fernández, 2004). These toxins reduce the *G. scutellatus* numbers, but parasitism rates by *A. nitens* are also negatively affected (Carbone and Fernández, 2004). The biopesticide *Bacillus thuringiensis* showed minimal activity in killing both *G. scutellatus* and *A. nitens*. Alpha-cypermethrin, a broad-spectrum insecticide tested in South Western Australia was found to kill many beneficial arthropods as well as *G. scutellatus* (Loch, 2005). Insecticides that have a negative impact on the biological control of *G. scutellatus* should be used only in areas where biological control fails (Hanks *et al.*, 2000). These toxins are both expensive and damaging to the environment, thus other means of controlling *G. scutellatus* may be more viable and should be developed.

1.5 *Eucalyptus* diversity and their volatiles

The genus *Eucalyptus* has been subdivided into seven polytypic subgenera and six monotypic subgenera (Brooker, 2000). Most of these trees occur naturally in Australia and

Tasmania and a few species are also found in Indonesia (Eldrige *et al.*, 1993). Today these trees are valued for their timber, bark, essential oils and ornamental properties.

The Tasmanian blue gum (*E. globulus*) was among the first *Eucalyptus* trees to be planted outside of Australia (Poynton, 1979). This tree was regarded as the "prince" among eucalypts and it was favored as a plantation tree due to its rapid growth and the fact that its juvenile leaves are unpalatable to grazing animals (Eldrige *et al.*, 1993). Juvenile leaves can be distinguished from adult leaves based on their shape and the amount of wax on their surface. Juvenile leaves are ovate (egg shaped and broader towards the base) with higher quantities of wax than the adult leaves which are sickle shaped (Brooker and Kleinig, 1996). Juvenile leaves are generally found on *E. globulus* trees that are younger than three years old (Nunes and Pio, 2001).

Eucalyptus globulus is still planted today in countries such as Portugal, Spain, Bolivia, Chile, China, Columbia, Ethiopia, Peru and USA (California). *Eucalyptus globulus* was planted in South Africa in the past, but planting was halted since 1937 due to the many pests that occur on this species. Among the major reasons for halting the planting of *E. globulus* was the high levels of infestation by *G. scutellatus* (Poynton, 1979).

Species grown commercially in South Africa include *Eucalyptus grandis, E .dunnii, E. saligna, E. macarthurii, E. nitens, E. fastigata, E. viminalis, E. smithii, E. paniculata, E. cloeziana* and *E. microcorys* (Poynton, 1979). Some hybrids are also planted and these include those between *E. urophylla*, *E. tereticornis*, and *E. camaldulensis*. Of these *E. grandis* is the most widely planted eucalypt in South Africa (DWAF, 2007-2008).

1.5.1 Volatile compounds found in *Eucalyptus* plantations

Many parameters determine the diversity of volatile compounds found in forests. Among these are numerous environmental factors and biological stresses that impact on the physiological processes of the vegetation. Species diversity also adds to the diversity of volatiles found in forests. It is thus expected that monocultures of trees would have a lower diversity of volatiles than forests of high species diversity. Most *Eucalyptus* plantations are usually monocultures and these trees are often clones, which also limits genetic diversity.

Numerous alkanes, alkenes, carbonyls, alcohols, esters, ethers and acids are emitted into the atmosphere by plants, but it is usually the isoprenoids that are the most abundant in *Eucalyptus* forests (Pio *et al.*, 2001). The isoprenoids can be subdivided according to the number of basic C5 building block units. This class consists of hemiterpenes (C5), monoterpenes (C10), sesquiterpenes (C15), diterpenes (C20), triterpenes (C30),

tetraterpenes (C40) and polyterpenes (>C45) (Kesselmeier and Staudt, 1998). These compounds are mostly hydrophobic. The monoterpenes alone may have non-, mono-, bi- or tri-cyclic structures (Kesselmeier and Staudt, 1998). Isoprene, α-pinene, β-pinene, 1,8-cineol, limonene and trans-ocimene, were found to be the most abundant monoterpenes within *E. globulus* plantations (Nunes and Pio, 2001; Pio *et al.*, 2001).

Variation in the emission rates of these volatiles is known to exist and it has been shown that these monoterpenes are emitted in a diurnal cycle with the highest quantities emitted at night and during the early afternoon (Cooke *et al.*, 2001; Nunes and Pio, 2001; Pio *et al.*, 2001). Variability in emission rates of isoprene and monoterpenes was also observed between individual leaves of the same *E. globulus* plants under the same environmental conditions (Guenther, 1991). Such variability is also observed between adult and juvenile leaves. The daily emission variation in the emission of volatiles for *E. globulus* adult and juvenile leaves have been recorded (Figure 1.2). Usually leaves of young trees (juvenile leaves) have higher isoprene and monoterpene emission rates than leaves of adult trees (Guenther, 1991; Nunes and Pio, 2001). Young trees were shown to have a standard isoprene emission rate of 48 $\pm$ 11 $\mu g g^{-1} h^{-1}$, while adult trees had an emission rate of 32 $\pm$ 10 $\mu g g^{-1} h^{-1}$ (Nunes and Pio, 2001). Nunes and Pio (2001) observed that juvenile leaves also emit a higher diversity of monoterpenes (1-8 cineol, limonene and a-pinene) than adult leaves (1-8 cineol) while other authors have reported that some *Eucalyptus* species (*E. nitens* and *E. regnans*) show no difference in their terpene content (Gras *et al.*, 2005).

Plants emit a different bouquet of volatiles when they are under stress or have been damaged. These volatiles are known as the inducible volatile organic compounds or IVOCs (Kessler and Baldwin, 2001). Among the IVOCs are the ubiquitously occurring group of green leaf volatiles (GLV). In general, GLVs constitute monounsaturated six carbon aldehydes i.e., hexanal, (E)-2-hexenal, (E)- and (Z)-3-hexenal and their corresponding alcohols and esters (Ruther, 2000). GLVs have been shown to be the products of enzymatic degradation of membrane fatty acids (Gailliard and Matthew, 1976; Matsui *et al.*, 2000) and have also been found in the ambient air around *E. globulus* trees (Yassaa *et al.*, 2000). These compounds are expected to be present in stressed *Eucalyptus* forests. *Eucalyptus globulus* trees are known to emit more monoterpenes when the leaves are disturbed especially the young leaves (Nunes and Pio, 2001). This increase in emission rate is known to last for more than four hours after the disturbance (Nunes and Pio, 2001).

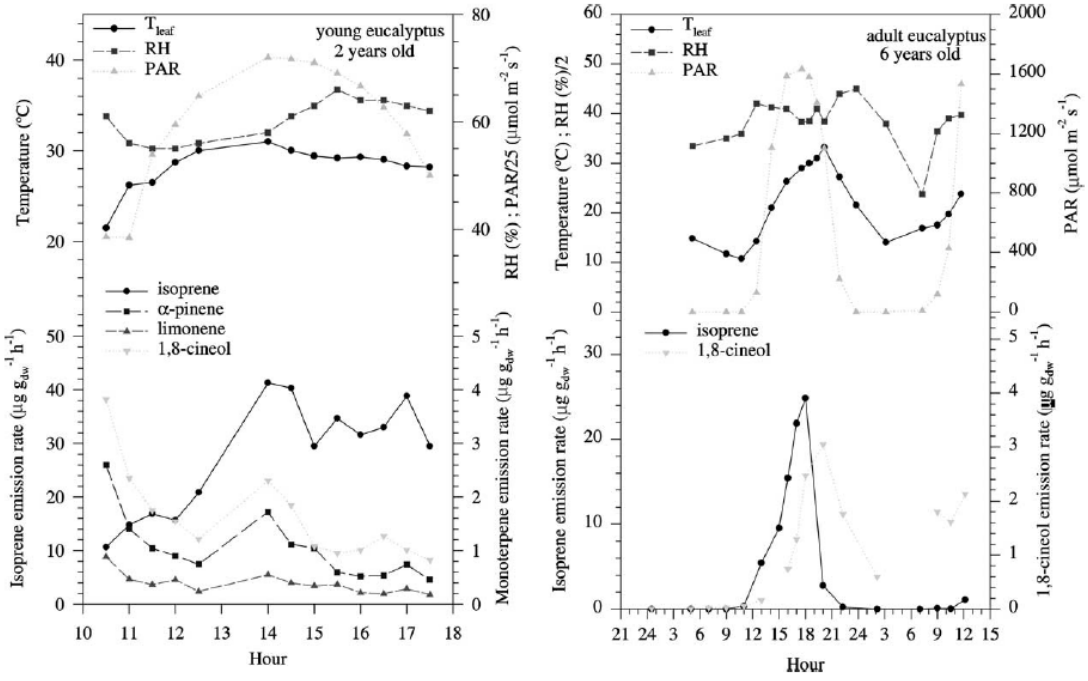

FIGURE 1.2: Emission of VOC's by young and adult *Eucalyptus globulus* trees. Example of daily cycles, also showing temperature, humidity and PAR (Radiation) variation. Adapted from Pio et al. (2001).

1.5.2 Compounds found in *Eucalyptus* essential oils

Essential oil yield and composition varies among different species and provenances of eucalypts (Li and Madden, 1995). Because of the complexity of these oils, which includes hundreds of compounds, classification is usually based on their major constituents. Essential oils made from *E. globulus* adult leaves contain α-pinene, p-cymene and eucalyptol (cineol) as the major constituents with very little phelandrene (Li and Madden, 1995; Tooke, 1953). Its oil is used pharmaceutically and has bio-pesticide properties (Yang *et al.*, 2004). Essential oils made from *E. grandis* adult leaves contain α-pinene and eucalyptol (cineol) as the dominant constituent with no β-pinene (Lucia *et al.*, 2007).

Li and Madden (1995) suggested that differences in leaf oil composition is probably due to genetic variation. They found a large difference between essential oils of the ashes (*E. delegatensis, E. regnans*) and southern blue gum (*E. globulus*). Among other differences, oils made from *E. delegatensis* (Boland *et al.*, 1982) and *E. regnans* leaves contained α- and β-phelandrene as major constituents, while *E. globulus* contained virtually no phelandrene (Li and Madden, 1995).

Li and Madden (1995) found that there are differences in oil composition of juvenile and adult leaves. Of the twelve species of *Eucalyptus* in their experiments, they found that differences were usually quantitative, with qualitative differences occurring only for

some compounds. Piperitone was found to be higher in the juvenile leaves for all but one (*E. pauciflora*) of the twelve species of *Eucalyptus* tested.

1.6 Host detection strategies for flying insects

1.6.1 Insect host location

The central nervous system of a flying insect is the controlling body that allows it to find suitable hosts based solely on its inputs. Some of these inputs originate from the insects sensory equipment (olfactory, gustatory, visual and mechano-receptive organs) which is able to detect information originating from its environment (Miller and Stickler, 1984). Internal inputs also influence the behavior of the insect and Dethier (1982) has suggested that internal and external inputs function in a synergistic/antagonistic manner.

If both the internal and external inputs are positive for a given situation, the insect would "choose" to invest energy into locating and moving towards the source of information. If internal and external stimuli are negative then the insect would "choose" not to invest energy for this purpose. A trickier situation arises when some inputs contradict others. For example, an insect that has just fed would have a negative internal input, but may also experience a positive environmental input in the presence of a preferred food source. This insect would according to (Dethier, 1982), choose only to invest when the positive inputs outweigh the negative inputs. This positive negative ratio was clearly illustrated in a simplistic mechanical analogue by Miller and Stickler (1984) (Figure 1.3).

When insects select hosts they make many of these "accept" or "reject" decisions within a given time frame and they adjust their behavior accordingly (Visser, 1986). This process can be viewed as a chain of behavioral events with different encounters leading to different behavioral states. These culminate in oviposition or feeding on a host plant (for a herbaceous insect) when all of the events have a positive outcome (Miller and Stickler, 1984).

1.6.2 Role of olfaction in insect host location

Plants and insects have co-evolved for nearly 400 million years (Metcalf and Metcalf, 1992). During this time, herbivorous insects have exerted a selective force on the plants on which they feed on and *vice versa* (Metcalf and Metcalf, 1992). Evidence of this is present today in the immense diversity of plant secondary metabolites and the extraordinarily high specificity and sensitivity of olfactory receptors of insects (Dicke, 2000;

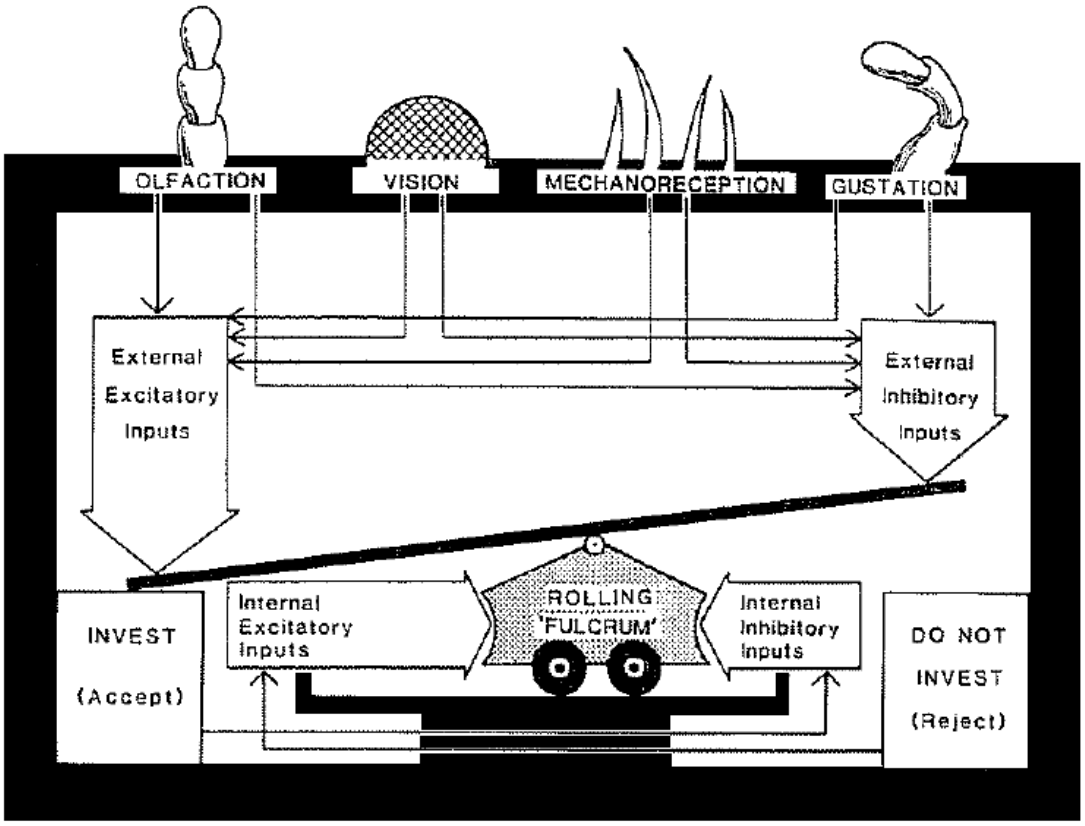

FIGURE 1.3: Millers' 1984 mechanical analogue of Dethiers 1982 model for the influence of external and internal factors on insect investment behaviors. Adapted from Miller and Stickler (1984).

Angioy *et al.*, 2003). Different plants may emit different chemicals into the air and these volatile organic chemicals form the basis of a complex communication network between the plant, herbivore and predator (Price *et al.*, 1980). Herbaceous insects use these olfactory cues to aid in the process of distinguishing between different plants (Price *et al.*, 1980; Dudareva *et al.*, 2004, 2006).

Some compounds that are emitted by plants may function as allomones or kairomones. Allomones are defined as "a chemical substance, produced or acquired by an organism, which, when it contacts an individual of another species in the natural context, evokes in the receiver a behavioral or physiological reaction adaptively favorable to the emitter" (Brown, 1968). A kairomone is defined as "a trans-specific chemical messenger, the adaptive benefit of which falls on the recipient rather than on the emitter" (Brown *et al.*, 1970).

Green leaf volatiles (GLV) are known to be involved in plant to plant communication (Engelberth *et al.*, 2004; Yan and Wang, 2005) and have been found to be involved in sexual communication between some male and female insects (Ruther *et al.*, 2002).

Some insects are able to detect GLVs (Hansson *et al.*, 1999) and studies have shown that these compounds may function as attractants for parasitoids of herbaceous insects (Paré and Tumlinson, 1999; Kessler and Baldwin, 2001). GLVs have also been shown to enhance the attractiveness of insect pheromones (Light *et al.*, 1993). These GLVs may also aid herbaceous insects in finding their host plant species (Visser, 1986). Numerous electroantennography studies have shown that herbaceous insects are able to detect host chemicals (Bedard *et al.*, 1980; Weissbecker *et al.*, 1999; Barata *et al.*, 2000; Larsson *et al.*, 2001; Tol and Visser, 2002; Fraser *et al.*, 2003) and that these chemicals may influence the behaviour of these insects (Bedard *et al.*, 1980; Kessler and Baldwin, 2001; Syed and Guerin, 2004).

1.7 Conclusions and aims

A review of the litterature shows that very little is known about the host preference of *G. scutelatus*. *Eucalyptus globulus* and *E. viminalis* are the species most often reported in the literature as hosts of *G. scutellatus*. These reports are primarily from countries where *G. scutellatus* is an introduced species and where *E. globulus* and *E. viminalis* is or was planted in monocultures. Whether these trees are preferred by *G. scutellatus* has not been tested experimentally.

It is possible that *G. scutellatus* is a generalist *Eucalyptus* feeder that targets only less preferred species when those that are preferable are absent. The studies by Clarke *et al.* (1998) and Richardson and Meakins (1984) confirm that feeding and oviposition occurs on selected *Eucalyptus* species. This indicates that *G. scutellatus* is able to distinguish host trees from non-host trees and it is also able to distinguish more preferred from less preferred hosts. The involvement of host chemicals in host selection by *G. scutellatus* is, therefore, highly probable.

Some reports have stated that *E. globulus* juvenile leaves are preferred for oviposition above adult leaves (Tooke, 1953). This would indicate that there is some factor present or absent in the juvenile leaves that prevents *G. scutellatus* from feeding. The reports by, Nunes and Pio (2001); Guenther (1991) and Pio *et al.* (2001) confirm that there are differences between the volatiles emitted by young *E. globulus* trees and adult *E. globulus* trees. Essential oils made from juvenile and adult leaves of various eucalypts are also known to differ although these differences are usually quantitative. The behavior of *G. scutellatus* may, therefore, be influenced by these differences.

Tooke (1953) believed that attraction between eucalypts and *G. scutellatus* is primarily based on an olfactory mechanism. He investigated the essential oil components from

eight groups of *Eucalyptus* species. He attemted to correlate this *Eucalyptus* oil list to the compiled list of the susceptible *Eucalyptus* species. The data of the oils and susceptibility did not correlate, except for the fact that trees with cineol were more palatable to *G. scutellatus*. This was contradictory to other studies showing that cineol content may not have an effect on *G. scutellatus* oviposition (Dungey and Potts, 2003).

Host volatiles play an important role in host selection for many insects. Clearly there is a large diversity of volatiles that are emitted by the different *Eucalyptus* species. The possibility, therefore, exists that *G. scutellatus* is able to detect some volatile organic compounds that originate from these hosts. The large number of reported *Eucalyptus* hosts implies a high probability that *G. scutellatus* is able to detect compounds which are common among most of these *Eucalyptus* species. The aim of this study is thus to confirm whether *G. scutellatus* is able to detect volatile compounds from some *Eucalyptus* species. Furthermore, to identify some of the volatiles that are detected from *E. globulus* juvenile leaves. The identified volatiles could then be tested in future studies for behavioural activity.

Chapter 2

Methodology to identify semiochemicals from host plants

2.1 Introduction

The first electroantennography (EAG) experiments were reported by Schneider in 1957 and these resulted in the development the single sensillum recording (SSR) technique by Schneider and Boeckh in 1962. EAG and SSR were powerfull techniques that provided information on the neurological functioning of insect antennae. However, identification of semiochemicals on a routine basis was not realized until EAG and SSR were linked to a separation technique such as gas chromatography (Moorhouse *et al.*, 1969; Wadhams, 1984). Today, these techniques are at the heart of numerous scientific breakthroughs in the field of chemical ecology.

Identification of host semiochemicals commences by following a logical process. First, an adequate sample needs to be obtained. Secondly, the material has to be analyzed and lastly, the generated data should be interpreted. The interpretation of the data is only possible when the entire process is understood. The aim of this chapter is, therefore, to explain the techniques and principles used in identifying semiochemicals. It briefly elaborates on some sampling techniques, but mainly focuses on the purge and trap method. Principles used in detection techniques such as electroantennography (EAG), single sensillum recording (SSR) and gas chromatography electroantennographic detection (GC-EAD) are explained. The separation process during chromatography is also explained in some detail. Mass spectrometry as an identification technique is expanded on and a special focus is placed on the ion trap mass analyzer.

2.2 Air sampling techniques

The analysis and subsequent identification of a semiochemical compound is a complex process that begins with the sampling of the EAG active material. Numerous sampling methods have been developed for this purpose, and a decision regarding which to use in such experiments is often difficult. Simple sampling techniques are known to give a more accurate representation of the actual volatile profile existing in the air space around a plant. For this reason, many researchers are chosing to move away from older techniques including distillation and subsequent solvent fractionation. Techniques that involve the sampling of the headspace, such as the purge and trap method or solid phase micro extraction (SPME), are now preferred. Common methods to obtain sample material are displayed in table 2.1:

TABLE 2.1: Sampling techniques that have been used in previous studies

Number	Sampling technique	Authors
1.	Steam or vacuum distillation	Millar and Sims, 1998
2.	Direct sampling of the airspace	Agelopoulos and Pickett, 1998
3.	Solid phase microextraction (SPME)	Chai and Pawlizyn, 1995
4.	Purge and trap techniques	Millar and Sims, 1998

A short description of the first three techniques is given here but for more detail the reader is referred to the reviews by Harper (2000); Augusto *et al.* (2003) and Tholl *et al.* (2006). The purge and trap method is described in more detail in section 2.2.1.

The distilation technique is often followed by solvent fractionation. The distillation procedure involves heating that may change the chemical nature of the sample. Solvent fractionation is subsequently needed because the resulting oils are very complex mixtures which may complicate the analysis (Millar and Sims, 1998). One of the advantages of this technique is that it provides enough sample material for multiple analyses. The disadvantage is however that the process is very complicated and may result in sample contamination or sample degradation (Millar and Sims, 1998).

Direct sampling of the headspace with a syringe is the simplest technique and gives the best representation of the sample air. However, it suffers from a major disadvantage: This is that the analyte concentrations are usually below the detection limits of the analysis techniques.

Solid phase microextraction (SPME) is a relatively new technique that utilizes an adsorbent coated fiber. The fiber may be directly inserted into a GC injector and desorbed. This makes the SPME technique simple with regards to sample preparation; however

SPME may not always be ideal as reported by Agelopoulos and Picket (1998). These authors show that compound ratios were significantly different when using SPME as compared to the actual headspace and solid sorption techniques using Tenax® TA and Porapak Q. This is probably because SPME is a single extraction technique and the solid sorption techniques utilize multiple extraction whereby all compounds are trapped onto the trap before breakthrough.

2.2.1 Solid sorption headspace sampling (purge and trap)

One of the simplest headspace sampling methods is the purge and trap method. Purge and trap implies that the method is a dynamic method rather than a static method as in e.g. SPME (Tholl *et al.*, 2006). Generally the sample is enclosed in a container made from inert material such as glass, metal or Teflon (Millar and Sims, 1998). Purified air is passed through the headspace chamber and through a trapping device for a certain amount of time. The trapping device may contain an adsorbent implying that molecules are adsorbed onto the surface of the solid material.

The purge and trap method has many advantages over the other techniques. Firstly, the obtained sample usually represents the actual sample relatively accurately (Agelopoulos and Picket, 1998). Secondly, the use of solvents can be circumvented by using thermal desorption as a GC injection technique. An added benefit is that modern thermal desorption instrumentation allows for recapture of the split flow during the desorption process and allows for multiple analysis of the same sample. Solid sorption headspace sampling has also been reported to collect a higher diversity of compounds when compared to vacuum steam distillation (Takeoka *et al.*, 1988). This is probably due to a higher sensitivity that can be obtained by using thermal desorption as a GC injection technique.

The dynamic headspace sampling technique can be subdivided into two major categories when sampling from living material such as plants. The first is called *in situ*- sampling and the second *ex situ*- sampling. *In situ*- sampling is the term used when volatiles are sampled from the intact plants and *ex situ* refers to sampling volatiles from detached plant parts (Dudareva *et al.*, 2006). Figure 2.1 represents an *in situ* dynamic headspace sampling system. Generally *in situ* techniques provide a more accurate representation of the actual volatile profile from the plant (Dudareva *et al.*, 2006). *Ex situ* techniques may also include volatiles that originate from damaging plant material such as the green leaf volatiles (Augusto *et al.*, 2003). Most volatile organic compounds have been shown to be released at different times and rates after a plant has been disturbed (Nunes and Pio, 2001) and the leaf chemistry of different aged cloned trees may even differ (Donaldson

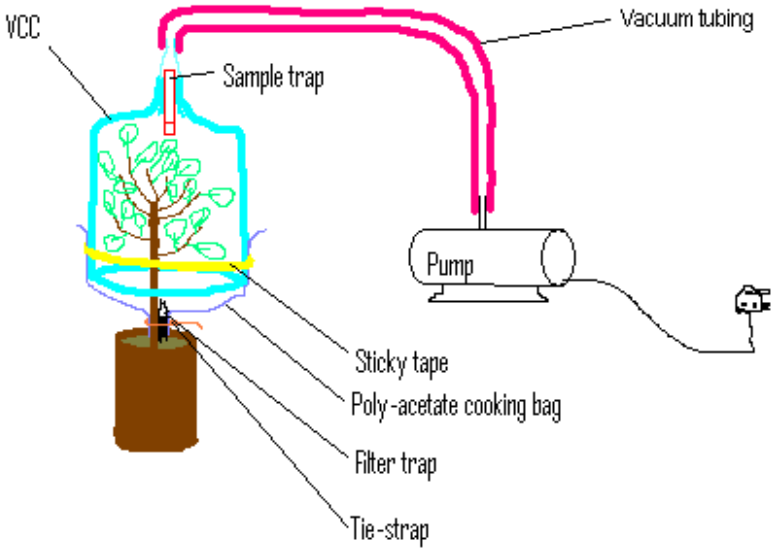

FIGURE 2.1: Dynamic headspace sampling system. Air is purified through a filtering device before entering the Volatile collection chamber (VCC). It passes through the trap at the top of the VCC where volatiles are adsorbed onto a sampling trap.

et al., 2006). These aspects make it very difficult to obtain a consistent sample source. Samples that are taken at different times may differ from one another even when they are taken from the same tree, branch or leaf. The purge and trap method is ideal for detecting such differences.

The purge and trap method is not without disadvantages. These disadvantages have to be considered before this method is used (Table 2.2).

TABLE 2.2: Some disadvantages of the purge and trap method

1.	Incomplete adsorption of volatiles may occur because different VOC's may have different adsorption affinities for different adsorbents (Tholl et al. 2006).
2.	Sample volumes are small and do not allow for the use of identification techniques like NMR and X-ray crystallography (Millar and Sims, 1998).
3.	Thermal desorption of samples may cause changes in the composition of the sample (Millar and Sims, 1998).
4.	Samples can often be analyzed only once when thermal desorption is used as opposed to liquid extraction where multiple injections are often possible.

2.2.1.1 Selectivity during the adsorption process

Samples are generally taken from a sample matrix which is a complex mixture of different compounds. Only a few of these compounds are usually of interest in a given situation and are referred to as the analytes. Low concentrations of analyte compounds have to be sampled selectively above the matrix in order to to concentrate them. The purge and trap method allows for such selective trapping of analyte molecules. To understand selectivity for the purge and trap method the single compound system has to be considered before the multiple compound system. In this regard the selectivity is generally governed by two factors. The first is the type of adsorbent used during the sampling process and the second is the distribution ratio of the compound between the adsorbent and the air inside the sampling chamber.

The Langmuir isotherm (Figure 2.2) relates the degree of adsorption (sites filled) to the concentration or partial pressure of one compound under constant temperature. The number of active sites for a given amount of adsorbent is determined by the pore size and total surface area of the adsorbent (Frigge *et al.*, 1987). Under infinitely low concentrations sites will never fill to their maximum level (m_{max}) and the system is said to operate under linear chromatographic conditions. At high concentrations (for the single compound) the active sites may be filled and multi-layer adsorption may even occur. In these cases the adsorption properties of the adsorbent is influenced by the nature and number of adsorbed molecules. This in turn may change the distribution ratio of the compound.

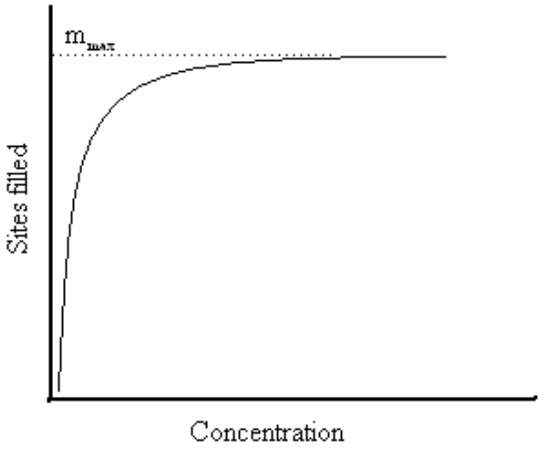

FIGURE 2.2: The Langmuir isotherm for one compound at a constant temperature.

The accumulation of an analyte occurs before it is lost due to breakthrough. Breakthrough occurs when the compound has moved through the adsorbent as in a chromatographic run. This occurs when a sufficient volume of gas has been passed through

the trap. The moment in time when a compound breaks through the trap is called the breakthrough time and has been defined according to Harper (2000) as the point in time when the outlet stream concentration is equal to 5% of the inlet stream concentration. Breakthrough time of a specific compound is dependent on a variety of factors (Table 2.3) including the flow rate and can be related to the breakthrough volume through the average volumetric flow rate through the trap. Breakthrough volume stays constant for a compound at a specific temperature and pressure and only depends on the distribution constant (see equation 2.4). The breakthrough volume of a compound is thus independent of the flow rate (Baya and Siskos, 1996; Harper, 1993). Breakthrough is not desired during a quantitative analysis and the sampling process should be stopped before the analyte is lost due to breakthrough.

TABLE 2.3: Some factors influencing breakthrough time

1.	The specific adsorbent used (Harper, 1993).
2.	Temperature (Harper, 1993).
3.	Concentration of the adsorbed molecule (Harper, 1993).
4.	The presence of other compounds that compete for adsorption space (Harper, 1993).
5.	Volume passed through the trap (Harper, 1993).

Different compounds may break through the trapping device at different times during the adsorption process and this difference can then be used to selectively concentrate certain molecules above others (Figure 2.3) in a multiple component system.

From figure 2.3 it becomes clear that the sampling process can be stopped before breakthrough of any analyte molecules (carrier air or matrix is intentionally allowed to breakthrough). Such a procedure is very useful especially if it is required to sample multiple analytes in a mixture without analyte loss. In this case the relative ratio of the analytes should reflect the actual composition sampled. Larger samples need to be processed effectively to accumulate detectable amounts of very dilute compounds. This obviously requires larger breakthrough volumes. The breakthrough volume can be increased by increasing the amount of adsorbent in a trap or by changing the adsorbent. Very complex mixtures may also be sampled by combining more than one type of absorbent in one trapping device as in Baya and Siskos (1996).

The adsorption process in multicomponent systems may become different from the single component system because different molecules may compete for sites available on the adsorbent and because different compounds are usually not at the same concentration within a sample. The theory for predicting breakthrough volumes in such multiple component systems becomes complex and can be found in Comes *et al.* (1993).

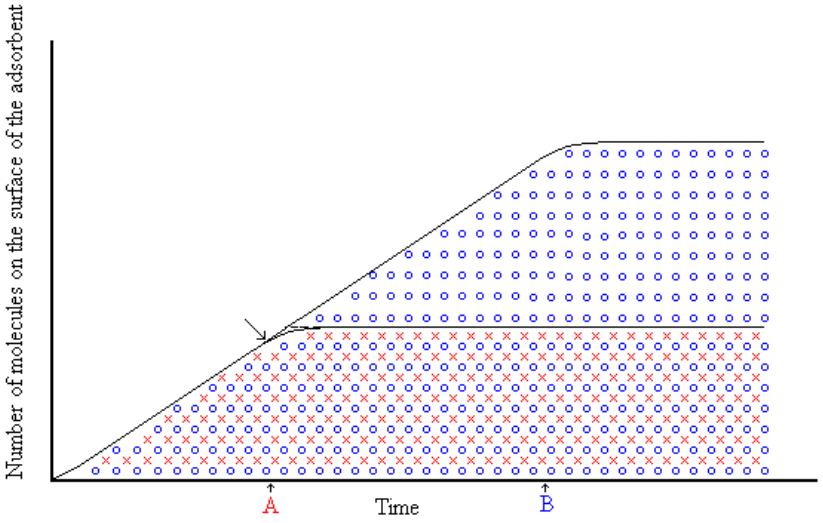

FIGURE 2.3: The adsorption process (in time) for two compounds of the same initial concentration. The red molecules have a smaller distribution constant than the blue molecules and thus a shorter breakthrough time than the blue molecules. Breakthrough times for these two molecules are indicated with A and B on the X axis. The adsorbent used here shows a higher selectivity for the blue molecules. Notice that the relative amount of the two substances collected will stay constant until the first breakthrough volume (arrow) is reached.

2.2.1.2 Tenax® as an adsorbent

Thermal desorption is a GC injection technique that utilizes high temperatures to rapidly volatilize a sample. The thermal desorption process both simplifies sample preparation and increases sensitivity (Harper, 2000) when compared to solvent extraction of traps. One of the adsorbents that is used for selectively sampling C7-C26 volatiles from air is Tenax® which is a 2,6-diphenyl-p-phenyleneoxide polymer. Tenax® has a high thermal stability, and its hydrophobicity results in low retention of water that facilitates its use in thermal desorption. This is advantageous because water is known to influence chromatographic peak shape and may even block the cryogenic trap of a thermal desorber system (McCaffrey and MacLachlan, 1994). Table 2.4 lists the criteria which are required for an ideal adsorbant.

Although the ideal adsorbent does not exist, Tenax® comes close to being one. Tenax® is, however, not without disadvantages. It has a low specific surface area of about 35 m^2g^{-1} that limits its application to atmospheres of relatively higher concentrations (Harper, 2000). It is not suitable for solvent desorption (Harper, 2000) and Tenax® is sensitive to light (Peters *et al.*, 1994). Artifacts such as benzaldehyde, acetophenone and other larger aldehydes are known to originate from Tenax® (Peters *et al.*, 1994). Certain terpenes (a-pinene and sabinene) have also been known to degrade when sampling with Tenax® (Coeur *et al.*, 1997). Other terpenes are also known to react with various

TABLE 2.4: Dettmer and Engewald (2002) identified the following criteria for the ideal adsorbent

1.	It should have the ability to enrich and thus pre-concentrate analytes.
2.	Desorption of analytes should be fast and complete.
3.	The surface of the adsorbent should be inert with respect to the analyte.
4.	It should have a low affinity for water.
5.	It should have a low adsorbtion capacity for inorganic gases present in air.
6.	It should have high mechanical and thermal stability.
7.	It must be able to be used multiple times.

oxidative chemicals that may be present during the sampling process (Calogirou *et al.*, 1999).

Tenax® is conditioned at temperatures as high as 330 °C, while under constant flow of an inert gas such as helium or nitrogen. The conditioning process both minimizes the presence of artifacts and removes any particles that may have originated from other sources. Conditioning procedures may be very tedious and a cleaner version of Tenax®, Tenax® TA is now also available (Millar and Sims, 1998). Various other adsorbents exist but are beyond the scope of this thesis. For additional information, the reader is referred to the reviews by Harper (2000) and Dettmer and Engewald (2002).

2.3 Electrophysiological techniques

Electroantennography (EAG) (Schneider, 1957) and single cell recording (SCR) (Scneider & Boeckh, 1962) are both techniques that have been used to identify compounds involved in olfactory processes in insects. Both techniques rely on the measurement of voltage fluctuations that occur when molecules interact with receptor proteins in cell membranes within insect antennae.

Electrodes and a suitable amplifier are required to measure the small currents originating from the antennae of the insect. Chlorinated silver or gold wires immersed in suitable electrolytes have replaced the older sharpened tungsten electrodes. Glass capillary electrodes can easily be made in the laboratory by drawing a glass capillary tube to a fine tip manually in a flame. Chemical and electromagnetic noise is unfortunately a reality with these electrophysiological techniques and a Faraday cage is often used to minimize electromagnetic interferences. Sometimes a simple foil covering of the recording electrode is sufficient (Millar and Sims, 1998). The use of glass capillary electrodes

can also result in a reduction in the signal to noise ratio especially when compared to the electrode fork which is used for larger antennae in EAG.

Simple electrolyte solutions have been found to function the best in many cases and these are typically prepared from a potassium chloride salt. Small amounts of polyvinyl pyrolidone can be added to the solution to prevent evaporation and subsequent desiccation of the antennal preparation. More complex solutions have also been used in single cell recordings and EAG especially when antennal lifetime is a problem. A list of recipes for these electrolytes can be found in Bjostad (1998).

2.3.1 Single cell recording (SCR)

The single cell technique measures the potential change that occurs across a single sensillum. According to Boeckh (1984), electrical impulses are created when the conductance/resistance at the distal end of a single receptor cell changes, due to the interaction of molecules with the receptor membrane proteins. Figure 2.4 is a schematic representation of one of these sensilla.

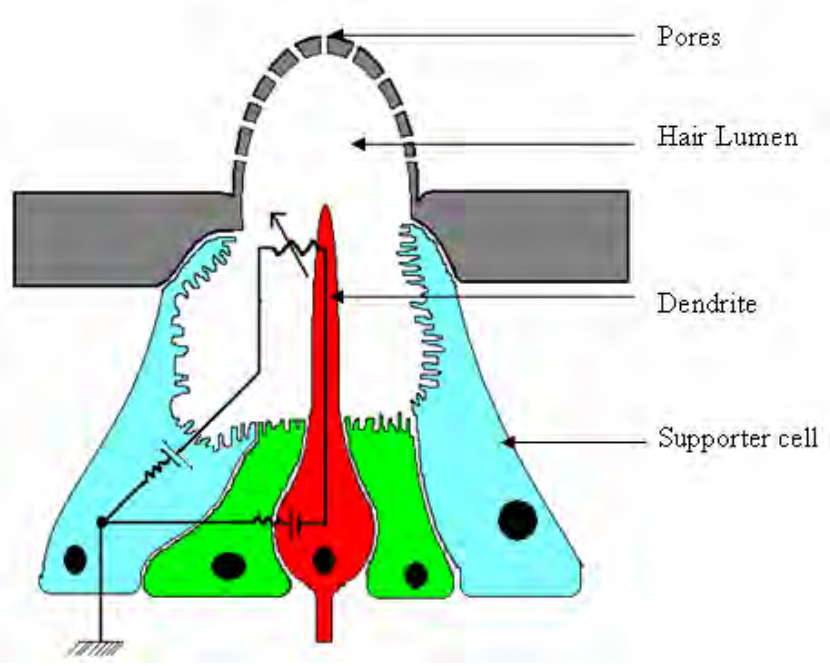

FIGURE 2.4: A schematic view of the antennal sensillum. Odour molecules enter the hair lumen via the pores on the surface. Supporter cells transport the odour molecules to the receptor cell (red). Current is generated by receptor cell and supporting cells across the cell membranes as indicated by the circuit diagram. The potential across the circuit changes when the resistance of the circuit changes. Redrawn from Boeckh (1984).

In single sensillum recording the recording electrode is placed at the tip of one sensilla with the reference electrode inserted into the antenna. The reference electrode is moved while stimulating the antenna with a compound until single action potentials or spikes are observed in the output (Wadhams, 1984; Blight *et al.*, 1995). When the amplitude of all the spikes are the same, the spikes are said to originate from one cell (Bjostad, 1998). Figure 2.5 displays a simulated output that would be observed for one sensillum in such a recording. Compounds that are more active give higher frequency of spikes in the output. The high frequency nature of the response necessitates the use of an alternating current amplifier rather than a direct current amplifier as in EAG. Researchers commonly use this technique to classify sensilla based on compounds that stimulate them (Wibe *et al.*, 1997; Bichao *et al.*, 2005). The single cell recorder has also been coupled to gas chromatography (Wadhams, 1984).

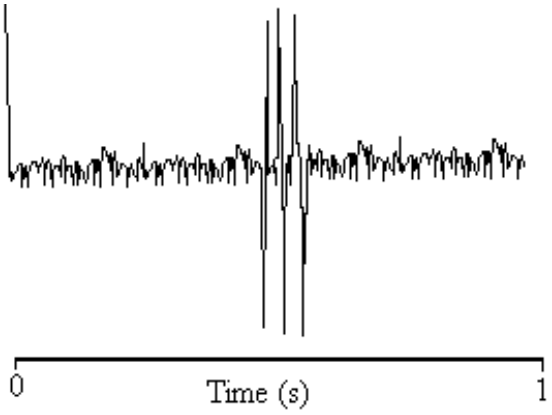

FIGURE 2.5: Hypothetical output for single cell recording. Spikes are observed after a stimulus is given.

2.3.2 Electroantennography (EAG)

Thousands of sensilla contribute to the overall large potential change that can be measured from the tip to the base of the antenna in EAG (Nagai, 1981). This results in a relatively slow deflection of the potential across the antenna. Live insects or removed antennae Malo *et al.* (2000) can be used in these recordings, however, movement by live insects can influence the recording quality and a suitable restraining device is often necessary. A response during an EAG experiment can be used to indicate that some EAG active molecules exist within a given sample. This response can only be linked to the behaviour of an insect by adequate bioassay experiments.

The recording electrode is placed on the tip of the antenna with the reference electrode on the insect head or eye for live insects. This allows for the recording of a negative deflection in potential once stimulation is achieved. An example of such a recording is

displayed in Figure 2.6. Some researchers have reported that superior connectivity can be obtained by removing the first few segments from the antenna before coupling the recording electrode (Struble and Arn, 1984).

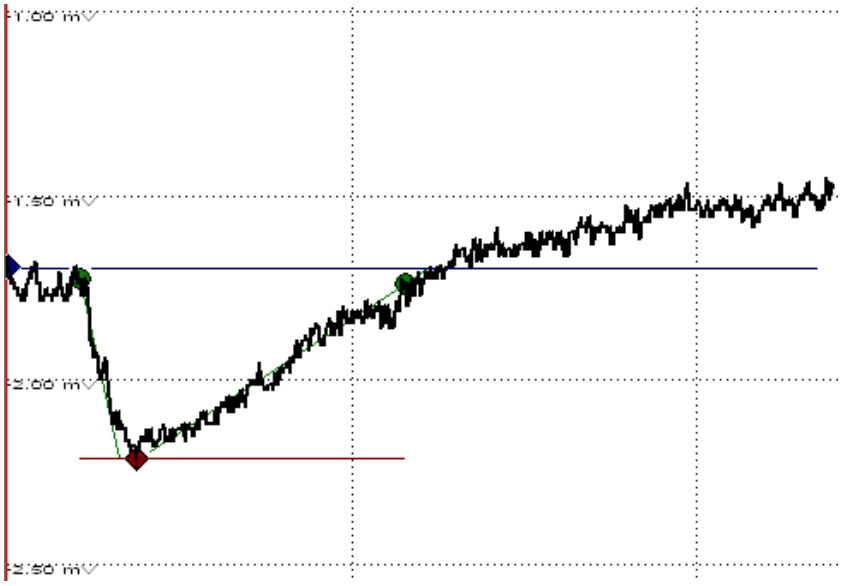

FIGURE 2.6: The EAG response observed when a live *G. scutellatus* female insect was stimulated with host volatiles from a crushed *Eucalyptus viminalis* leaf.

Typically a sample is placed in a disposable Pasteur pipette and clean humidified air is passed over the sample and blown into a stimulus delivery tube. The stimulus delivery tube facilitates a gentle stimulation of the antennae that limits the response from mechanoreceptors. An excessive airflow in the stimulus delivery tube can lead to stimulation of mechanoreceptors and subsequently high noise in the recording output. An excessive airflow through the Pasteur pipette can also result in false positives for the same reason. Clean air can be obtained from bottled canisters or by filtering laboratory air through a suitable filtering device. Modern EAG equipment is usually equipped with suitable filters that should be replaced once contamination is suspected.

When measured correctly, a response is observed if the sample contained some EAG-active compound. The responses are typically in the milli- to micro- volt range and are stimulus concentration dependent. These responses may vary for different species of insects mainly because differences occur in their antennal morphology and because receptors can vary in number and type. A good example of morphological differences can be seen when comparing antennae from two different families of insects. Weevils, which belong to the beetle Order (Coleoptera), usually have club shaped antennae while the butterflies and moths (Lepidoptera) have an elongated segmented shape. The sensitivity of the antennae may be localized to a specific area in the antenna as reported by Nagai (1981) and Tol and Visser (2002).

A decline in antennal sensitivity is usually observed especially when removed antennae are used for EAG recordings (Malo *et al.*, 2000). The decline in antennal sensitivity makes it difficult to compare results from different recording sessions and responses are subsequently normalized to a response from a known EAG active compound at a known concentration. The antennae can also suffer from a recovery period after a stimulus is given, and an appropriate recovery time is usually necessary between consecutive sample puffs.

2.3.3 Gas chromatography electroantennography detector (GC-EAD)

Identifying a semiochemical normally involves separating a mixture of compounds in a sample. Compounds which are volatile at room temperature are generally separated by using gas chromatography. Moorhouse *et al.* (1969) reported the first GC-EAD coupling and since then GC-EAD has become a fundamental tool for the identification of chromatographic peaks that elicit responses from insect antennae. GC-EAD is accomplished by synchronizing the response of a detector such as a flame ionization detector (FID) with that of the electro-antennogram detector (EAD) in time. This synchronization is vital and can be achieved by splitting the GC effluent with a splitting device with equal lengths of deactivated silica tubing. The column leading to the EAD detector is heated with a suitable transfer line. The transfer line is usually kept at the maximum temperature of the GC oven when it can not be programed to match the GC oven temperature program.

GC-EAD has some advantages over EAG. Firstly the technique combines the high resolving power of a GC with the high sensitivity of an insect antenna. This means that responses to chromatographic peaks may be observed rather than responses to mixtures of chemicals. GC-EAD may even be used to separate and identify suspected EAD active isomers (Struble and Arn, 1984). Secondly, there is no disturbance in the airflow as in EAG and thus fewer false positive responses in a GC-EAD run.

Different species of insects are inherently different and often display different properties during GC-EAD. This means that optimal conditions can usually only be determined by experimentation. GC-EAD runs tend to be long in comparison with EAG and a decline in antennal sensitivity can be a problem. Live insects can be used to prevent this problem but a suitable mounting system is again necessary to prevent movement of the insect. Some researchers use Plexiglas and wax to prevent movement of the insect (Barata *et al.*, 2000). Inserting the live insect into a micropipette tip with a cotton piece behind the insect can also help prevent movement of the insect. Other researchers simply remove the antennae Struble and Arn (1984) and suspend it through adhesion

forces between the two electrodes. Removing the antennae may have a negative effect on antennal lifetime and humidifying the air passing over the antennae is often necessary. Cooling the incoming air could also enhance antennal lifetime (Struble and Arn, 1984).

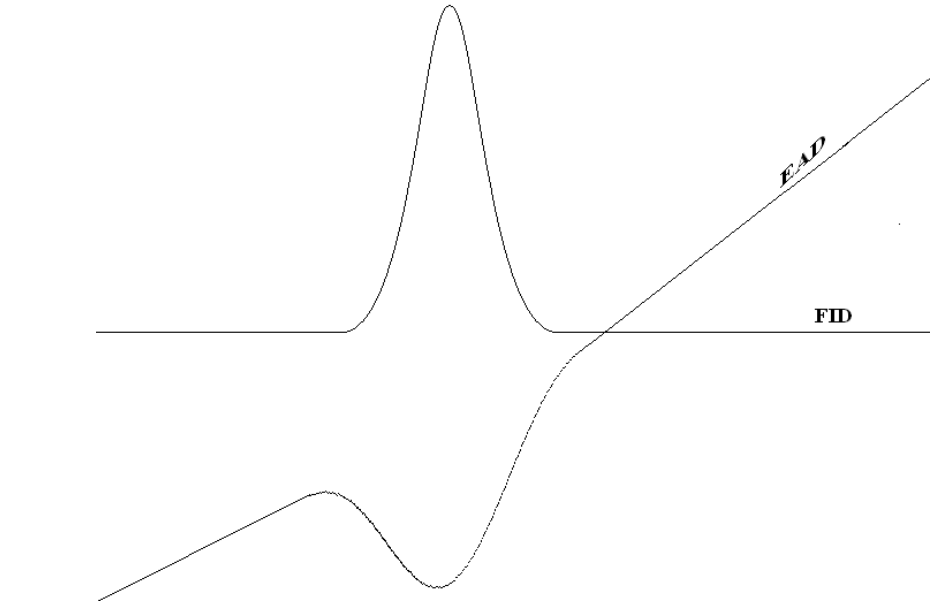

FIGURE 2.7: The shape of a raw EAD signal in comparison to a FID signal. Adapted from Slone and Sullivan (2007)

Recording raw direct current (DC) EAD data can be a problem because baseline drift causes the signal to wander off-scale. Therefore, modern EAD equipment allows for the electronic zeroing of EAD signals to keep the baseline within an acceptable range. Automatic and frequent zeroing the signal, however, comes at a cost. The raw data are not displayed, which makes it difficult to interpret the signals. Slone and Sullivan (2007) have developed a means to mathematically identify true EAD signals from the raw DC data based on the signal's characteristic amplitude, wavelength and symmetry and correlation to FID peak width. Slone and Sullivan (2007) clearly show that the raw EAD data arising from a eluting GC peak has the same Gaussian curve shape as the peak in the FID signal (figure 2.7). The zeroing of the data can then be performed manually in Excel using equation 2.1 (Slone and Sullivan, 2007). This equation effectively measures the differences in signal as time moves on (slope) and incorporates a scaling factor to amplify these differences. Where Z specifies the modified EAD data and E is the raw direct current (DC) EAD data. The factor r can be related to chromatographic peak width at half height ($w_{\frac{1}{2}}$) manually using equation 2.2 as in Slone and Sullivan (2007). The zeroed data would then have peaks that are not Gaussian but rather in the form of a *sine* wave as in figure 2.8.

$$Z_t = E_t - E_{t-1} + rZ_{t-1} \tag{2.1}$$

$$r = 0.8w_{\frac{1}{2}}^{0.05} \tag{2.2}$$

$$r = 0.37^{\frac{1}{f_s TC}} \tag{2.3}$$

Zeroing the EAD data electronically requires specification of a time constant (TC) in the r term which is defined as the time (seconds) required to reduce the EAD deflection to 63% of its deflection maximum. The time constant is then incorporated in the r term as in equation 2.3, where f_s is the sampling rate and TC is the time constant (Slone and Sullivan, 2007). The required time constant can be determined by correlating GC peak width with the EAD peak width. The EAGPro software automatically adjusts the baseline electronically with the SYNTECH IDAC 2/3 recording device when alternate current (AC) data is recorded and a time constant is thus not entered into the software. The software programmed into the IDAC 2/3 automatically detects when the baseline moves out of the scale range which is specified during the recording and auto adjusts the baseline back to zero. This can result in some large responses being sinusoidal in shape and other peaks being Gaussian in shape.

Another problem with GC-EAD data is that noise often mask responses from the antenna. Electronic filtering is used to solve these types of problems, but also modifies the data and it is thus very important to look at the raw data first before deciding on whether filtering the data would help improve the situation. One option is to filter the data only after the recording was made. A frequency window with the lower frequency specifying the longest wavelength (widest chromatographic peak) and the higher frequency the shortest wavelength (spikes) that is allowed to pass can however be adjusted in the software. The longer wavelength should obviously not be shorter than the width of a non overloaded GC peak because the response would then not pass the filter.

2.3.3.1 Separation theory

The separation process often provides inadequate resolution, especially when complex mixtures are separated in single dimensional gas chromatography. A sound understanding of the separation theory is thus essential to any chromatographer and it is for this reason that the basics of the theory is presented here. The heart of the separation in

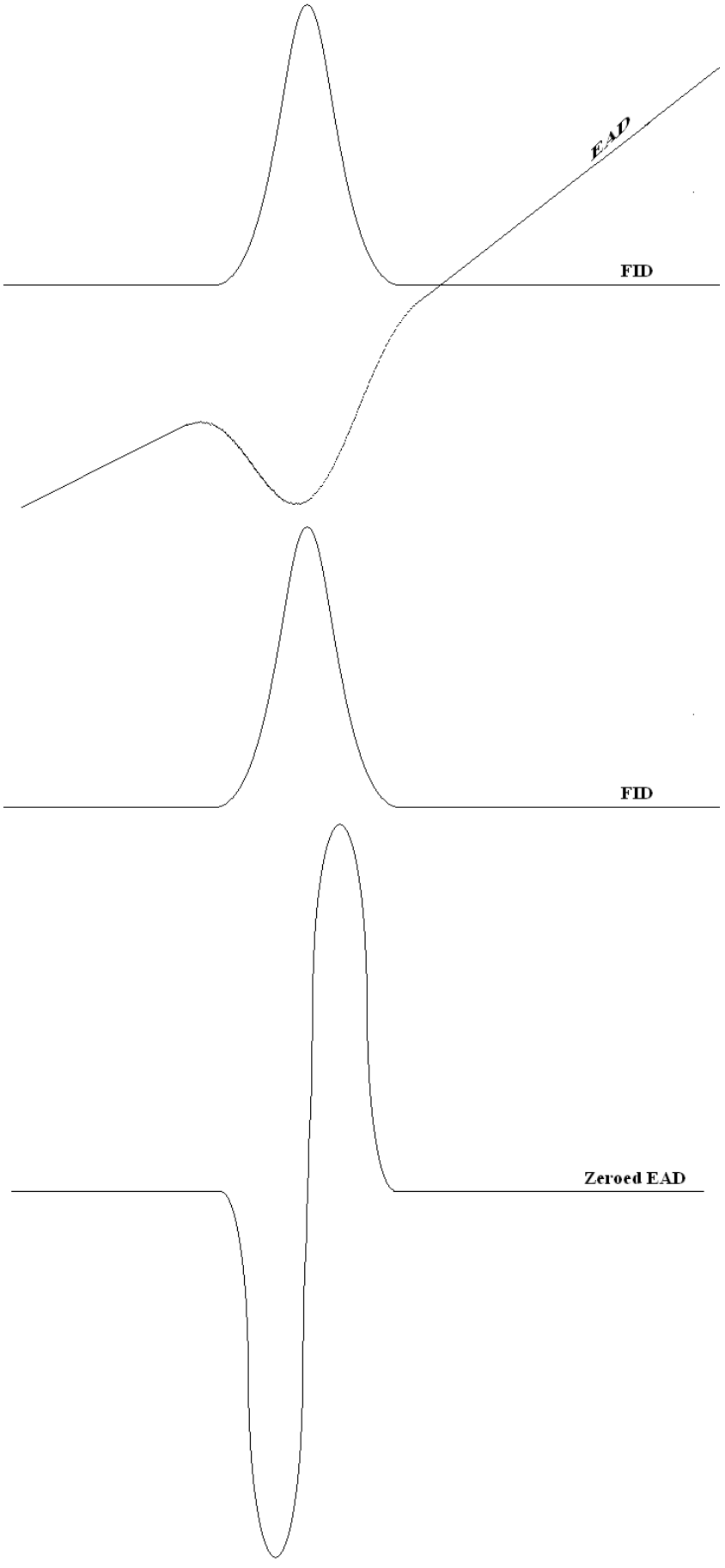

FIGURE 2.8: The shape of a baseline corrected EAD signal in comparison to a FID signal. Adapted from Slone and Sullivan (2007)

gas chromatography is the equilibria that exist between the stationary phase and the mobile phase in the capillary column. These are displayed in figure 2.9.

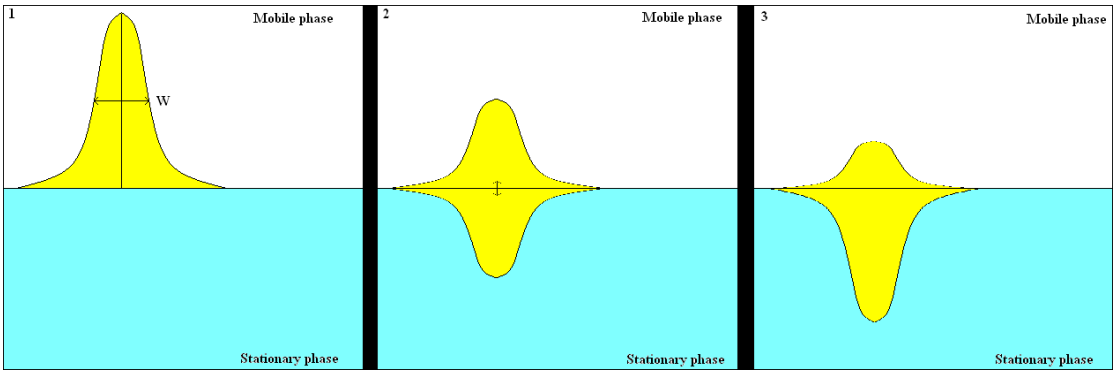

FIGURE 2.9: The distribution of three different molecules in the stationary and mobile phases. Frame one: The distribution of an non retained compound. Frame two: The distribution of a compound which is 50% retained. Frame three: The distribution of a compound which is 75% retained.

The equilibrium that exists between the stationary phase and the mobile phase can be described with a distribution constant (Equation 2.4).

$$A_m \rightleftharpoons A_s$$

$$K = \frac{[A_s]}{[A_m]} \tag{2.4}$$

The difference in distribution constants for different compounds at a specific temperature, is the driving force for separation during a chromatographic process. Large distribution constants mean that the compounds have a large proportion of the total number of molecules in the stationary phase. In time, a band of molecules with a large distribution constant would require a longer time to travel the same distance as a band of molecules with a small distribution constant (Figure 2.9). Therefore, a clear relationship exists between the distribution constant and the retention time of a compound. This relationship is displayed in equation 2.5 and 2.6.

$$\upsilon = \mu \left(\frac{1}{1 + K\frac{V_s}{V_m}} \right) \tag{2.5}$$

The KVs/Vm term is known as the retention factor (k) and is an important parameter that defines the migration rate of a compound. The retention factor can also be written

in terms of retention times for each peak in a chromatogram. Where t_r is the retention time of a retained compound and t_m is the retention time of a non retained compound.

$$k = \frac{t_r - t_m}{t_m} \tag{2.6}$$

The retention factor should ideally be between 2 and 10 for the peaks in a chromatogram. This is not always possible in an isothermal run but changing the temperature during a run can keep the retention factor values in this optimal range.

Selectivity (α) is another term that describes the relative retention behaviour between two compounds (a and b) in a chromatogram. It can also be written in terms of retention times as in equation 2.8. In gas chromatography the selectivity factor is generally changed by changing the stationary phase chemical properties.

$$\alpha = \frac{K_b}{K_a} = \frac{k_b}{k_a} \tag{2.7}$$

$$\alpha = \frac{t_b - t_m}{t_a - t_m} \tag{2.8}$$

The peaks in a chromatographic profile have a Gaussian distribution and thus a width. The width of a peak in the column may be defined in a number of ways. One of these is the standard deviation (σ) of the distribution (σ is half the width of the profile at 68% of its area around the mean) and another way is the width at half the height ($W_{1/2}$) of the peak as in figure 2.9-1. These two widths are proportional to each other.

The efficiency of a column is related to the width of the peak and the distance moved in the column, more specifically the variance, σ^2 (cm), per distance moved (Equation 2.9) and has been defined as the plate height (H) of a column. In order to determine the plate height from a chromatogram which is measured in time units the standard deviation of a peak in time (τ) has to be related to the standard deviation of the peak at the end of the column in distance (σ). This is done by using the migration rate (cm/s) of the compound as an added factor (Equation 2.10). Migration rate is defined as the length (L) of the column divided by the retention time (t_r) of the compound. A width is defined at the base of a Gaussian distribution which is equal to four times the standard deviation of the distribution and is used to approximate the width (W) of a non-overloaded pure chromatographic peak. Thus $4\tau = W$ in time.

$$H = \frac{\sigma^2}{L} \tag{2.9}$$

$$\sigma = \tau \frac{L}{t_r} \tag{2.10}$$

$$\sigma = \frac{W}{4} \frac{L}{t_r} \tag{2.11}$$

$$H = \frac{W^2}{16} \frac{L}{t_r^2} \tag{2.12}$$

The term plate number (N) is related to plate height (H) as in equation 2.13 and has been related to the width of a chromatographic peak at half its height ($W_{1/2}$) as in equation 2.14. In general larger N values are more closely associated with better resolution (Equation 2.16) than H values only, as N also takes into consideration the column length.

$$N = \frac{L}{H} = 16 \frac{t_r^2}{W^2} \tag{2.13}$$

$$N = 5.54 \left(\frac{t_r}{W_{1/2}} \right)^2 \tag{2.14}$$

The width of a peak increases during the separation process and is mainly caused by the three effects listed in table 2.5. These effects have been added in a general expression known as the Van Deemter equation (2.15). The shape of the Van Deemter curve is displayed in Figure 2.10. It is desired to use a flow rate near the minimum in these curves. At the curve minimum, the plate height is at a minimum which allows for a maximum number of plates for a given column. The three common carrier gases (N_2, H_2 and He) used in gas chromatography give different Van Deemter curves as in figure 2.10. Nitrogen has an optimal flow rate around 10 cm/sec Heath and Duben (1998) and helium at around 20 cm/sec Heath and Duben (1998) for columns with 0,25 mm internal diameter. It is important to realize that two identical systems operating at the same linear flow rate but with a different carrier gas would normally provide different column efficiencies (H) and thus different N values and resolution.

$$H = A + \frac{B}{\mu} + C\mu \tag{2.15}$$

The number of theoretical plates (N), retention factor (k) and the selectivity (α) all contribute to the resolution (R) between two closely eluting compounds (Sandra, 1989*a*,*b*).

TABLE 2.5: The width of a peak increases due to three effects

1.	Diffusion of the molecules in the mobile phase from the centre of the distribution (or band) towards the outer edges (B/u).
2.	Variability in the different flow paths which exist in the column (A). This effect does not exist in an open tubular column.
3.	Resistance to mass transfer (Cu) referring to the non-instantaneous re-establishment of equilibrium as the mobile phase constantly moves the top profile forward.

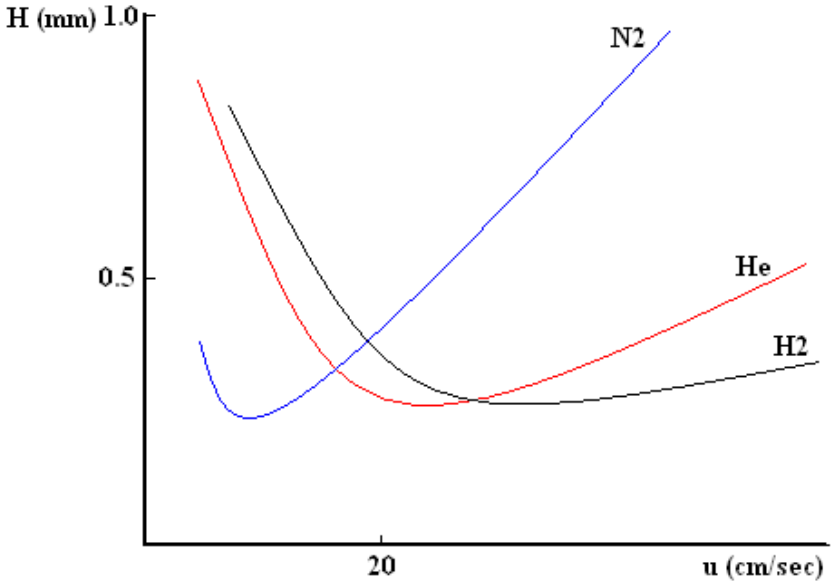

FIGURE 2.10: The shape of the Van Deemter curves for different carrier gases for open tubular columns with a 0.25 mm internal diameter.

These factors have been combined into a resolution equation (2.16). In this equation k_b refers to the k value of the latter eluting peak of two peaks in a chromatogram. (Generally a resolution of 1 gives an acceptable separation for any two peaks in a chromatogram.)

$$R = \frac{\sqrt{N}}{4}\left(\frac{\alpha - 1}{\alpha}\right)\left(\frac{k_b}{k_b + 1}\right) \tag{2.16}$$

"Column efficiency" between two chromatographic systems can also be compared experimentally by calculating the average number of peaks that can be fitted in between two consecutive hydrocarbon peaks for both systems. This value (equation 2.17) is referred to as the separation number (SN) or TZ value and can be calculated both for isothermal

and temperature programmed runs (Sandra, 1989*a*,*b*). It is the latter feature that often favours this "column efficiency" determination as N and H can only be determined from isothermal runs because constant migration rate is implied when deriving equation 2.12 from equation 2.9.

$$SN = \frac{t_{r2} - t_{r1}}{W_2 + W_1} - 1 \tag{2.17}$$

2.4 Mass spectrometry

Mass spectrometry relies on the ionization and subsequent fragmentation of molecules. Fragmentation of the molecules results due to excessive energy available after the ionization process. All ions are accelerated within a vacuum under a known electric field in the ion source so that all the ions end up with the same kinetic energy. Ions with different mass (or more specifically mass to charge ratios) are separated by the mass analyser. A mass spectral pattern (Figure 2.11) is obtained when the intensities of each ion is counted at each specific mass to charge ratio (m/z). The mass spectra that are obtained are unique to each compound provided that the ionization process is standardized. Electron impact ionization is a very common method for ionizing molecules in the ion source of a mass spectrometer and is standardized by using an electron beam with a constant energy of 70 eV per electron.

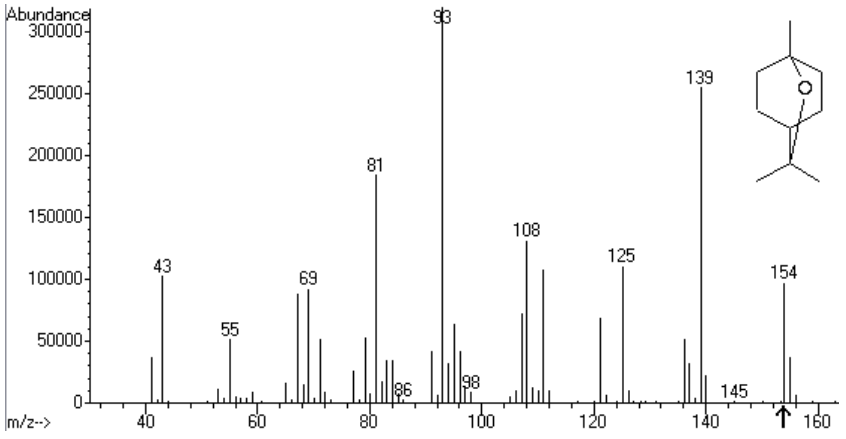

FIGURE 2.11: The mass spectrum of 1-8 Cineol. Notice the molecular ion at m/z value 154.

Mass spectra emerging from investigations are usually matched to known mass spectra in mass spectral libraries such as the NIST and Wiley libraries. The mass spectra can be very similar for different types of isomers. Chromatography can be used to solve such problems provided the isomers are separated in the chromatographic run. In this way,

the chromatogram adds an extra dimension to the identification process. Mass spectra together with retention times (or retention indices) are thus preferred to tentatively identify unknown compounds.

Many different mass analysers have been developed each with its own characteristics. A discussion on each different analyzer is beyond the scope of this thesis but the reader is referred to the review by Webster *et al.* (1998) for more information. The ion trap mass analyzer was used in this study and is discussed in more detail below.

2.4.1 Ion trap Mass spectrometry

The ion trap mass analyzer is very similar to the quadropole mass analyzer. This can be seen by looking at the similarities in their design. Both analyzers rely on the generation of two radio frequency (Rf) potentials that are imposed on top of two direct current (DC) potentials. Each Rf DC combination is applied to a pair of rods in the quadropole and to the two lids and the side in the ion trap (Figure 2.12). In the quadropole different combinations of the DC and Rf frequencies allow different ions to pass through the analyzer to the detector, thus providing an ion separation mechanism. The ion trap uses similar combinations to selectively eject trapped ions into the detector.

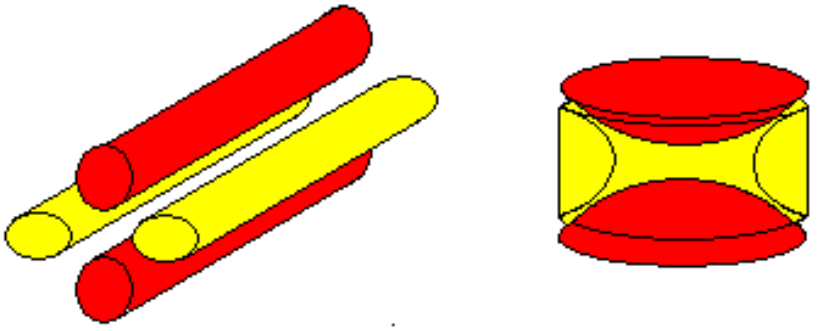

FIGURE 2.12: A schematic representation of a quadrupole mass analyzer (left) and the ion trap mass analyzer (right). Similarly coloured areas are electrically connected and operate at the same frequency potentials for both types of analyzers.

Ions can be injected into the ion trap mass analyzer from an external ion source by means of a potential drop between the ion source and ion trap. These ions are usually focused by a series of lenses which are electrically isolated from each other before they enter the trap. What makes the ion trap special, is the fact that it allows for detection of all ions comming from the ionizer which means that the sensitivity is very high. (In some models of the ion trap selected ions can also be singled out and fragmented again to produce daughter ions. Daughter ion spectra provide extra information that can be used to aid in the identification of unknown compounds.)

There are a number of warnings in the literature regarding mass spectra obtained from an ion trap mass analyzer. These caveats concern the comparison of acquired spectra to library spectra which were obtained from a different mass analyzer and ion source (Webster *et al.*, 1998). Interaction between the ions and molecules in the ion trap may cause a number of phenomena that are not usually observed with other mass analyzers. Protonation of ions via ion molecule reactions in the ion trap may cause large M+1 ion peaks that can deviate from a true electron impact (EI) mass spectrum. These comparisons can result in a false identification of a compound. A tentative identification should thus first be made. The mass spectra of the suspected pure standard should then be compared to that of the mass spectra of the sample itself on the same instrument. These comparisons are usually much more accurate and can give more certainty to the assigned identity of an unknown.

2.5 Conclusion

The semiochemical identification process comprises a combination of many different technologies and methodologies. For successful experimentation in this field, it is both logical and essential to have a sound understanding of these techniques. This chapter has sought to provide some background regarding the most important of these techniques.

Chapter 3

Instrumental and method development

3.1 Introduction

A successful and repeatable semiochemical identification process was the goal in this chapter and required the use of three different techniques namely, electroantennography (EAG), gas chromatography electroantennography detection (GC-EAD) and gas chromatography mass spectrometry (GC-MS). The GC-EAD system was used for both electroantennographic (EAG) experiments and GC-EAD experiments. Results from the EAG experiments provided a means for scanning through numerous samples while the results from the GC-EAD experiments gave valuable data on differential antennal activity towards chromatographic peaks. The GC-MS system was used to provide mass spectral data that allowed for tentative identification of EAD active chromatographic peaks.

This chapter aims to illustrate the challenges encountered while doing EAG, GC-EAD and GC-MS experiments. Firstly a brief description of the instrumentation is given and secondly the methodologies and modifications that were necessary to obtain repeatable and trustworthy results are described. This process required the use of two chromatographic systems that were situated in two different buildings at the University of Pretoria. The GC-EAD system was situated in the Forestry and Agricultural Biotechnology Institute (FABI) building and the GC-MS system was situated at the department of chemistry of the University of Pretoria. These systems ran on different carrier gases and a compromise between the two systems had to be found in order to be able to compare their respective results. This resulted in one of the biggest challenges because the EAD data had to be linked to the MS data through the FID data. The

problems and modifications for each of these systems are illustrated with appropriate pictures and examples of results. In each case a short description of the experiment is given before a conclusion is made on the results that were obtained. These experiments led to the tentative identification of thirteen compounds from the *E. globulus* volatile profile.

3.2 *Gonipterus scutellatus* samples

Live *Gonipterus* samples were obtained from numerous areas in South Africa (Appendix A table A1). These *Gonipterus* samples were assumed to belong to the *Gonipterus scutellatus* species, although it is recognized that the taxonomic status of this species is currently in revision (Slippers, Personal communication). These insects were kept alive in wooden cages (Figure 3.1) by feeding them fresh *Eucalyptus* foliage. The cages were kept within temperature controlled rooms (25 °C). Insect samples were stored in ethanol after each experiment for later classification purposes.

FIGURE 3.1: *Gonipterus scutellatus* cages.

3.3 *Eucalyptus* samples

All *Eucalyptus* samples were obtained from either the FABI nursery on the experimental farm of the University of Pretoria or the zoo plantation near Tom Jenkins Drive in

Pretoria, South Africa. The *Eucalyptus* samples were usually sampled on the day of collection unless stated otherwise.

3.4 Electroantennography

3.4.1 System

The electroantennography system (IDAC 2, Syntech, Hilverstrum, The Netherlands, Figure 3.2) consisted of three separate devices which were linked to each other, to a computer and a chromatography system (6890N, Agilent Technologies, Chemetrix, Midrand, South Africa). The chromatography system was linked to a thermal desorption system (MKIUNITY, Markes). This system was used for all EAG and GC-EAD recordings. The transfer line heater was used during GC-EAD recordings and controls and displays the temperature of the column transfer line between the GC oven and EAD detector (Figure 3.2). The stimulus controller controlled the air flow through the stimulus delivery tube and sample delivery tube and had three valves marked A, B and C (Figure 3.2). Valve A allowed for a controlled puff of air that was used to move air over a sample and subsequently into the stimulus delivery tube. Valves B and C allowed for a controlled delivery of a continuous flow of air through the stimulus delivery tube. Air entered through the back of the stimulus controller system and was filtered through a charcoal filter. Air exiting this system was humidified by passing it through an external glass wash bottle filled with distilled water. The two channel acquisition controller (IDAC 2) simultaneously acquired data from the GC's FID detector and the EAD detector and allowed for the synchronization of the two signals.

3.4.2 Shape of an EAG response

An electroantennography response was identified by a sharp change in the slope from the baseline and a slow recovery to the baseline potential. This shape allowed for the measurement of two variables: the deflection intensity measured in Volts and the surface area measured as Volts×seconds. The surface area and intensity was measured automatically with the EAGPro software (Version 2, Syntech, Hilverstrum, The Netherlands). Defining the signal area with the appropriate placement of the signal markers was essential to obtain the correct value for the surface area (Figure 3.3).

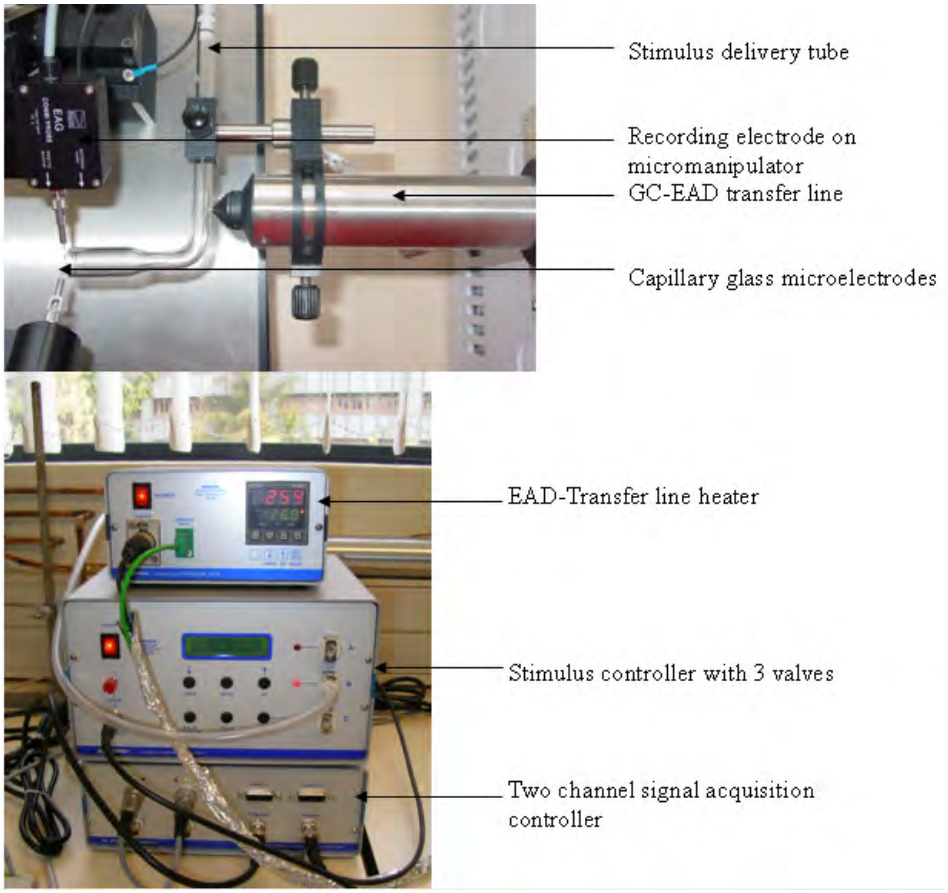

FIGURE 3.2: The EAG system by Syntech. Top: Stimulus delivery system. Bottom: Controlling electronic system

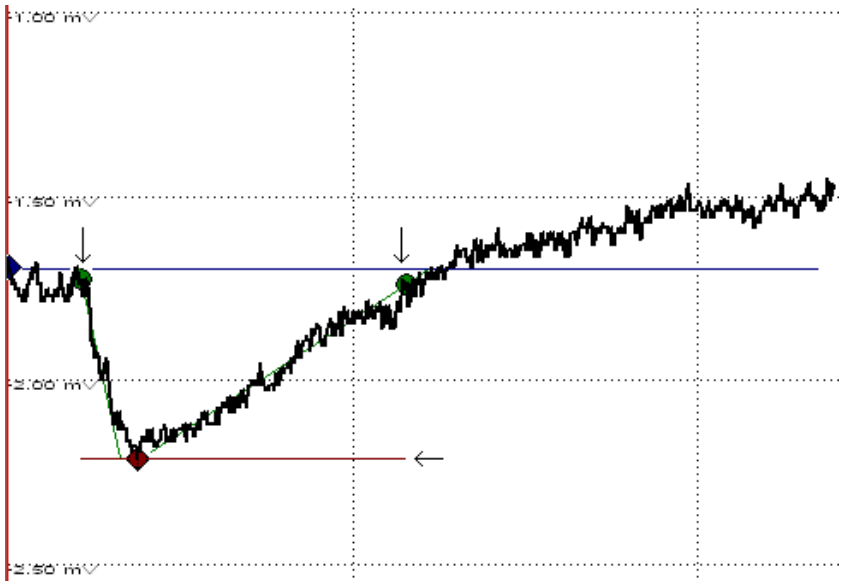

FIGURE 3.3: The EAG response. Arrows indicate where the markers were placed to obtain the correct recording of surface area and response intensity.

3.5 Electrode selection

Two different electrodes were available that could be used during EAG and GC-EAD recordings. Both electrode types were tested in a series of EAG experiments. The experiments were done by observing the response to leaves from two known *Eucalyptus* hosts, *E. globulus* and *E. smithii*. The experiments were performed on the two excised antennae of one *Gonipterus scutellatus* female. The first antenna was used with the electrode fork and Spectra electrolyte gel and the second antenna was used with glass capillary micro electrodes with 0.1 M KCl solution as an electrolyte.

A puff (0.4 sec) of filtered air was passed through a Pasteur pipette which contained a small (1cm×1cm) piece of *Eucalyptus* leaf in the case of the sample and nothing in the case of the blank. Notice the unstable nature of the recordings (Figure 3.4) and the improvement when using the capillary micro electrodes (Figure 3.5). The electrode fork and gel clearly did not give the same quality signal as the capillary micro electrodes. The micro electrode recordings showed that the responses observed for the *E. globulus* and *E. smithii* samples were significantly larger than responses to sample blanks but did not differ significantly from each other when looking at the voltage deflection intensity (Appendix A Table A2 and Figure A1).

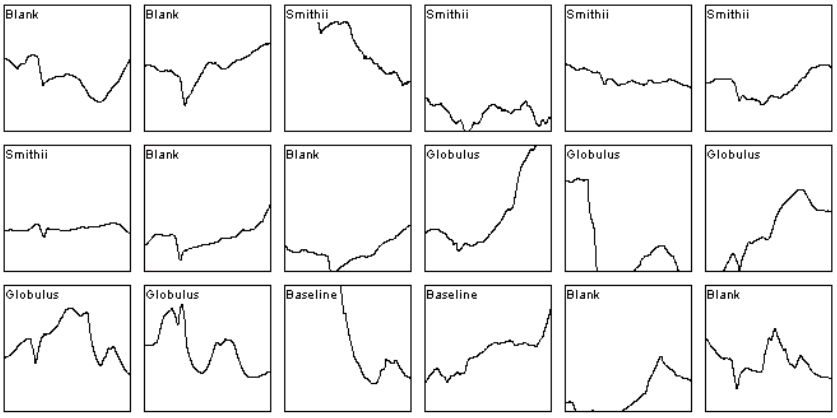

FIGURE 3.4: Responses observed with the electrode fork and electrolyte gel. The type of stimulus is indicated in the top left corner of each window. Globulus: *Eucalyptus globulus* leaf; Smithii: *Eucalyptus smithii* leaf.

3.6 Flow rates during EAG and EAD stimulation

It was realized that a response could be observed for a sample blank (section 3.5) which was not desirable in the EAG recordings. The flow rate through the stimulus delivery tube was subsequently investigated. Flow rates through the stimulus delivery tube

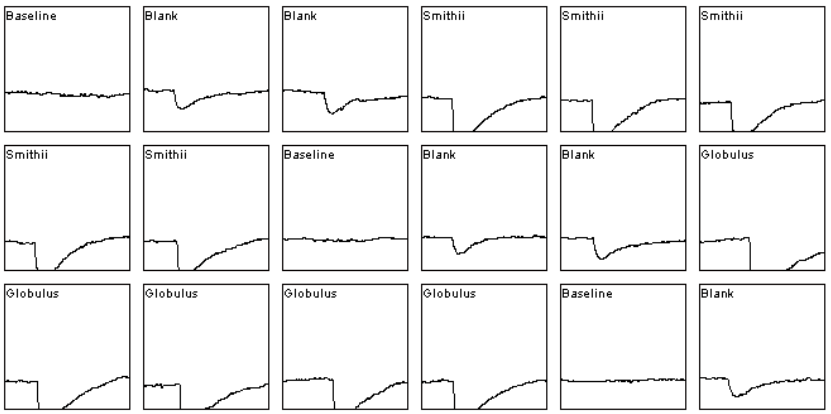

FIGURE 3.5: Responses observed when capillary micro electrodes were used.

and sample delivery tube had to be adjusted so that mechanical stimulation of the antennae could be minimized. The stimulus controller allowed for seventeen different flow settings. The flow setting was set to the lowest possible flow setting and measured with an electronic flow meter (Flow Tracker 2000, Agilent). The flow corresponded to 150 ml/min.

The flow rate through the stimulus delivery tube was adjusted to a setting of 2 and the stimulus delivery tube was modified to allow for a gradual increase in flow to a maximum of 30 ml/min (Sullivan, Private communication) (Figure 3.6). This modification decreased disturbance in the airflow reaching the antenna preparation and thus responses due to mechanical stimulation. The Experiment was repeated with the lower flow rates through the system and *E. scoparia* was tested. The results (Figure 3.7) showed responses due to mechanical stimulation was decreased because responses to the blank was considerably less.

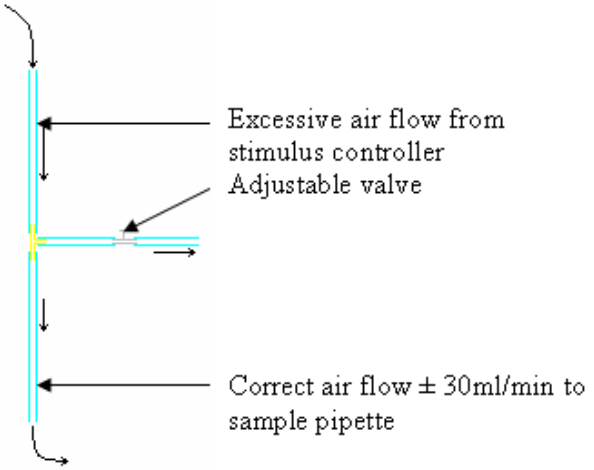

FIGURE 3.6: The modification that was needed in the stimulus delivery tube

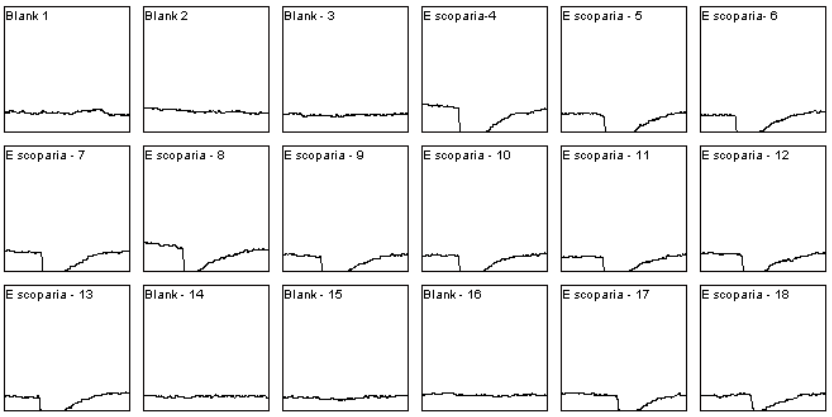

FIGURE 3.7: Responses that were observed for *Eucalyptus scoparia* leaf after a flow rate adjustment.

3.7 Antennal sensitivity during EAG recordings

In order to test the sensitivity of excised antennae from a female *G. scutellatus* insect over time, the antenna was sequentially exposed to 0.4 second puffs of either sample volatiles or sample blanks (Figure 3.8). Sample volatiles originated from a 1 cm^2 piece of *E. globulus* leaf. A one minute recovery period was allowed in between consecutive puffs. The experiment lasted for 38 minutes.

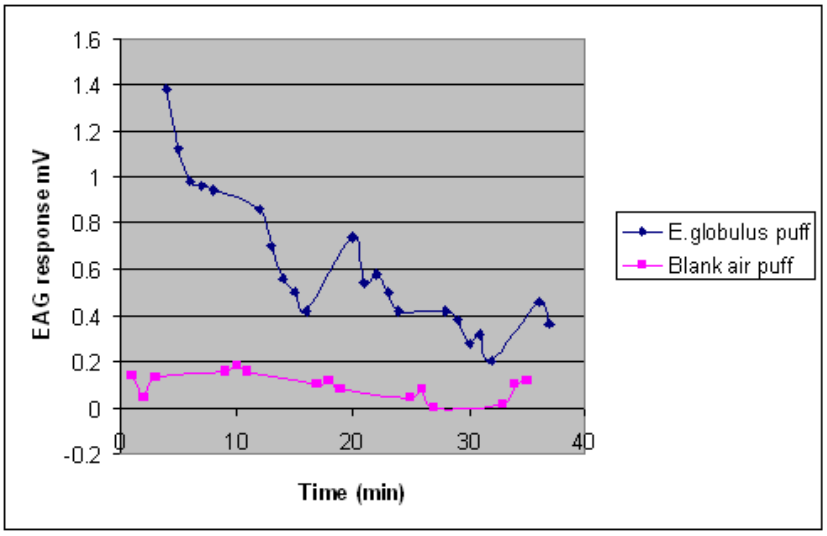

FIGURE 3.8: A decline in antennal sensitivity was observed during the antennal lifetime test. (pink:blank puff of air, blue:volatiles from a *Eucalyptus globulus* leaf

Larger responses to *E. globulus* volatiles were observed in comparison to blanks. Furthermore, a decline in antenna sensitivity was present during extended EAG recordings. Finaly, the antenna showed some recovery of responsiveness after blank puffs. These

data suggested that the use of live insects would be beneficial, especially during long EAG recording sessions.

3.8 Headspace sampling

The dynamic headspace sampling system was modeled on a system proposed by Tholl *et al.* (2006) and Raguso and Pellmyr (1998) (Figure 3.9). Care was taken to use materials like glass and poly-acetate that do not contribute to the overall volatile profile in the system. This system was used to obtain volatile samples from *Eucalyptus* leaves for subsequent GC-EAD analysis.

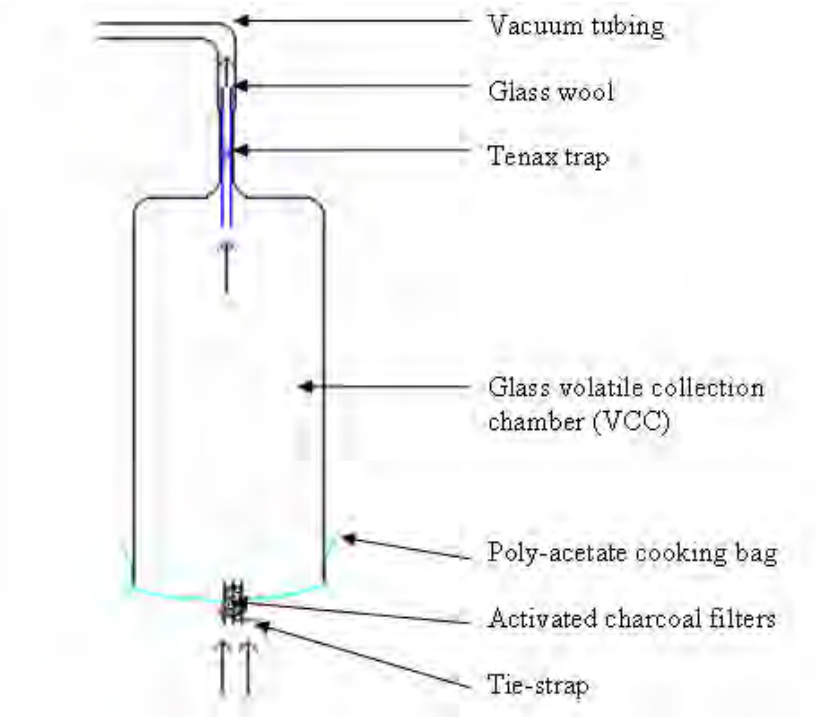

FIGURE 3.9: A schematic diagram of the dynamic headspace sampling apparatus

During the process air was filtered through activated charcoal filters before entering a volatile collection chamber. The air passed over the sample which was inserted in the chamber and through the Tenax® TA trap at the top of the sampling chamber. The flow rate through the system was measured at 512 ml/min . The entire sampling process lasted for one and a half hours with a total volume equal to 46 l. This system was cleaned after sampling by washing with sope and water and wiping the entire chamber with acetone. Samples were weighed (wet weight) after collection.

A system blank was taken to prove that volatiles were predominantly originating from the *Eucalyptus* samples. This blank was run on the GC-FID-EAD system and on the

GC-MS system. Peaks were observed in the system blank and retention indices were calculated for the 12 larger peaks that were observed on the GC-FID-EAD system (Table A 3 in appendix A). The system blank peak sizes were relatively small in comparison to the peak sizes of *Eucalyptus* volatiles, which indicates that small leaks or residual compounds were present during the sampling process (Figure 3.10).

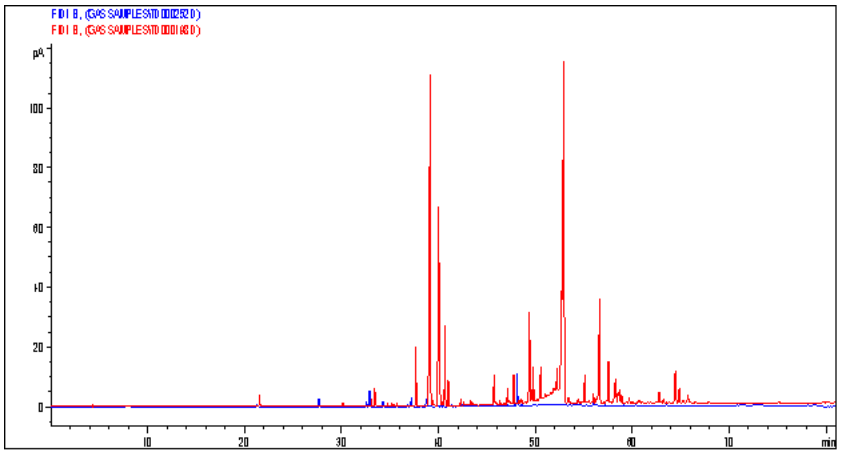

FIGURE 3.10: The System blank (Blue) overlain with a *E. globulus* sample (Red) on the GC-EAD system

3.9 Chromatography

3.9.1 Thermal desorption

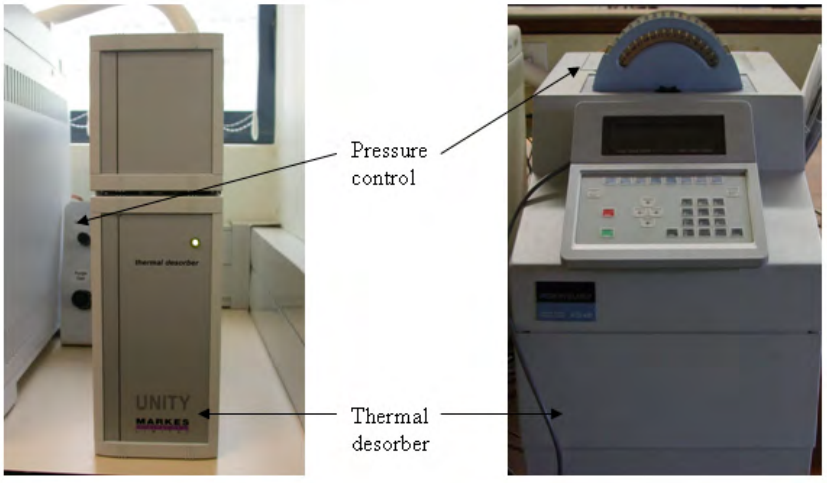

FIGURE 3.11: The two thermal desorption systems. Left: The Unity Markes thermal desorber used in conjunction with the GC-FID-EAD. Right: The Perkin Elmer thermal desorber system used in conjunction with the GC-MS system.

The thermal desorption systems of the GC-EAD (MKIUNITY, Markes, Chemetrix, Midrand, South Africa) and GC-MS (Perkin Elmer) both used a two stage injection technique whereby volatiles are desorbed from the sample tube onto a cold trap and then onto the column. The sample split performed during primary and secondary desorption depended on desorption and split flows used in each case. The Unity Markes system coupled to the GC-EAD allowed for recapture of desorbed samples. Recaptured samples could therefore be analyzed multiple times on the GC-EAD system but not on the GC-MS system.

The column head pressure could be adjusted manually in both systems and the Van Deemter plot of the C9 n-alkane was drawn for the GC-EAD system at an isothermal temperature of 130 °C (Figure 3.12). This was used to give an indication of what the optimal pressure would be for maximum resolution. The results indicated that the plate height of 400 μm was achieved at a pressure equal to 14.7 psi. This plate height was theoretically not the lowest value that could be attained for this system (250 μm). Lowering the column head pressure to achieve the optimum linear flow rate for N_2 carrier gas used in this system would mean that the GC-MS system (He as carrier gas, identical linear flow rate) would have a significantly larger plate height than that of the GC-EAD system. Such a difference would cause major differences in the total number of peaks resolved for the two systems (see Chapter 2: Figure 2.10). This difference is due to the fundamental differences which occur in the diffusion coefficients and subsequently Van Deemter plots for the two carrier gases. Nitrogen has a much larger C term than helium which is responsible for the sharp rise in the curve at higher flow rates. Higher flow rates (25 cm/sec) are not within the optimal flow rate range for nitrogen but are in the optimal flow rate range for helium. A compromise between these systems can be obtained by operating them close to the intercept between their Van Deemter plots (see Figure 2.10). At the time of installation it was thought that nitrogen would be a more ideal carrier gas for the GC-EAD system. Nitrogen has more or less the same density as the air in the laboratory which meant that it would mix with the filtered air flow which passes over the antenna more so than a lighter carrier gas such as helium or hydrogen. This meant that the GC-EAD system had to be operated at low carrier gas flow rate for better resolution.

The desorption process in both systems was achieved by purging the sample tube for one minute at ambient temperature (to remove oxygen) and subsequently heating the tube to 280 °C for 5 minutes. The cold trap was desorbed by heating to 300 °C for 3 minutes. The transfer lines between the thermal desorbers and their respective GC′s were kept at a maximum temperature of 190 °C. Desorption efficiency (sample carry-over) was tested on both systems. This was done to ensure that cross contamination among samples was

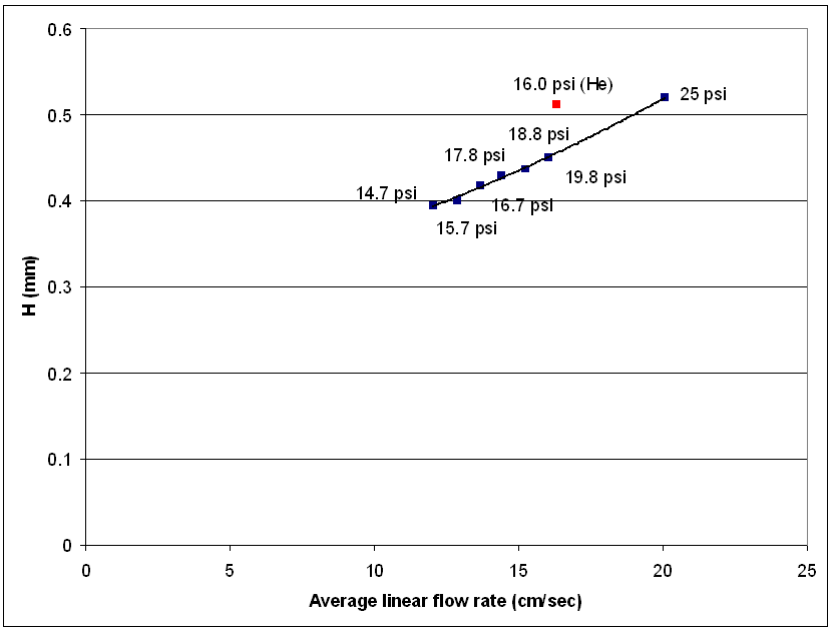

FIGURE 3.12: Van Deemter plot for the GC-EAD system for the n-alkane C9 and N_2 as carrier gas with a single plate height position for C9 on the GC-MS system run with He carrier gas. (Isothermal at a hundred and thirty degrees Celsius)

minimal (Figure 3.13 and 3.14) Complete desorption was obtained on both the GC-EAD and GC-MS systems.

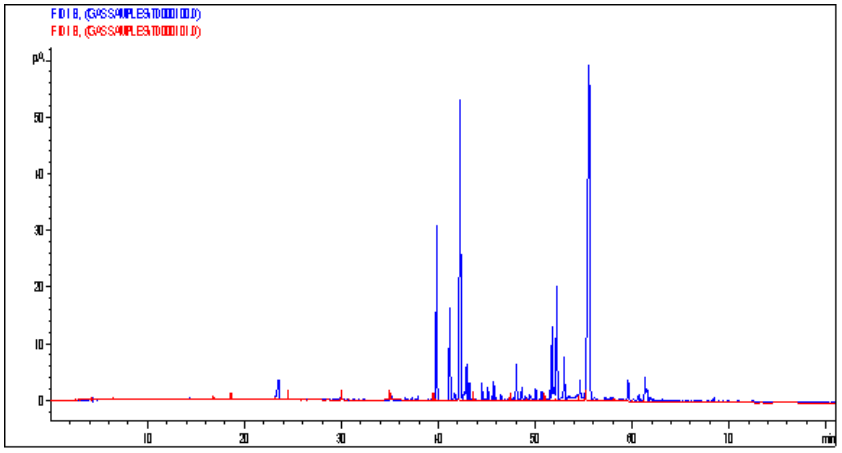

FIGURE 3.13: Here a *Eucalyptus globulus* sample (blue) was desorbed and n-alkanes were subsequently injected (red). This showed that the cold trap was clean after desorption on the GC-EAD system. Thus minimal sample carry over.

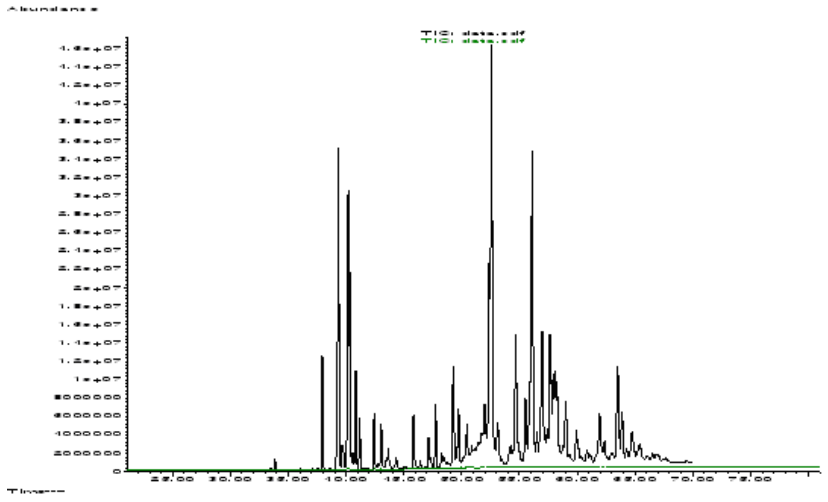

FIGURE 3.14: GC-MS desorption efficiency. The black chromatogram is the *Eucalyptus globulus* sample and the green line is the re-desorption of the same sample tube. Thus minimal sample carry over.

3.9.2 Gas chromatography electroantennography detector (GC-EAD)

3.9.2.1 System and method

The gas chromatography electroantennography (GC-EAD) system that was used consisted of a gas chromatograph (Agilent, 6890N, Chemetrix, Midrand, South Africa) with a standard FID and a EAD detector system (Syntech, Hilverstrum, The Netherlands). A 60 m DB624 column (94% dimethylpolysiloxane and 6% cyanopropylphenyl, J & W scientific) with an internal diameter of 250 μm and a film thickness of 1.4 μm was used to separate compounds and nitrogen was used as carrier gas. The thick film column was used to increase the column capacity. Often insects respond very strongly to very small peaks eluting next to large peaks this meant that a large column capacity was desired in order to see such small peaks without overloading larger peaks (see Figure 3.24). Overloaded larger peaks may hide these small peaks of interest (Barata *et al.*, 2000). A one to one split ratio at the end of the column was obtained by using a Y shaped glass splitter with equal lengths of deactivated silica tubing to each detector. This allowed for the simultaneous detection and synchronization of GC-FID and GC-EAD signals. The transfer line between the GC and EAD was kept at 260 °C which corresponded to the maximum oven temperature used during runs. The oven was held at 40 °C for 7 minutes and increased to 260 °C at a rate of 5 °C/min.

3.9.2.2 GC-FID Repeatability

A leak free chromatographic system is desirable because variation in retention times of non-overloaded peaks would then be extremely small. The degree of accuracy can be obtained by calculating the expected day to day variance in retention times. The repeatability of retention times of n-alkanes was therefore assessed on the GC-EAD system. These tests are reported for runs on different days for the two years of this study, 2008 and 2009 (Table 3.1 and 3.2).

TABLE 3.1: GC-FID-EAD repeatability in 2008 (14.8 psi, 143 ng). Retention times listed in minutes.

Day	10-Aug-08	8-Sep-08	5-Oct-08	30-Oct-08	3-Nov-08			
Run	197	180	156	208	211			
n-alkane						Mean	SD	CV
7	22.61	22.64	22.60	22.61	22.61	22.61	0.017	0.074
8	28.07	28.10	28.06	28.08	28.08	28.08	0.016	0.057
9	33.00	33.04	33.00	33.02	33.01	33.01	0.016	0.049
10	37.47	37.50	37.46	37.48	37.47	37.47	0.017	0.046
11	41.54	41.58	41.53	41.55	41.54	41.55	0.017	0.041
12	45.30	45.34	45.29	45.32	45.31	45.31	0.019	0.042
13	48.79	48.84	48.79	48.82	48.80	48.81	0.020	0.041
14	52.09	52.13	52.08	52.11	52.10	52.10	0.022	0.043
15	55.48	55.54	55.47	55.51	55.50	55.50	0.026	0.048

TABLE 3.2: GC-FID-EAD repeatability in 2009 (14.7 psi, 146 ng). Retention times listed in minutes.

Day	18-Apr-09	24-Apr-09	30-Apr-09	15-May-09	22-May-09			
Run	266	243	253	265	270			
n-alkane						Mean	SD	CV
7	22.47	22.45	22.41	22.45	22.45	22.45	0.021	0.095
8	27.93	27.91	27.87	27.91	27.91	27.91	0.022	0.078
9	32.87	32.85	32.81	32.84	32.84	32.84	0.022	0.066
10	37.33	37.32	37.27	37.31	37.31	37.31	0.023	0.061
11	41.41	41.39	41.35	41.39	41.39	41.39	0.023	0.055
12	45.18	45.16	45.11	45.15	45.15	45.15	0.023	0.052
13	48.68	48.66	48.61	48.66	48.66	48.65	0.024	0.050
14	51.97	51.95	51.90	51.94	51.94	51.94	0.025	0.049
15		55.34	55.28	55.33	55.33	55.32	0.027	0.048

The coefficient of variation (CV) of below 0.1% indicated that the repeatability of the GC-FID-EAD system was excellent. This repeatability gives an indication of how accurately the retention times of non-overloaded peaks could be determined.

3.9.2.3 Live insect EAD recordings compared to removed antennal recordings

Numerous pilot GC-EAD experiments were initially conducted on live insect preparations. The repeatability of these recordings was found to be unsatisfactory due to the many random responses that were superimposed on non-random responses (Figure 3.15) There were significantly less noise and random responses observed removed antenna preparations during the analysis of blank Tenax® sample traps. The large responses observed in the live coupling could be attributed to movement by the insect during the run.

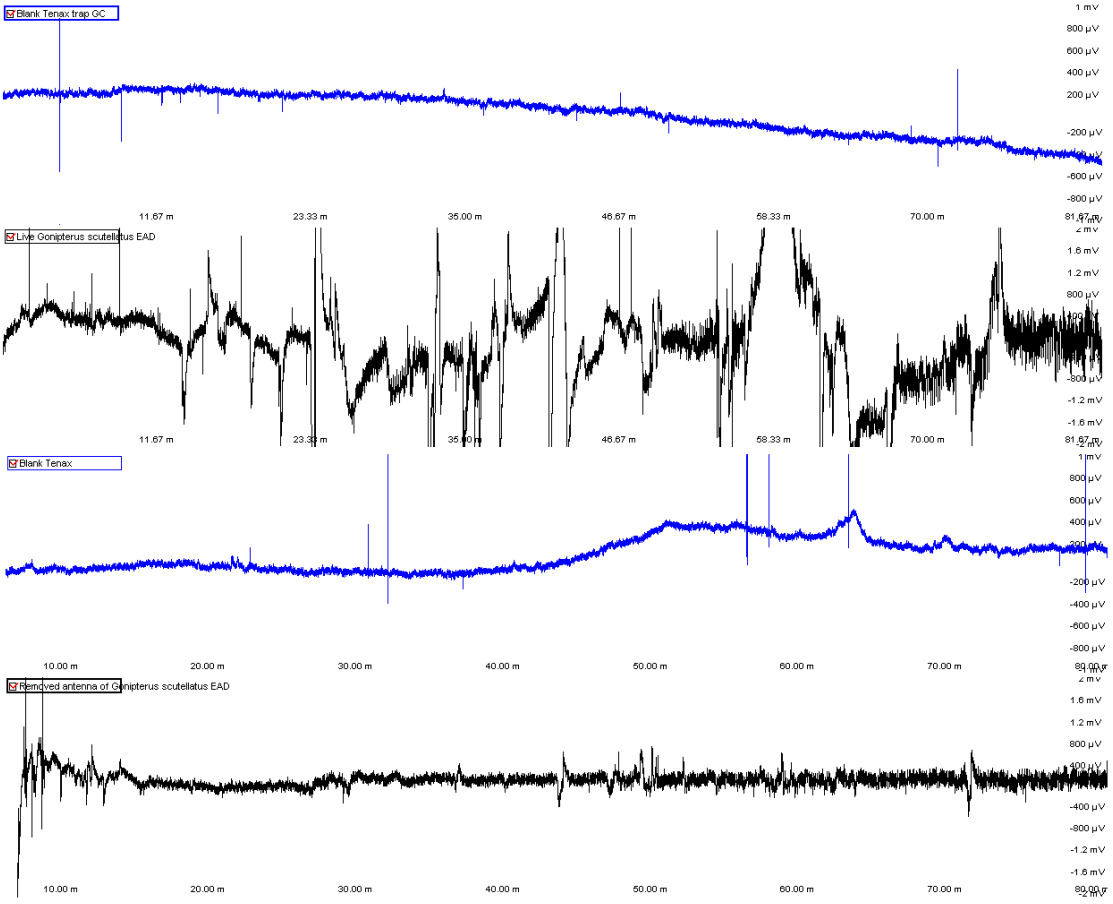

FIGURE 3.15: GC-EAD traces that were obtained for blank Tenax® traps. Top: Live insect coupled to the EAD detector. Bottom: Removed antennae coupled to the EAD detector. The EAD signals have not been electronically filtered for comparison purposes. Blue: FID, black: EAD

3.9.2.4 Antennal lifetime during GC-EAD

Removing the antennae from the insect for GC-EAD recordings meant that it would eventually die and show no sensitivity towards stimulatory compounds. Antennal lifetime information was therefore required. The lifetime of the female antenna was assessed during a continuous EAG experiment. In this experiment puffs of *Eucalyptus* leaf volatiles were used to indicate antennal activity. Two consecutive experiments were conducted on the two antenna of the same female beetle. The first antenna was stimulated every 10 minutes and the second every 5 minutes. This was done to give an indication of any differential antennal activity caused by a possible antennal poisoning due to *E. globulus* leaf volatiles.

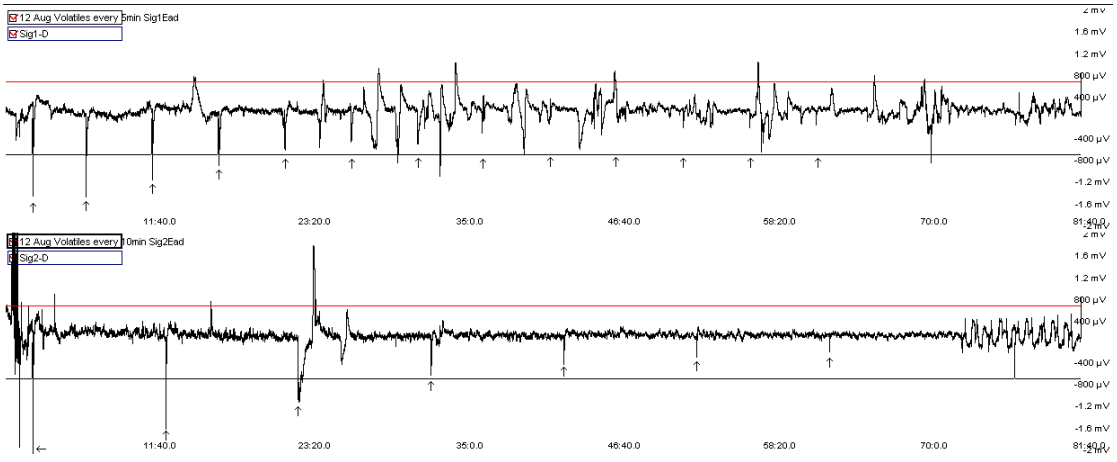

FIGURE 3.16: The antennal lifetime test. Arrows indicate when a puff of *Eucalyptus globulus* leaf volatiles was given during the experiment. The responses generally appear as lines at the x-axis time scale chosen.

The antenna that was stimulated every 10 min showed slightly larger responses, indicating that there may be some poisoning occurring (Figure 3.16). A gradual decline in antennal sensitivity could be observed in both runs (Figure 3.16 and 3.17). The decline was slightly different between the two antennae. These results indicated that the antennae could still detect volatiles for approximately 40 min after excision. GC-EAD runs were longer than 40 min and it was decided to couple the antenna during the run just before the first peaks were observed in the chromatogram. This allowed for maximal antennal sensitivity while compounds eluted.

3.9.2.5 System noise

The signal to noise ratio in EAD signals was very low and undesirable for removed antenna recordings. The origin of the noise could be ascribed to electromagnetic pulses

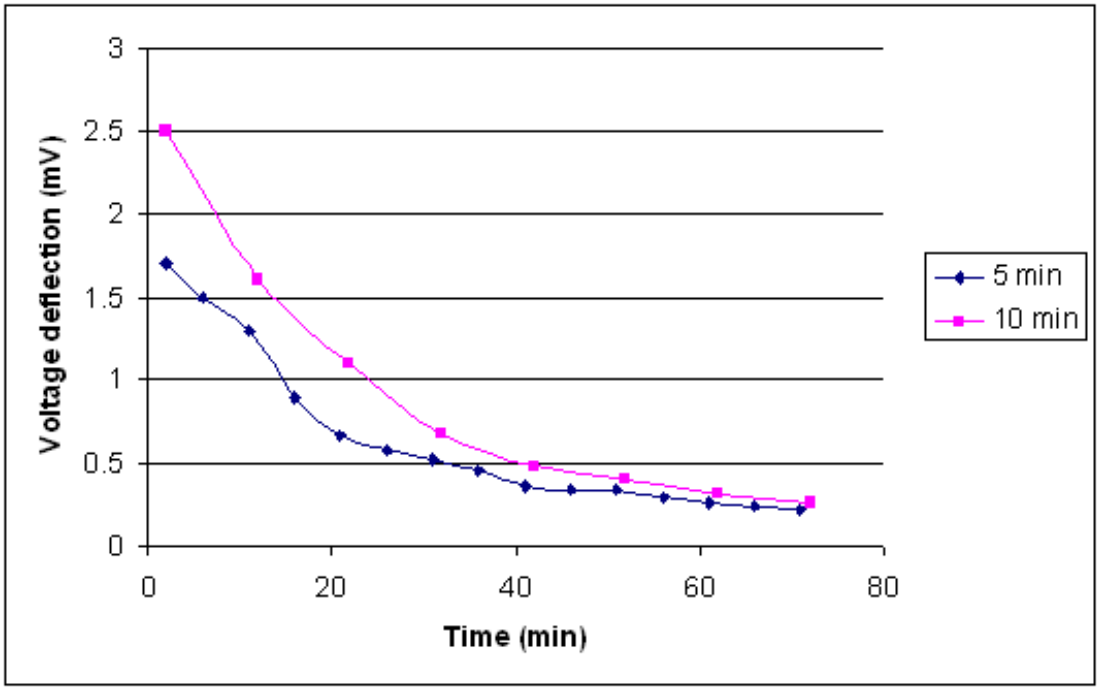

FIGURE 3.17: Graphic representation of the antennal lifetime test

originating from the EAD transfer line heater. Typically a spike in the EAD output was observed each time the transfer line heater switched on or off. A Faraday cage made from mesh wire placed over the entire preparation minimized this effect considerably (Figure 3.18 and 3.19). Foil was also wrapped over unshielded wires and a piece of foil was inserted between the transfer line heater and the EAD detector. Vibrations were minimized by placing the GC oven and thermal desorber on rubber stoppers and soft polyethylene foam. Electronically filtered EAD signals were subsequently recorded with a filter setting set to allow 0.05-3000 Hz to pass. The lower frequency corresponded to the width (approx. 20 seconds) of non-overloaded pure FID peaks. The resulting EAD signals were also digitally filtered after each run. The digital filter was set to allow only signals of 0 to 3 Hz to pass and resulted in substantially decreasing the background noise especially from the higher frequencies (Figure 3.20). The best results were obtained by using the Faraday cage and both the electronic and digital filters.

3.9.3 Gas chromatography-mass spectrometry

3.9.3.1 The GC-MS system

The GC-MS system consisted of a Thermo Quest trace GC 2000 series directly coupled (column end evacuated) to a Finnigan Polaris Ion Trap Detector (ITD). Helium was used as a carrier gas. The GC-MS needed to be synchronized with the GC-EAD system

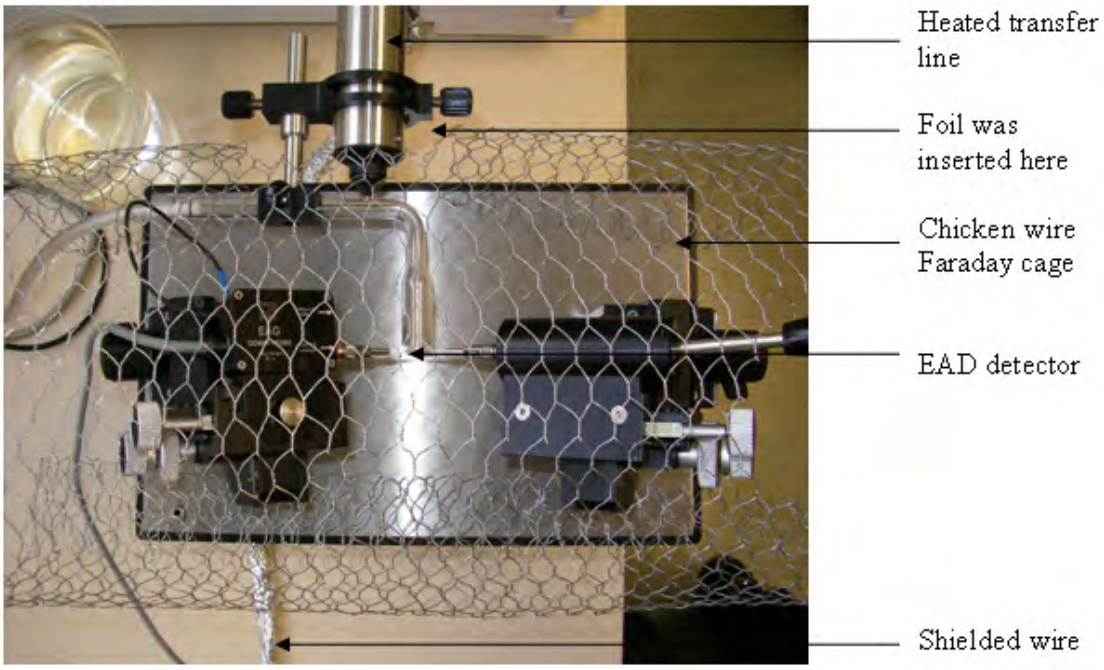

FIGURE 3.18: Top view of the EAD detector with a homemade Faraday cage.

and therefore an identical DB624 column was installed and operated with the same temperature program and linear flow rate. This was done to match retention times between the two systems. The transfer line between the GC and MS was kept at 260 °C. The Finnigan Polaris ITD was operated with an ion source temperature equal to 200 °C and 70 eV ionization energy. The mass scan range was either 45-350 or 50-285.

3.9.3.2 Retention time synchronization

Retention time synchronization between the GC-EAD and GC-MS systems was obtained by matching the retention time of the C12 n-alkane peak at 45.30 minutes. The column head pressure was changed and the retention time of C12 was recorded during consecutive temperature programmed runs. In order to obtain this match a column head pressure equal to between 9.0 and 9.1psi had to be used on the GC-MS system. The oven temperature was set at 40 °C for 7 minutes and increased to 260 °C at a rate of 5 °C/minute.

The linear flow rate of the two systems was subsequently measured by injecting butane during isothermal runs at 40 °C. As expected the flow rate corresponded to 12.5 cm/sec in both systems (Appendix A, Figure A 2 and A 3). A flow rate of 12.5 cm/s is close to the optimal flow rate for nitrogen in a 0.25 mm open tubular column but is below the optimal flow rate for helium in the same column (Heath and Duben, 1998). It

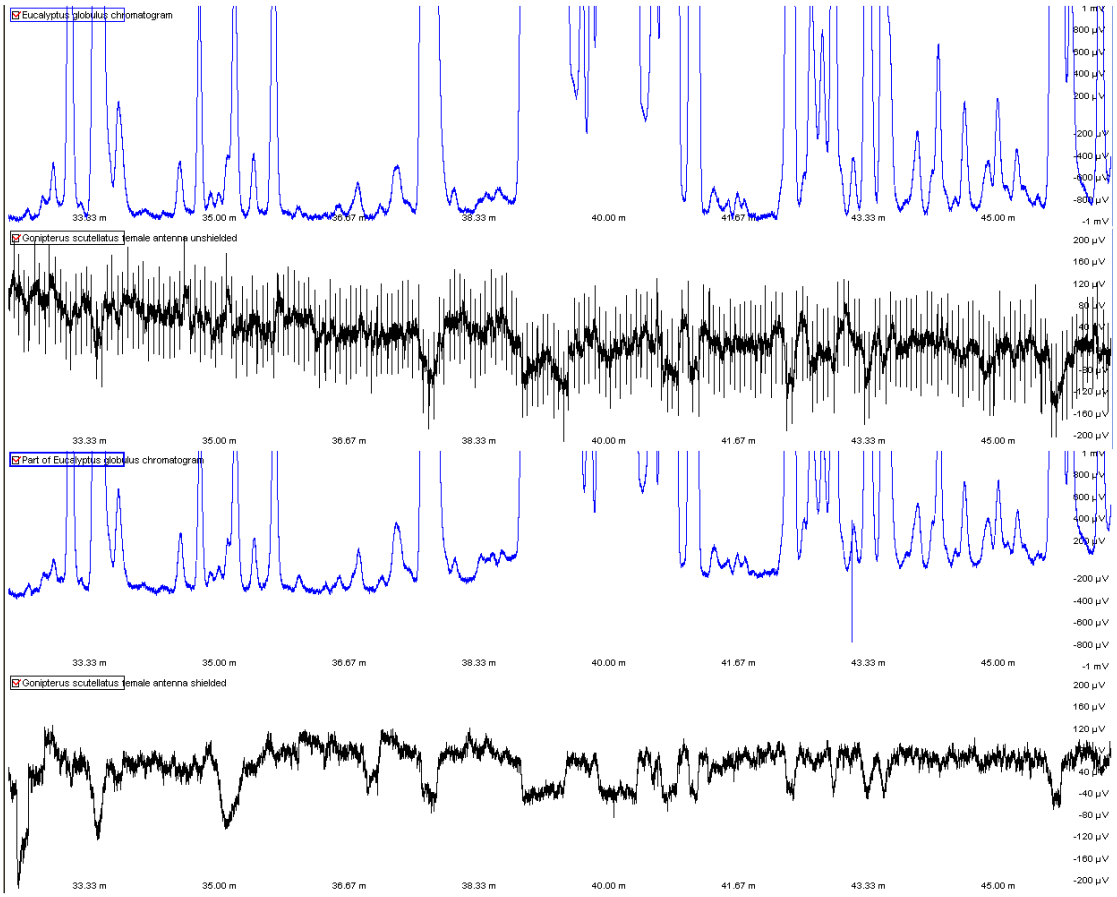

FIGURE 3.19: The effect of the Faraday cage on the GC-EAD signal (black). Top: Part of the *Eucalyptus globulus* chromatogram with an unshielded EAD signal from the removed antenna of *Gonipterus scutellatus*. Bottom: A repeat of the same chromatogram and EAD signal shielded with the Faraday cage. FID traces recorded simultaneously in blue.

was expected that the GC-MS system would have a lower resolution than the GC-EAD system (see also Van Deemter curves in section 2.3.3.1).

3.9.3.3 GC-MS repeatability

The retention time repeatability on the GC-MS system was assessed by calculating the coefficient of variation for n-alkane peaks on different days (Table 3.4.) The low coefficient of variation indicated acceptable repeatability.

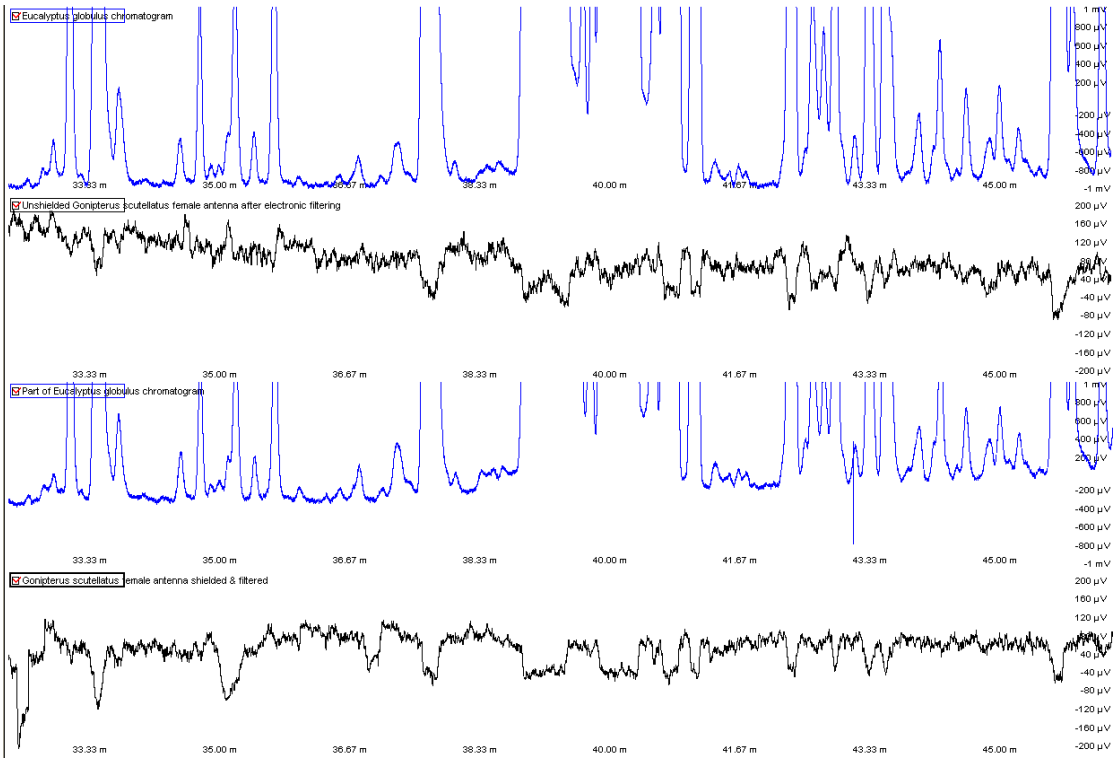

FIGURE 3.20: The effect of the digital filter on the GC-EAD signals. Top: Digitally filtered GC-EAD trace (black) that was not shielded with the Faraday cage. Bottom: Electronically filtered GC-EAD trace that was shielded with the Faraday cage. FID traces recorded simultaneously in blue.

3.10 Separation number comparison between GC-EAD and GC-MS

Temperature programmed runs (same linear flow rate, Figure A 2 and A 3) of n-alkanes on both systems allowed for a comparison of the separation number (SN) of both systems (see section 2.3.3.1). The GC-FID-EAD system had a higher SN value compared to the GC-MS (Table 3.5 and 3.6). A difference in resolution between the two systems was expected (see section 2.3.3.1 and 3.9.1). This difference could be ascribed to the differences in diffusion coefficients of the different carrier gases used in the two systems and the subsequent influence on the B and C terms of the Van Deemter equation. A decrease in SN value during the run was observed on both systems and was greater on the GC-MS system (see Table 3.5 and 3.6).

There was a linear decrease in SN value during the temperature programming of the run in both systems. The slope of the lines in these graphs (Figure 3.21) becomes zero as the oven reaches its maximum temperature and becomes isothermal at 260 °C. This data indicated that the separation efficiency was much better in the beginning of

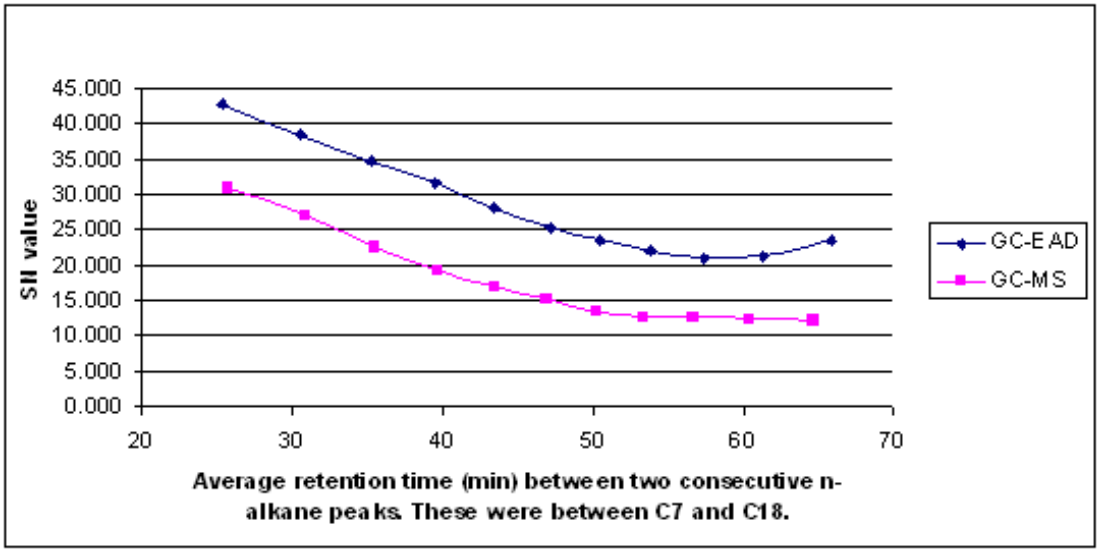

FIGURE 3.21: Graphic representation of the SN values for the GC-EAD (14.7 psi, 12.5 cm/sec at 40 °C isothermal) and GC-MS (9.9 psi, 12.5 cm/sec at 40 °C isothermal) systems. The runs become isothermal (260 °C) at 51 minutes.

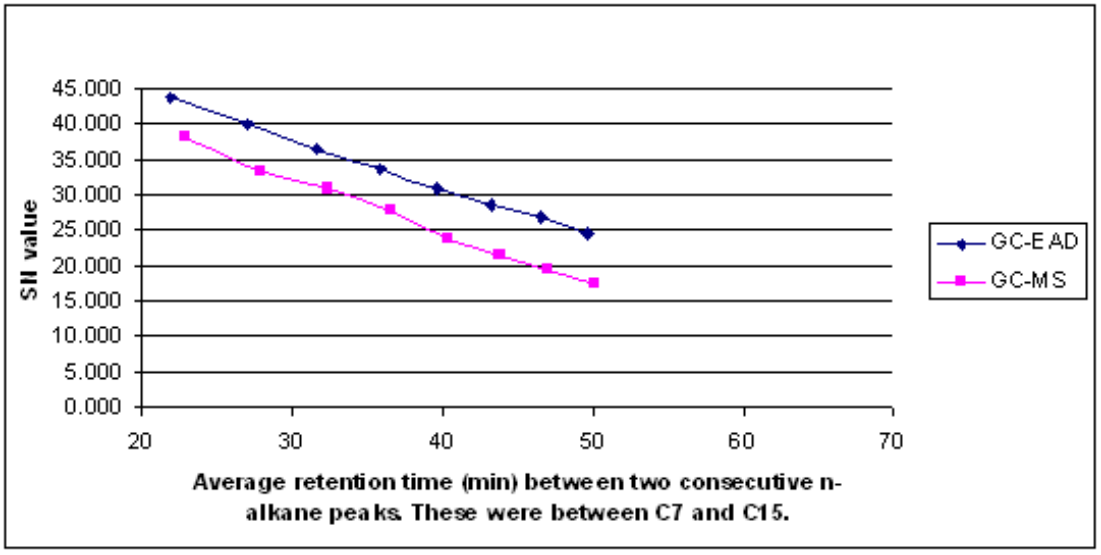

FIGURE 3.22: Graphic representation of the SN values for the GC-EAD and GC-MS systems. The runs become isothermal (260 °C) at 51 minutes. A column head pressure 20.1 psi was used on the GC-FID (16.23 cm/sec isothermal at 130 °C) and 16.0 psi (16.31 cm/sec isothermal at 130 °C) was used on the GC-MS system.

TABLE 3.3: n-alkane synchronization between GC-FID and GC-MS. The best matching was obtained for the C12 n-alkane.

n-alkane	GC-FID RT (min) (14.8 psi, N_2)	GC-MS RT (min) (9.0 psi, He)
7	22.64	23.11
8	28.10	28.50
9	33.04	33.33
10	37.50	37.69
11	41.58	41.65
12	45.34	45.30
13	48.84	48.67
14	52.13	51.83
15	55.54	55.05
16	59.20	58.49
17	63.36	62.41
18	68.28	67.10

TABLE 3.4: GC-MS repeatability at 9.0 psi

Day of Run	5-Nov-08 5Noval1	6-Nov-08 6Noval1	24-Jul-09 24JulMS2	27-Jul-09 27JulMS2	29-Jul-09 29JulMS			
n-alkane						Mean	SD	CV
7	23.05	23.11	23.08	23.06	23.10	23.08	0.027	0.118
8	28.44	28.50	28.45	28.43	28.48	28.46	0.030	0.104
9	33.28	33.33	33.28	33.26	33.31	33.29	0.029	0.086
10	37.63	37.69	37.64	37.62	37.67	37.65	0.029	0.076
11	41.60	41.65	41.61	41.58	41.63	41.61	0.028	0.067
12	45.24	45.30	45.26	45.23	45.29	45.26	0.030	0.066
13	48.61	48.67	48.65	48.62	48.67	48.64	0.029	0.059
14	51.77	51.83	51.82	51.79	51.85	51.81	0.032	0.062
15	54.98	55.05	55.04	55.02	55.08	55.03	0.037	0.067

the chromatograms for both the GC-EAD and GC-MS systems and that a decline in resolution occurs through the run as the temperature increases.

The decline in SN value might be explained by the increase in gas viscosity as the temperature increases. This increase effectively lowers the linear flow rate through the system and causes a detrimental shift on the Van Deemter plot for each compound (see Section 2.3.3.1). A rapid decrease in retention factor (k) for late eluting peaks as they move into the length of the column may also have a negative effect on the resolution as indicated by a smaller $\frac{k}{k+1}$ term in the resolution equation (see Section 2.3.3.1). This is due to the high temperature increase rate of 5 °C/minute for the long 60 m column. The temperature increase rate of the oven was kept constant to simplify the retention

TABLE 3.5: GC-FID system N_2 column head pressure 14.7 psi (148 ng, Run 180)

N-alkane	RT (min)	Start (min)	End (min)	ΔRT (min)	Width at base (min)	Width at half height (min)	W1+ W2	SN or TZ value
7	22.64	22.55	22.76	5.46	0.20	0.062	0.12460	42.9
8	28.10	28.02	28.22	4.94	0.20	0.063	0.12540	38.4
9	33.04	32.95	33.15	4.46	0.20	0.062	0.12520	34.6
10	37.50	37.41	37.62	4.08	0.21	0.063	0.12540	31.5
11	41.58	41.49	41.69	3.76	0.21	0.063	0.12970	28.0
12	45.34	45.25	45.46	3.50	0.22	0.067	0.13260	25.4
13	48.84	48.74	48.96	3.30	0.21	0.065	0.13400	23.6
14	52.13	52.03	52.26	3.40	0.22	0.069	0.14730	22.1
15	55.54	55.43	55.67	3.67	0.24	0.079	0.16760	20.9
16	59.20	59.08	59.35	4.16	0.27	0.089	0.18760	21.2
17	63.36	63.22	63.54	4.92	0.32	0.099	0.20010	23.6
18	68.28	68.11	68.49		0.38	0.101		

TABLE 3.6: GC-MS system He column head pressure 9.09 psi (148 ng, Run 5NOVAL1)

N-alkane	RT (min)	Start (min)	End (min)	ΔRT (min)	Width at base (min)	Width at half height (min)	W1+ W2	SN or TZ value
7	23.05	22.82	23.25	5.40	0.43	0.084	0.16900	30.9
8	28.44	28.21	28.67	4.84	0.46	0.085	0.17200	27.1
9	33.28	33.07	33.43	4.35	0.36	0.087	0.18500	22.5
10	37.63	37.42	37.91	3.97	0.49	0.098	0.19700	19.2
11	41.60	41.46	41.74	3.63	0.28	0.099	0.20200	17.0
12	45.23	45.11	45.39	3.38	0.28	0.103	0.21000	15.1
13	48.61	48.45	48.80	3.15	0.35	0.107	0.21800	13.5
14	51.76	51.59	51.93	3.21	0.34	0.111	0.23400	12.7
15	54.97	54.80	55.17	3.44	0.38	0.123	0.25400	12.5
16	58.41	58.16	58.64	3.91	0.49	0.131	0.29000	12.5
17	62.32	62.07	62.57	4.66	0.51	0.159	0.35600	12.1
18	66.97	66.72	67.29		0.57	0.197		

index calculation of peaks and for the analysis time to stay within the antennal lifetime of approximately 40 minutes.

A higher pressure and subsequent faster linear flow rate was used for all results of chapter 5. A column head pressure 20.1 psi was used on the GC-FID and 16.0 psi was used on the GC-MS system. This corresponded to a linear flow rate of 16.23 cm/sec on the GC-FID and 16.31 cm/sec on the GC-MS isothermally at 130 °C (also see Figure 3.12). This increase in column head pressure for both systems resulted in a more accurate match between these two systems (see Figure 3.22 as compared to 3.21).

3.11 Retention index calculation

Retention indices were used as an added comparison method between the GC-EAD and GC-MS systems. Retention indices for the temperature programmed runs were calculated by linear interpolation between neighbouring n-alkane peaks and sample peaks (Figure 3.23 and Formula 3.1).

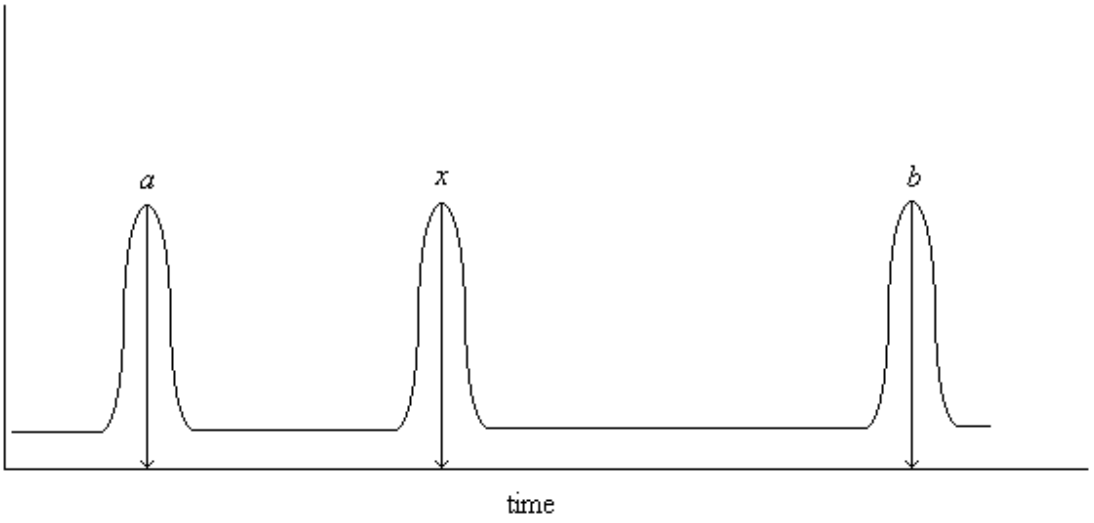

FIGURE 3.23: Simulated chromatogram of an unknown peak x between two consecutive hydrocarbon peaks a and b. Arrows indicate retention time at each individual peak apex.

$$KI_x = (KI_b - KI_a)\left(\frac{tr_x - tr_a}{tr_b - tr_a}\right) + KI_a \tag{3.1}$$

The linear interpolation method allowed for an accurate calculation of retention indices in the Excel spreadsheet program. It also allowed for calculating retention indices based on peak start time and end time. This is usefull for peaks that deviate from the expected Gaussian distribution such as peaks that were not separated properly or when column overload and activity was observed. In these cases the peak apex and end retention times may shift, but the peak start time stays relatively constant (Figure 3.24). Retention index comparisons based on peak start time was thus more accurate in these cases.

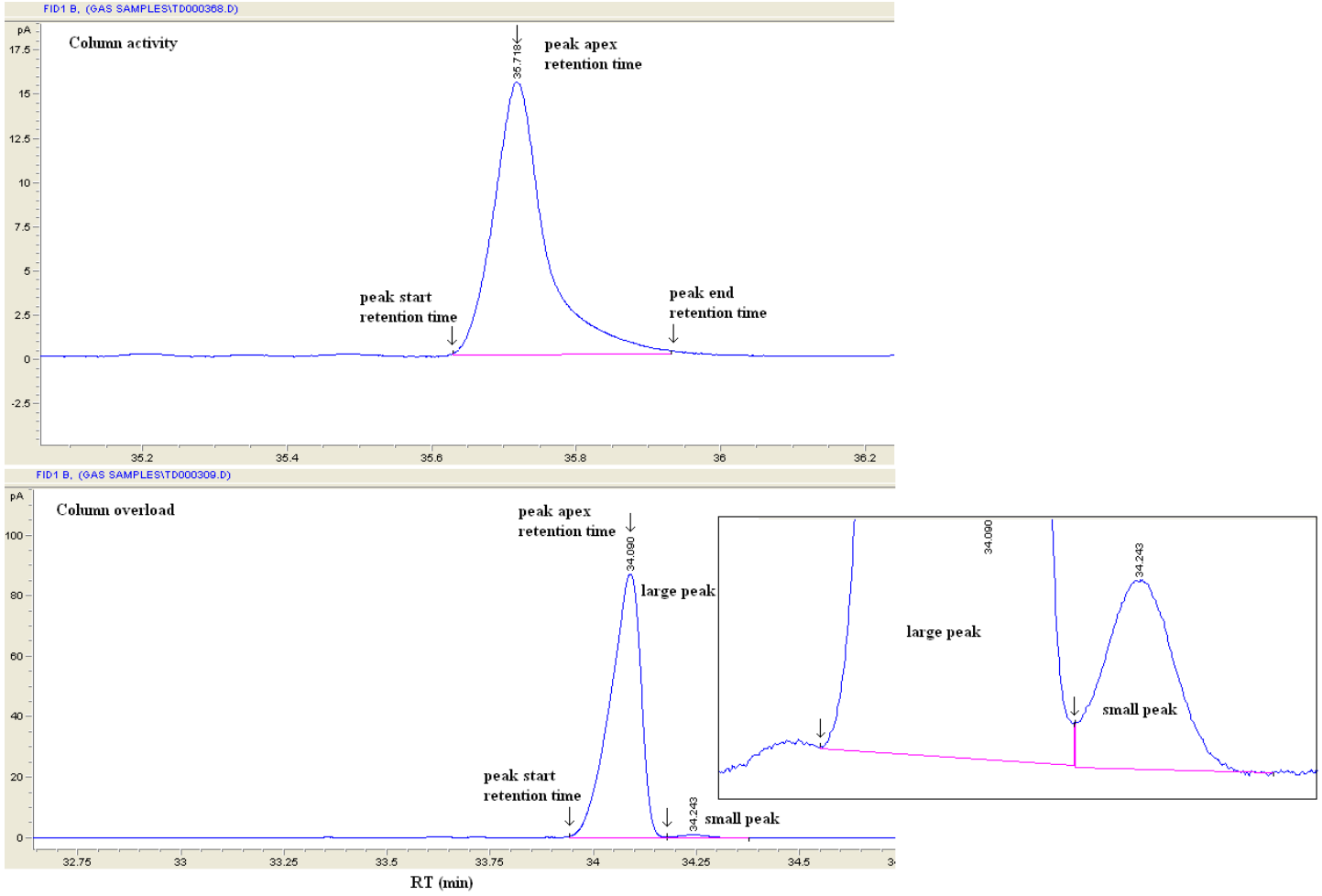

FIGURE 3.24: The effect column activity and overload has on retention times. (Notice that the peak apex times are not in the middle of the peak start and end times as expected for a Gaussian distribution. Right: A larger dynamic range makes smaller peaks visible when larger amounts are injected.

3.12 GC-EAD repeatability

Consistency in response pattern during GC-EAD was desired so that responses from different *Eucalyptus* samples could be compared. An assessment on the repeatability of the EAD detector was subsequently done by desorbing the same *E. globulus* sample multiple times and coupling antennae from different *G. scutellatus* female insects to the EAD detector. This experiment revealed the complexity of the crushed *E. globulus* leaf sample and the complexity in the EAD response pattern (Figure 3.25). Chromatographic overload was present for some of the larger peaks in these chromatograms and variance in EAD response pattern was present between runs for different insects. The EAD variation was evident both in the presence and intensity of certain peaks.

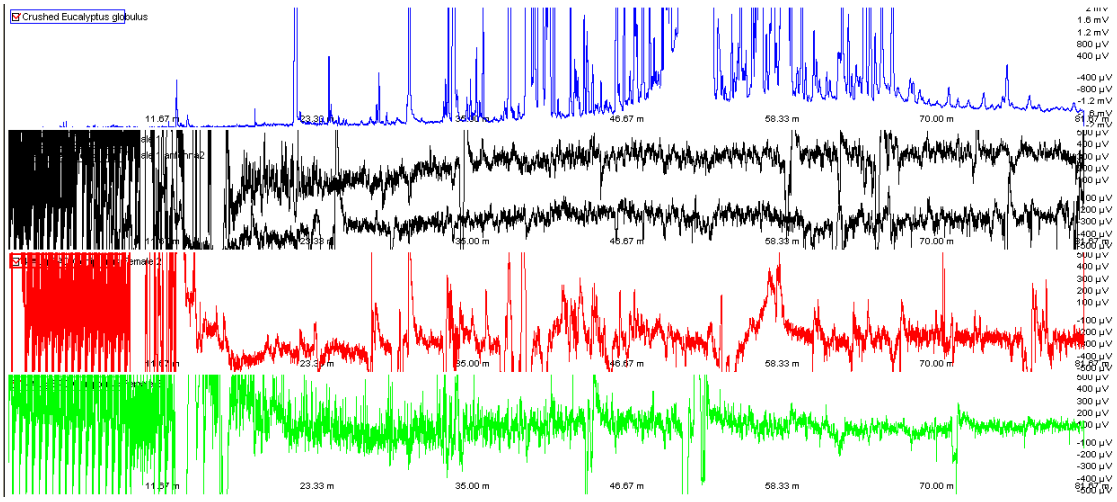

FIGURE 3.25: An illustration of the variation in EAD responses that were obtained for different insects. Top (Blue): Crushed *Eucalyptus globulus* leaf sample (FID). Middle (black): Two consecutive EAD responses of one female insect. Bottom (red and green) two EAD responses from two other female insects.

The variation was considerably less when comparing consecutive runs with the same insect′s two antennae. Repeatable responses could be obtained only when the two antennae from the same individual insect was compared for the same *Eucalyptus* sample. This variation in EAD response pattern made comparisons between different insects difficult. It was subsequently decided that a repeatable response would be defined as a response which is present in the EAD response patterns from both antennae of the same insect. This type of repeatable response was then confirmed if it was observed in at least one other insect′s EAD response pattern (although it could also be absent in some of these response patterns). The width (in time) of the response was also compared with the width (in time) of the chromatographic peak and responses which were narrower than their respective chromatographic peak was either eliminated or in the case of very wide chromatographic peaks it was concluded that the chromatographic

peak may be complex. This criterion was used to identify thirteen repeatable responses from the crushed *E. globulus* leaf volatile profile (Section 3.13). Most of the repeatable responses occurred in the 28-55 min region within the chromatograms. This specific region subsequently became the area of interest for these *E. globulus* volatile profiles.

3.13 EAD responses of *G. scutellatus* to crushed *E. globulus* leaf volatile profile

Three consecutive volatile samples were collected from the crushed juvenile leaves of one *E. globulus* plant. This was done in an attempt to keep at least the volatile profile constant. These samples were run repeatably on *G. scutellatus* female insects and allowed for the tentative GC-MS identification of peaks that could be said to be repeatable (as defined in section 3.12). Eight chromatograms and eight EAD traces were obtained for four female *G. scutellatus* insects (Appendix A Figure A4 to A16). EAD results allowed for the identification of thirteen repeatable responses (Figure A12 to A16). These *E. globulus* samples were subsequently run on the GC-MS system for tentative identification of the thirteen chromatographic peaks responsible for the EAD signals (Figure A17 to A19).

TABLE 3.7: 13 tentatively identified EAD active peaks from the crushed *E. globulus* leaf volatile profile and their retention indices (based on run 181 on GC-FID)

Response # on EAD	RT start Trx	RT Apex Trx	KI Start Kix	KI Apex Kix	tentative compound names
1,2	30.11	30.20	840.75	842.55	4,4-dimethyl-2-pentene
3	33.36	33.57	907.27	912.02	Z-3-hexen-1-ol
4	38.89	39.48	1034.06	1048.53	α-phelandrene,(Z)-3-hexenyl acetate, 3-carene,α-terpinene
5	39.88	40.47	1058.33	1072.80	limonene,cymene
6	40.71	40.86	1078.78	1082.54	1,8-cineol
7	41.18	41.31	1090.37	1093.42	γ-terpinene
8	42.37	42.45	1120.97	1123.29	α-terpinolene
9	43.32	43.41	1146.25	1148.82	2,4,6-Octatriene, 2,6-dimethyl-, (E,Z)-
10	45.72	45.95	1210.81	1217.46	2-phenylethanol
11	46.34	46.46	1228.73	1231.96	benzyl acetate
12	47.67	47.87	1266.56	1272.39	α-terpineol acetate
13	49.12	49.26	1308.56	1312.96	ethylphenylacetate

Similarities in chromatographic profile between the GC-EAD and GC-MS systems together with matching retention indices were used to identify the correct EAD active

peaks in the GC-MS total ion chromatograms. The difference in retention indices for the samples run on the GC-MS and GC-EAD systems were calculated (Table A4). Discrepancies between retention indices were sometimes more obvious. This was especially evident when chromatographic overload was observed on the GC-EAD system. The difference in resolution between the two systems caused some peaks to be slightly separated on the GC-FID whereas the same peaks were complex on the GC-MS. Detector overload was also observed for some of the larger peaks on the GC-MS system (Figure 3.26). In these cases the peak start time was used to calculate a more accurate retention index. The MS spectra of the compounds found in the thirteen peaks of the *E. globulus* sample were obtained and compared to the NIST library spectra and the spectra of the synthetic standard (when available) (Appendix A figure A20 to A33). The retention times, Kovats index and tentative identities of these peaks were summarized (Table 3.7). The retention time of each of the standard compounds was obtained by individually injecting them on the GC-EAD system (Figure A 40). A mixture of these standards was subsequently made in dichloromethane and their Kovats retention indices were calculated by co-injection with an n-alkane standard on both the GC-MS (Figure A36) and GC-EAD (Figure A37) systems. The difference in each retention index was again calculated (Table 3.8). The comparison of the retention index of the synthetic standards to the sample peaks resulted in the realization that 4,4-dimethyl-2-pentene was falsely identified by GC-MS. This compound had a retention index of 623 in stead of 842.

TABLE 3.8: The difference in Kovats retention indices (ΔKI) for the standards run on the GC-MS (44 ng) and GC-EAD (340 ng)

GC-MS run 29Jul		GC-FID run280			ΔKI	ΔKI
KI Start	KI Apex	KI Start	KI Apex	Compound name	Start	Apex
906.86	913.69	907.36	910.94	(Z)-3-hexen-1-ol & (E)-2-hexenal	0.50	-2.75
956.17	961.90	959.63	961.49	α-pinene	3.46	-0.42
976.81	985.07	982.50	984.41	camphene	5.69	-0.66
1011.01	1015.58	1012.68	1014.85	β-pinene	1.67	-0.73
1034.72	1039.57	1035.12	1037.16	(Z)-3-hexenyl acetate	0.40	-2.41
1039.97	1041.59	1039.14	1041.13	3-carene	-0.84	-0.46
1045.91	1049.34	1046.52	1048.47	α-terpinene	0.61	-0.87
1053.33	1060.93	1059.14	1060.63	d-limonene	5.81	-0.30
1063.36	1064.19	1062.17	1063.27	cymene	-1.19	-0.92
1068.54	1077.85	1074.71	1076.82	eucalyptol	6.17	-1.04
1082.88	1087.50	1084.91	1087.07	g-terpinene	2.04	-0.43
1213.79	1225.03	1210.19	1213.27	2-phenylethanol	-3.59	-11.76
1305.22	1316.38	1310.80	1313.76	ethylphenylacetate	5.58	-2.63

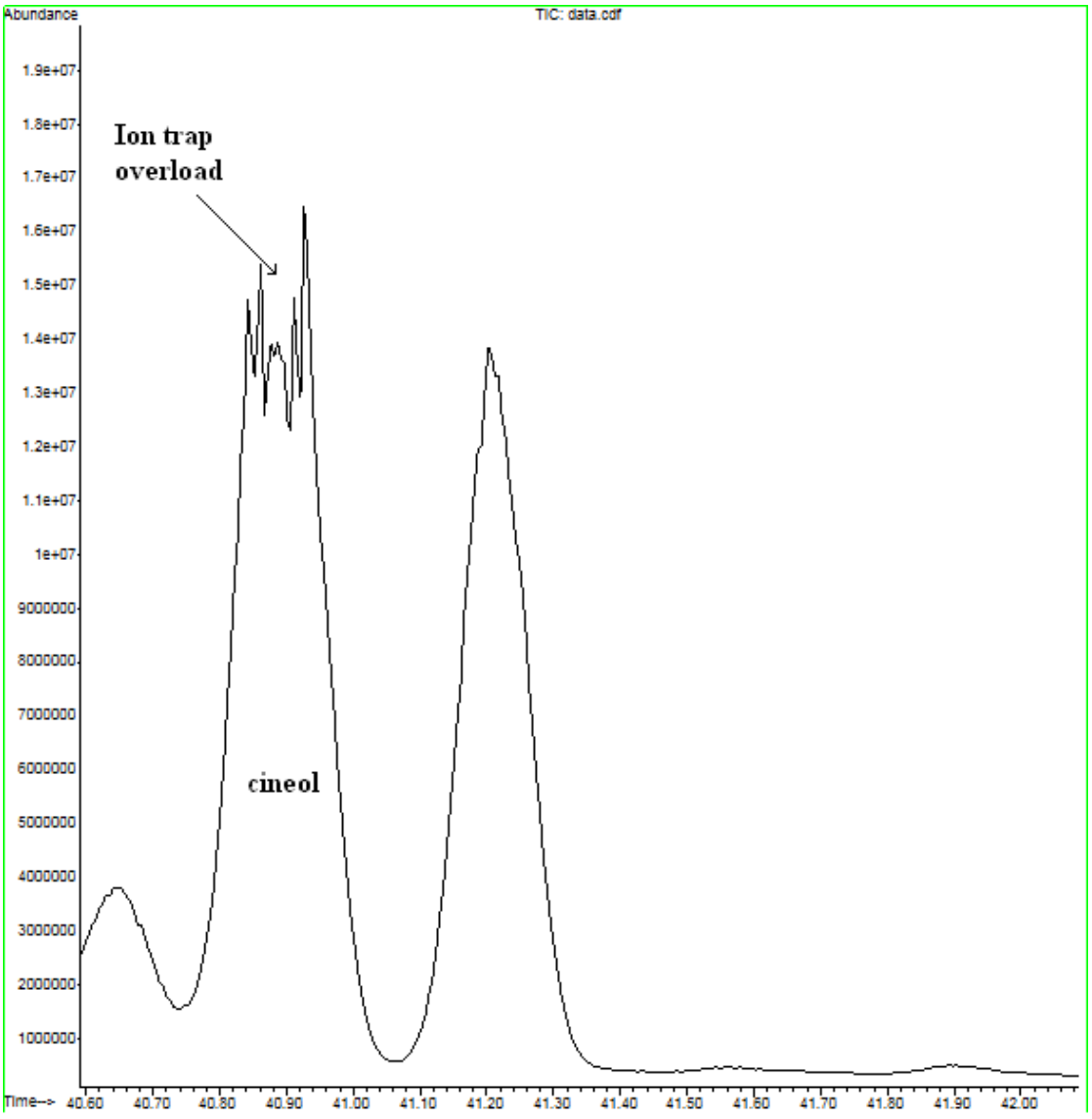

FIGURE 3.26: Part of a total ion chromatogram of volatiles isolated from *Eucalyptus globulus*. An illustration of what an overloaded peak looks like on the ion trap detector.

A number of ionization effects complicated the initial tentative identification of these compounds. These effects were usually observed when the ion trap detector was overloaded due to large peaks. Effects like protonation in the ion trap was especially evident for cineol which contained oxygen, but not for other terpines like γ-terpinene (Figure 3.27). Molecule ion interaction was observed for (Z)-3-hexenylacetate (Figure 3.28). This resulted in a molecular ion at m/z = 285 in stead of 142 ($285 = 142 \times 2 + 1$).

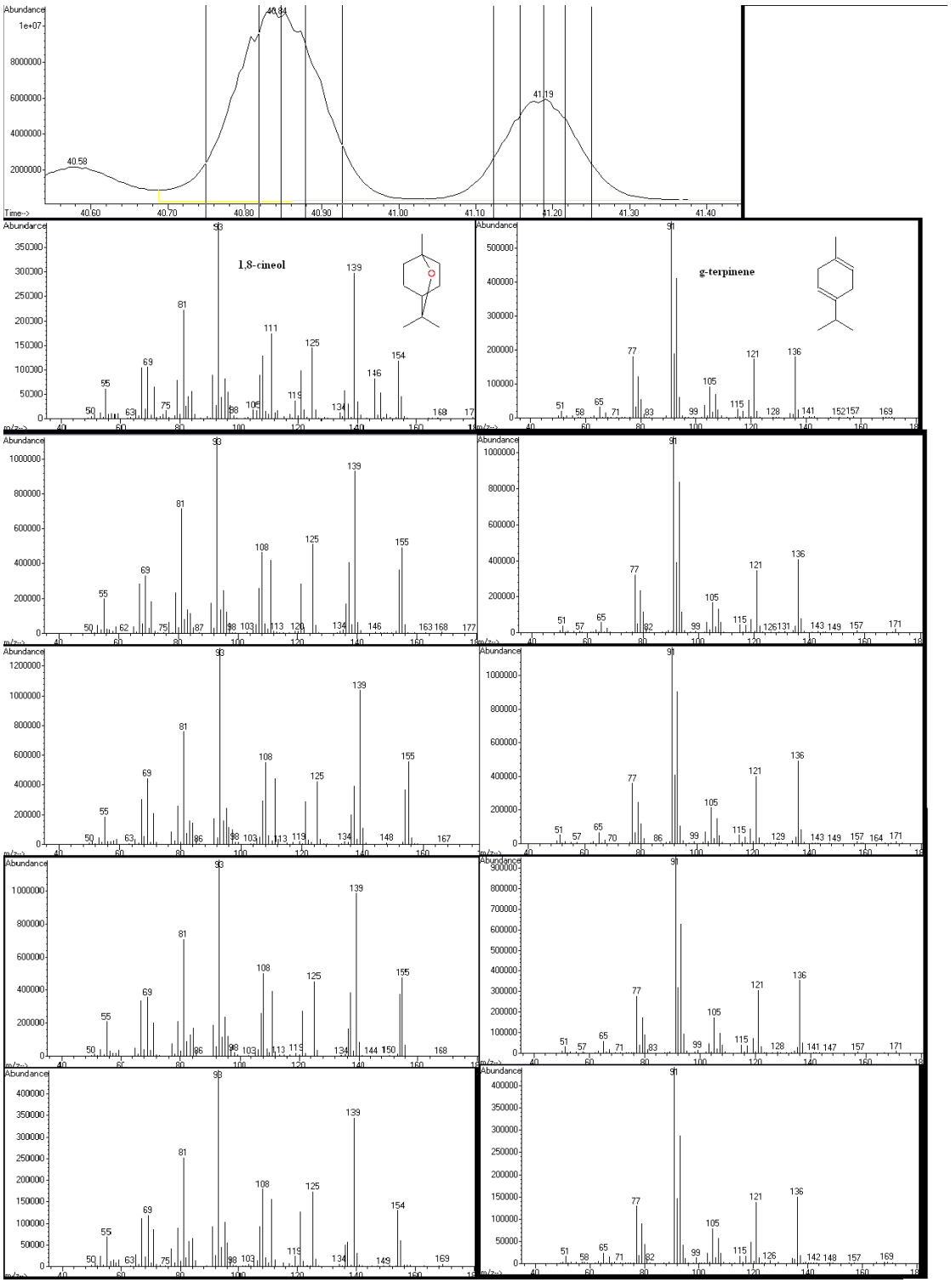

FIGURE 3.27: A comparison between the sequential mass spectra of two compounds: Cineol and γ-terpinene. Notice that protonation occurs only with cineol and to a greater extent at the peak apex

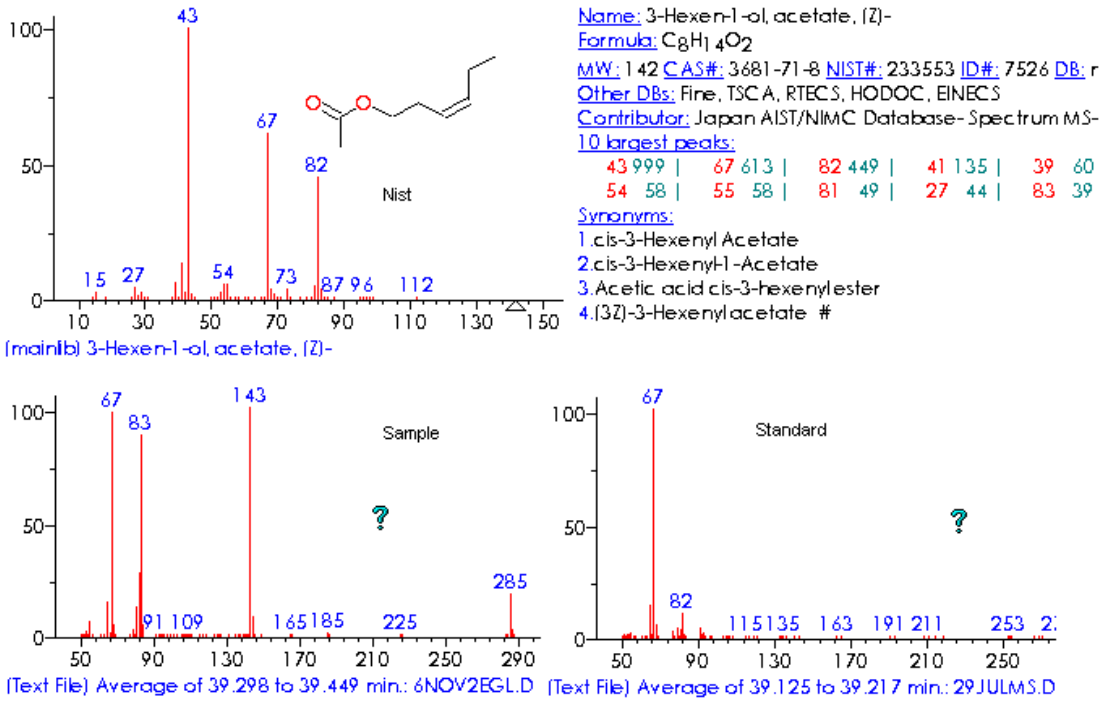

FIGURE 3.28: Tentative identification of (Z)-3-hexenyl acetate and confirmation with standard. Notice an adduct formation effect occurred in the ion trap due to overload and also protonaton of some ions of this compound.

3.14 Confirmation of EAD responses

Confirmation of the EAD response to the standards were obtained by using the exact same GC method that was used for the *E. globulus* volatile profile. From these results (Figure 3.29 and A 37,38,39) it became clear that the green leaf volatiles, (Z)-3-hexen-1-ol, (E)-2-hexenal, (Z)-3-hexenyl acetate, 2-phenylethanol and ethylphenylacetate give stronger responses than the terpenes: a-terpinene, d-limonene, cymene, eucalyptol and g-terpinene. α-Pinene, camphene, β-pinene appear not to give any significant response from *G. scutellatus* females.

3.15 Conclusions

Developing an EAG system for detecting differential antennal activity towards the total volatile profile for different *Eucalyptus* species was essential. Such a system can be used for detecting differences in the EAG response patterns for all the reported hosts of *G. scutellatus*. One host could potentially be singled out by using such an EAG system and GC-EAD analysis could be done on just this host. Developing such an EAG system was complicated mainly because antennae from insects such as *G. scutellatus* may have

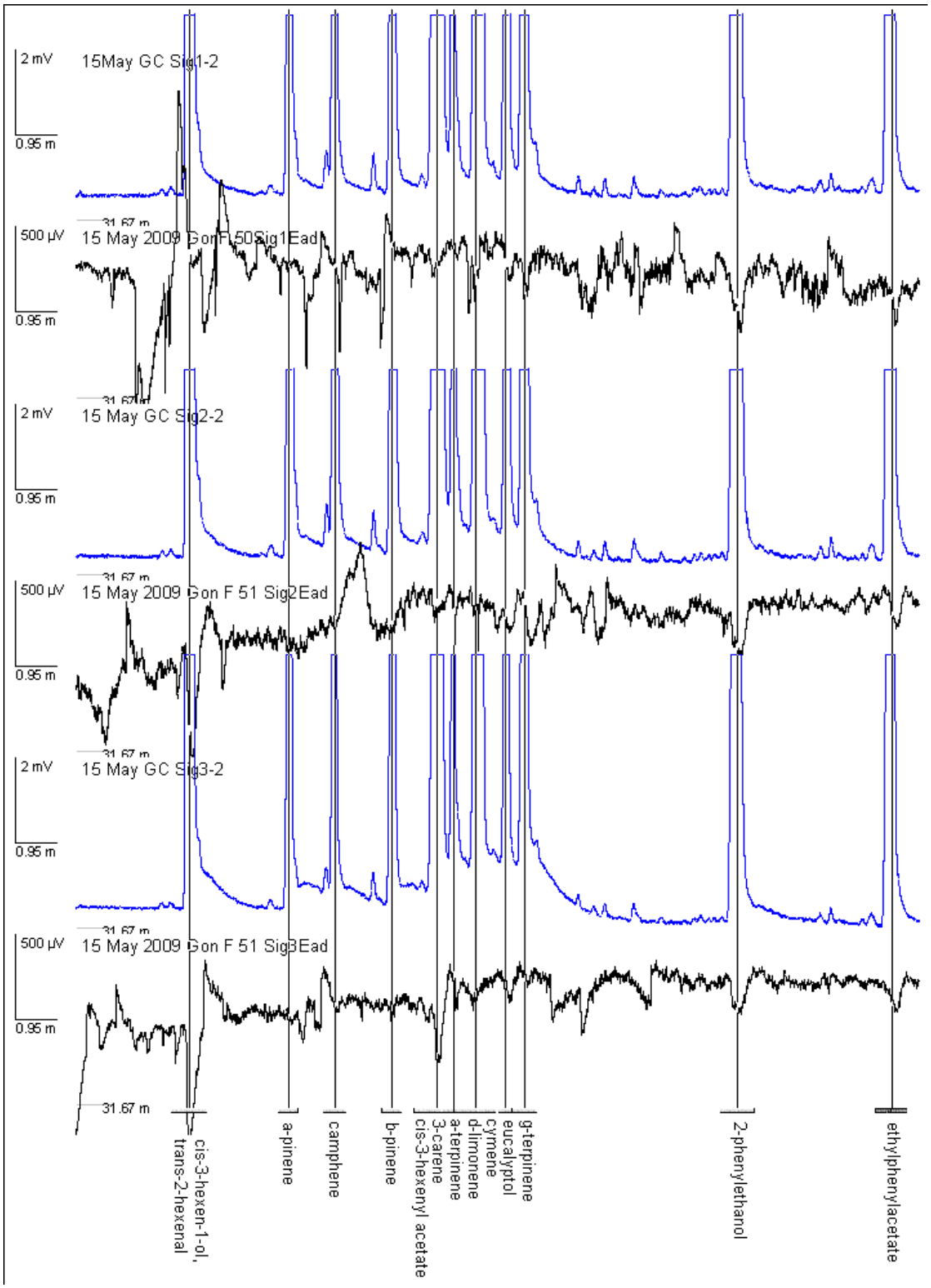

FIGURE 3.29: The GC-EAD responses which were observed for the standard compounds which were identified in the volatile profile of crushed *E. globulus* leaves. Blue: GC-FID trace, black: GC-EAD trace. The two bottom traces are from the same individual insect and the top is from another insect.

mechano-receptors which cause responses when high flow rates are used during EAG. This may cause added variation when multiple individuals are used during an EAG experiment.

A GC-EAD method was developed for this study. Random responses during GC-EAD were generally observed for live insects, especially when they moved. This degree of randomness necessitated the use of removed antennae. The removed antennae showed a relatively stable baseline that allowed for more reliable interpretation when multiple GC-EAD runs were compared. The removed antenna however had a limited lifetime during GC-EAD recordings and a balance between antennal lifetime, chromatographic runtime and resolution needed to be found.

A clear idea of a true EAD response was difficult to obtain and could only be seen after the electromagnetic interference originating from the EAD transfer line heater was removed with a Faraday cage and subsequent electronic and digital filtering. The experiments on the volatile profile from crushed *E. globulus* leaves showed that variation occurs even between two consecutive runs with the same volatile profile and the same insect's two antennae. This variation can be ascribed to variation in the process of removing the antennae and variation in the way electrical coupling of the antennae was achieved. The automated baseline correction mechanism in the IDAC 2 system also contributes to variation in antennal responses because antennal drift may be different for each coupling. Other effects may originate from degradation of unstable molecules during the thermal desorption process which may cause thermally labile compounds to break down. The greater inherent variation observed between female insects' EAD traces can be ascribed to effects such as differences in the age of the beetles and environmental and genetic differences between beetles. Nevertheless it was possible to show some degree of repeatability in EAD response patters for different insects.

These experiments led to the identification of 13 EAD active peaks in the GC-EAD chromatograms. Many of these peaks were observed to be overlapping on the GC-MS system which had a lower resolution than the GC-EAD system. Tentative identification of individual compounds were often difficult and extracted ion chromatograms resolved some of these problems, especially when ions were extracted that were not common between overlapping compounds. The larger peaks in the GC-EAD chromatograms were overloaded chromatographically which also caused uncertainty in the exact elution time and identity of peaks eliciting EAD responses. Re-sampling the volatiles and analyzing with a higher split ratio could solve such problems in future runs. Running both systems on the same carrier gas may also improve the resolution problem and the uncertainty in retention indices which were used to identify the compounds.

Many of the identified compounds (monoterpenes) appear to be common among different *Eucalyptus* species and some of the identified green leaf volatiles which elicited relatively large EAD responses are known to be common among many different plant species. This may suggest that *G. scutellatus* may differentiate among different trees based on the compound ratio differences rather than the absolute identity of compounds that are different among different trees. This analysis does not give any enantiomeric information on the different compounds which may also play a critical role in differentiating among different hosts for *G. scutellatus*.

Chapter 4

Electroantennographic responses of *Gonipterus scutellatus* to *Eucalyptus* species

4.1 Introduction

The *Eucalyptus* snout beetle (*Gonipterus scutellatus*) has been a significant pest in *Eucalyptus* plantations throughout South Africa for a long time (Tooke, 1953). *Gonipterus scutellatus* decreases timber quality and yield through its continual defoliation of young *Eucalyptus* shoots. In severe cases continual feeding may reduce the height of an adult *Eucalyptus* tree to a mere shrub (Tooke, 1953). Heavy infestations were particularly prominent before the introduction of *Anaphes nitens* as a bio-control agent in 1926 (Tooke, 1953). The introduction of *A. nitens* reduced the damage caused by *G. scutellatus* to acceptable levels in most areas; however, outbreaks are still known to occur in areas where the climate is not suitable for the *A. nitens* lifecycle (Tooke, 1953; Richardson and Meakins, 1984). It is also known that predator prey fluctuations may cause sporadic outbreaks of *G. scutellatus* (Rivera *et al.*, 1999). This insect is therefore still an economically significant pest, especially where bio-control fails in South Africa.

Gonipterus scutellatus appears to have a preference for certain *Eucalyptus* species (Tooke, 1953; Richardson and Meakins, 1984; Clarke *et al.*, 1998; Rivera and Carbone, 2000). In South Africa, *E. globulus*, *E. viminalis*, *E. scoparia* and *E. smithii* are reported as being among the most preferred hosts (Tooke, 1953; Richardson and Meakins, 1984). The planting of *E. globulus* as a plantation tree has been halted in South Africa due to heavy infestations by *G. scutellatus* in the past (Poynton, 1979). *Eucalyptus globulus*

is also known to be infested in California, North West Spain and South West Australia (Hanks *et al.*, 2000; Carbone and Fernández, 2004; Loch and Floyd, 2001).

A difference in the host preference of *G. scutellatus* in the native range in Tasmania, as opposed to countries where the beetle has been introduced, has been reported by Clarke *et al.* (1998). Their results indicated a higher number of eggs on *E. pulchella*, *E. tenuiramis* and *E. amygdalina* as compared to *E. viminalis* and *E. globulus*. These authors attribute this difference to various effects. Firstly, host preference was assessed through different methods in different countries, which obscures comparisons. Secondly, most of the reports originate from countries where *G. scutellatus* is regarded as a pest within monocultural plantations. Monocultures limit the diversity of *Eucalyptus* species to choose from and may not include preferred hosts. Thirdly, specific provenances of *Eucalyptus* species may show higher susceptibility in certain areas (Richardson and Meakins, 1984). Lastly, *G. scutellatus* may be a complex of sibling species each with different host preferences (Clarke *et al.*, 1998).

The exact preferred hosts of *G. scutellatus* therefore still remains unclear. Furthermore, nothing is known about the chemical ecology between *G. scutellatus* and its *Eucalyptus* hosts. If there is a host preference, as reported in the literature, then it is likely that chemical cues might be involved in female host choice. These chemical cues may ether be distinct or similar for each of the reported hosts. The aim of this study was, therefore, to confirm the electro-antennographic responses of *G. scutellatus* towards some of the reported hosts. Such results could could potentially clarify the host preference conundrum for *G. scutellatus*.

4.2 Methods

4.2.1 Insect samples

Gonipterus scutellatus samples were obtained from a *Eucalyptus* plantation in Pretoria, South Africa near Tom Jenkins drive (S25°44' 07,97 E28°14' 18.08). Insects were fed *E. smithii* and *E. globulus* foliage while being kept in wooden cages within a temperature controlled (20-25 °C) room. Female insects were used in EAG recordings because they are the ones that find suitable oviposition material. Females were identified based on the differences in the penultimate sternites as reported by Carbone and Rivera (1998).

4.2.2 *Eucalyptus* samples

Eleven different *Eucalyptus* species were sampled from two sites in Pretoria (Table 4.1). All of these species except *E. saligna* were reported as susceptable in South Africa by ether Tooke (1953) or Richardson and Meakins (1984). *E. grandis* is widely planted in South Africa (DWAF, 2007-2008) and is also known to be a host (Rivera and Carbone, 2000) and was therefore included in the analysis. *E. citriodora* was chosen as a non-host representative (Tooke, 1953) for comparison purposes. Six of the sampled *Eucalyptus* species were found on the same site as the insects. The remaining five *Eucalyptus* species were obtained from the Forestry and Agricultural Biotechnology Institute (FABI) nursery at the University of Pretoria. Cross contamination between individual samples were avoided by separating them, upon sampling, by placing each sample in a separately sealed poly-acetate cooking bag. These bags were stored in a fridge at 5 °C before analysis.

TABLE 4.1: *Eucalyptus* samples collected

Tree species	Location	Date	Time
E. globulus	Farm	25-Mar-09	14:32
E. smithii	Farm	25-Mar-09	14:34
E. grandis	Farm	25-Mar-09	14:36
E. camaldulensis	Farm	25-Mar-09	14:38
E. territicornis	Farm	25-Mar-09	14:42
E. saligna	Farm	25-Mar-09	14:40
E. viminalis	Tom Jenkins	25-Mar-09	14:00
E. rubusta	Tom Jenkins	25-Mar-09	14:12
E. puntata	Tom Jenkins	25-Mar-09	14:07
E. scoparia	Tom Jenkins	25-Mar-09	14:00
E. citriodora	Tom Jenkins	25-Mar-09	14:05

4.2.3 Electroantennography

All EAG recordings were made with an EAG detector system by Syntech (Hilversum, The Netherlands). Live female beetles were used in these recordings because a decline in antennal sensitivity was observed when antennae were removed. Beetles were secured with cotton wool inside a micropipette tip with only their head and antennae protruding from the end of the pipette tip. The pipette was secured to a mounting device and a stereo microscope and micromanipulator were used to position and connect glass capillary microelectrodes to the insect antennae and head. The recording electrode was connected to the tip of the club shaped antennae with the reference electrode connected to the eye on the opposite side of the insect′s head. Ag/AgCl electrodes were made from silver wire that were immersed in a 0.1 M KCl electrolyte solution with 2 % PVP

(polyvinyl pyrolidone) added to prevent dessication. The entire preparation was moved to within one centimeter from a glass stimulus delivery tube. Filtered and humidified air was blown onto the insect preparation through the stimulus delivery tube at a flow rate of 150 ml/min and sample volatiles were introduced into this air flow 170 mm upstream from the antennal preparation as 0.4 second puffs, at 30 ml/min at puff maximum.

Clean surgical blades were used to cut a 1 cm^2 piece of leaf from each of the eleven different *Eucalyptus* samples. Each piece was inserted into a different Pasteur pipette and an empty pipette was used as a sample blank. A blank recording was made before and after sets of five sample recordings for each of the *Eucalyptus* samples. Each of the samples was mechanically damaged by damaging the cuticle of the leaf with a clean piece of glass. Five additional recordings were subsequently made of the damaged plant material. A recovery period of one minute was allowed between each individual recording. The whole experiment was repeated three times with three different female insects. The order in which these recordings were made was kept constant for all three insects.

4.3 Results and Discussion

The absolute response intensity (mV) and surface area (s×mV) of each recording was measured. Eighteen outliers (1.5 IQR) were identified based on both deflection intensity and surface area and discarded from the analysis. All the remaining data were used in the analysis (Table 4.2).

Relative response intensity during EAG experiments is often measured by comparing the response to a known stimulant (see for example Barata *et al.* (2000)). The data in our experiments were not manipulated in this way, because a clear comparison between the blank recordings and the sample recordings was desired. This necessitated a test to determine the validity of pooling the recordings for the three different insects. This was done by pooling each individual insect′s data across the *Eucalyptus* species for both surface area and response intensity (excluding blank recordings). Student's t and Tukey-Kramer tests were done with an α level equal to 5 %. From this analysis (Figure 4.1) it could be shown that the two parameters contradicted each other. The surface area data showed that surface area values did not differ significantly between insects. The response intensity, which is a more sensitive parameter than the surface area, showed that intensity recordings from insect 1 differed from insect 3, but did not differ significantly form insect 2. The surface area data also appeared not to be normally distributed, with the majority of recordings producing low surface area values. This is in contrast with the deflection intensity recordings that was normally distributed in most cases. A possible

explanation for this variation is the difference in the electronic coupling achieved for each insect. Differences in sensitivity along the length of the antenna may exist as indicated for European corn borer *Ostrinia nubilalis* (Nagai, 1981).

TABLE 4.2: Frequency of EAG recordings for each *Eucalyptus* species

Level	Count	Prob
blank	66	0.17143
crushed *E. camaldulensis*	14	0.03636
crushed *E. citriodora*	15	0.03896
crushed *E. globulus*	16	0.04156
crushed *E. grandis*	15	0.03896
crushed *E. punctata*	14	0.03636
crushed *E. robusta*	15	0.03896
crushed *E. saligna*	15	0.03896
crushed *E. scoparia*	14	0.03636
crushed *E. smithii*	13	0.03377
crushed *E. territicornis*	15	0.03896
crushed *E. viminalis*	15	0.03896
E. camaldulensis	15	0.03896
E. citriodora	13	0.03377
E. globulus	14	0.03636
E. grandis	15	0.03896
E. punctata	15	0.03896
E. robusta	15	0.03896
E. saligna	15	0.03896
E. scoparia	13	0.03377
E. smithii	13	0.03377
E. territicornis	15	0.03896
E. viminalis	15	0.03896
Total	385	1.00000

All blanks and respective recordings for each *Eucalyptus* species were pooled and a global ANOVA analysis was done based on both the surface area and deflection intensity. We used Student's t and Tukey-Kramer tests with an α level equal to 5% in order to determine which *Eucalyptus* species had larger responses than the blank recordings (Figure 4.2). Some differences were observed between the surface area data and response intensity data. One overall difference was that the variance in response intensity data was larger than the variance in the response surface area data, especially when the blank responses were compared (Figure 4.2). The larger variance in the blanks observed for the response intensity data caused species such as *E. globulus*, *E. robusta* and *E. smithii* not to be significantly different from the blank values as compared to the surface area data (Figure 4.2). *Eucalyptus* species that were not significantly different from the blank values when comparing the surface area data included *E. camaldulensis*, *E. citriodora*, *E. grandis*, *E. punctata*, *E. saligna* and *E. scoparia*.

Similarities between the two data sets (response intensity vs. surface area) could also be seen (Figure 4.2). Both the surface area data and the response intensity data showed that *E. citriodora* always gave the lowest responses of all the *Eucalyptus* species tested. This could be observed for both the crushed and non-crushed leaves. These data corresponded to the fact that *E. citriodora* is not known as a host for *G. scutellatus* (Tooke, 1953). It was also observed that among the known hosts, *E. viminalis*, *E. globulus*, *E. smithii*, *E. robusta*, gave the largest responses (Tooke, 1953).

When looking at both variables for the non-crushed leaves it can be concluded that most of these responses did not differ significantly from the blank recordings except for *E. viminalis* and *E. territicornis* these results were consistent with reports from South Africa (Tooke, 1953; Richardson and Meakins, 1984) where *E. viminalis* is known as

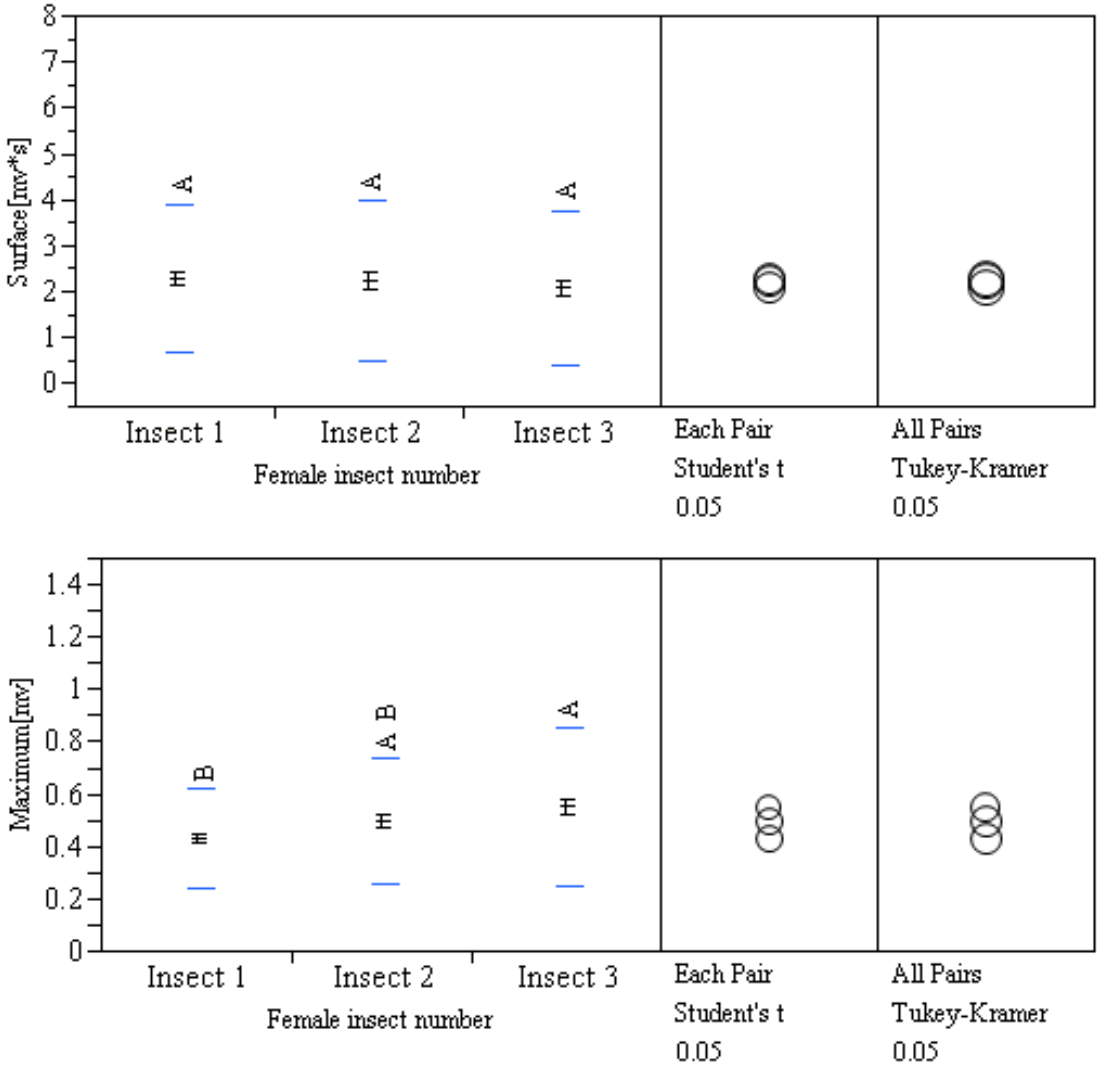

FIGURE 4.1: ANOVA analysis on EAG recordings between different female *G. scutellatus* insects excluding outliers and blank values. Top: Surface area. Bottom: Deflection intensity. Blue = standard deviation lines, Black = mean error bars.

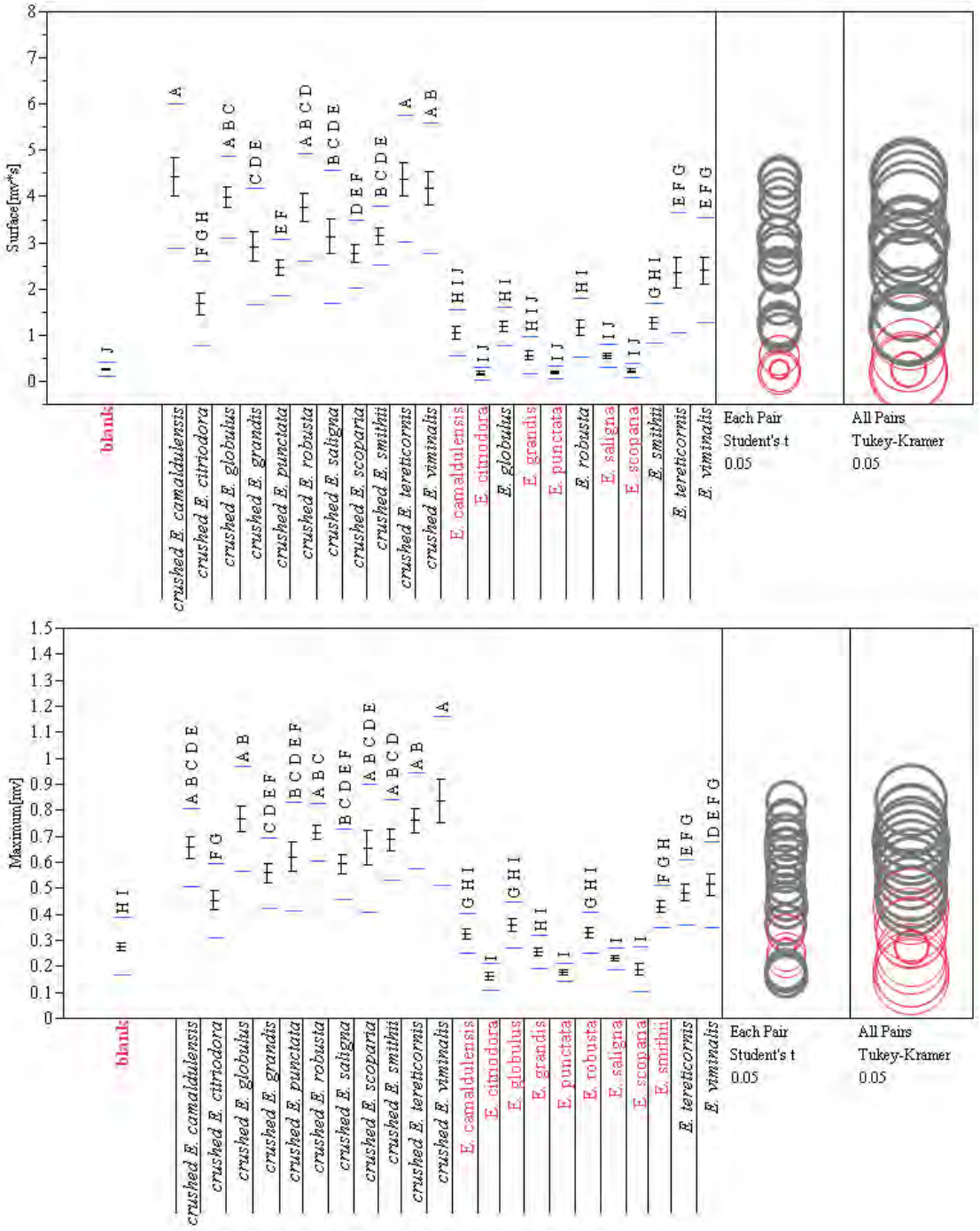

FIGURE 4.2: ANOVA analysis on EAG surface area (Top) and response intensity (Bottom) between the different *Eucalyptus* species. Names which are highlighted red (not in italics) are not significantly different from blank recordings α =5%. Blue = standard deviation lines, Black = mean error bars.

being one of the most preferred hosts. *E. territicornis* was noted by Tooke (1953) as a circumstantial host especially under the influence of unfavourable locality factors.

Crushing the leaves produced significant responses in all cases, and here the non-host, *E. citriodora* again gave the weakest responses. This may indicate that *G. scutellatus* females are able to detect green leaf volatiles that are common across the different *Eucalyptus* species but may not be as prevalent in *E. citriodora*. These compounds are products of enzymatic breakdown of membrane fatty acids (Gailliard and Matthew, 1976; Matsui *et al.*, 2000) and originate from damaged or stressed plants. Green leaf volatiles are known to be detected by phytophagous insects (Visser, 1986; Metcalf and Metcalf, 1992). Other factors that may cause the significance in response, is that as soon as the leaves are crushed there is a increase in concentration of volatiles that may stimulate the antenna. Differences in the composition of the wax layers on the leaves may also influence the differences in responses observed for the different species.

4.4 Conclusions

Differences in EAG responses could be observed for the different *Eucalyptus* species tested in this experiment. Larger responses were observed when the *Eucalyptus* leaves were crushed indicating that *G. scutellatus* may detect volatiles that originate from damaged foliage. These volatiles may include common isoprenoids and green leaf volatiles, which are known to stimulate antennae in various phytophagous insects (Visser, 1986; Metcalf and Metcalf, 1992). The differences that were observed between the different *Eucalyptus* species could have originated from volatiles unique to each species of tree. Synergistic effects between the different compounds and differences in ratios of these compounds may also have given rise to differences in EAG response patterns between the different *Eucalyptus* species. Overall *E. viminalis*, *E. globulus*, *E. territicornis* and *E. smithii* gave larger EAG responses when compared to the non-host *E. citriodora* and some of the other *Eucalyptus* species tested in this experiment.

Chapter 5

GC-EAD responses of *Gonipterus scutellatus* to *Eucalyptus globulus*, *E. viminalis* and *E. citriodora*

5.1 Abstract

The ability of *G. scutellatus* females to detect volatiles from crushed *Eucalyptus* foliage was confirmed in a prior electro-antennography study (Chapter 4). The aim of this study was to identify the volatiles responsible for the observed EAG responses. For this purpose a comparison between the volatile profiles of three different *Eucalyptus* species was made. Volatiles were collected from the crushed foliage of two known hosts: *E. globulus* and *E. viminalis*, and one non-host, *E. citriodora*, by adsorption on Tenax® traps for subsequent GC-EAD analysis. Crushed *E. globulus* leaves contained 2-phenyl ethanol, benzyl acetate, ethylphenylacetate, eucalyptol, α-pinene, (Z)-3 hexenyl acetate, (Z)-3-hexen-1-ol and (E)-2-hexenal that appeared to elicit EAD responses from female *G. scutellatus* antennae. The *E. viminalis* profile had very little 2-phenylethanol and virtually no benzyl acetate. The *E. citriodora* volatile profile contained very little (Z)-3-hexen-1-ol, (E)-2-hexenal, benzyl acetate, ethylphenylacetate and virtually no 2-phenylethanol. α-pinene, β-pinene and camphene did not elicit large EAD responses from *G. scutellatus* females, and β-pinene and camphene were below the detection limits for all three the *Eucalyptus* trees. The GC-EAD analysis suggest that compounds identified here may influence the host selection behaviour of *G. scutellatus* females.

5.2 Introduction

The *Eucalyptus* snout beetle *Gonipterus scutellatus* originates from South-east Australia and Tasmania (Tooke, 1953) and is a significant pest in *Eucalyptus* plantations, especially where it has been introduced. These beetles have been known to cause major damage in plantation forests in numerous countries (Mally, 1924; Clark, 1932; Williams *et al.*, 1951; Hanks *et al.*, 2000; Rivera and Carbone, 2000; Lanfranco and Dungey, 2001; Loch and Floyd, 2001), including South Africa (Tooke, 1953; Richardson and Meakins, 1984). This insect feeds on leaves of *Eucalyptus* trees during both larval and adult stages and causes economic losses by stunting the growth of susceptible trees (Tooke, 1953; Richardson and Meakins, 1984).

The literature is unclear as to which *Eucalyptus* species is the true preferred host for *G. scutellatus* (Clarke *et al.*, 1998). Different countries plant different *Eucalyptus* species in their plantations and use different techniques to score damage by *G. scutellatus*. For example, *E. globulus* has been reported as one of the most highly infested hosts for *G. scutellatus* in countries like South Africa (Mally, 1924; Tooke, 1953; Richardson and Meakins, 1984), New Zealand (Clark, 1932), USA (Hanks *et al.*, 2000), Spain (Rivera and Carbone, 2000), Chile (Lanfranco and Dungey, 2001) and Australia (Loch and Floyd, 2001). These observations appear to contradict its behaviour in Tasmania where a wider host range is available. Here *G. scutellatus* prefer *E. pulchella* above *E. globulus* trees (Clarke *et al.*, 1998).

The uncertainty about the preferred host of *G. scutellatus*, might be because the host selection behaviour of these beetles are linked to many factors. This includes the availability of preferred hosts (Clarke *et al.*, 1998), and environmental factors influencing the hosts and the beetles themselves. Temperature is known to influence the beetle's activity levels (Tooke, 1953) and volatile emission rates of *Eucalyptus* trees (Guenther, 1991; Nunes and Pio, 2001). Another source of confusion comes from the fact that many of these *Eucalyptus* trees carry two distinct types of foliage, which have different characteristics physically (Brooker and Kleinig, 1996) and chemically (Guenther, 1991; Nunes and Pio, 2001; Pio *et al.*, 2001). These differences may influence the host choice for *G. scutellatus* (Richardson and Meakins, 1984; Rivera *et al.*, 1999).

The ability of herbaceous insects to detect volatile organic compounds from plants is well known (Visser, 1986; Metcalf and Metcalf, 1992; Dicke, 2000). Tooke (1953) strongly argued that *G. scutellatus* host selection behaviour was linked to an olfactory mechanism. He attempted to link the host preference of *G. scutellatus* to the essential oil composition of different *Eucalyptus* species by correlating the host susceptibility in the field to the major components in the essential oils made from these trees. This experiment had

little success and Tooke (1953) could only show that the majority of preferred hosts had eucalyptol (cineol) in their essential oils.

This study aims to identify host volatiles that elicit GC-EAD responses for *G. scutellatus* females. Volatiles were sampled from the crushed leaves of two apparently susceptible hosts, *E. globulus* and *E. viminalis* and one non-host, *E. citriodora* (Tooke, 1953) by an adsorption process. GC-EAD active peaks were tentatively identified from the *E. globulus* volatile profile by GC-MS and confirmed with standards. The presence of the identified volatiles was subsequently investigated for these three hosts.

5.3 Methods

5.3.1 Insect samples

Gonipterus scutellatus samples were obtained from a Sappi *Eucalyptus* plantation in South Africa (GPS coordinates: S28°32.758' E032°10.736' 36 m). Insects were fed *E. smithii* foliage while being kept in wooden cages in a temperature controlled (20-25 °C) room. Female insects were used in GC-EAD recordings and were identified based on the differences in their penultimate sternites (Carbone and Rivera, 1998).

5.3.2 *Eucalyptus* samples

Volatiles from the crushed juvenile foliage of three different *Eucalyptus* species were sampled by adsorption onto standardized Tenax® TA (200 μg) traps (MKIUNITY, Markes, Chemetrix, Midrand, South Africa). The sampling material was obtained from three trees on two sites in Pretoria. *Eucalyptus citriodora* and *E. viminalis* were obtained from a *Eucalyptus* plantation near Tom Jenkins drive (S25°44' 07,97 E28°14' 18.08) and *E. globulus* was obtained from the Forestry and Agricultural Biotechnology Institute (FABI) nursery at the University of Pretoria. Cross contamination between individual samples were avoided by separating them, upon sampling, by placing each sample in a separately sealed poly-acetate cooking bag. The leaves of each *Eucalyptus* species was cut into pieces of approximately 5 cm^2. The crushed leaves were sampled for 30 minutes at a flow rate of 512 ml/minute in duplicate for each *Eucalyptus* species and a sample blank was taken. The dry weight of the sampled leaves was measured afterwards (Table 5.1).

5.3.3 GC-EAD

All GC-EAG recordings were made with an EAD detector system by Syntech (Hilversum, The Netherlands) coupled to an Agilent 6890N gas chromatography system (Chemetrix, Midrand, South Africa). EAD signals were recorded at a sampling rate of 100 samples/s. A 10× external amplification was used and the low cutoff filter was set to 0.05 Hz. High frequency noise was digitally removed after the recording was made by adjusting the low pass filter after the run to allow only a window of 0.05 Hz to 3 Hz to pass. These settings were used for all thermally desorbed samples.

Samples were injected onto a 60 m DB 624 column (J & W scientific) with a thermal desorption system (MKIUNITY, Markes, Chemetrix, Midrand, South Africa) at a 17:1 split ratio. The transfer line between the thermal desorption system and GC was kept at 190 °C. Nitrogen was used as carrier gas and constant column head pressure of 20.1 psi was used during separation. The GC oven was kept at 40 °C for 7 minutes and increased at 5 °C per minute to a maximum of 260 °C.

Antennae were removed from live female *G. scutellatus* beetles by cutting at the base of the antenna with a surgical blade. A stereo microscope and micromanipulator were used to position and connect glass capillary microelectrodes to the insect antenna. The recording electrode was connected to the tip of the club shaped antennae with the reference electrode connected to the base of the removed antenna. Ag/AgCl electrodes were made from silver wire immersed in a 0.1 M KCl electrolyte solution with polyvinyl pyrolidone (2 %) added to prevent antennal dessication. The preparation was moved to within 0.5 cm from a glass stimulus delivery tube. Filtered and humidified air was blown onto the antennal preparation through a stimulus delivery tube at a flow rate of 150 ml/minute and the GC effluent was introduced into the air steam 90 mm upstream from the preparation. The transfer line between the GC and EAD detector was kept at a maximum temperature of 260 °C. Six GC-EAD recordings were performed for each *Eucalyptus* species in order to identify repeatable responses (Figure A 12 to A 16 and B 11, B 19 and B 26).

GC-EAD responses to the identified standard compounds were also confirmed on the GC-EAD system by liquid injection of a mixture made in dichloromethane (Figure 5.5 and B

TABLE 5.1: *Eucalyptus* samples and their dry weight.

Eucalyptus species	Dry weight (g)	samples
E. citriodora	6.14	2
E. globulus	9.50	2
E. viminalis	4.78	2
System blank	0	1

27 to B 34). The liquid injector was operated in split mode (20:1) at a temperature equal to 200 °C and direct current (DC) recordings were performed during the liquid injection runs. Baseline correction was performed on the resulting EAD data (Time constant TC = 0.88) (Slone and Sullivan, 2007) and retention indices were used to match peaks between the two sample injection methods (Table B 1 to B 4).

5.3.4 GC-MS

GC-MS analysis was done in order to tentatively identify some of the EAD active peaks. A Thermo Quest trace GC 2000 series coupled to a Finnigan Polaris ITD and a Perkin Elmer thermal desorption system with an identical 60 m DB624 analytical column was used. A split ratio equal to 43.7:1 was used during desorption of samples on the GC-MS system. Helium was used as carrier gas and the average linear velocity was matched with the GC-EAD system isothermally at 130 °C and required a column head pressure of 16.0 psi. The oven of the GC-MS system was set at 40 °C for 7 minute and increased at 5 °C/minute to a maximum of 260 °C. The transfer line between the thermal desorption system and GC was kept at 190 °C and the transfer line between the GC and MS was kept at 260 °C. The Finnigan Polaris ITD was operated with an ion source temperature equal to 200 °C and 70 eV ionization energy. The mass scan range was 50-285 m/z.

5.4 Results and Discussion

Complex EAD traces were observed for the complex chromatographic profiles of the crushed *Eucalyptus* leaves (Figure B 11, B 19 and B 26). Many of these antenna responses were observed not to originate from the eluting compounds, but rather from baseline drift. This drift is known to hide responses during long GC-EAD recordings (Moorhouse *et al.*, 1969) and is removed from the recording by applying a baseline correction algorithm (see Slone and Sullivan (2007)). This mechanism is automatically incorporated when electronic filtering is applied before the recording starts and may result in these random responses. Therefore, only repeatable responses were investigated further. EAD response patterns were successfully matched to GC-FID signals for *E. globulus* (Figure 5.1), *E. viminalis* (Figure 5.2) and *E. citriodora* (Figure 5.3).

EAD active peaks were identified from the *E. globulus* volatile profile because these runs showed the highest repeatability in terms of EAD response width corresponding to FID peak width (see Figure A 12 to A 16). Sixteen compounds were tentatively identified that were associated with 13 EAD active peaks in the *E. globulus* volatile profile (Table 5.2). Many other peaks were also EAD active for *G. scutellatus*, but for the purpose of

this study the focus was on the repeatable responses that could clearly be distinguished from baseline noise (see Figure A 12 to A 16).

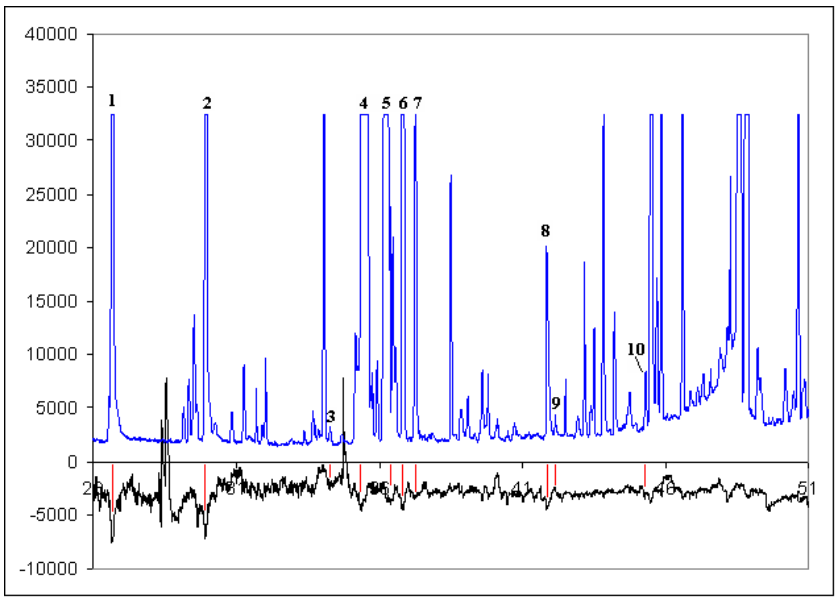

FIGURE 5.1: The numbering of chromatographic peaks which correspond to standards and EAD responses observed for *E. globulus* as in Table 5.5.

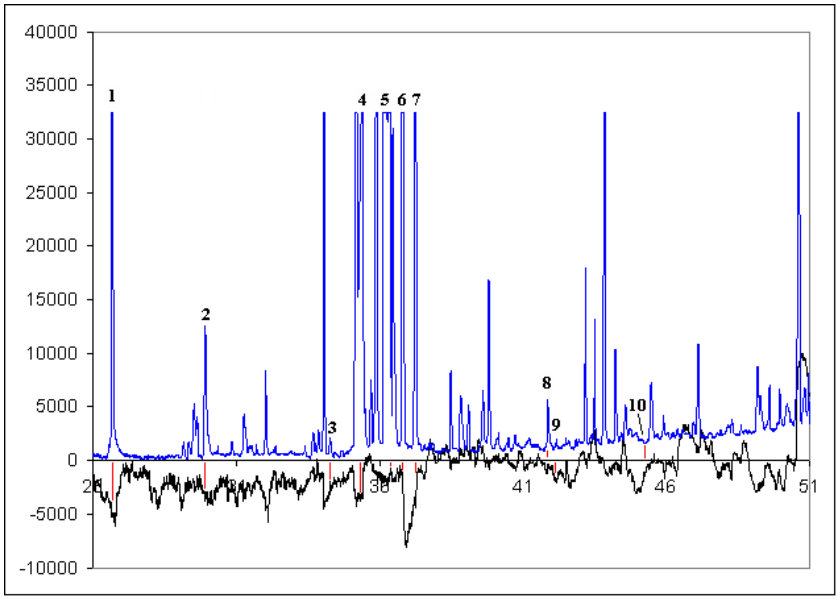

FIGURE 5.2: The numbering of chromatographic peaks which correspond to standards and EAD responses observed for *E. viminalis* as in Table 5.5.

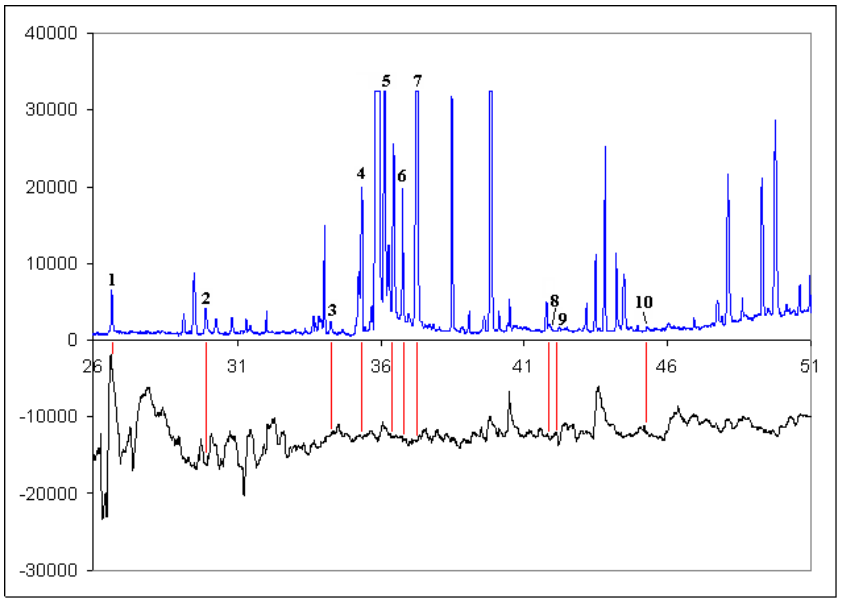

FIGURE 5.3: The numbering of chromatographic peaks which correspond to standards and EAD responses observed for *E. citriodora* as in Table 5.5.

TABLE 5.2: The standard compounds and purities

Standard No	Name	Cas no	% purity	manufacturer
1	(E)-2-hexenal	6728-26-3	98	Aldrich
2	(Z)-3-hexen-1-ol	928-96-1	99	Dr. Ehrenstorfer
3	a-pinene	80-56-8	98	Chem Service
4	camphene	79-92-5	99.3	Chem Service
5	b-pinene	127-91-3	99.5	Chem Service
6	(Z)-3-hexenyl acetate	1708-82-3	99	Dr. Ehrenstorfer
7	3-carene	13466-78-9	96.5	Dr. Ehrenstorfer
8	a-terpinene	99-86-5	94	Dr. Ehrenstorfer
9	m-cymene	535-77-3	99.0	Dr. Ehrenstorfer
10	limonene	5989-27-5	99.3	Chem Service
11	eucalyptol	470-82-6	-	Chem Service
12	g-terpinene	99-85-4	97	Aldrich
13	2-phenylethanol	60-12-8	-	Sigma
14	benzyl acetate	140-11-4	99.5	Chem Service
15	ethyl phenylacetate	101-97-3	99	Aldrich
16	terpenyl acetate	80-26-2	-	Chem Service

Kovats retention indices were calculated and used to match peaks between the GC-EAD and GC-MS systems (Table 5.3). The only inconsistency (large difference in KI between the two systems) was observed for the alcohols 2-phenylethanol and (Z)-3-hexen-1-ol. The inconsistencies could be explained by column surface activity on the GC-MS, which caused band broadening of alcohols through hydrogen bonding. The presence of these compounds were investigated for the three *Eucalyptus* species and the sample blank. The

comparison was made on both the GC-EAD and GC-MS and was based on retention indices for the peak apex (Table 5.4, B 5 and B 6), and peak start times (Table 5.5 and 5.6).

TABLE 5.3: The retention indices for the standard compounds on both the GC-EAD and GC-MS systems.

	GC-MS			GC-EAD			ΔKI		
Compound name	start	apex	end	start	apex	end	start	apex	end
(E)-2-hexenal	909	911	914	908	910	913	-1	-2	-1
(Z)-3-hexen-1-ol	914	918	938	-	-	-	-	-	-
α-pinene	955	958	962	956	958	961	2	0	-1
camphene	978	980	983	978	980	983	1	0	0
β-pinene	1007	1010	1015	1008	1011	1013	1	0	-2
(Z)-3-hexenyl acetate, 3-carene	1034	1037	1042	1035	1038	1041	1	0	-2
α-terpinene	1042	1046	1052	1044	1046	1048	1	0	-3
m-cymene, d-limonene	1052	1057	1059	1054	1058	1059	3	1	0
eucalyptol	1068	1073	1076	1071	1073	1076	3	0	-1
γ-terpinene	1078	1084	1088	1083	1085	1087	4	1	0
2-phenylethanol	1216	1229	1243	1207	1209	1216	-9	-20	-27
benzyl acetate	1226	1229	1232	1226	1228	1231	0	-1	-1
ethyl phenylacetate	1307	1312	1317	1308	1311	1315	1	-1	-3
terpenyl acetate	1408	1411	1416	1408	1411	1415	0	0	-1

TABLE 5.4: Tentative identities of compounds in the sample blank. Based on run 9OCTR1 on the GC-MS

RT at peak apex (min)	Kovats Index	Compound name
25.32	796.06	Toluene
30.37	853.44	xylene
32.80	958.41	α-pinene
35.01	1010.99	β-pinene
35.99	1035.89	Benzene derivative
44.09	1258.47	unknown
44.83	1280.55	naphthalene
48.62	1400.00	C14
49.07	1415.81	naphthalene derivative

TABLE 5.5: Identities of the compounds associated with EAD active peaks and the retention indices for these peaks for the three tested *Eucalyptus* species on the GC-EAD. These retention times and indices are based on peak start time.

			E. globulus		*E. viminalis*		*E. citriodora*	
Peak No	Standard No	Compound	Rt(min)	KI	Rt(min)	KI	Rt(min)	KI
1		C6 alcohol	26.48	838.51	26.55	839.93	26.53	839.47
2	1	(E)-2-hexenal,	29.79	907.64	29.79	907.49	29.79	907.47
	2	(Z)-3-hexen-1-ol	present	present	present	present	-	-
	3	α-pinene	31.91	956.31	31.89	955.47	31.92	956.11
	4	camphene	-	-	-	-	-	-
3	5	β-pinene	-	-	-	-	-	-
4	6	3-carene	-	-	-	-	-	-
	7	(Z)-3-hexenyl acetate	35.24	1035.49	35.23	1034.98	35.25	1035.49
	8	α-terpinene	present	present	35.59	1043.99	35.57	1043.44
5	10	limonene	36.02	1055.04	36.05	1055.46	36.03	1055.00
		cymene	present	present	36.28	1061.25	36.20	1059.24
6	11	eucalyptol	36.74	1072.99	36.70	1071.91	36.66	1070.80
7	12	γ-terpinene	37.17	1083.67	37.15	1083.10	37.15	1083.11
8	13	2-phenylethanol	41.72	1206.13	41.73	1206.15	-	-
9	14	benzyl acetate	42.38	1225.22	-	-	-	-
10	15	ethyl phenylacetate	45.19	1307.47	-	-	-	-
	16	terpenyl acetate	48.39	1407.96	-	-	-	-

TABLE 5.6: Identities of the compounds associated with EAD active peaks and the retention indices for the three different *Eucalyptus* species on the GC-MS. These retention times and indices are based on peak start time.

			E. globulus		*E. viminalis*		*E. citriodora*	
Peak No	Standard No	Compound	Rt(min)	KI	Rt(min)	KI	Rt(min)	KI
1		C6 alcohol	27.54	842.31	27.55	842.50	27.52	841.82
2	1	(E)-2-hexenal,	30.68	909.23	30.72	910.19	30.74	910.65
	2	(Z)-3-hexen-1-ol	present	present	present	present	-	-
	3	α-pinene	32.65	955.08	32.68	955.69	32.70	956.13
	4	camphene	-	-	-	-	-	-
3	5	β-pinene	-	-	-	-	-	-
4	6	3-carene	-	-	-	-	-	-
	7	(Z)-3-hexenyl acetate	36.04	1037.24	36.03	1036.78	35.99	1035.79
	8	α-terpinene	36.33	1044.56	36.32	1044.35	36.35	1045.02
5	10	limonene	36.75	1055.19	36.75	1055.19	36.76	1055.54
		cymene	present	present	36.97	1060.80	36.96	1060.57
6	11	eucalyptol	37.41	1071.96	37.39	1071.55	37.39	1071.58
7	12	γ-terpinene	37.78	1081.52	37.81	1082.28	37.76	1080.93
8	13	2-phenylethanol	42.71	1217.55	-	-	-	-
9	14	benzyl acetate	43.09	1228.92	-	-	-	-
10	15	ethyl phenylacetate	45.80	1310.30	-	-	-	-
	16	terpenyl acetate	48.82	1407.33	-	-	-	-

Confirmation of the observed responses were obtained for the identified standard compounds (Figure 5.4). During these recordings the direct current (DC) EAD data were obtained by recording without any filters. This data, however, required mathematical baseline correction and smoothing after data collection (Slone and Sullivan, 2007). Responses to the standard compounds revealed that (E)-2-hexenal, (Z)-3-hexen-1-ol, (Z)-3-hexenyl acetate, eucalyptol, γ-terpinene, β-pinene, 2-phenylethanol, benzyl acetate and ethyl phenylacetate were correctly identified as being antenna active compounds. The largest responses, amongst these, were observed for the green leaf volatiles (E)-2-hexenal, (Z)-3-hexen-1-ol, (Z)-3-hexenyl acetate and phenolic compounds 2-phenylethanol, benzyl acetate and ethyl phenylacetate (see Figure 5.4).

Compounds that were confirmed as antenna active that could not be detected in the chromatographic profiles of any of the *Eucalyptus* samples included camphene, β-pinene and 3-carene. These compounds were tentatively identified as being present in these profiles, but retention index differences between the sample peaks and standard compounds showed that the initial tentative identification, which was based on a library mass spectra was incorrect. β-pinene and cymene were possibly present in these samples, but in different isomeric forms from those in the standard (Figure 5.5 and 5.6). The 3-carene mass spectrum could not be found in the sample profiles of any of the *Eucalyptus* species at the expected elution time of 35.97 minutes (start) on the GC-MS (see Table 5.5 and 5.6 as compared to Table B 1, B 2).

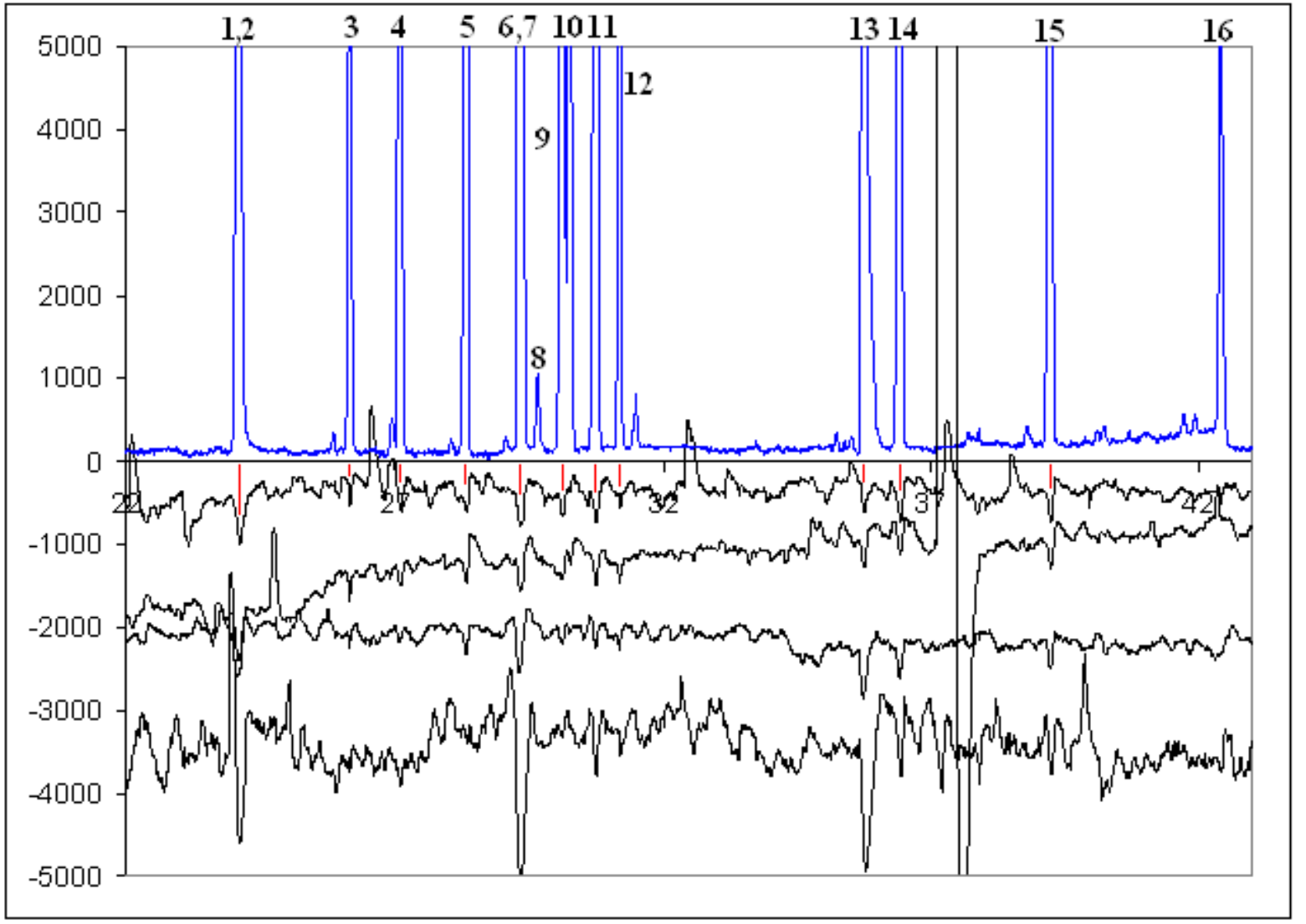

FIGURE 5.4: The confirmed, repeatable responses observed for two different *Gonipterus scutellatus* female insects. These were obtained after liquid injection of the standard compounds on the GC-EAD system (150 ng). Numbers refer to standard numbers in Table 5.3, 5.5 and 5.6.

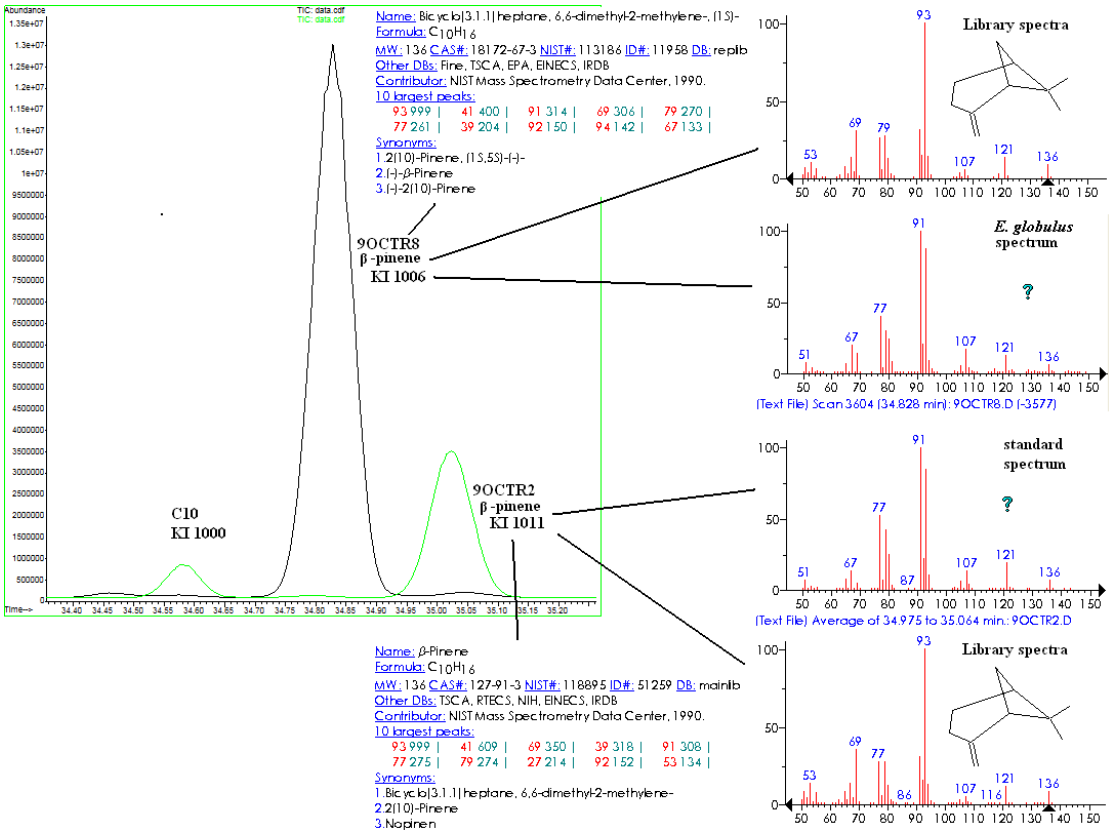

FIGURE 5.5: A comparison of the mass spectra obtained for the β-pinene (cas no: 127-91-3) in the standard and the compound found in the *E. globulus* volatile profile. These results show that the mass spectra of these two peaks are identical but their elution times differ. It can be concluded that these two are different compounds.

Co-elution occurred for some of the compounds in the standard mixture (Table 5.4 and B 1 to B 4). For example, two cymene peaks were observed in the standard mixture that eluted on ether side of d-limonene (Figure B 36). m-cymene was identified as the earlier co-eluting peak with d-limonene. The source of the second cymene peak was traced to the α-terpinene standard (Figure 5.6). The similarity in the structure of α-terpinene and p-cymene led to the conclusion that α-terpinene could have been converted to p-cymene (Figure 5.6). This conversion could have taken place in the *Eucalyptus* samples themselves because both *alpha*-terpinene and p-cymene was present in these profiles. Degradation of terpene compounds through oxidation is well known (Calogirou *et al.*, 1999). These two cymene isomers can easily be distinguished from limonene based on their molecular ion mass differences (136 vs 134) (Apendix B, Figure B 36).

Quantitative differences of EAD active compounds occurred for the three *Eucalyptus* species investigated. Major differences were observed for compounds such as 2-phenylethanol, benzyl acetate, ethyl phenylacetate, terpenyl acetate and (Z)-3-hexen-1-ol. The majority of these compounds occurred in the *E. globulus* volatile profile and

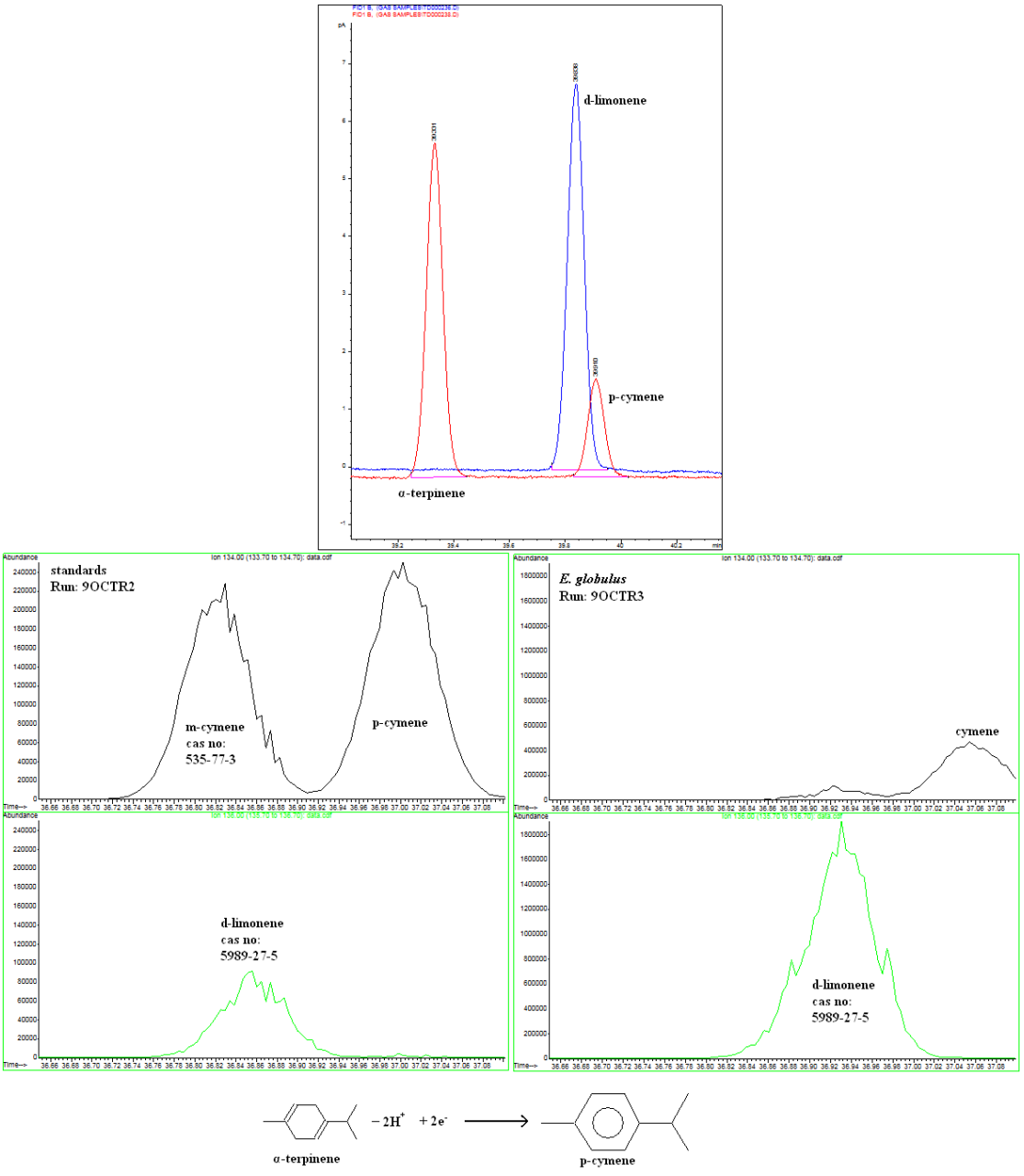

FIGURE 5.6: Top: Individually injected standards on the GC-FID system. Bottom left: Extracted ion chromatograms for d-limonene (136) (cas no: 5989-27-5) and m-cymene (134) (cas no:535-77-3) and the other cymene peak observed in the standard mixture. The d-limonene peak co-eluted with m-cymene in the standard run. It was concluded that the second cymene peak in the standard run is a breakdown product of α-terpinene. Bottom right: Extracted ion chromatograms for limonene and cymene found in the *E. globulus* volatile profile. As can be seen here m-cymene is not present in the *E. globulus* sample, only another cymene that is possibly p-cymene. The d-limonene peak was the largest peak in the *E. globulus* volatile profile and was chromatographically overloaded.

The hypothesized conversion of α-terpinene to p-cymene is indicated below.

2-phenylethanol was observed to be present in both the *E. globulus* and *E. viminalis* profiles, but not in the *E. citriodora* profile. These differences should be interpreted with caution because these compounds may be present at below detection levels in all three *Eucalyptus* species investigated. The relative differences between these compounds were, however, easily noticed when comparing the three *Eucalyptus* species (Figure 5.7 and B 35).

The majority of the identified compounds that elicited EAD responses for *G. scutellatus* are known to be antennally active for other insect species as well. This includes 2-phenyl ethanol and (Z)-3-Hexen-1-ol that were EAG active for the Colorado potato beetle, *Leptinotarsa decemlineata* (Weissbecker *et al.*, 1999) and (Z)-3-hexen-1-ol, α-pinene, β-pinene, cymene, 1,8-cineole, and limonene being EAD active for the *Eucalyptus* woodborer, *Phoracantha semipunctata* (Barata *et al.*, 2000). The Sphinx moth *Manduca sexta* was shown to give EAG responses to (Z)-3-hexenyl acetate (Fraser *et al.*, 2003) and this compound was found to increase the attractiveness of pheromones for the corn earworm, *Helicoverpa zea* and codling moth, *Cydia pomonella* (Light *et al.*, 1993).

Five of the antenna active compounds identified here (2-phenylethanol, 1,8-cineol, (Z)-3-hexenyl acetate, (Z)-3-hexen-1-ol, (E)-2-hexenal) was found to be EAG active for another weevil species (the cabbage seed weevil *Ceutorhynchus assimilis*) (Blight *et al.*, 1995). These authors could show single sensillum responses to the same compounds for that weevil. It is therefore possible that *G. scutellatus* has the same type of receptors for these compounds. 2-phenylethanol was also identified as being antenna active for the pollen beetle, *Astylus atromaculatus* and was shown to be behaviourally attractive for this species (Van den Berg *et al.*, 2008). It is, therefore, possible that this compound is behaviourally attractive for *G. scutellatus*. This compound was not found in the non-host profile of *E. citriodora*.

The relatively larger responses (Figure 5.5) that were observed for the green leaf volatiles ((Z)-3-hexen-1-ol, (E)-2-hexenal and (Z)-3-hexenyl acetate) indicated that *G. scutellatus* females primarily detect green leaf volatiles. Our results show that *G. scutellatus* female antennae are less sensitive towards terpenes like α-pinene, β-pinene, 1,8-cineol and γ-terpinene (Figure 5.5). This result is consistent with the findings in Chapter 4 and with an EAG study on the vine weevil *Otiorhynchus sulcatus*. The vine weevil was shown to give EAG responses to (Z)-3-hexenol-1-ol, (E)-2-hexenal, 2-phenylethanol and (Z)-3-hexenyl acetate, but showed weak responses towards terpenes (Tol and Visser, 2002). If these compounds are used to differentiate among hosts then the relative difference in the concentrations of these common compounds are critically important when differentiating between different hosts.

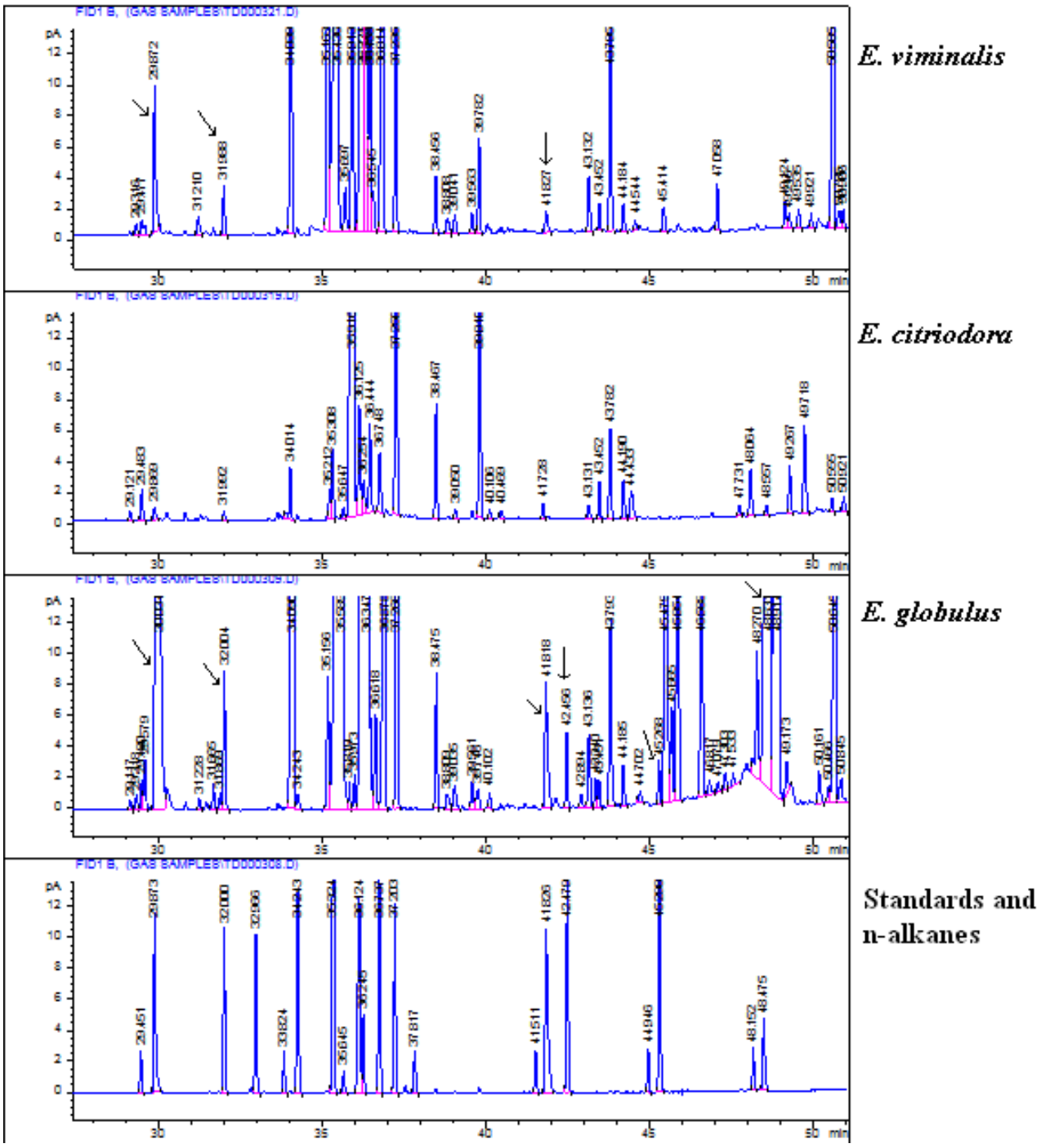

FIGURE 5.7: A comparison between the FID chromatograms for *E. globulus*, *E. viminalis* and *E. citriodora* compared to the standard mixture and n-alkanes. Arrows indicate the major differences for antenna active peaks for the three chromatographic profiles.

The fact that *G. scutellatus* detects such common compounds may be explained by the high number of different *Eucalyptus* species that have been reported as hosts for this insect (see Clarke *et al.* (1998)). Green leaf volatiles are known to originate from enzymatic reactions that occur when plant material is damaged (Gailliard and Matthew, 1976; Matsui *et al.*, 2000). These compounds are almost ubiquitous among all green plants. It is therefore possible that weevils like *G. scutellatus* detect these compounds, because they convey information about the stress level and general health of a plant (DAlessandro and Turlings, 2006). This might also explain the variability in host susceptibility observed for the same *Eucalyptus* species under different environmental conditions (Tooke, 1953; Richardson and Meakins, 1984; Clarke *et al.*, 1998).

5.5 Conclusions

Our results confirm a chemical interaction between *G. scutellatus* female antennae and different *Eucalyptus* species. This possibly explains the wide host range reported for this beetle. Differences in volatile profiles for the investigated *Eucalyptus* species were identified and 2-phenyl ethanol has been identified as a possible attractant for *G. scutellatus*. Compounds like 1,8-cineol, γ-terpinene, β-pinene, (Z)-3-hexen-1-ol, (E)-2-hexenal, (Z)-3-hexenyl acetate, benzyl acetate, ethyl phenylacetate and 2-phenyl ethanol show antennal activity for *G. scutellatus* females and should be investigated in a bioassay to determine behavioural activity.

Chapter 6

Conclusions

The main goal of developing semiochemical identification expertise and methodology at the University of Pretoria was achieved. During the developmental procedure *Gonipterus scutellatus* was used as a model insect. Results have shown that *G. scutellatus* females are able to detect compounds that originate from the crushed foliage of certain *Eucalyptus* species. Furthermore, it can be concluded that *Eucalyptus globulus* and *E. viminalis* always give larger responses when compared to the non-host *E. citriodora*. These results were obtained by utilizing electro-antennography (EAG) as a tool to investigate differences in response patterns to the total volatile profile of eleven distinct *Eucalyptus* species. This type of process was required because uncertainty in the literature as to the exact preferred host of *G. scutellatus* complicated the choice of host for GC-EAD investigation.

Volatiles were collected from the crushed leaves of these three *Eucalyptus* species by an adsorption process. EAD active chromatographic peaks were identified by removing the antennae from different individual insects and investigating the repeatability of EAD responses in the resulting GC-EAD response patterns. These responses had to occur at the exact elution time of the corresponding FID peak in the chromatographic profile. Variation in GC-EAD response patterns complicated the identification of these antenna active peaks. The main source of this variation was identified as changes in the antenna drift pattern that inevitably occurs and cannot be seen when recording alternating current EAD recordings. This is because antenna drift is removed by the baseline correction algorithm that is automatically implemented during an alternating current EAD recording. The software (EAGPro, Version 2, Syntech, Hilverstrum, The Netherlands) used in these recordings is specifically designed to remove this antenna drift because it keeps the recording trace within the allowed voltage range that is detected during these recordings.

Recording the direct current EAD trace allowed for viewing the nature of the antenna drift and allowed for the identification of true EAD responses. This method however required manual baseline correction for presentation purposes.

The use of live insects during GC-EAD was not feasible, because movement of the live insect increased random responses during GC-EAD recordings that complicated the data recordings. The method of using micro pipette tips as a restraining device for live insect preparations during GC-EAD recordings was simply inadequate for *G. scutellatus*. Developing a different way of incapacitating these live insects without limiting neural activity could potentially eliminate false responses observed during insect movement. This process would simultaneously extend the analysis time available and could allow for more than two GC-EAD recordings on the same insect (as opposed to only two from the removed, limited-lifetime antennae of one individual insect). Such a procedure would limit response variation that occurs during the antenna removal and coupling process. This variation inevitably occurred when removed antennae were used during GC-EAD. Multiple live insect recordings would then allow for the direct statistical comparison of GC-EAD response patterns between individual insects.

Tentative compound identification was achieved by investigating the identified EAD active peaks by GC-MS. Retention indices were used in order to correlate these peaks with the total ion chromatogram peaks of the GC-MS runs. Confirmation of the tentatively identified compounds was obtained by investigating differences in retention indices and mass spectra of sample peaks and commercial synthetic standard compounds. This procedure was essential because it is well known that certain terpenes have almost identical mass spectral patterns and can only be distinguished by retention time differences. Extensive effort was required to calculate and match retention indices for runs on the GC-EAD and GC-MS systems, which ran on different carrier gases. These two systems were synchronized based on the same average linear flow rate during isothermal runs. Resolution differences between the two systems further complicated the analysis. This resolution difference occurs because there is only one point on the Van Deemter curves where the plate height for the two systems are equal. The exact linear flow rate at this point can only be kept there during isothermal runs, which are long and non-practical. Discrepancies in retention indices were observed especially when peaks were either not separated properly, chromatographically overloaded or detector overloaded in the case of the ion trap. In these cases the peak integration software can provide incorrect retention times. This type of problem can be circumvented by incorporating the EAD detector directly with the GC-MS to form a GC-EAD-MS. In this way retention indices would not be needed. Alternatively, both systems should at least be run with the same carrier gas.

The EAD activity of the antenna towards the identified compounds was confirmed by investigating its response towards commercial standard compounds. The presence of these compounds was investigated in the samples isolated from the crushed leaves of *E. globulus*, *E. viminalis* and *E. citriodora*. Differences in peak size and presence of antennally active compounds were especially evident for the green leaf volatiles (Z)-3-hexen-1-ol, (E)-2-hexenal and (Z)-3-hexenyl acetate. Other differences were also noted for the aromatic compounds 2-phenylethanol, benzylacetate and ethylphenylacetate. Surprisingly 1,8-cineol (eucalyptol) showed antennal activity, confirming Tooke's approximations on the oils isolated from various eucalypts (Tooke, 1953). Other terpenes that were identified as antennally active included α-pinene, β-pinene and γ-terpinene, although response to these compounds was generally weaker than that observed for the green leaf volatiles and aromatic compounds.

The behavioural activity of these compounds is still unknown for *G. scutellatus*. Future bioassay experiments may reveal the nature of this activity. The compounds identified in this thesis are known to be EAD active for phytophagous and predatory insects other than *G. scutellatus*. This may suggest that they are not species specific enough to be used in specific mass trapping experiments. It is known that some of the identified compounds act in a synergistic way with pheromones to enhance their attractiveness. Identifying specific pheromones for this species might lead to more specific applications.

Appendix A

TABLE A.1: *Gonipterus scutellatus* samples used

Date	Location	GPS co-ordinates	Tree species
26-Feb-08	Wits University	-	-
23-Apr-08	Busby Lothair area	-	E. smithii
Jul-08	Zululand	S28°41.431' E031°58.173' 108m	GC clone
24-Jul-08	Busby Lothair area	-	E. smithii
14-Aug-08	Nyalazi boomerang Farm	S28°14.777' E032°20.020' 57m	GC clone
22-Aug-08	Winterton	S28°52.317' E029°26.013' 1267m	E. nitens
16-Sep-09	Sappi Mavuya A24	S28°32.758' E032°10.736' 36m	GU clone

TABLE A.2: EAG recordings for one removed antenna from a female *G.scutellatus* stimulated with *E.globulus* and *E.smithii* leaf volatiles and a system blank

StimID	Recording	Surface[v*s]	Maximum[v]	Surface[mv*s]	Maximum[mv]
2	*E.smithii*	-0.003735	-0.001465	3.735	1.465
2	*E.smithii*	-0.003251	-0.001292	3.251	1.292
2	*E.smithii*	-0.003095	-0.001224	3.095	1.224
2	*E.smithii*	-0.002557	-0.001169	2.557	1.169
2	*E.smithii*	-0.003094	-0.001163	3.094	1.163
2	*E.smithii*	-0.002617	-0.001002	2.617	1.002
3	*E.globulus*	-0.004676	-0.001552	4.676	1.552
3	*E.globulus*	-0.003615	-0.001297	3.615	1.297
3	*E.globulus*	-0.003441	-0.001204	3.441	1.204
3	*E.globulus*	-0.003585	-0.001237	3.585	1.237
3	*E.globulus*	-0.003499	-0.001236	3.499	1.236
3	*E.globulus*	-0.004033	-0.001214	4.033	1.214
1	Blank	- 0.001166	-0.000595	1.166	0.595
1	Blank	-0.000921	-0.000683	0.921	0.683
1	Blank	-0.000769	-0.000533	0.769	0.533
1	Blank	-0.000984	-0.000673	0.984	0.673
1	Blank	-0.001104	-0.000565	1.104	0.565
1	Blank	-0.001103	-0.000626	1.103	0.626

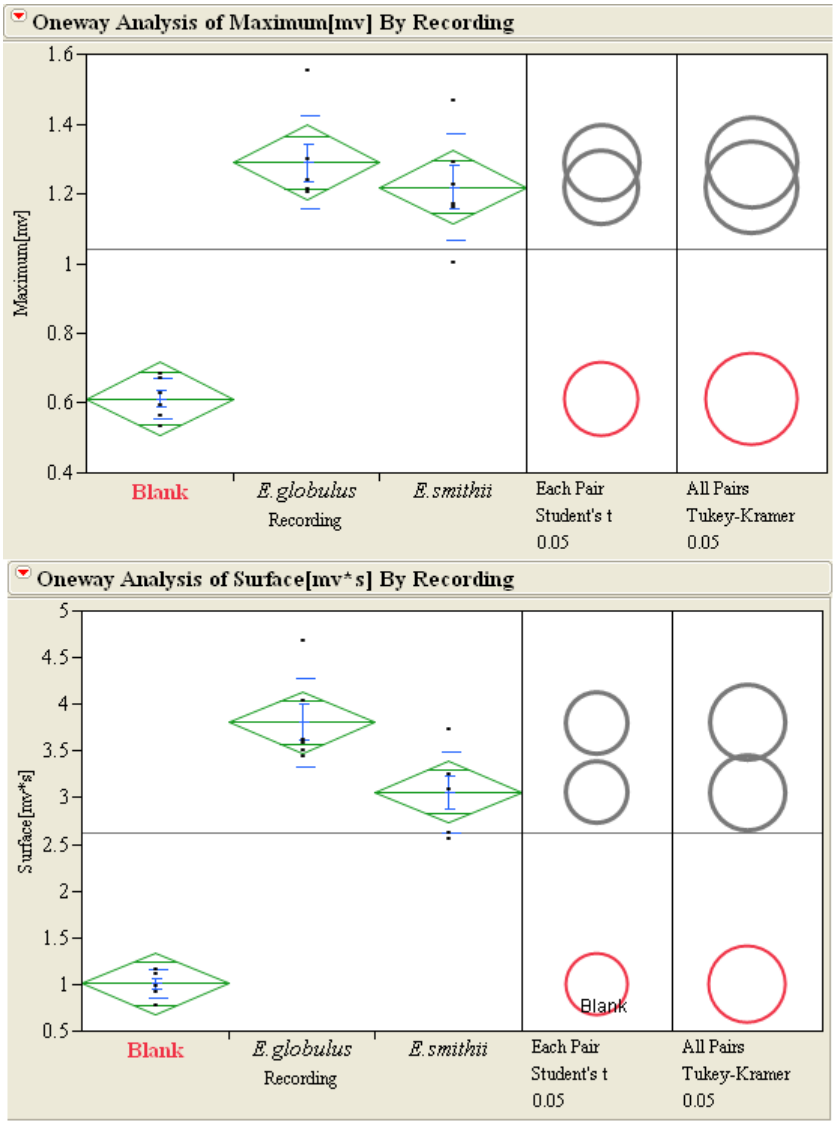

FIGURE A.1: Graphic representation of the EAG data (Table A1) indicating significantly larger responses to *Eucalyptus* volatiles compared to the blank. Top:Voltage deflection analysis. Bottom:Surface area analysis

TABLE A.3: Peaks found in a system blank on the GC-FID-EAD with their retention indices

#	RT Apex	Type	Area	height	width	RT start	RT End	start	KI apex	KI end
1	21.29	BB	3.33	0.80	0.06	21.22	21.39	678.10	679.39	681.25
2	27.70	BB	10.66	2.62	0.06	27.62	27.81	795.40	796.82	798.86
3	32.57	BB	7.19	1.72	0.06	32.49	32.68	893.53	895.17	897.53
4	32.79	BV	3.46	0.88	0.06	32.70	32.85	851.42	852.33	852.93
5	32.93	VB	24.76	5.35	0.07	32.85	33.06	900.89	902.83	905.71
6	34.30	BB	8.01	1.81	0.07	34.22	34.42	931.58	933.53	936.24
7	36.90	BB	2.90	0.70	0.07	36.81	37.01	989.74	991.57	994.17
8	37.16	BV	6.97	1.72	0.06	37.07	37.20	995.44	997.45	998.43
9	37.26	VB	12.74	3.01	0.06	37.20	37.37	998.28	999.66	1002.44
10	38.78	BB	18.23	2.51	0.10	38.61	38.96	1032.93	1036.88	1041.35
11	48.13	BB	50.95	10.43	0.08	48.03	48.27	1283.31	1286.13	1290.15
12	55.95	BB	11.48	2.12	0.09	55.85	56.10	1515.59	1518.52	1522.58

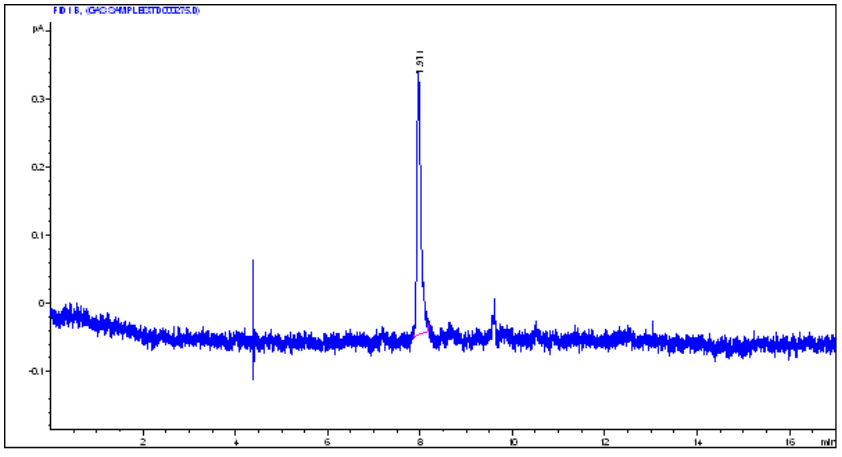

FIGURE A.2: The peak at 7.971 min is butane injected on the GC-FID-EAD (isothermal 40 °C). This corresponded to a flow rate of 12.5 cm/s at a pressure of 14.8 psi.

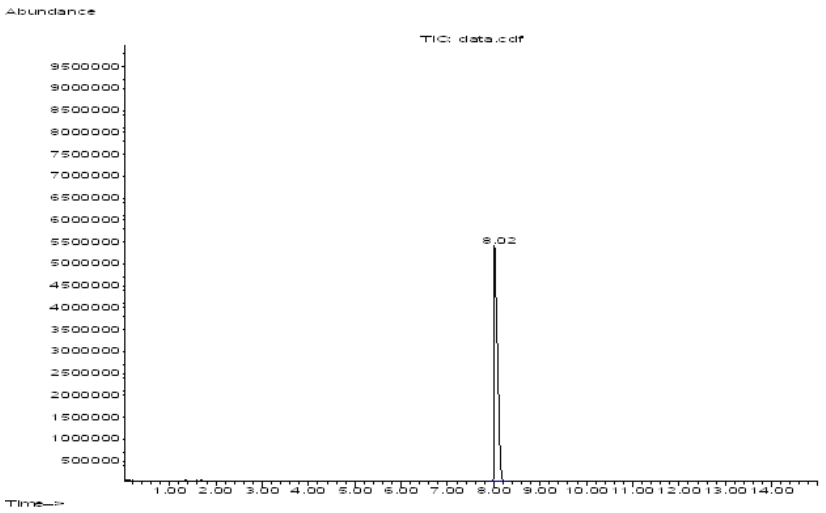

FIGURE A.3: The peak at 8.02 min is butane injected on the GC-MS (isothermal 40 °C). This corresponded to a flow rate of 12.5 cm/s at a pressure of 9.0 psi.

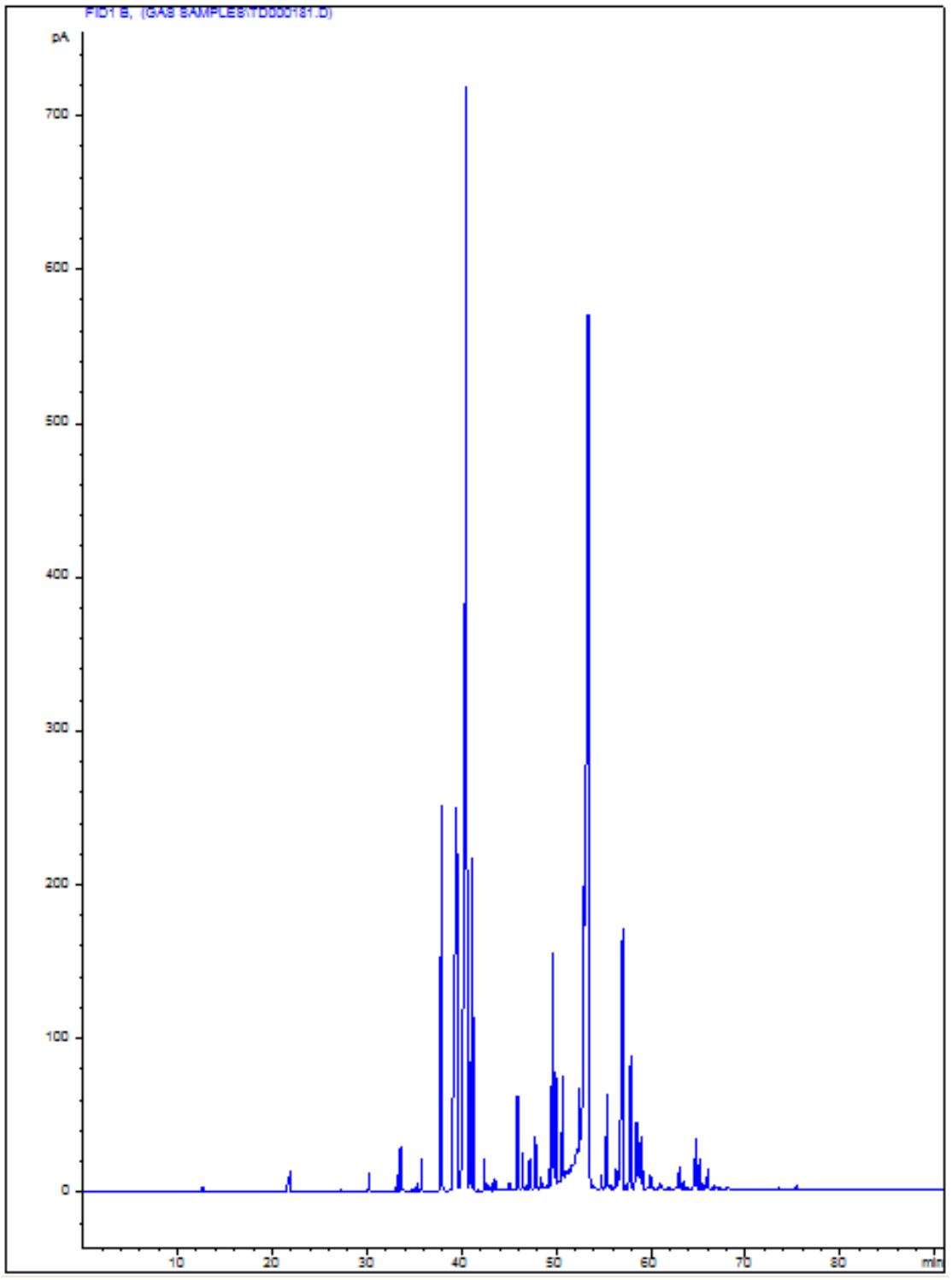

FIGURE A.4: GC-FID chromatogram for volatiles isolated from crushed *Eucalyptus globulus*. Run 181, 6:1 split

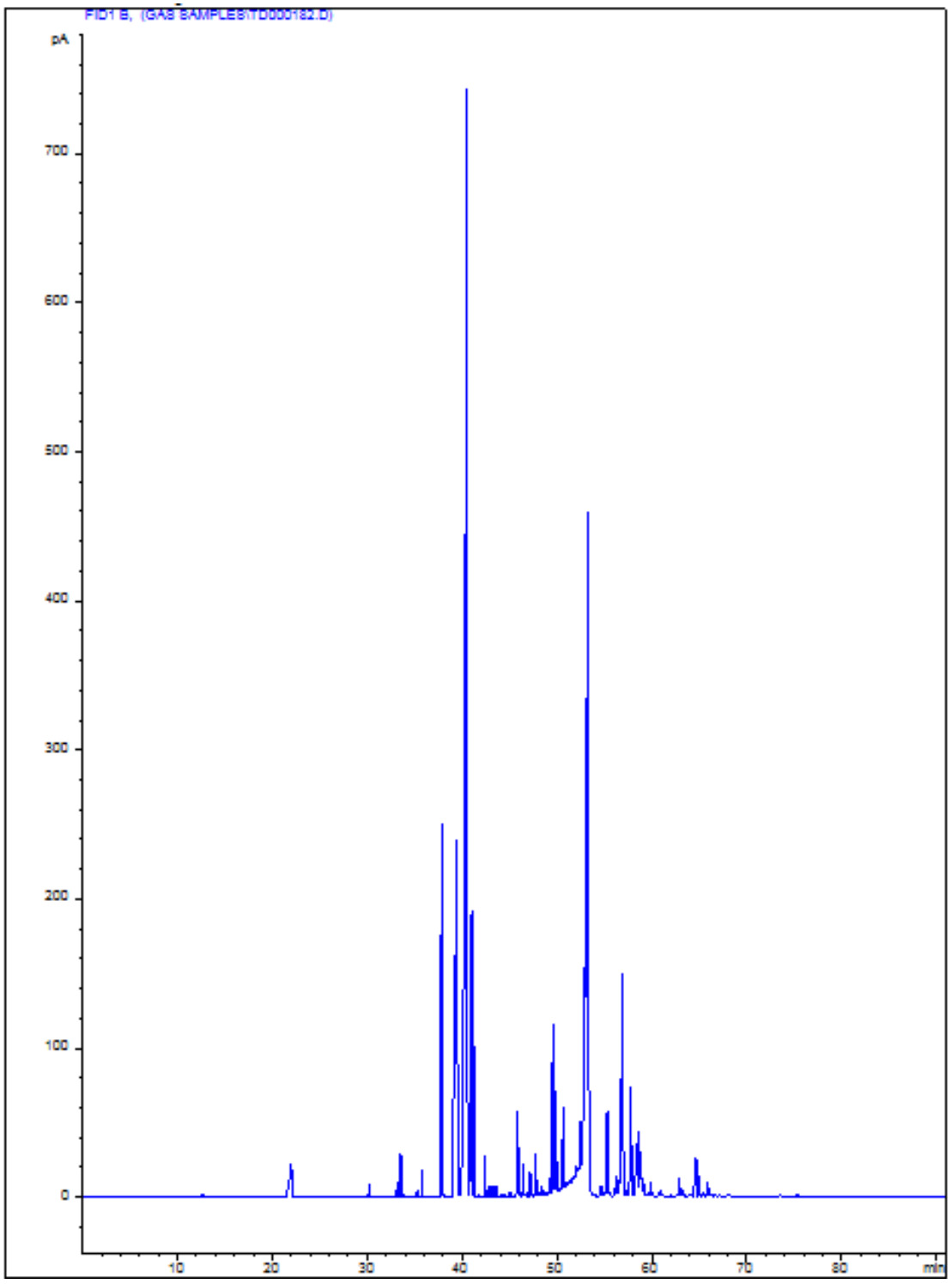

FIGURE A.5: GC-FID chromatogram for volatiles isolated from crushed *Eucalyptus globulus*. Run 182, 6:1 split

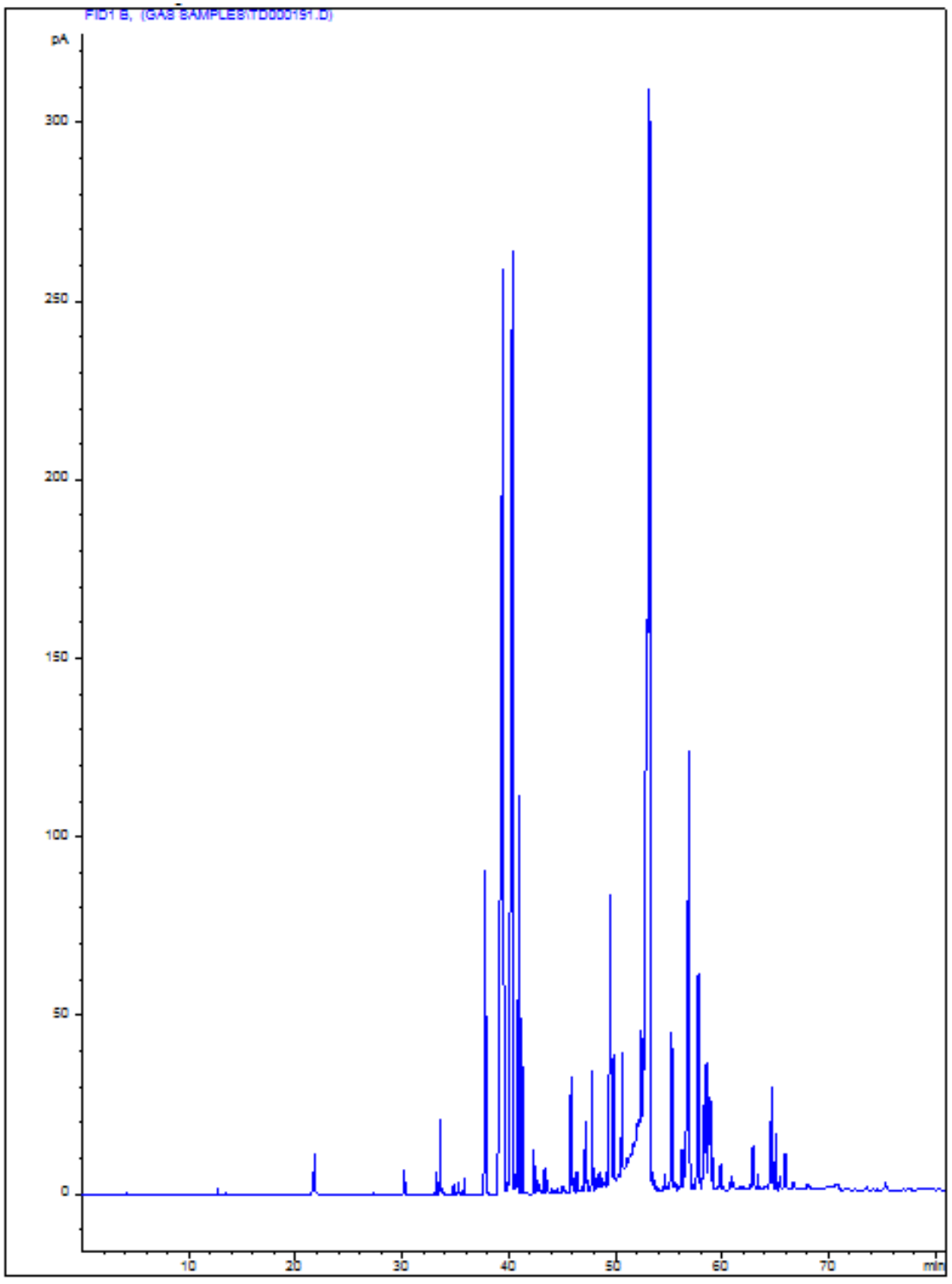

FIGURE A.6: GC-FID chromatogram for volatiles isolated from crushed *Eucalyptus globulus*. Run 191, 6:1 split

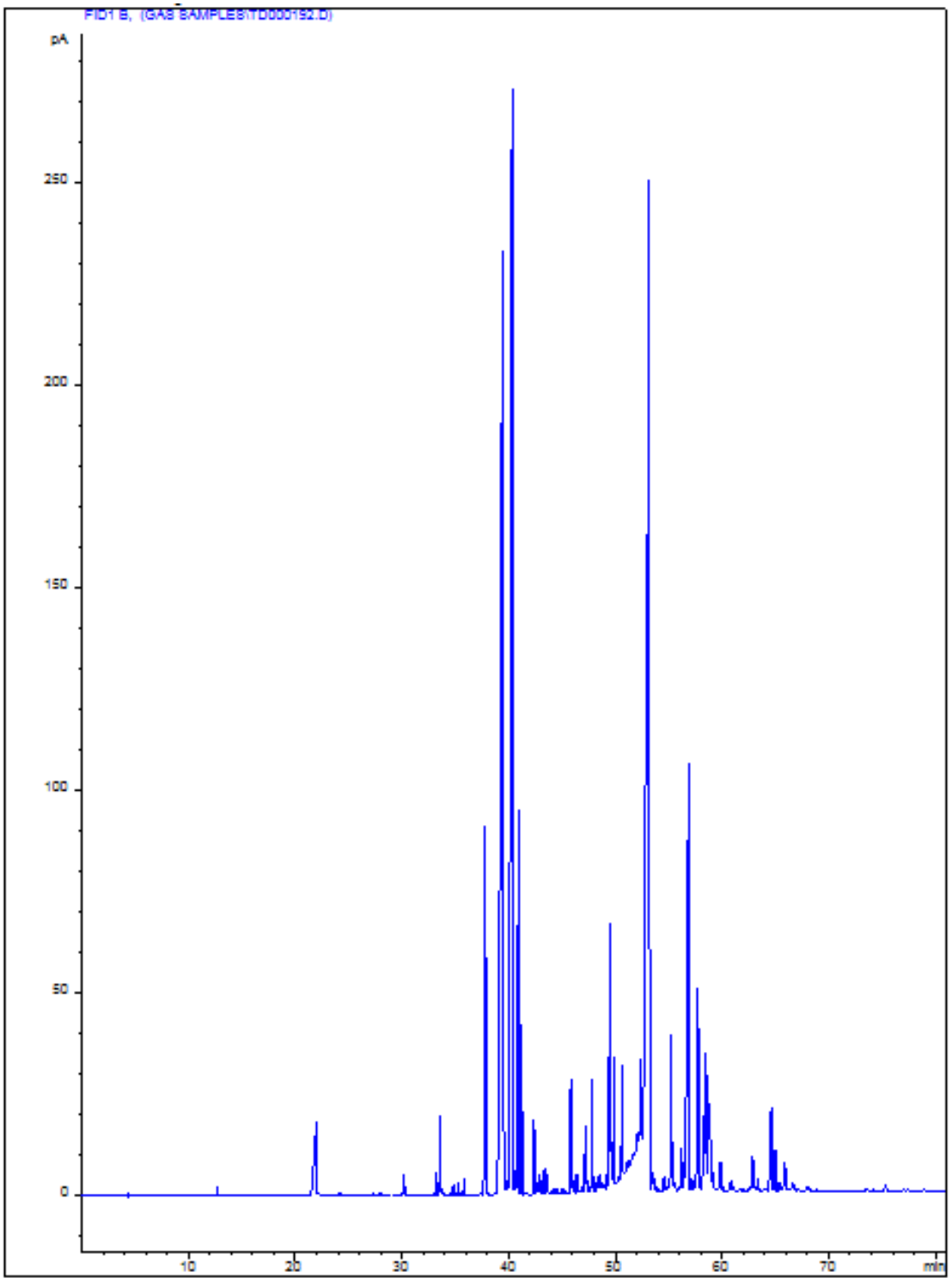

FIGURE A.7: GC-FID chromatogram for volatiles isolated from crushed *Eucalyptus globulus*. Run 192, 6:1 split

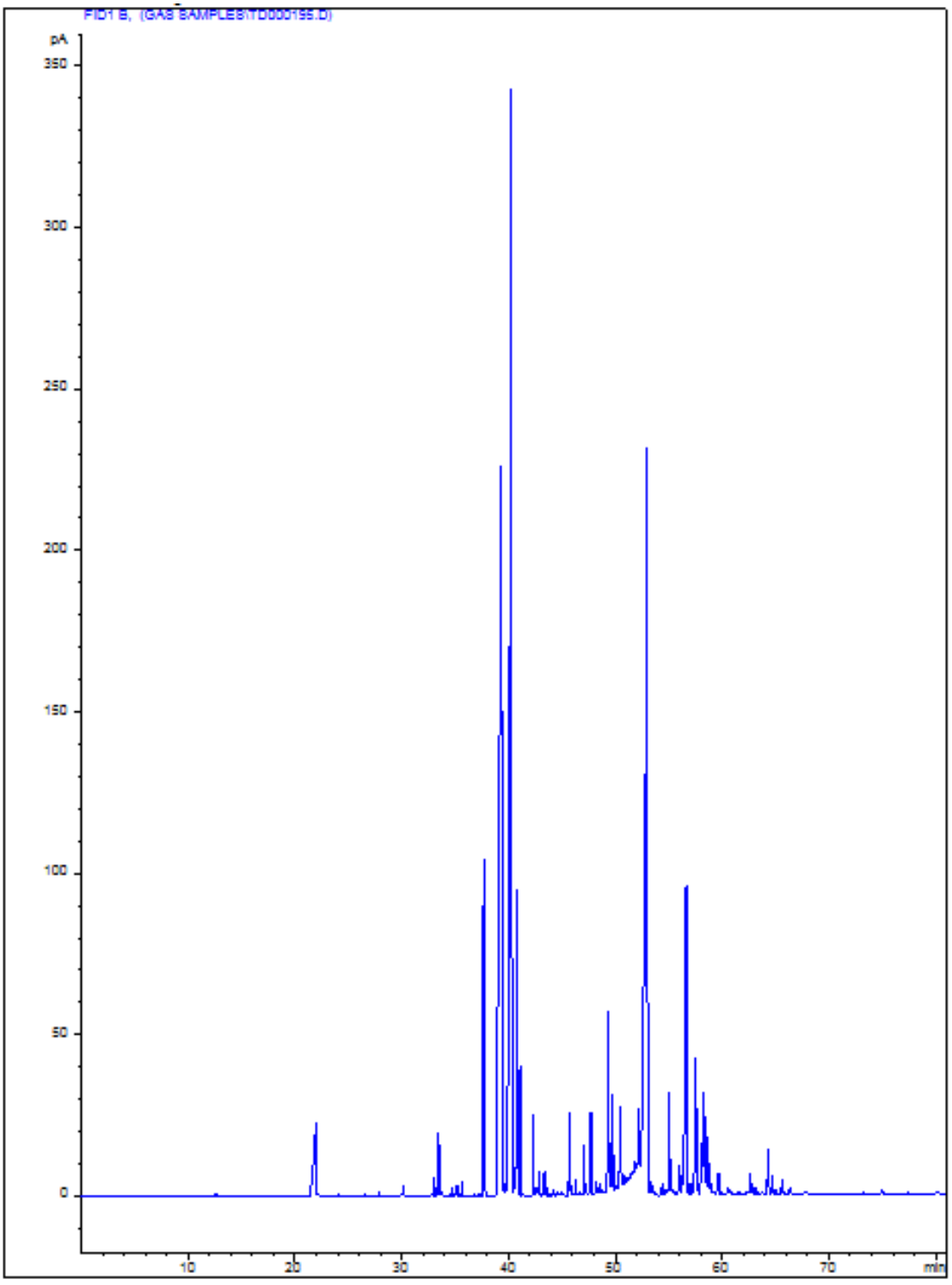

FIGURE A.8: GC-FID chromatogram for volatiles isolated from crushed *Eucalyptus globulus*. Run 195, 6:1 split

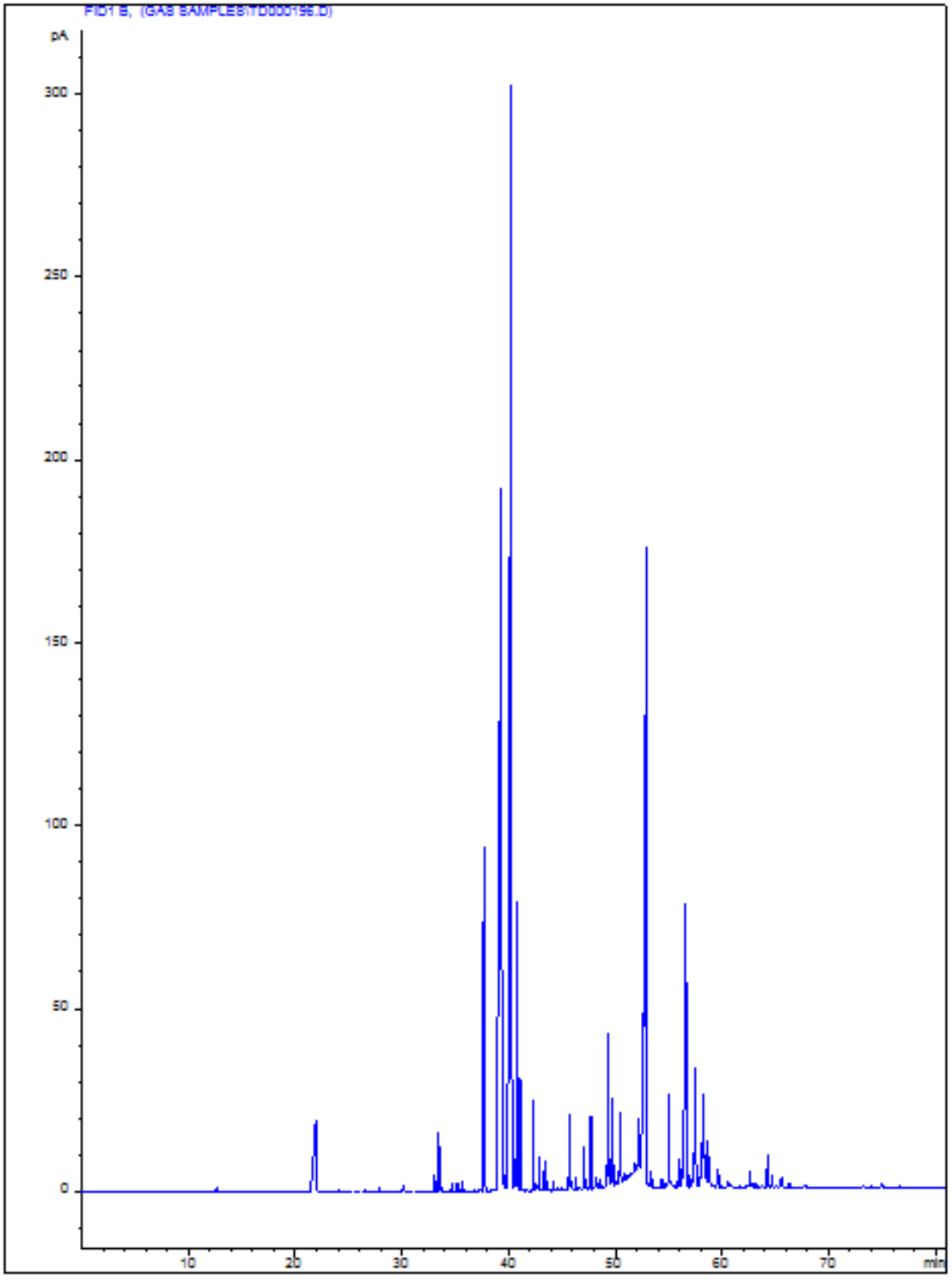

FIGURE A.9: GC-FID chromatogram for volatiles isolated from crushed *Eucalyptus globulus*. Run 196, 6:1 split

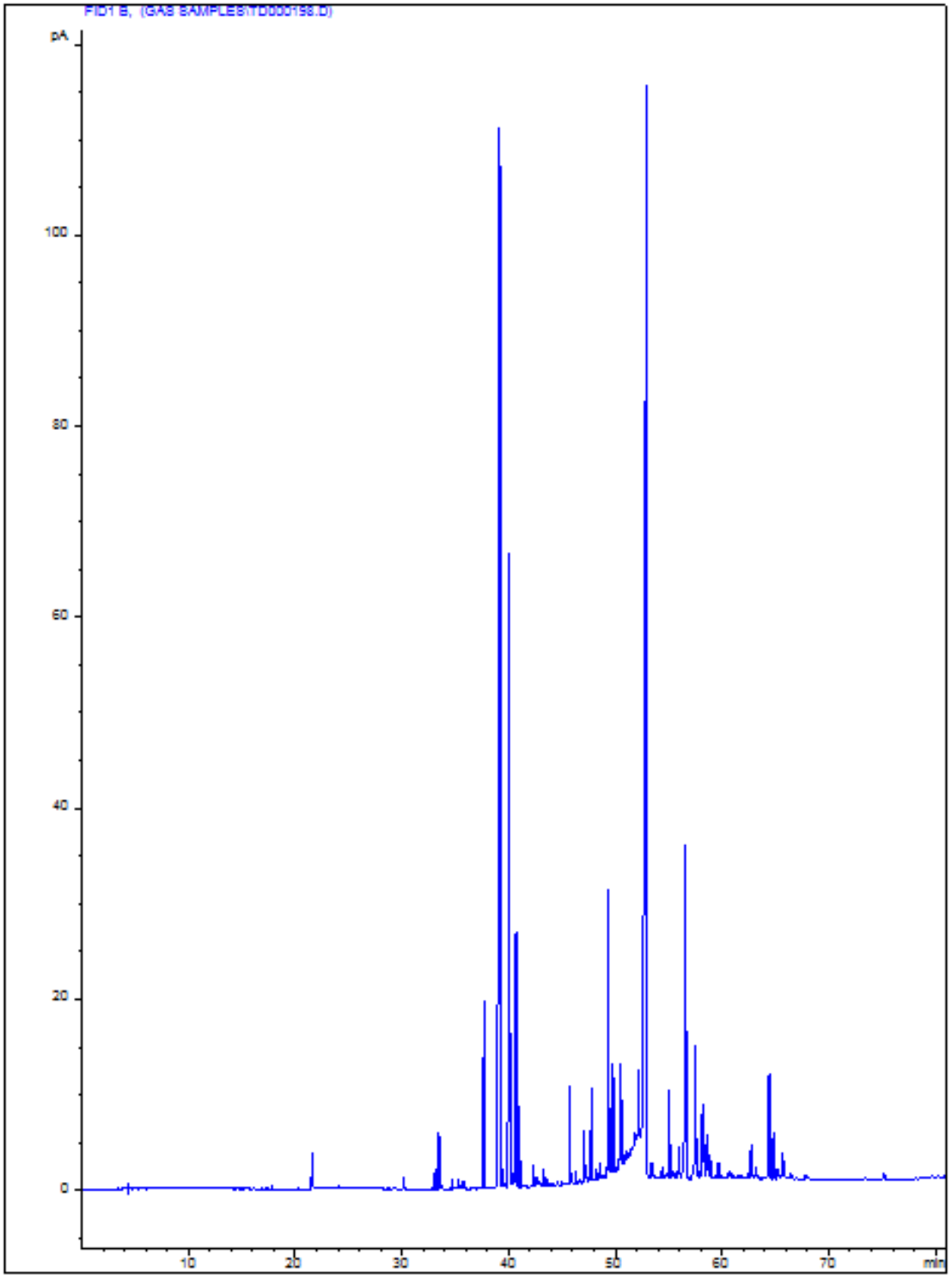

FIGURE A.10: GC-FID chromatogram for volatiles isolated from crushed *Eucalyptus globulus*. Run 198, 21.1:1 split

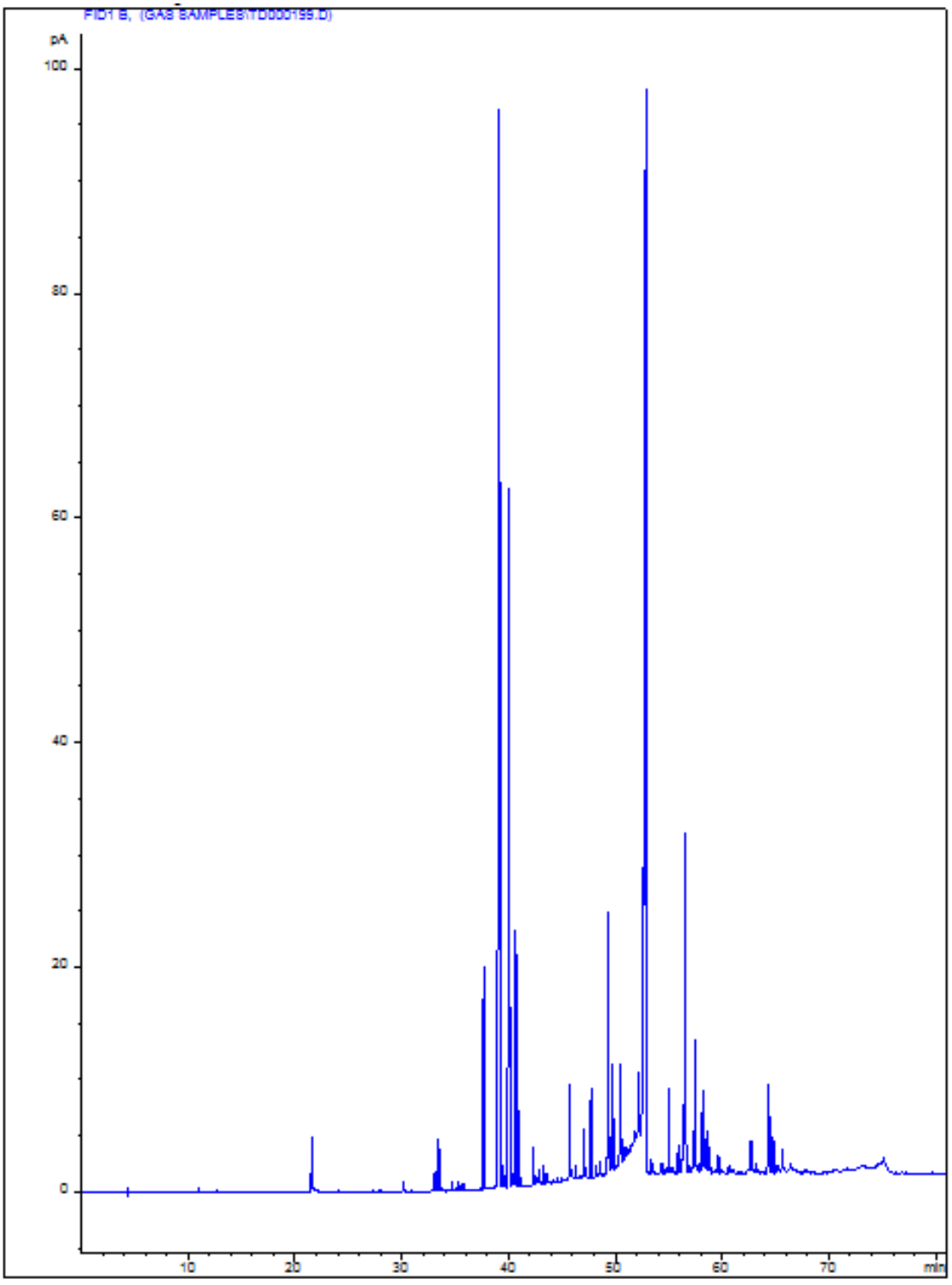

FIGURE A.11: GC-FID chromatogram for volatiles isolated from crushed *Eucalyptus globulus*. Run 199, 21.1:1 split

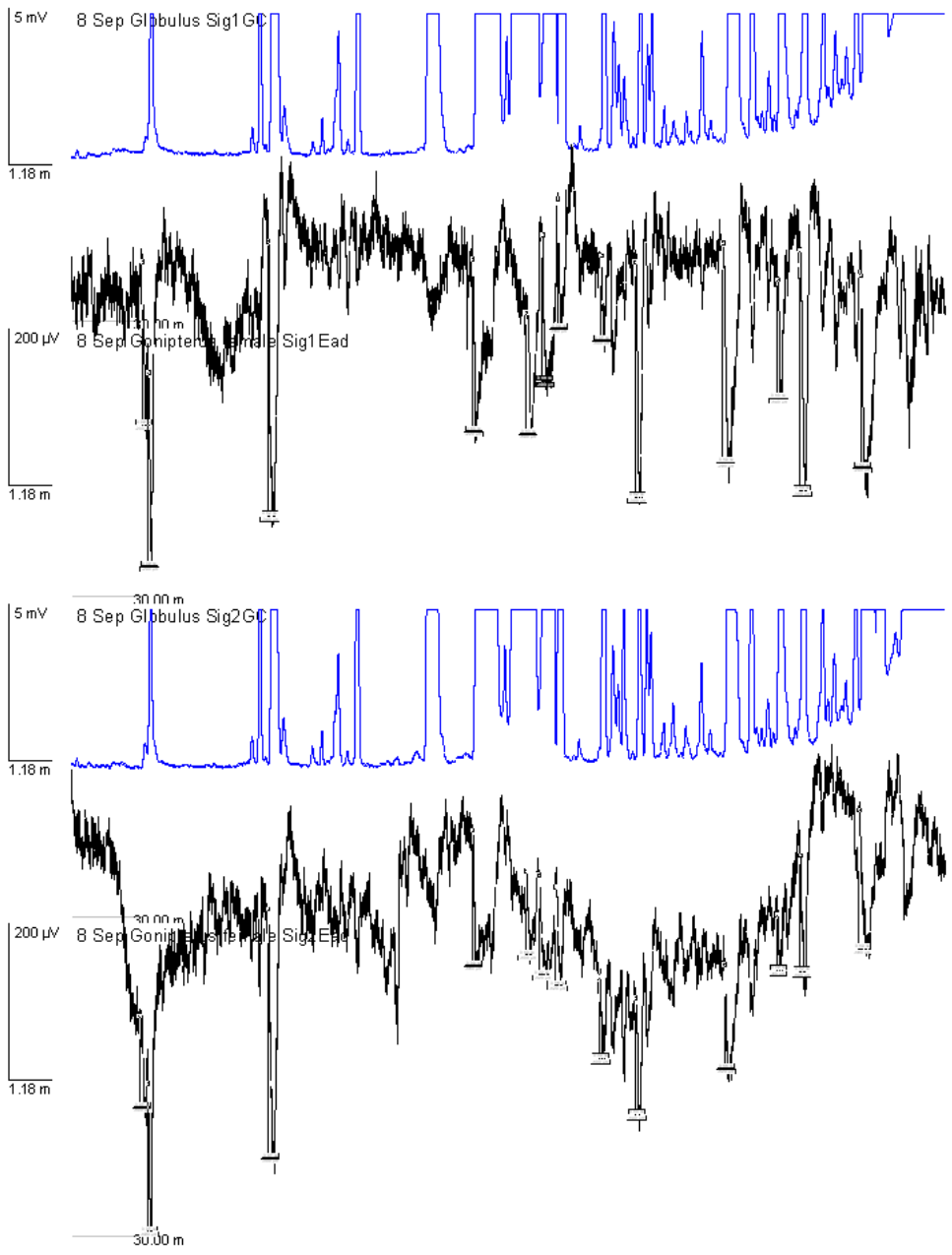

FIGURE A.12: GC-FID chromatograms for volatiles isolated from crushed *Eucalyptus globulus*. Run 181,182, 6:1 split with the respective EAD traces

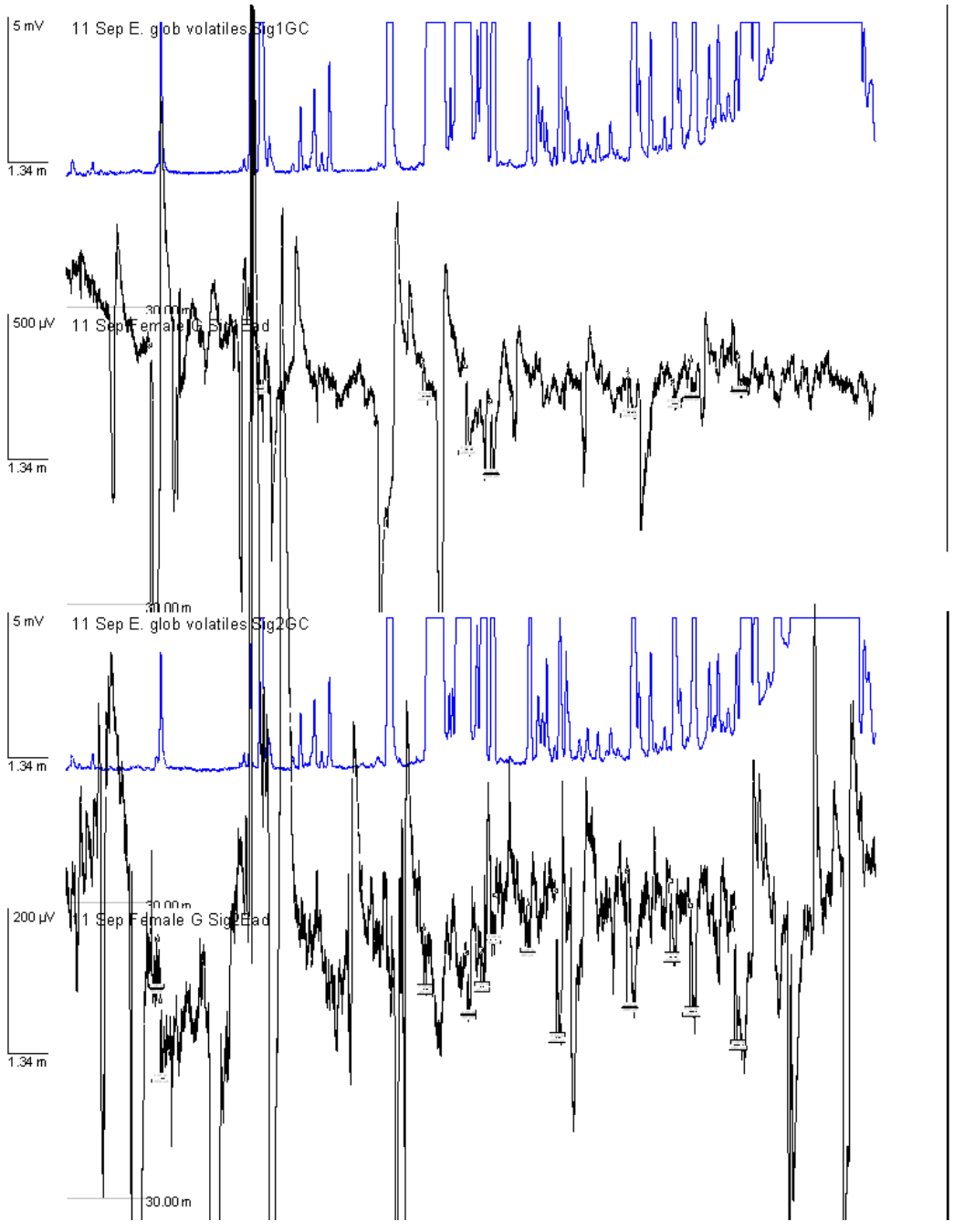

FIGURE A.13: GC-FID chromatograms for volatiles isolated from crushed *Eucalyptus globulus*. Run 191,192, 6:1 split with the respective EAD traces

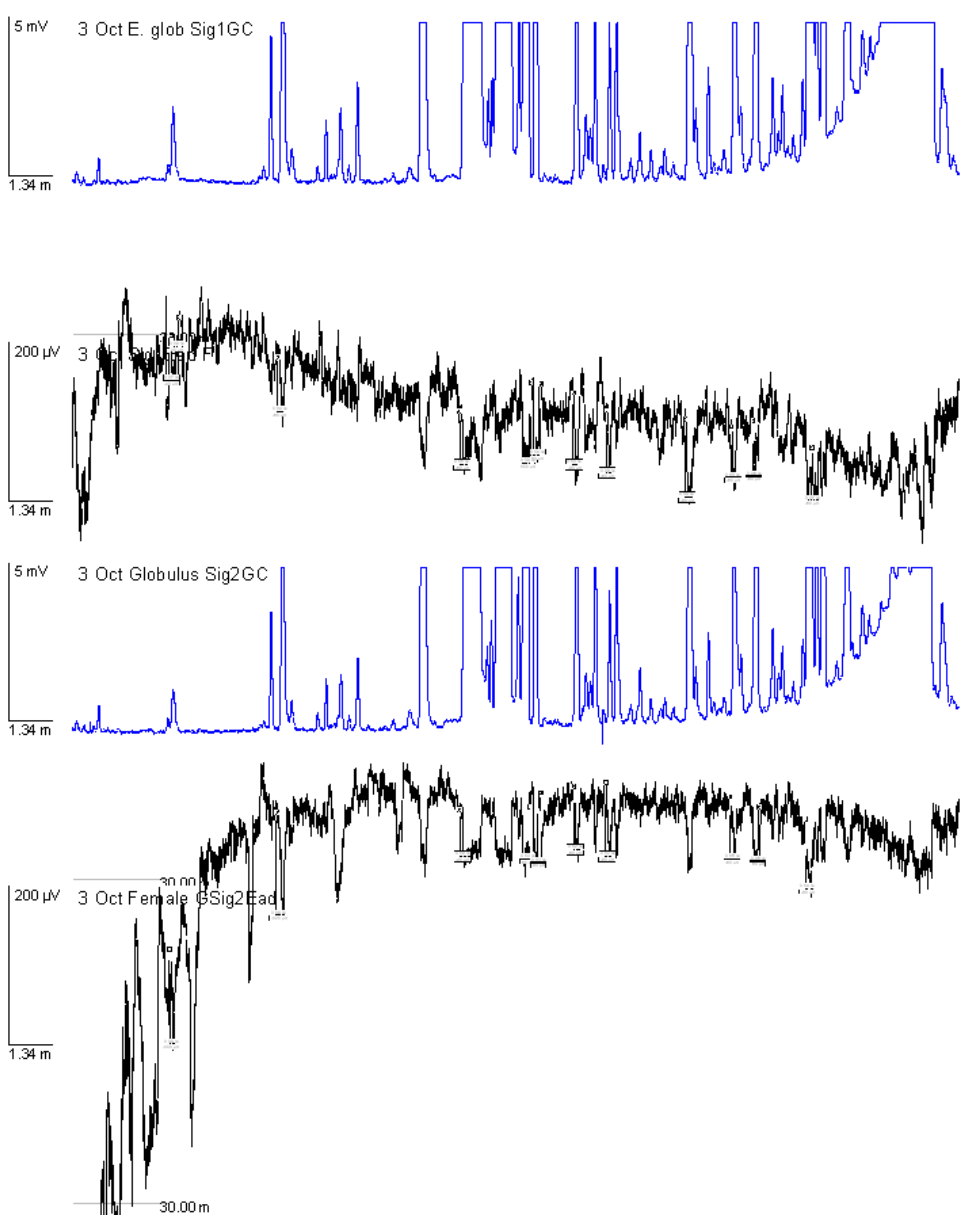

FIGURE A.14: GC-FID chromatograms for volatiles isolated from crushed *Eucalyptus globulus*. Run 195,196, 6:1 split with the respective EAD traces

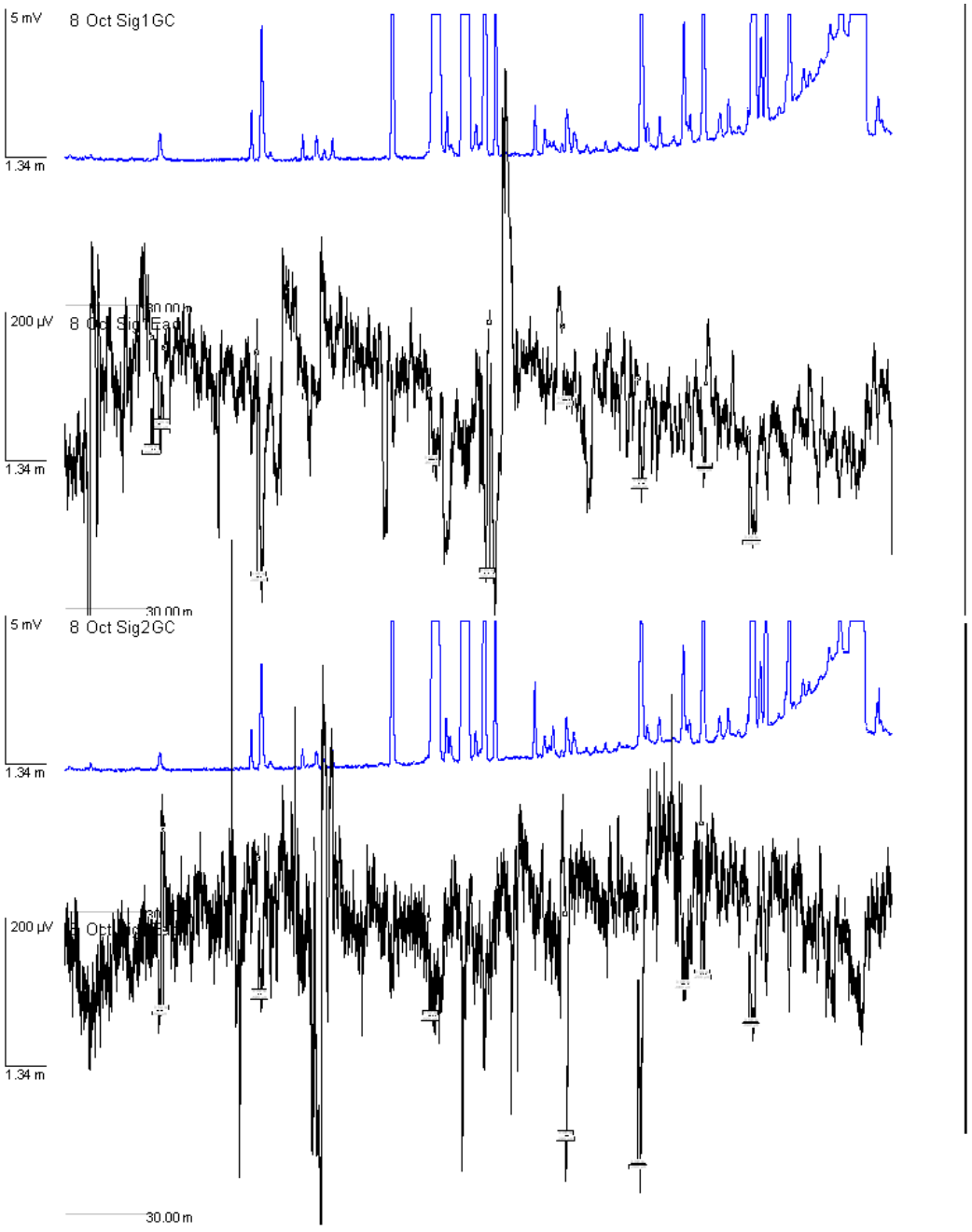

FIGURE A.15: GC-FID chromatograms for volatiles isolated from crushed *Eucalyptus globulus*. Run 198,199, 21.1:1 split with the respective EAD traces

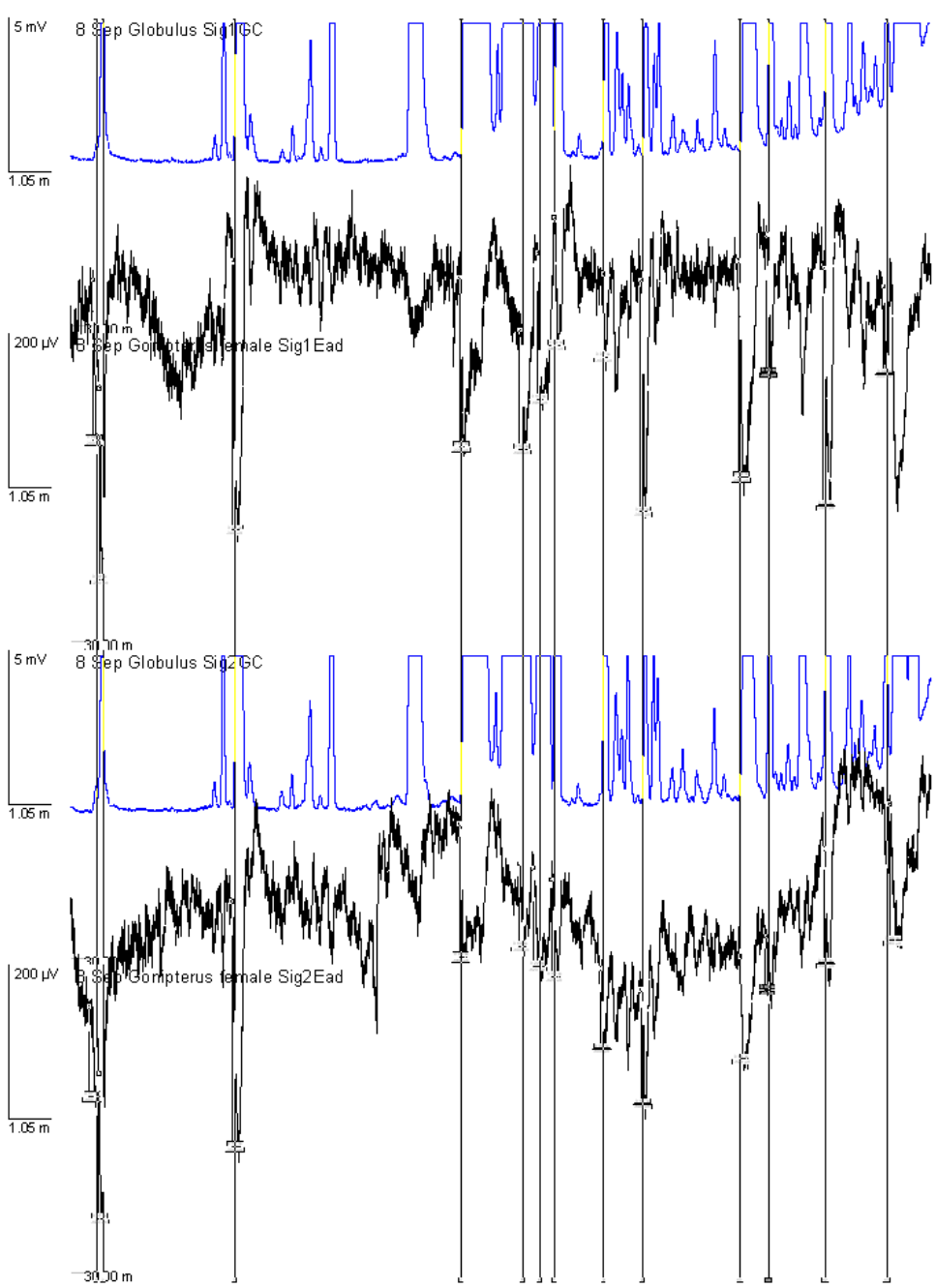

FIGURE A.16: GC-FID chromatograms for volatiles isolated from crushed *Eucalyptus globulus*. Run 181,182. Vertical lines indicate the repeatable responses and were numbered from left to right

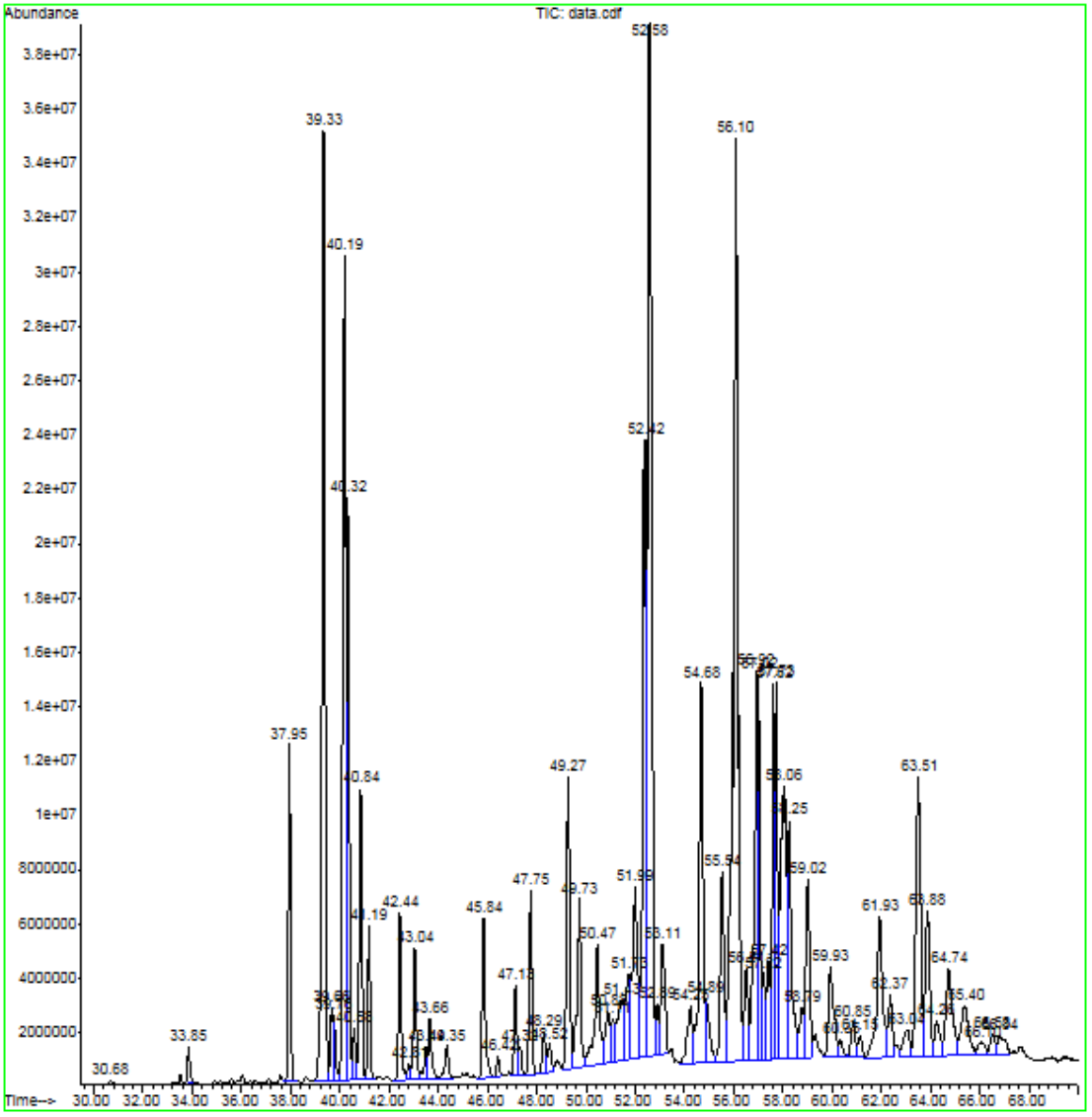

FIGURE A.17: Total ion GC-MS chromatogram for volatiles isolated from crushed *Eucalyptus globulus*. This chromatogram is the same sample that was run in Run 198,199 and 206 on the GC-EAD. Run name: 5NOV5EGl.

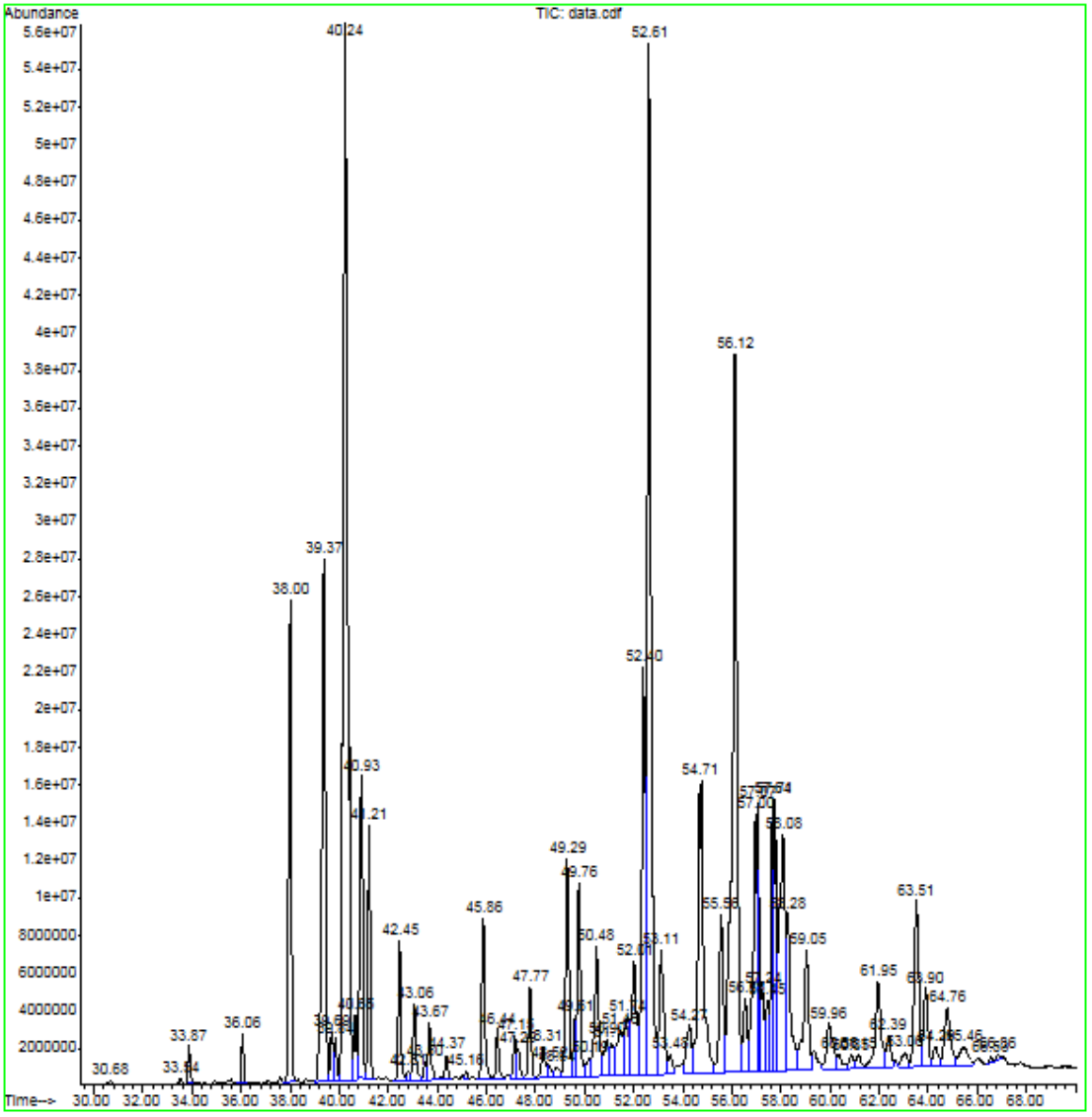

FIGURE A.18: Total ion GC-MS chromatogram for volatiles isolated from crushed *Eucalyptus globulus*. This chromatogram is the same sample that was run in Run 180 and 181 on the GC-EAD. Run name: 6NOV2EGl.

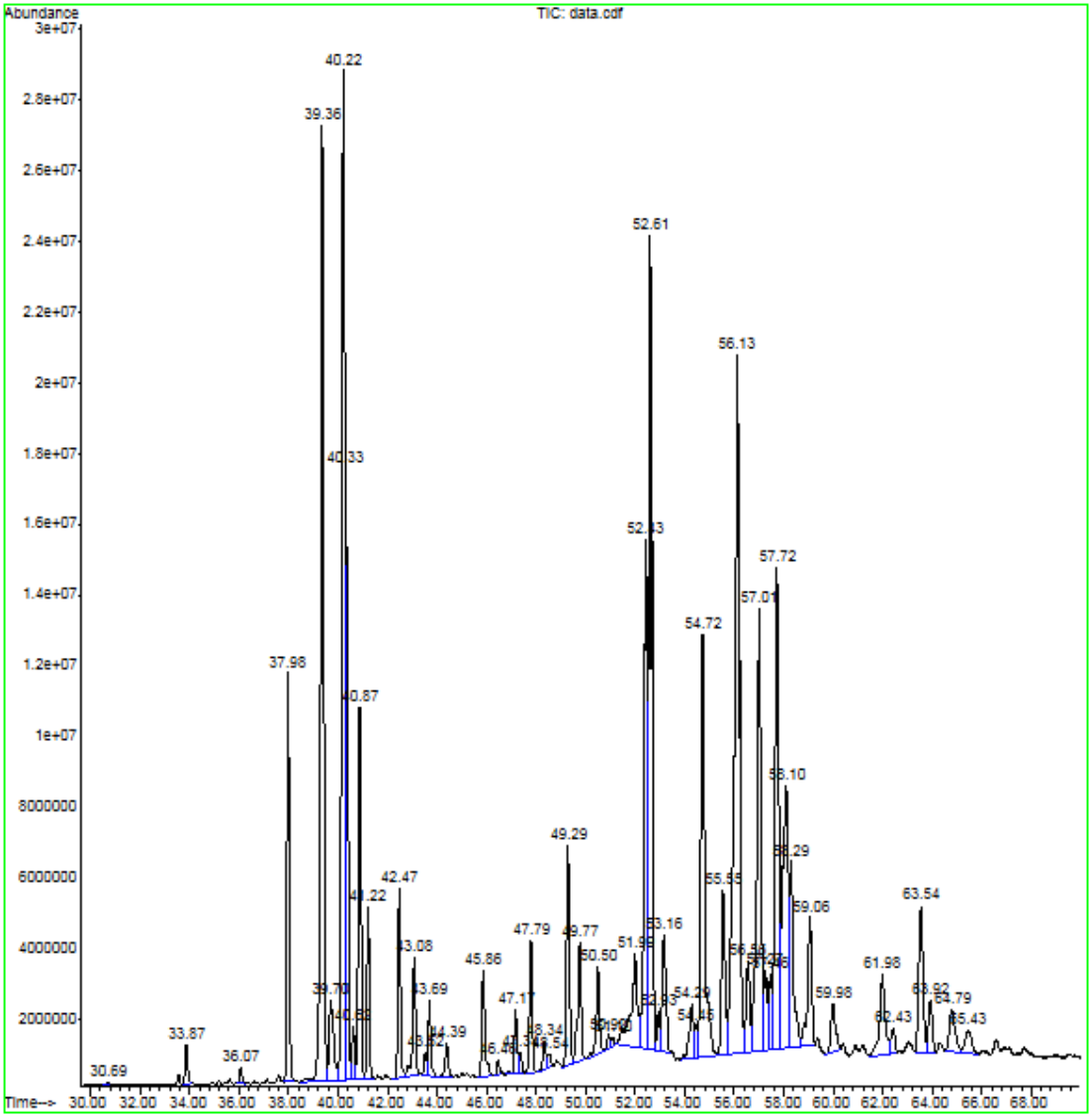

FIGURE A.19: Total ion GC-MS chromatogram for volatiles isolated from crushed *Eucalyptus globulus*. This chromatogram is the same sample that was run in Run 191, 192, 195 and 196 on the GC-EAD. Run name: 6NOV3EGl.

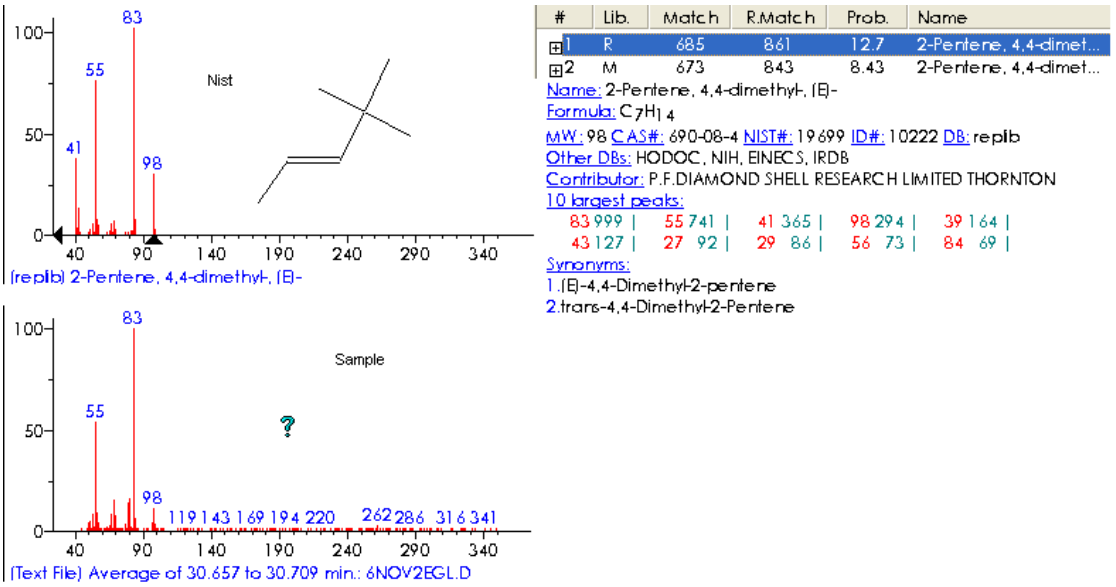

FIGURE A.20: Tentative identification of 4,4-dimethyl-2-pentene

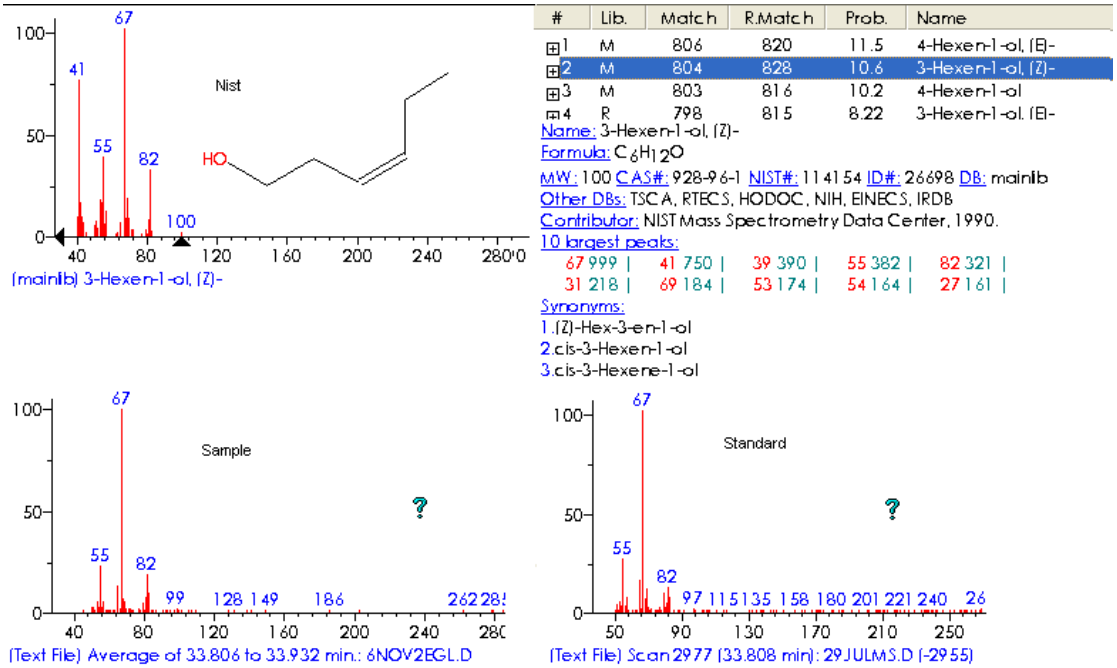

FIGURE A.21: Tentative identification of Z-3-hexen-1-ol and confirmation with standard

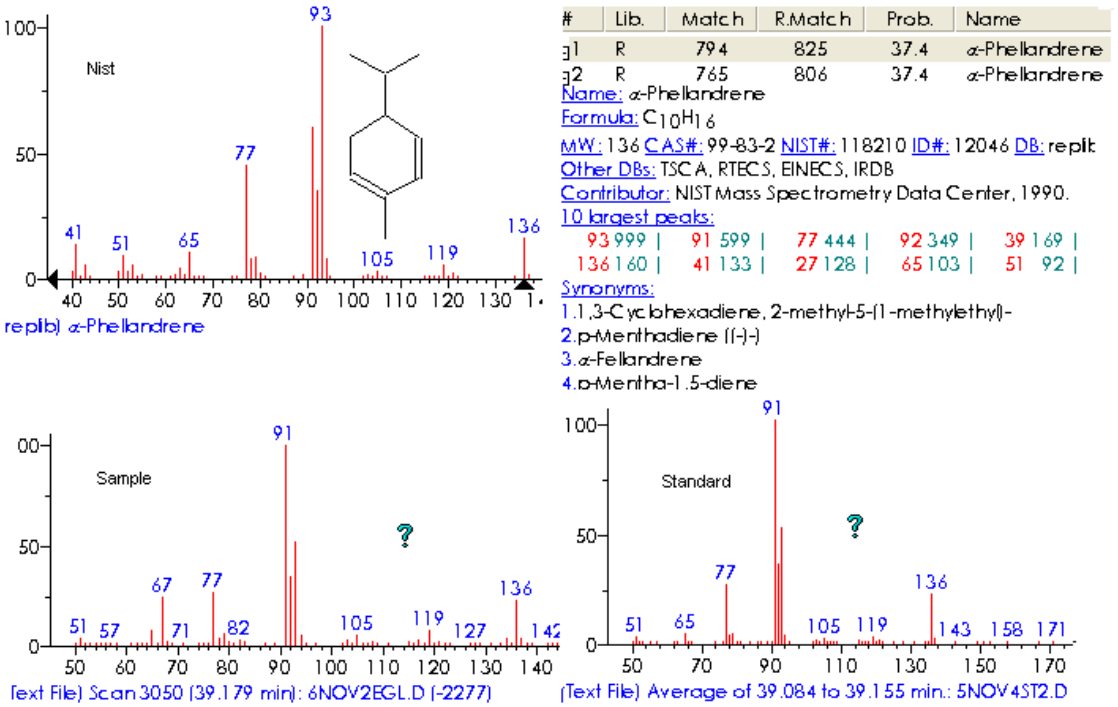

FIGURE A.22: Tentative identification of α-phelandrene and confirmation with standard

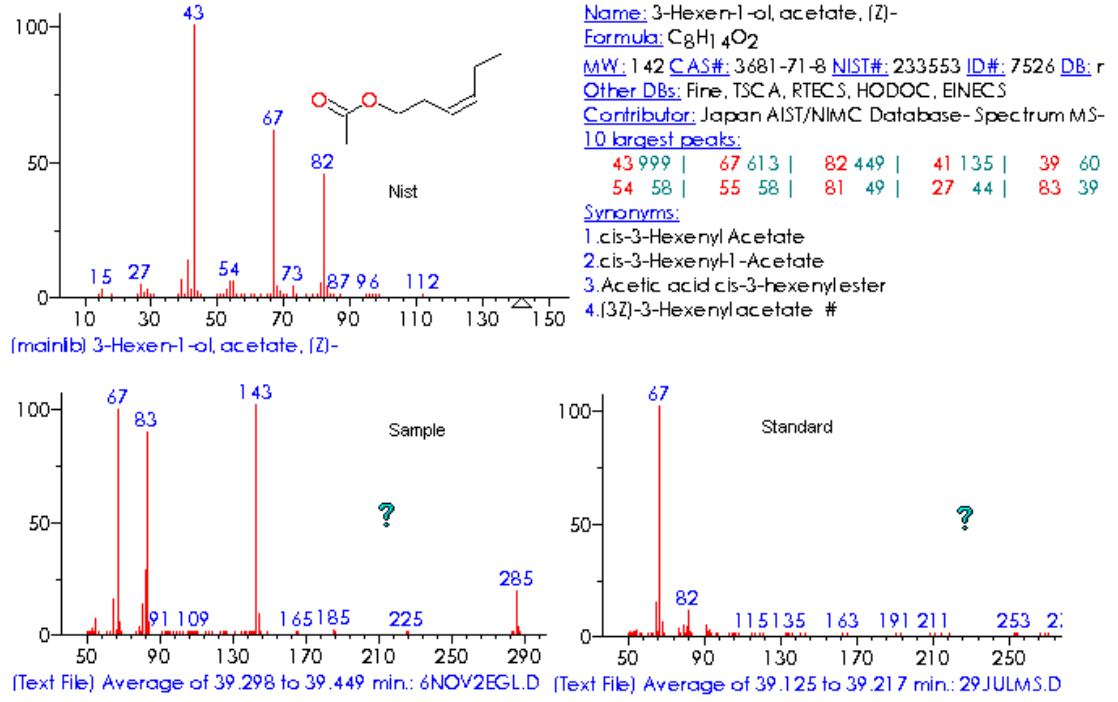

FIGURE A.23: Tentative identification of (Z)-3-hexenyl acetate and confirmation with standard. Notice an adduct formation effect occurred in the ion trap due to overload

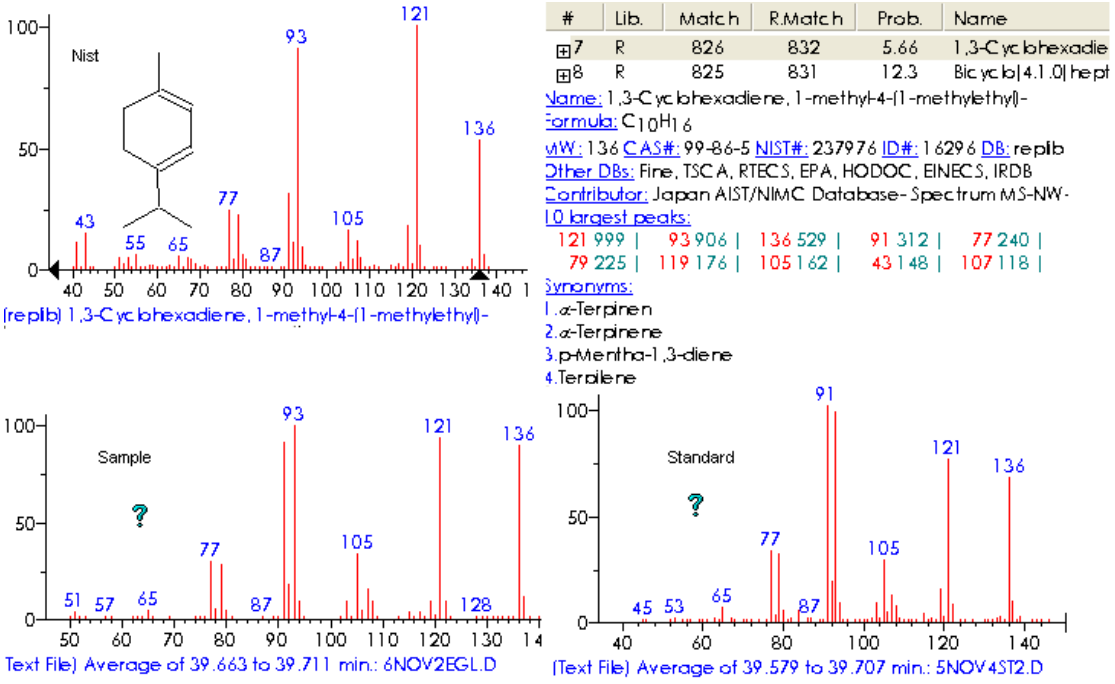

FIGURE A.24: Tentative identification of α-terpinene and confirmation with standard

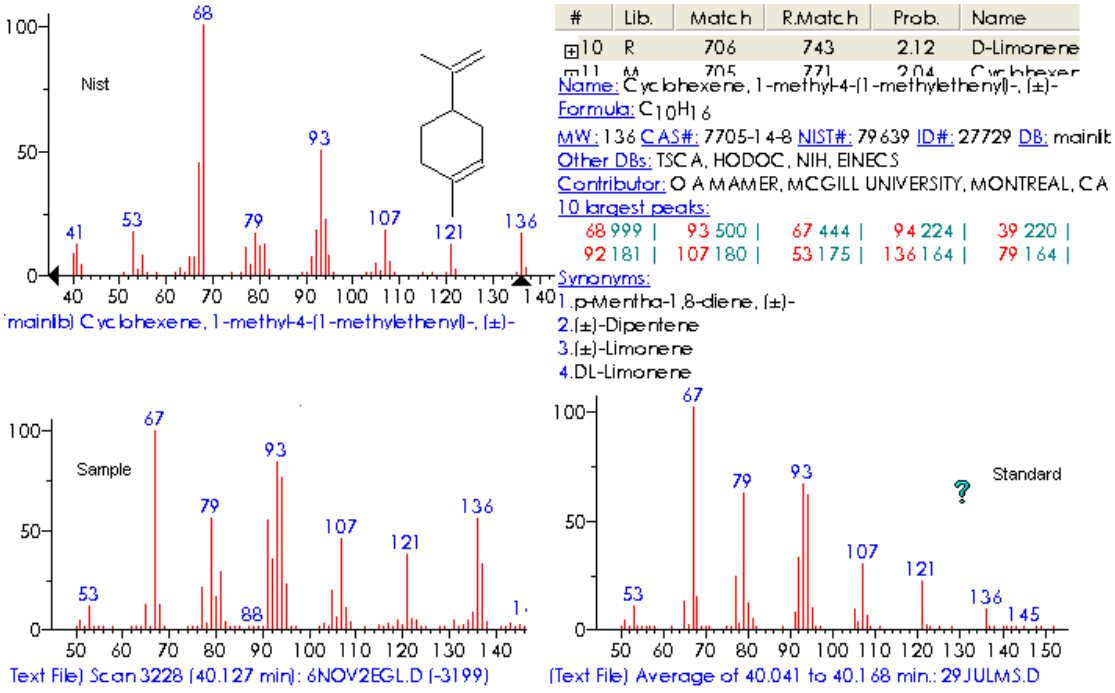

FIGURE A.25: Tentative identification of d-limonene and confirmation with standard

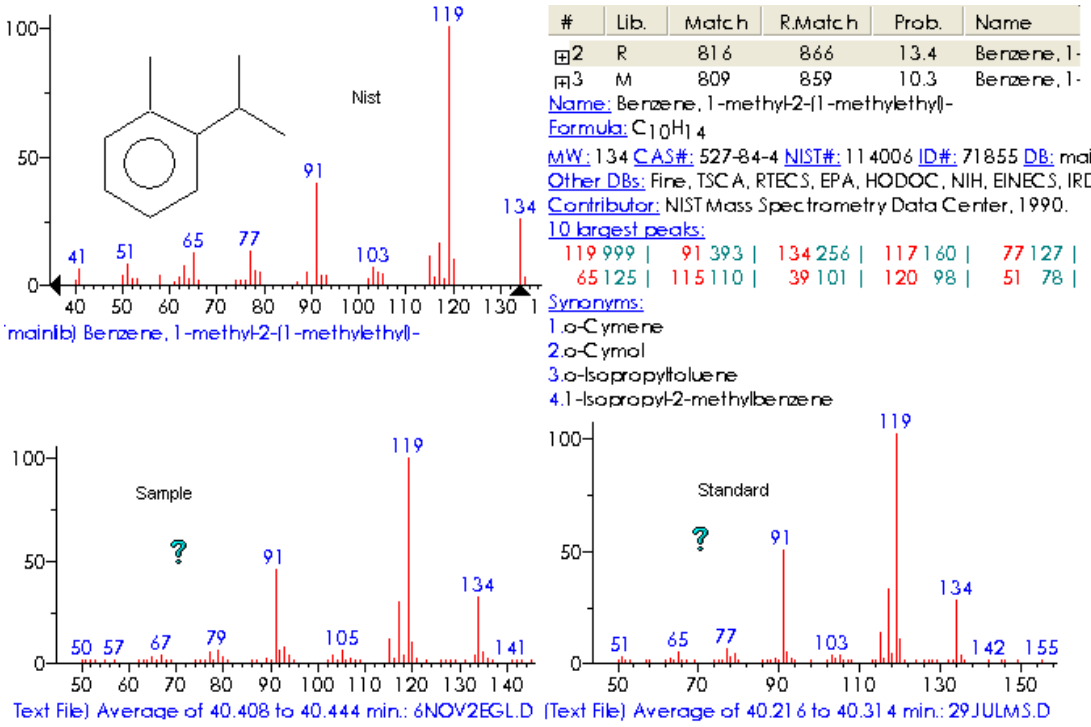

FIGURE A.26: Tentative identification of cymene and confirmation with standard

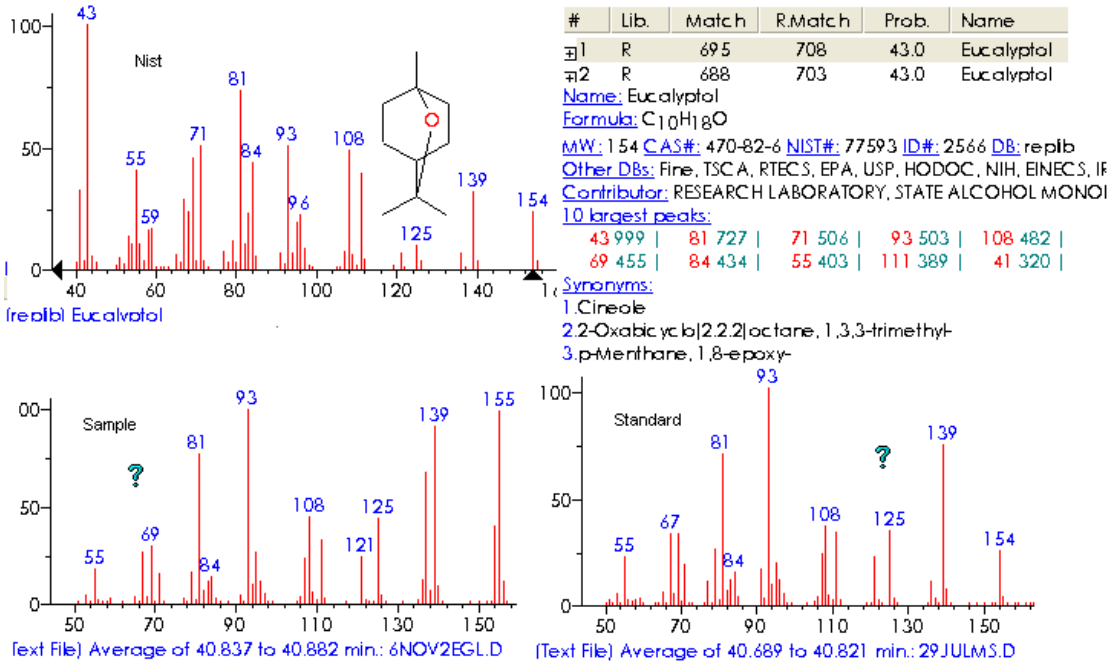

FIGURE A.27: Tentative identification of cineol and confirmation with standard

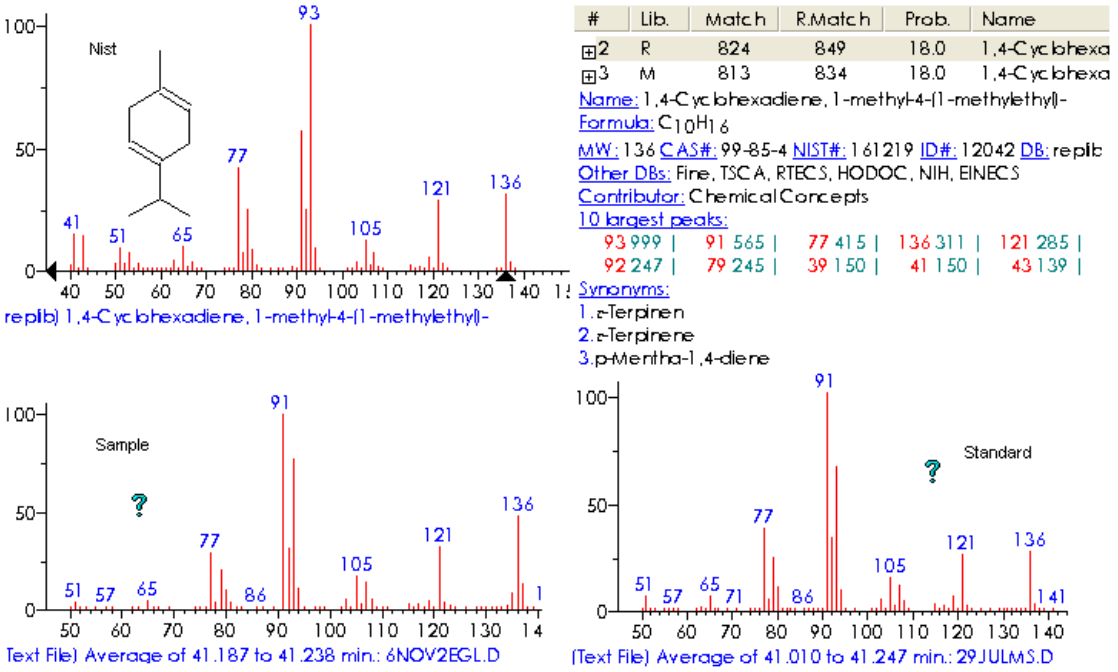

FIGURE A.28: Tentative identification of γ-terpinene and confirmation with standard

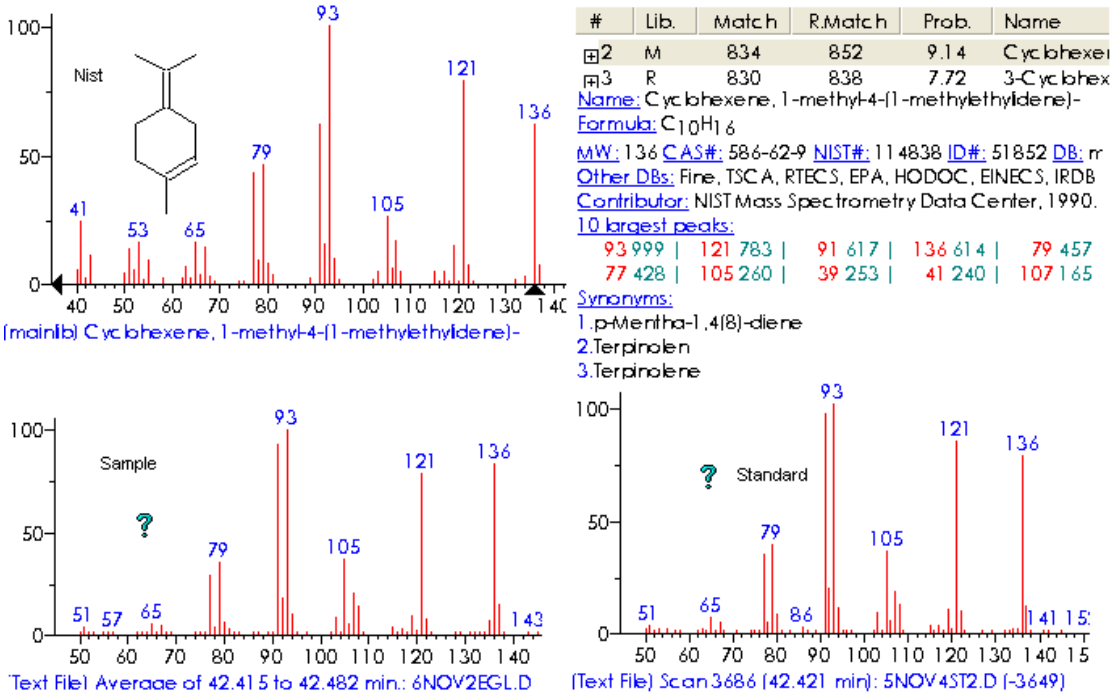

FIGURE A.29: Tentative identification of α-terpinolene and confirmation with standard

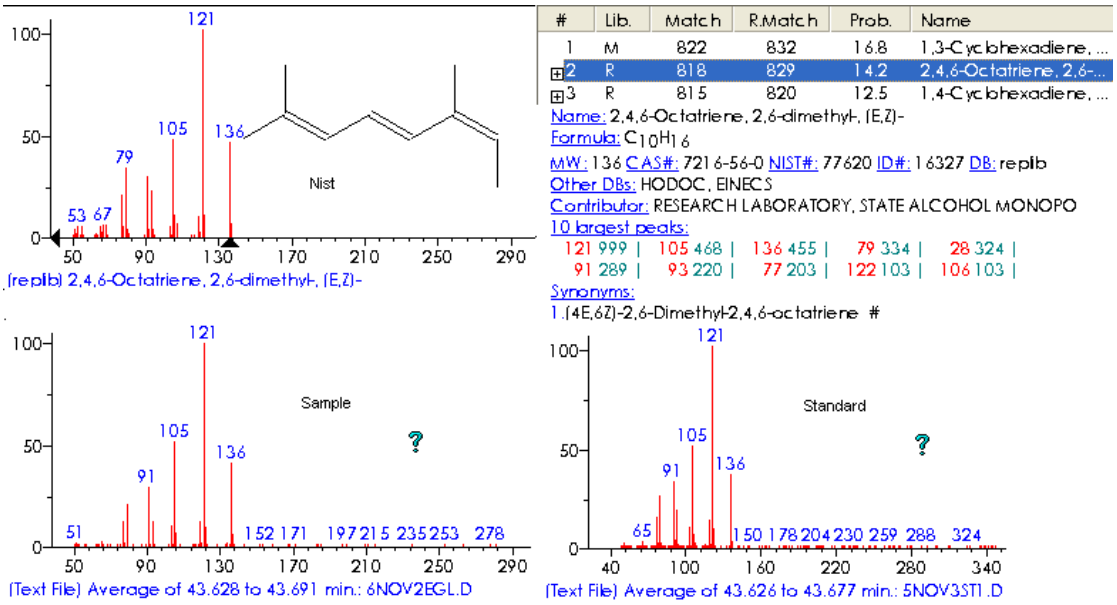

FIGURE A.30: Tentative identification of 2,4,6-Octatriene, 2,6-dimethyl-, (E,Z)- and confirmation with standard which was Ocimene

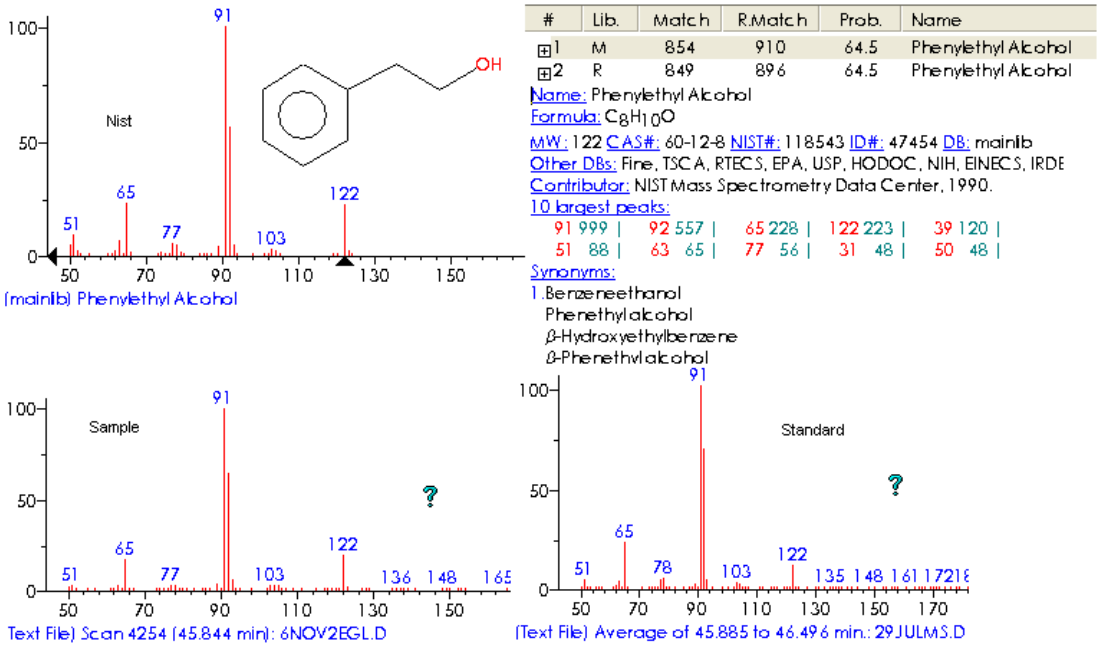

FIGURE A.31: Tentative identification of 2-phenylethanol and confirmation with standard

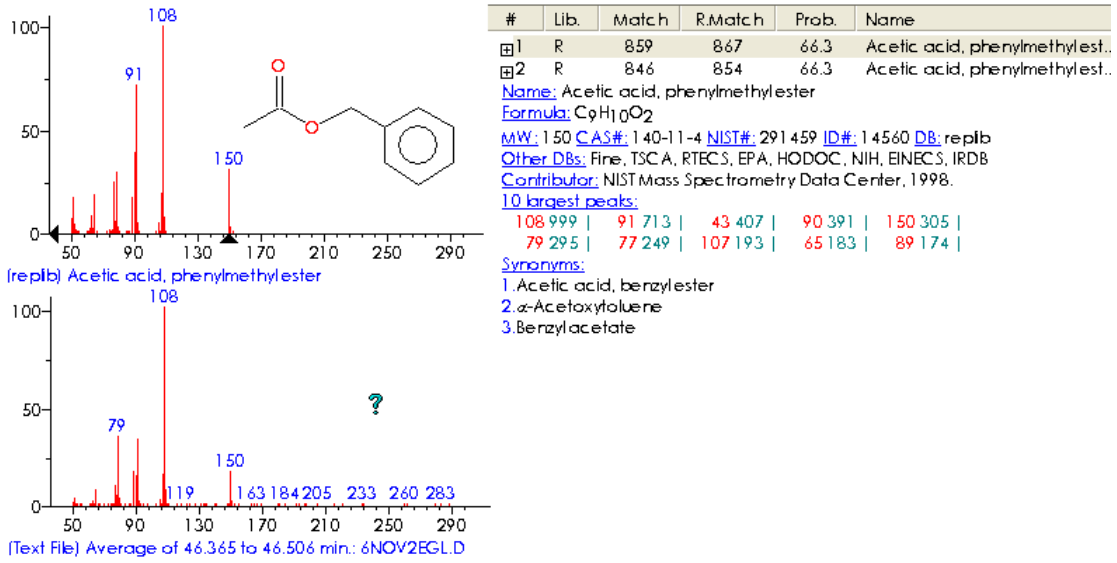

FIGURE A.32: Tentative identification of benzyl acetate

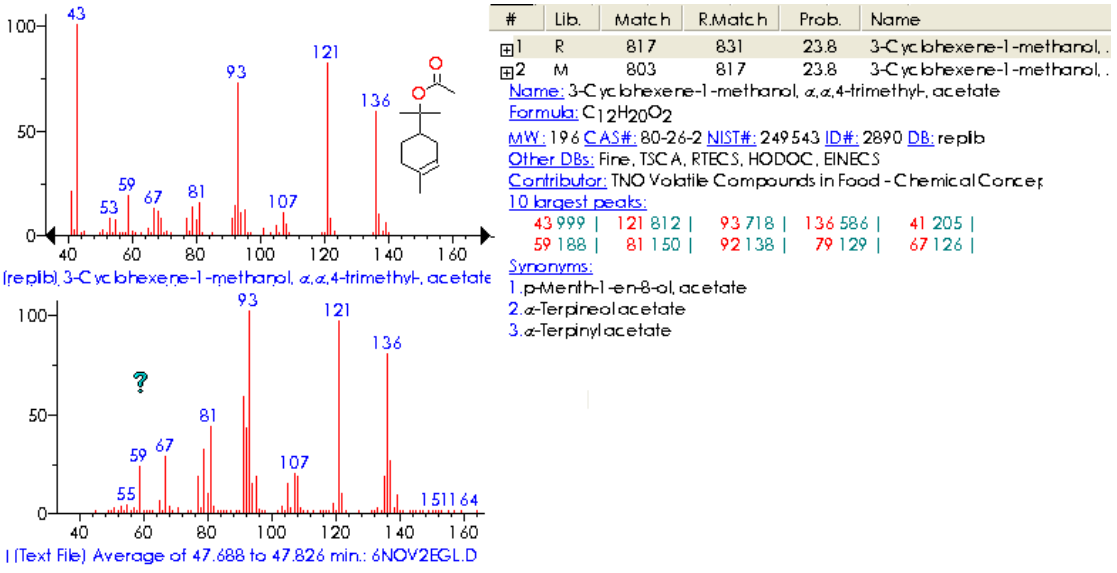

FIGURE A.33: Tentative identification of α-terpineol acetate

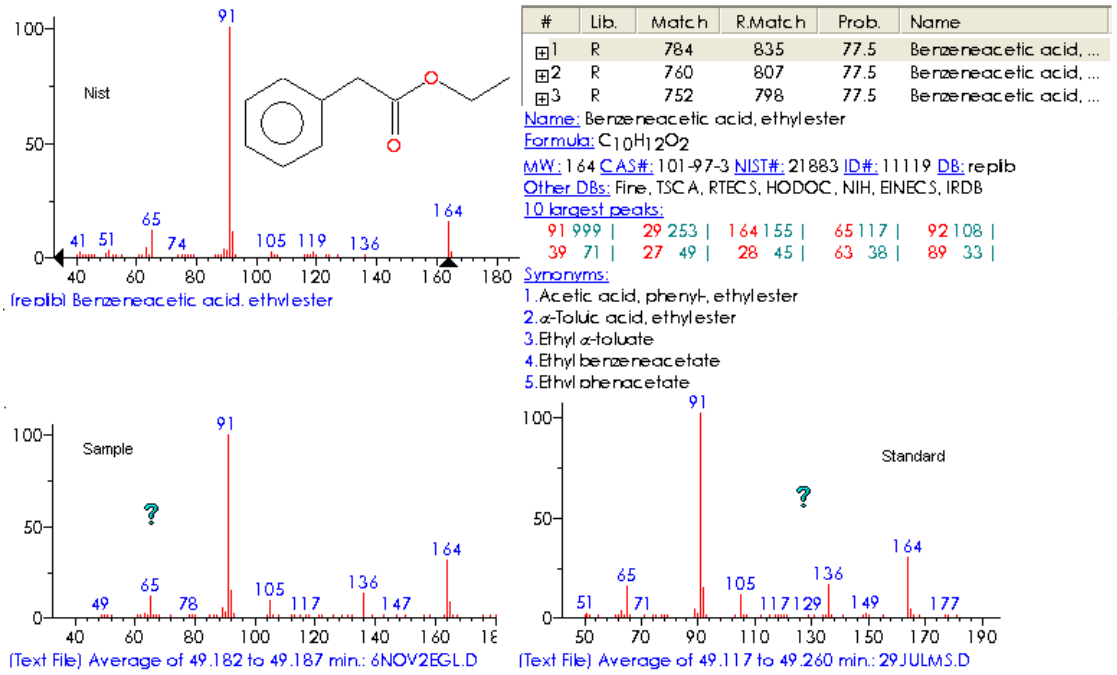

FIGURE A.34: Tentative identification of ethylphenylacetate and confirmation with standard

TABLE A.4: The differences that were observed between the retention indices for the 13 tentatively identified EAD active peaks (based on run 181 on GC-FID and run 6NOV2EGL)

Response #	GC-EAD Start	Apex	GC-MS Start	Apex	tentative identity	Start ΔKI	Apex ΔKI
1,2	840.75	842.55	843.26	845.10	4,4-dimethyl-2-pentene	2.52	2.55
3	907.27	912.02	908.22	912.35	(Z)-3-hexen-1-ol,(E)-2-hexenal	0.95	0.33
4	1034.06	1048.53	1033.38	1042.33	α-phelandrene,3-carene,α-terpinene	-0.68	-6.20
5	1058.33	1072.80	1057.57	1064.28	limonene,cymene	-0.76	-8.52
6	1078.78	1082.54	1077.32	1081.69	1,8-cineol	-1.46	-0.86
7	1090.37	1093.42	1085.19	1088.85	γ-terpinene	-5.18	-4.57
8	1120.97	1123.29	1114.59	1121.94	α-terpinolene	-6.38	-1.35
9	1146.25	1148.82	1147.17	1150.71	2,4,6-Octatriene, 2,6-dimethyl-, (E,Z)-	0.92	1.89
10	1210.81	1217.46	1209.06	1216.65	2-phenylethanol	-1.74	-0.81
11	1228.73	1231.96	1229.06	1233.77	benzyl acetate	0.33	1.81
12	1266.56	1272.39	1265.52	1273.10	α-terpineol acetate	-1.04	0.72
13	1308.56	1312.96	1311.75	1319.61	ethylphenylacetate (complex on ms)	3.19	6.65

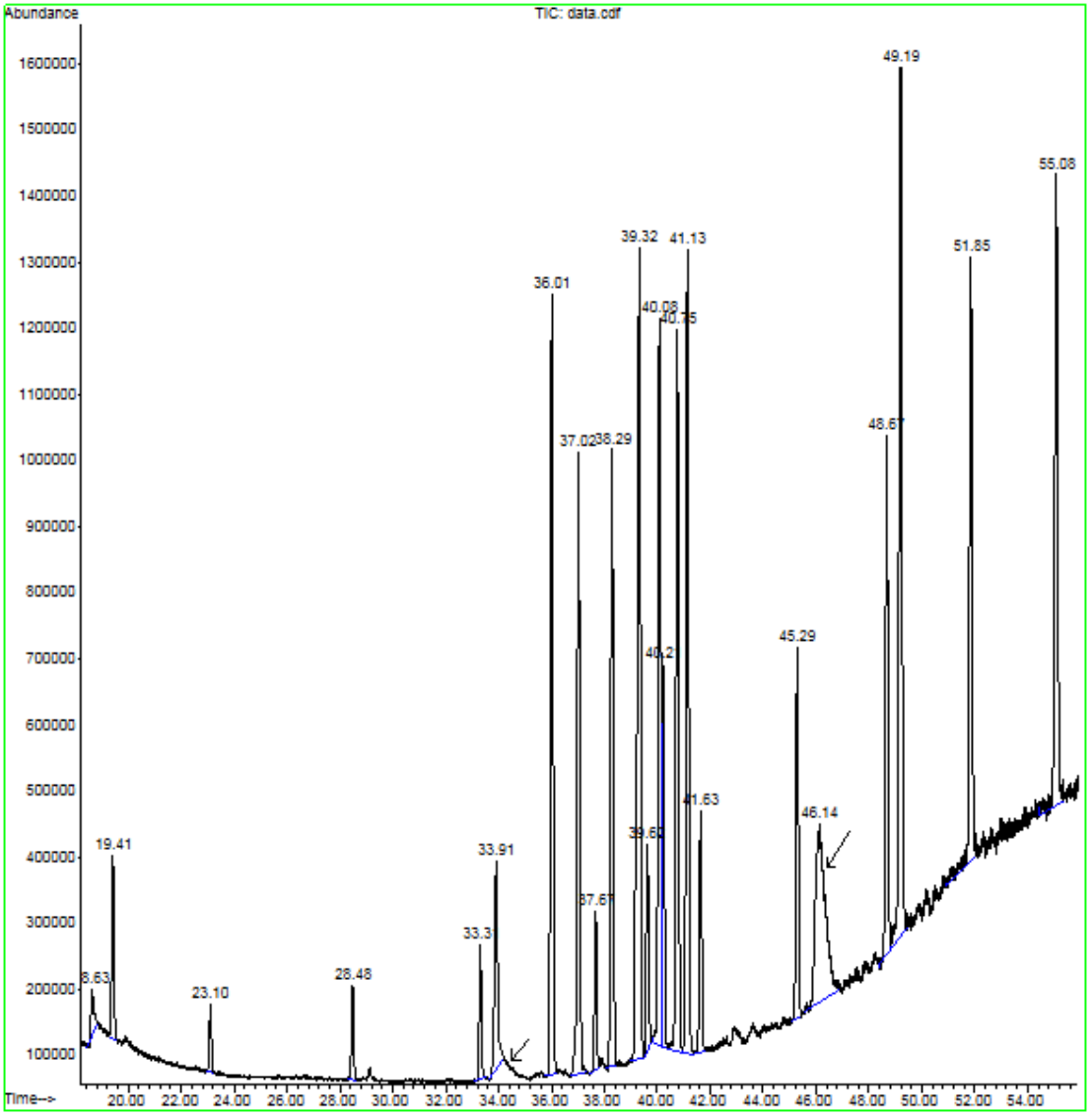

FIGURE A.35: GC-MS chromatogram of the standard compounds (44 ng) and n-alkanes (21 ng). Arrows indicate the two alcohols which were present in the standard mix. (z-3-hexen-1-ol Rt 33.19 and 2-phenyl ethanol Rt 46.14, Run name: 29Julms. 9.0 psi)

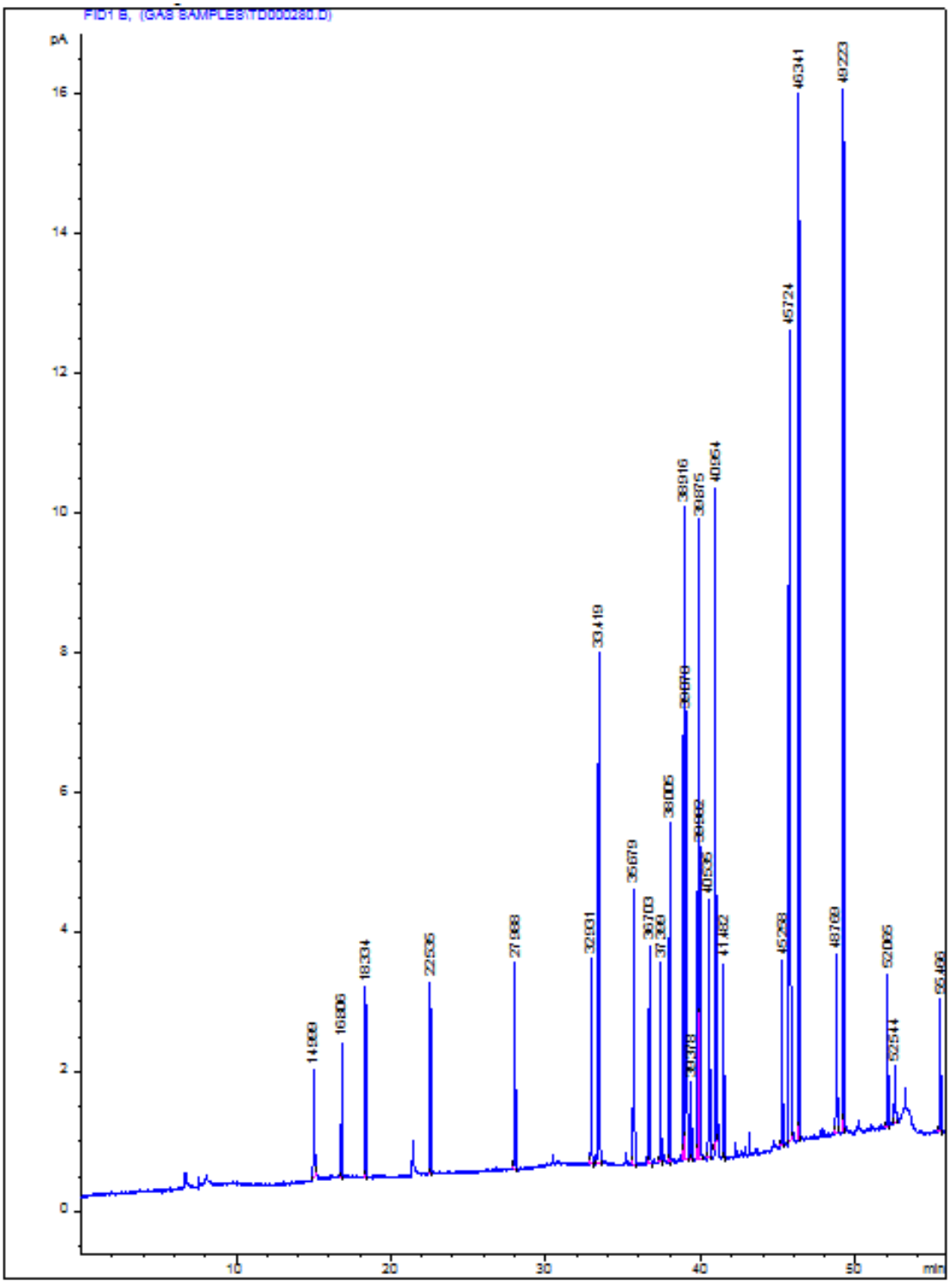

FIGURE A.36: GC-FID chromatogram of the standard compounds (370 ng) and n-alkanes (128 ng). Run 280 14.7 psi.

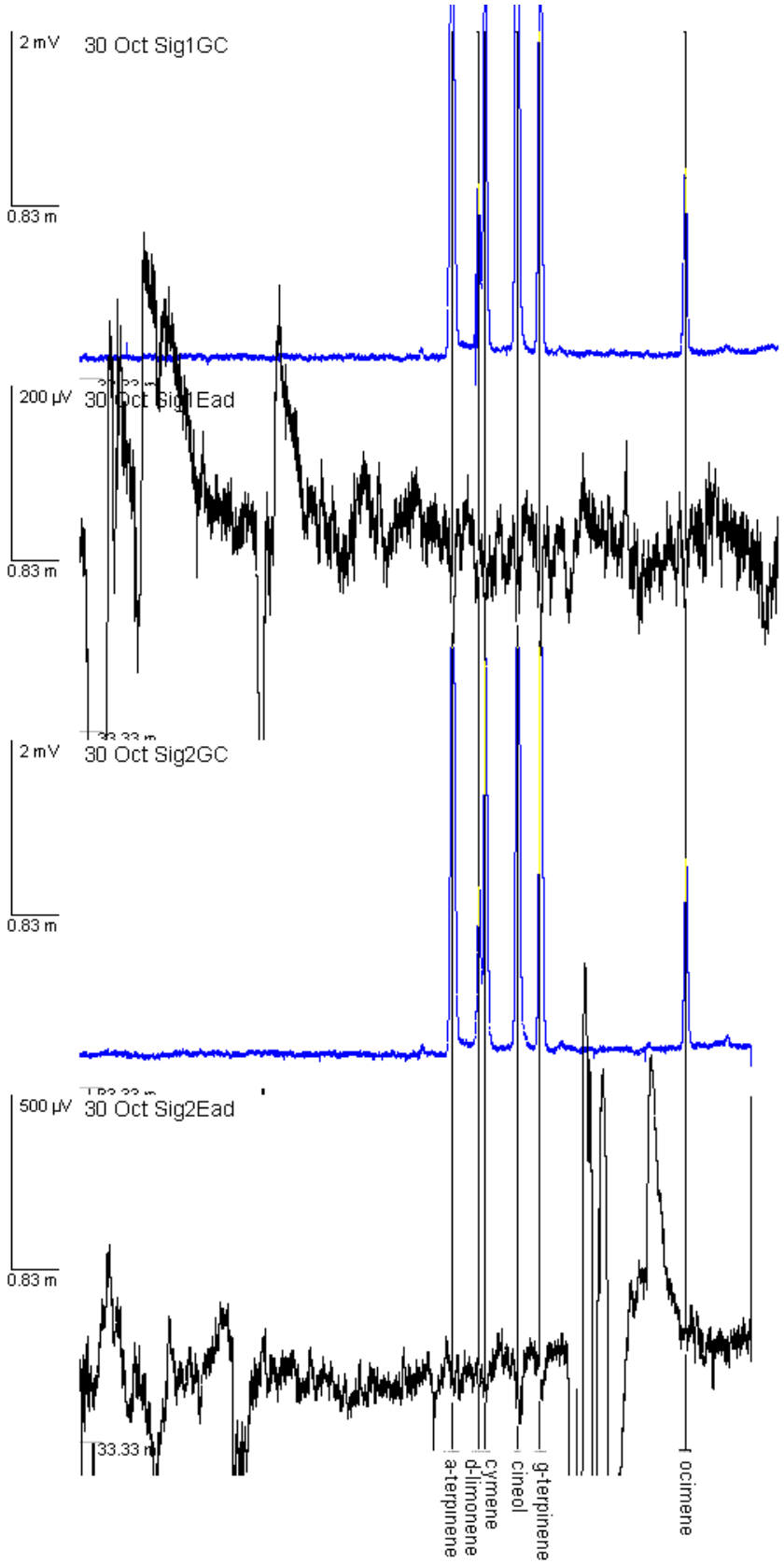

FIGURE A.37: GC-EAD responses to identified terpenes at low concentration (90 ng). Run 209 and 210.

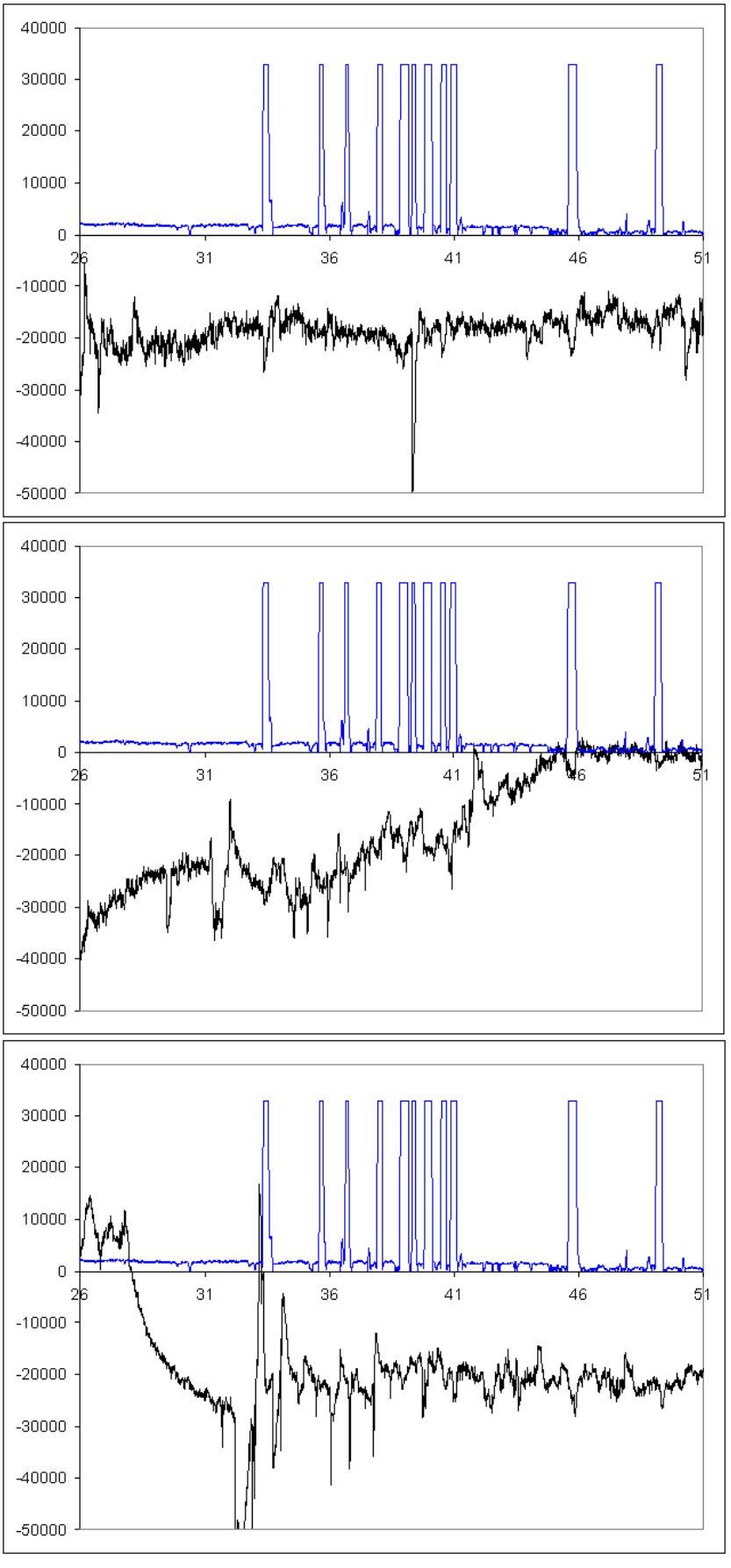

FIGURE A.38: GC-EAD responses to identified standards at high concentration (485 ng). Run 261 and 262.

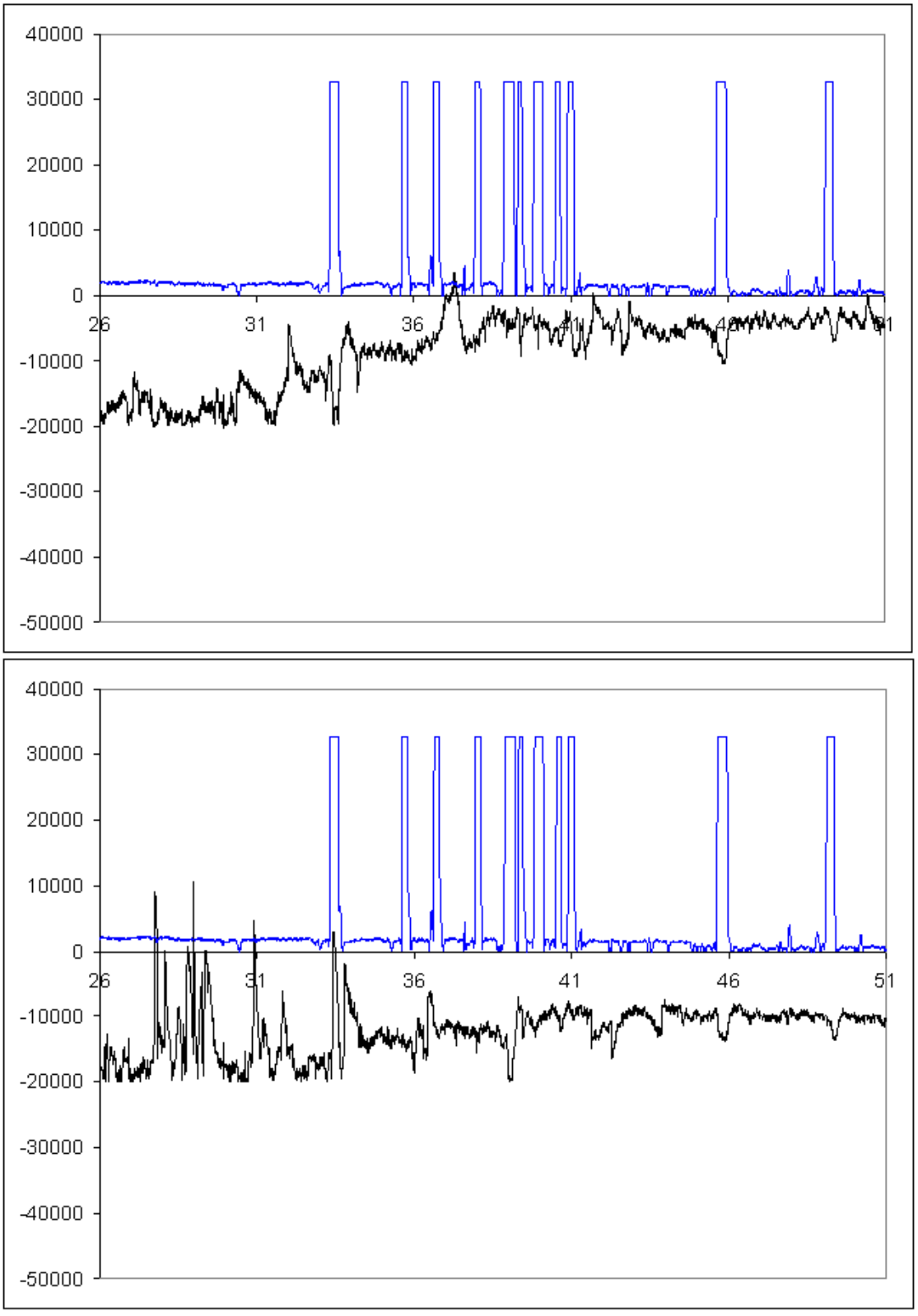

FIGURE A.39: GC-EAD responses to identified standards at high concentration (485 ng). Run 263 and 264.

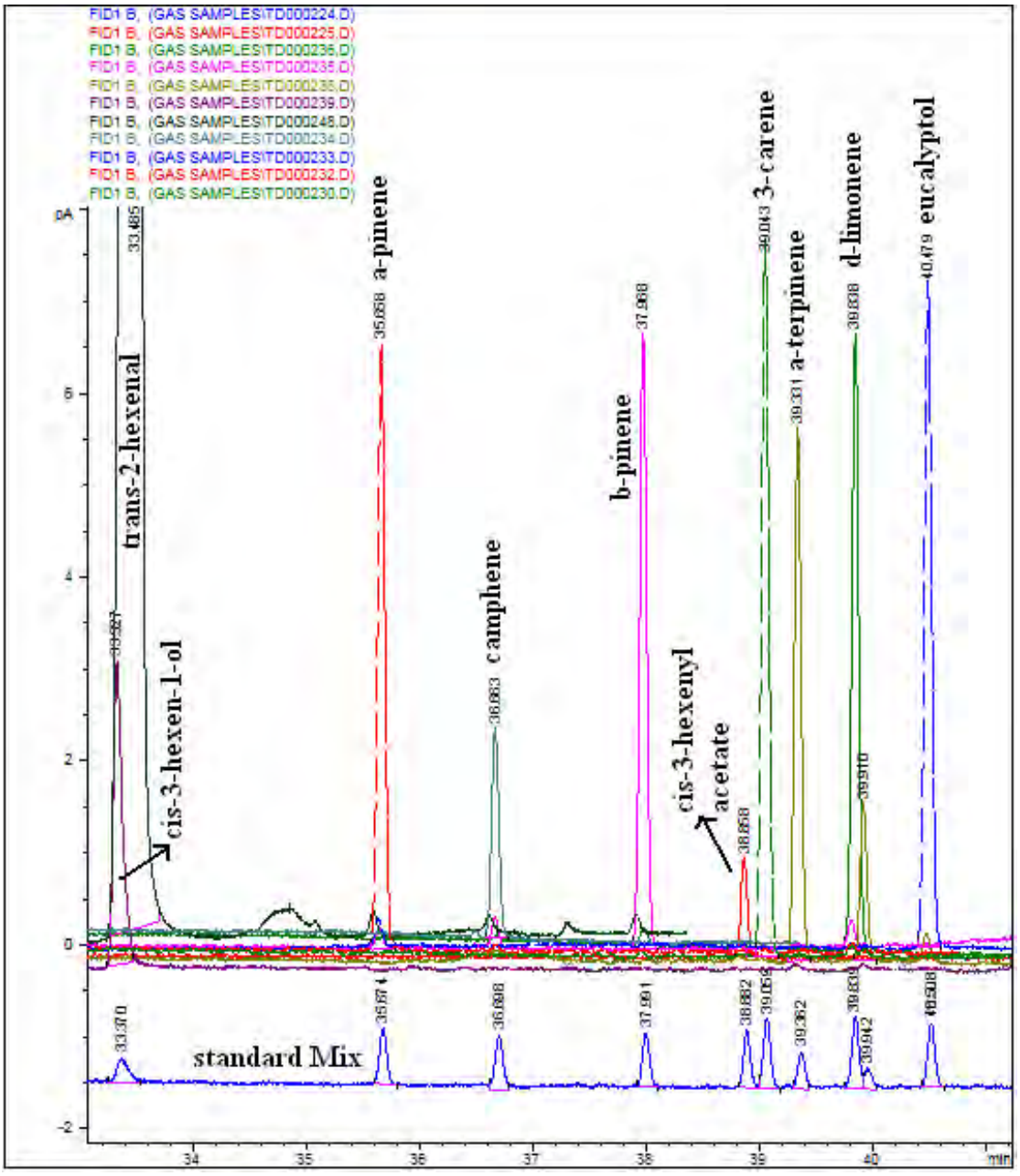

FIGURE A.40: The determination of elution order of standard compounds at 14.7 psi on the GC-EAD. Bottom a mixture made from the standards above.

Appendix B

TABLE B.1: Retention time (min) of standards based on peak start

	Run name	350	308	9OCTR2
	Instrument	GC-EAD	GC-EAD	GC-MS
Standard no	Compounds	RT liquid	RT thermal	RT thermal
1,2	(E)-2-hexenal, (Z)-3-hexen-1-ol	23.92	29.80	30.70
3	a-pinene	26.02	31.92	32.67
4	camphene	26.96	32.88	33.66
5	b-pinene	28.14	34.16	34.91
6,7	(Z)-3-hexenyl acetate, 3-carene	29.18	35.24	35.97
8	a-terpinene	29.51	35.57	36.28
9,10	m-cymene, d-limonene	29.85	35.99	36.64
-	cymene	30.17	36.19	36.94
11	eucalyptol	30.58	36.65	37.29
12	g-terpinene	31.04	37.13	37.69
13	2-phenylethanol	35.61	41.73	42.70
14	benzyl acetate	36.21	42.40	43.02
15	ethyl phenylacetate	39.01	45.21	45.76
16	terpenyl acetate	42.22	48.39	48.86

TABLE B.2: Retention index of standards based on peak start time

	Run name	350	308	9OCTR2
	Instrument	GC-EAD	GC-EAD	GC-MS
Standard no	Compound	RI liquid	RI thermal	RI thermal
1,2	(E)-2-hexenal, (Z)-3-hexen-1-ol	907	908	910
3	a-pinene	957	956	956
4	camphene	979	978	979
5	b-pinene	1008	1008	1008
6,7	(Z)-3-hexenyl acetate, 3-carene	1034	1036	1035
8	a-terpinene	1043	1044	1043
9,10	m-cymene, d-limonene	1052	1054	1053
-	cymene	1060	1059	1060
11	eucalyptol	1070	1071	1069
12	g-terpinene	1082	1083	1079
13	2-phenylethanol	1206	1206	1217
14	benzyl acetate	1223	1226	1227
15	ethyl phenylacetate	1306	1308	1309
16	terpenyl acetate	1406	1408	1409

TABLE B.3: Retention time (min) of standards based on peak apex

	Run name	350	308	9OCTR2
	Instrument	GC-EAD	GC-EAD	GC-MS
Standard no	Compounds	RT liquid	RT thermal	RT thermal
1,2	(Z)-3-hexen-1-ol, (E)-2-hexenal	24.07	29.87	30.81
3	a-pinene	26.13	32.00	32.81
4	camphene	27.07	32.97	33.77
5	b-pinene	28.30	34.24	35.03
6,7	(Z)-3-hexenyl acetate, 3-carene	29.33	35.32	36.09
8	a-terpinene	29.64	35.65	36.41
9,10	m-cymene, d-limonene	30.11	36.12	36.85
-	cymene	30.23	36.24	37.00
11	eucalyptol	30.72	36.74	37.48
12	g-terpinene	31.16	37.20	37.92
13	2-phenylethanol	35.73	41.83	43.15
14	benzyl acetate	36.38	42.48	43.15
15	ethyl phenylacetate	39.19	45.30	45.90
16	terpenyl acetate	42.37	48.48	48.98

TABLE B.4: Retention index of standards based on peak apex

	Run name	350	308	9OCTR2
	Instrument	GC-EAD	GC-EAD	GC-MS
Standard no	Compound	RI liquid	RI thermal	RI thermal
1,2	(Z)-3-hexen-1-ol, (E)-2-hexenal	910	910	912
3	a-pinene	959	958	959
4	camphene	982	980	981
5	b-pinene	1012	1011	1011
6,7	(Z)-3-hexenyl acetate, 3-carene	1038	1038	1038
8	a-terpinene	1046	1046	1047
9,10	m-cymene, d-limonene	1058	1058	1058
-	cymene	1061	1061	1062
11	eucalyptol	1074	1073	1074
12	g-terpinene	1085	1085	1085
13	2-phenylethanol	1209	1209	1226
14	benzyl acetate	1229	1228	1231
15	ethyl phenylacetate	1311	1311	1314
16	terpenyl acetate	1411	1411	1413

TABLE B.5: Identities of the compounds associated with EAD active peaks and the retention indices for these peaks for the three tested *Eucalyptus* species on the GC-EAD. These retention times and indeces are based on peak apex time.

			E. globulus		*E. viminalis*		*E. citriodora*	
Peak No	Standard No	Compound	Rt(min)	KI	Rt(min)	KI	Rt(min)	KI
1		C6 alcohol	26.66	842.28	26.67	842.29	26.62	841.28
2	1	(E)-2-hexenal	30.01	912.73	29.87	909.38	29.87	909.30
	2	(Z)-3-hexen-1-ol	present	present	-	-	-	-
	3	α-pinene	32.00	958.28	31.99	957.77	31.99	957.86
	4	camphene	-	-	-	-	-	-
3	5	β-pinene	34.24	1010.38	-	-	-	-
4	6	3-carene	-	-	-	-	-	-
	7	(Z)-3-hexenyl acetate	35.55	1043.28	35.44	1040.11	35.31	1036.90
	8	α-terpinene	present	present	35.70	1046.66	35.65	1045.41
5	10	limonene	36.32	1062.45	36.22	1059.80	36.13	1057.39
		cymene	present	present	36.35	1062.90	36.25	1060.62
6	11	eucalyptol	36.85	1075.90	36.81	1074.66	36.75	1072.99
7	12	γ-terpinene	37.25	1085.85	37.24	1085.20	37.25	1085.57
8	13	2-phenylethanol	41.81	1208.77	41.83	1209.02	-	-
9	14	benzyl acetate	42.45	1227.42	-	-	-	-
10	15	ethyl phenylacetate	45.27	1309.96	-	-	-	-
	16	terpenyl acetate	48.60	1414.74	-	-	-	-

TABLE B.6: Identities of the compounds associated with EAD active peaks and the retention indices for these peaks for the three tested *Eucalyptus* species on the GC-MS. These retention times and indeces are based on peak apex time.

			E. globulus		*E. viminalis*		*E. citriodora*	
Peak No	Standard No	Compound	Rt(min)	KI	Rt(min)	KI	Rt(min)	KI
1		C6 alcohol	27.63	844.30	27.63	844.16	27.62	843.95
2	1	(E)-2-hexenal	30.82	912.51	30.83	912.70	30.82	912.42
	2	(Z)-3-hexen-1-ol	present	present	-	-	-	-
	3	α-pinene	32.83	959.27	32.83	959.11	32.82	958.94
	4	camphene	-	-	-	-	-	-
3	5	β-pinene	35.05	1012.01	-	-	-	-
4	6	3-carene	-	-	-	-	-	-
	7	(Z)-3-hexenyl acetate	36.18	1040.66	36.14	1039.64	36.11	1038.92
	8	α-terpinene	36.44	1047.31	36.43	1047.11	36.41	1046.67
5	10	limonene	36.93	1059.85	36.89	1058.86	36.87	1058.30
		cymene	present	present	37.04	1062.58	37.02	1062.07
6	11	eucalyptol	37.53	1075.17	37.51	1074.64	37.50	1074.31
7	12	γ-terpinene	37.95	1085.85	37.94	1085.65	37.94	1085.50
8	13	2-phenylethanol	43.05	1227.67	-	-	-	-
9	14	benzyl acetate	43.17	1231.13	-	-	-	-
10	15	ethyl phenylacetate	45.92	1314.13	-	-	-	-
	16	terpenyl acetate	49.04	1414.66	-	-	-	-

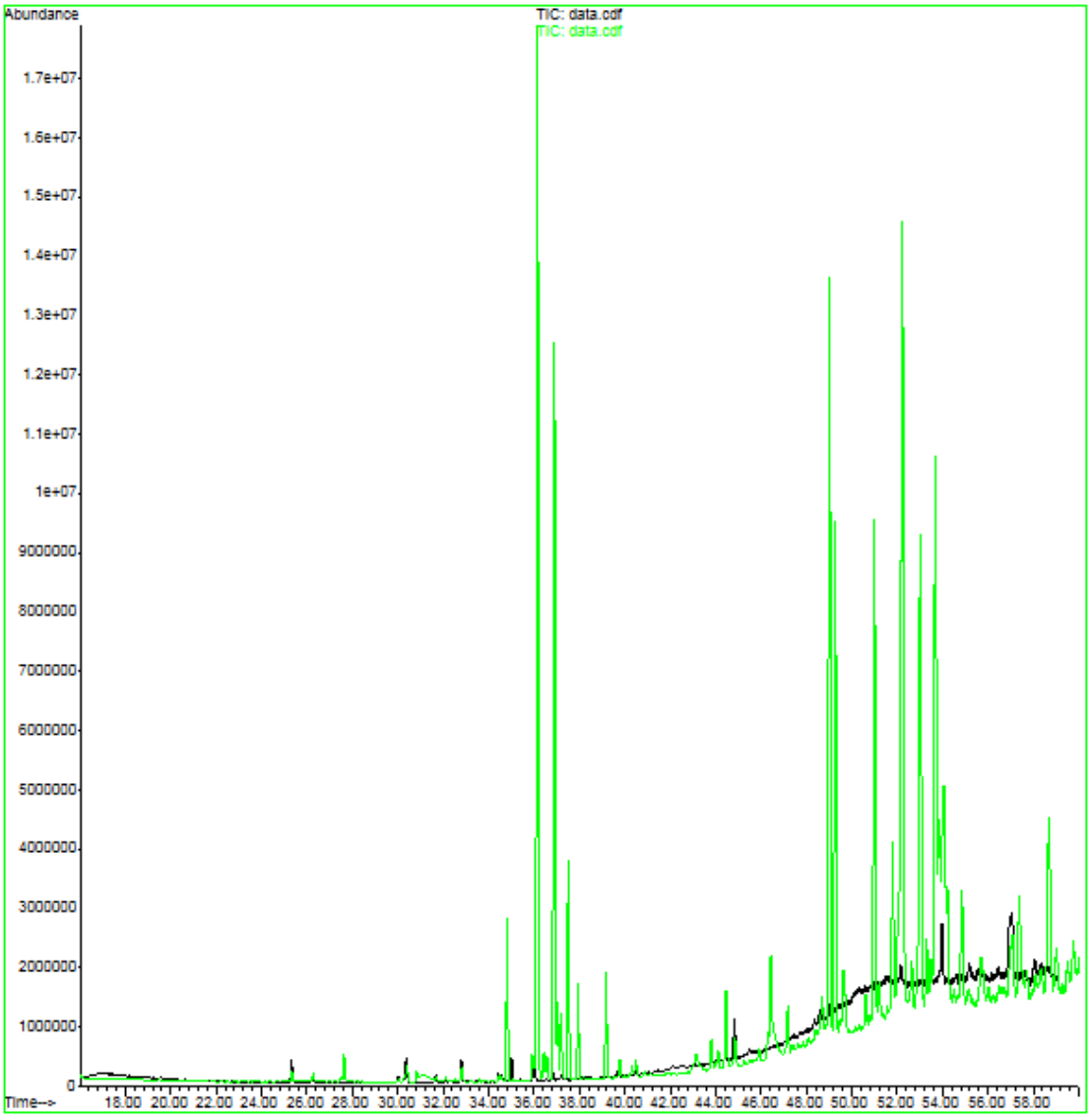

FIGURE B.1: Sample blank (Run: 9OCTR1) with a 43:1 split ratio at 16.0 psi on the GC-MS system compared to *E. globulus* volatile profile (Run: 9OCTR7).

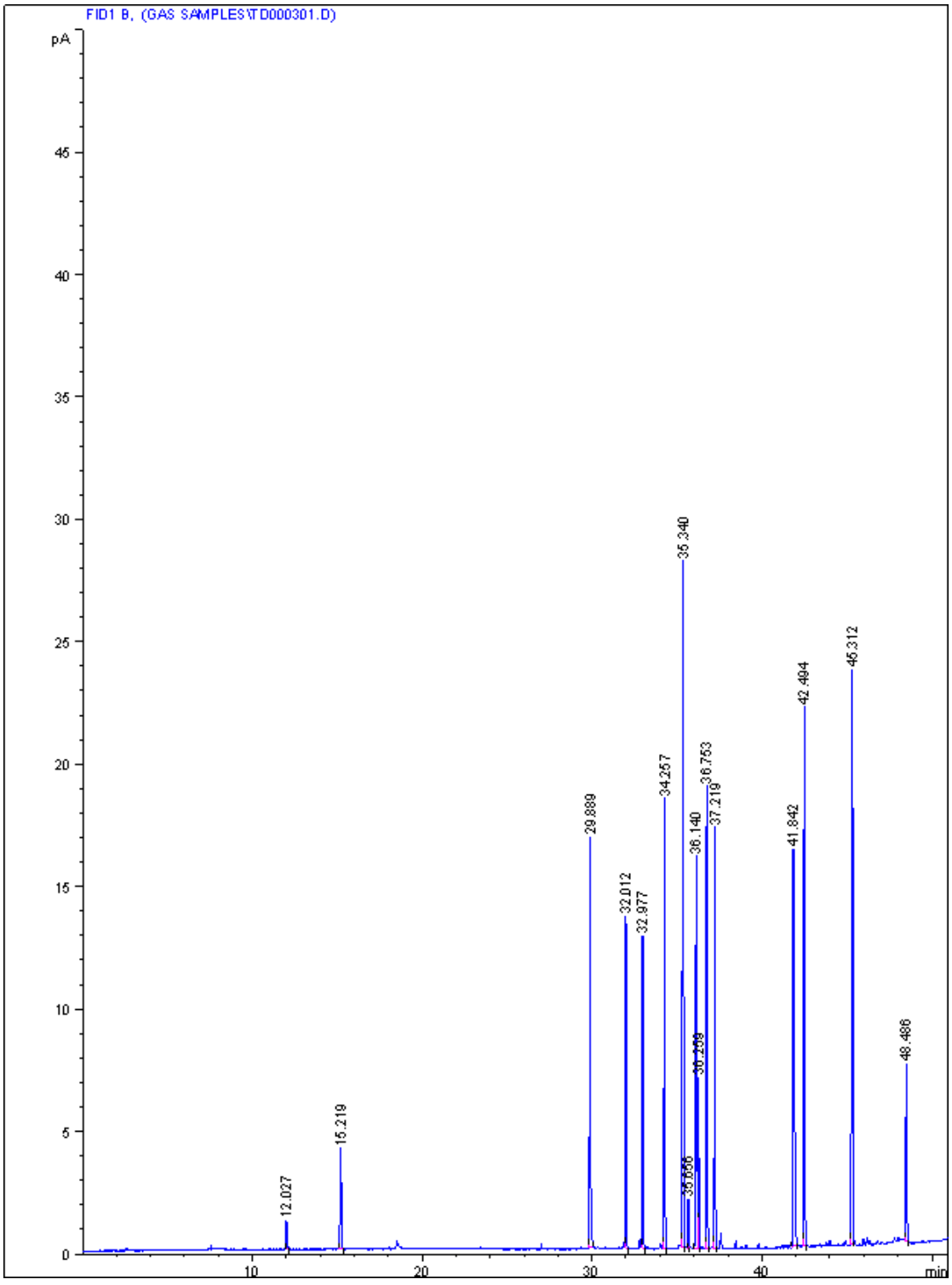

FIGURE B.2: GC-FID chromatogram of standard compounds(170 ng) on 21Sep2009 at 20.2psi

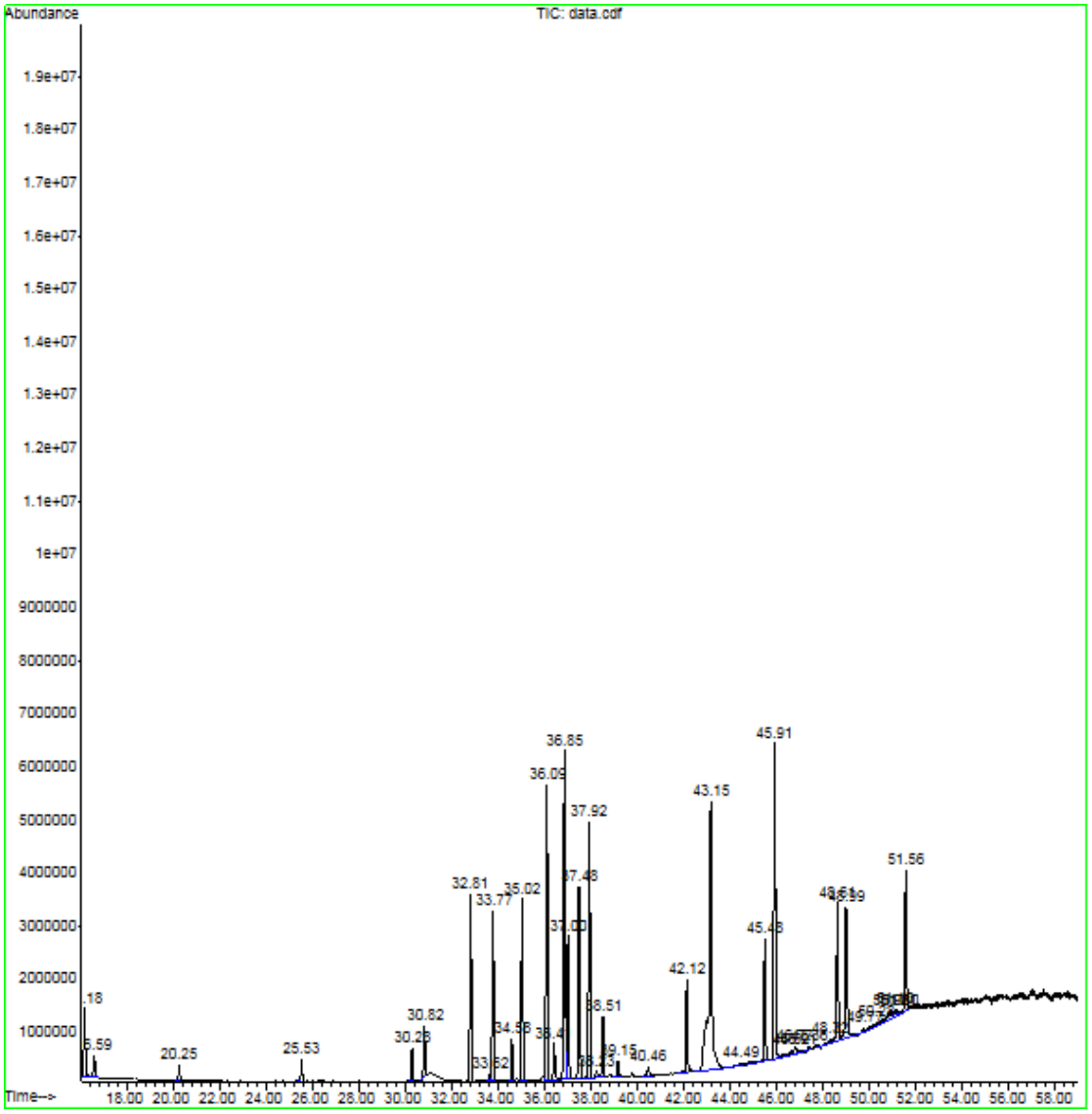

FIGURE B.3: GC-MS chromatogram of standard compounds(62 ng) and n-alkanes C5-C15 (32ng) on 9Oct2009 at 16.0 psi

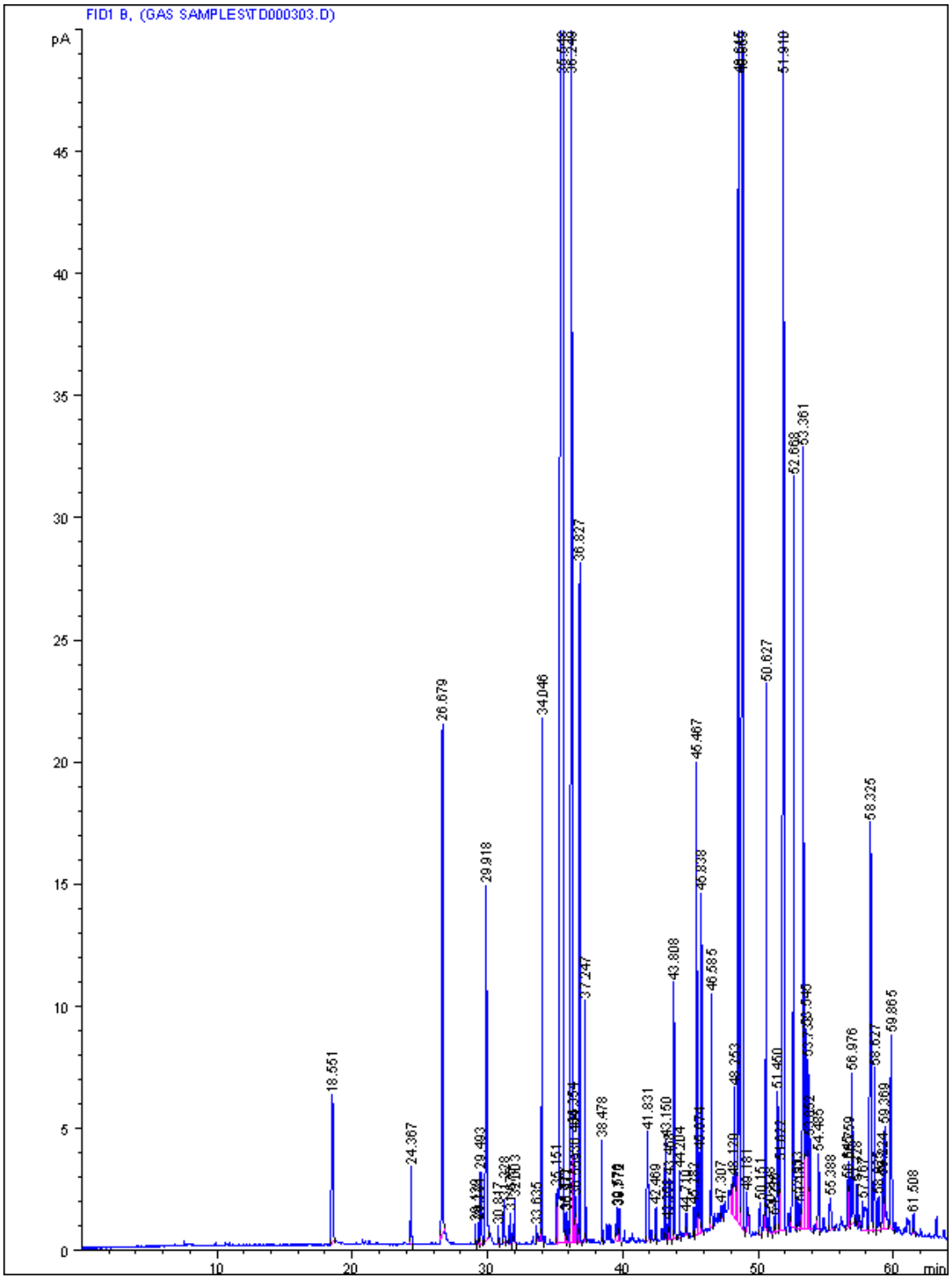

FIGURE B.4: FID chromatogram of *E. globulus* volatiles at 20.2 psi with 17.3:1 split ratio. Run 303

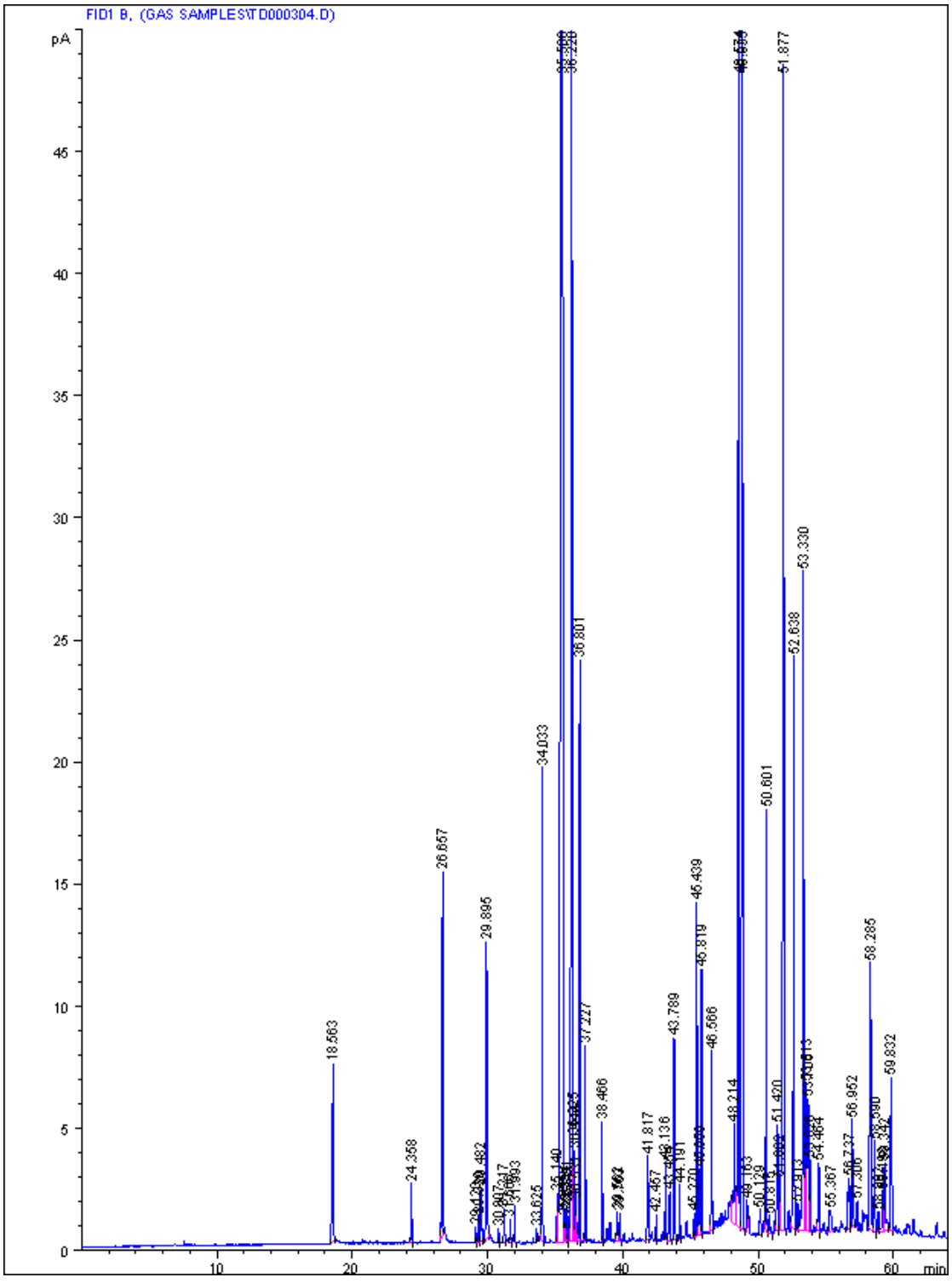

FIGURE B.5: FID chromatogram of *E. globulus* volatiles at 20.2 psi with 17.3:1 split ratio. Run 304

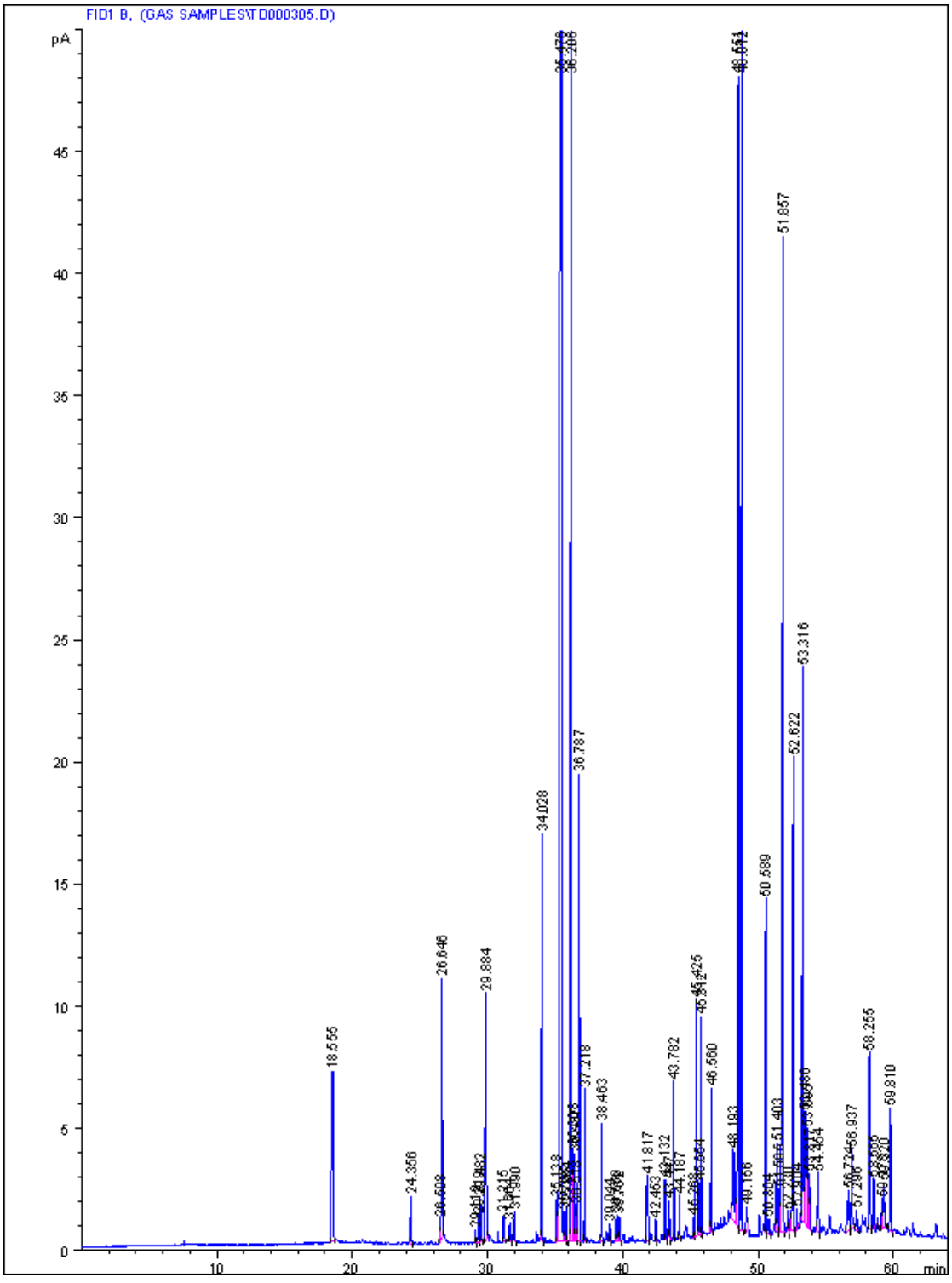

FIGURE B.6: FID chromatogram of *E. globulus* volatiles at 20.2 psi with 17.3:1 split ratio. Run 305

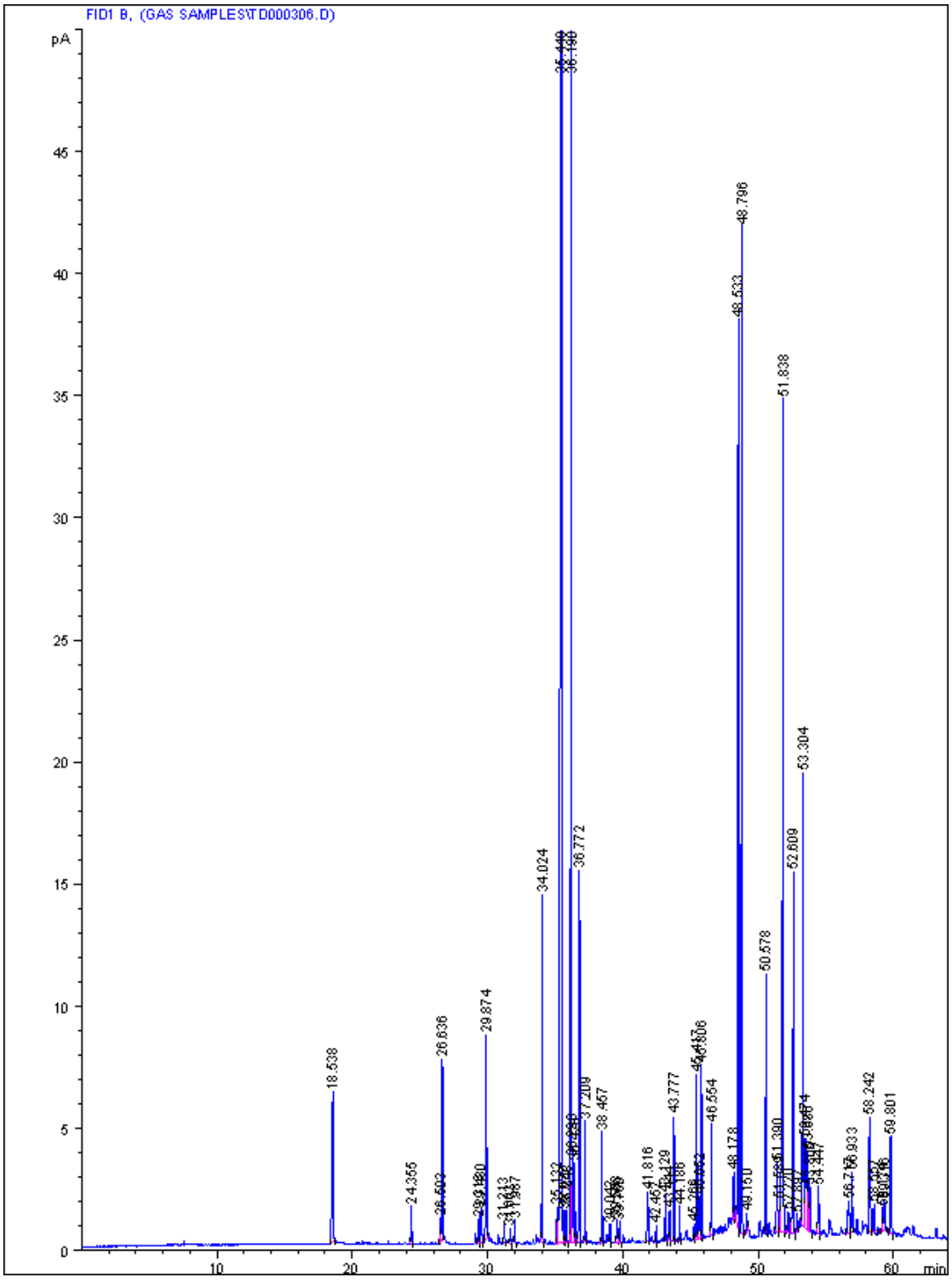

FIGURE B.7: FID chromatogram of *E. globulus* volatiles at 20.2 psi with 17.3:1 split ratio. Run 306

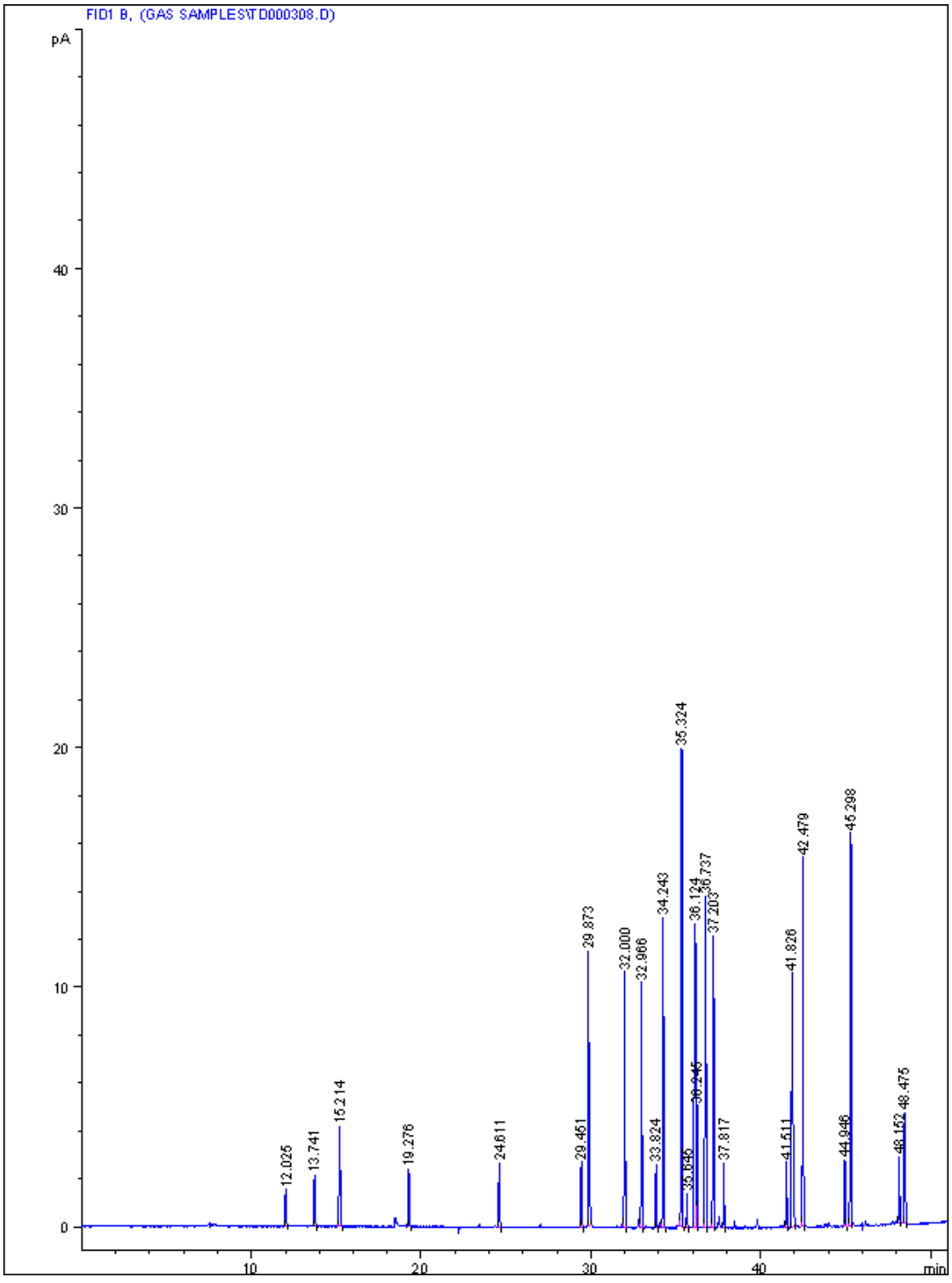

FIGURE B.8: Standard compounds (170 ng) and n-alkanes c5-c15 (42ng): 22Sep2009 at 20.2 psi on the GC-FID Run 308

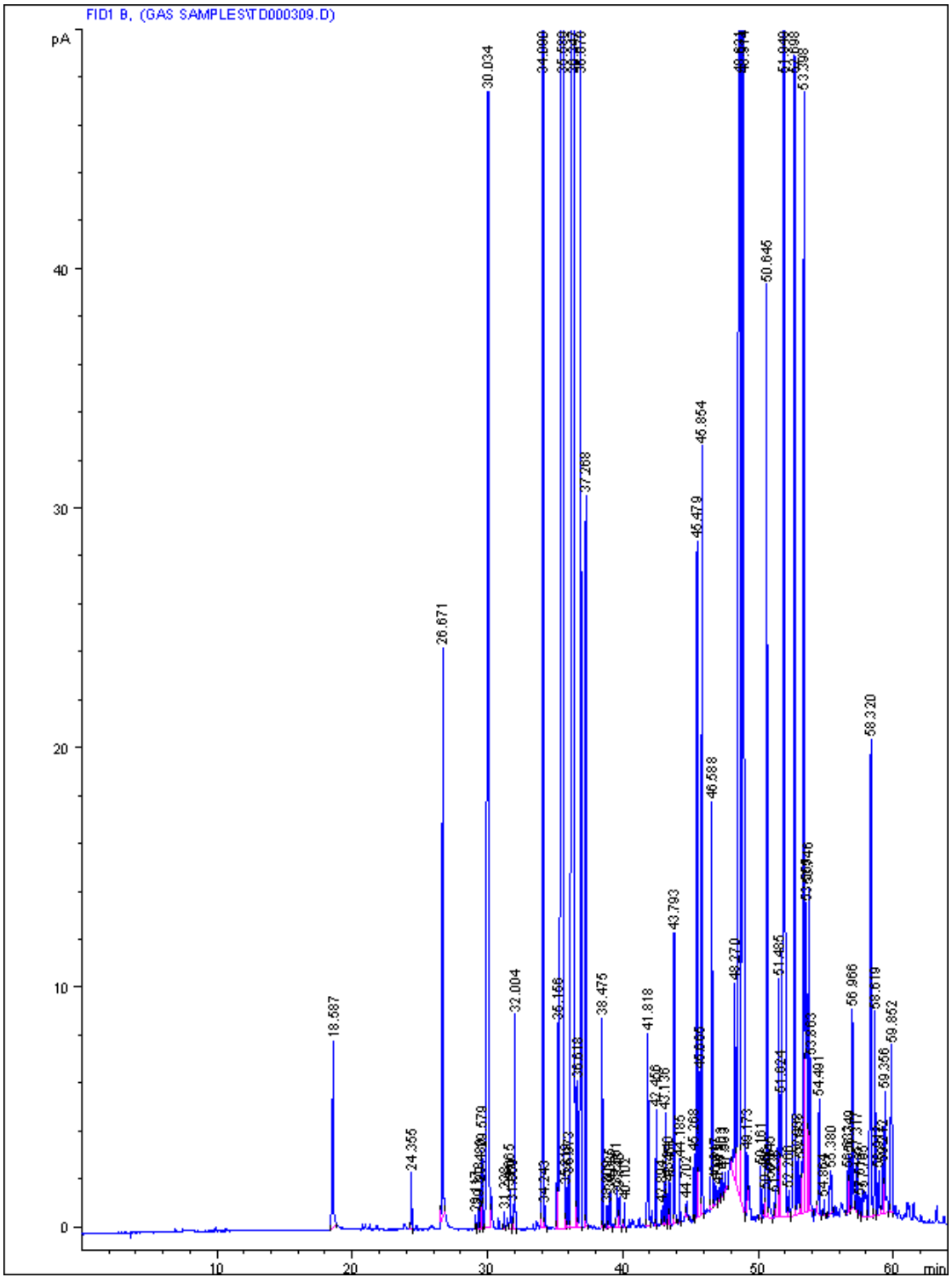

FIGURE B.9: FID chromatogram of *E. globulus* volatiles at 20.2 psi with 17.3:1 split ratio. Run 309

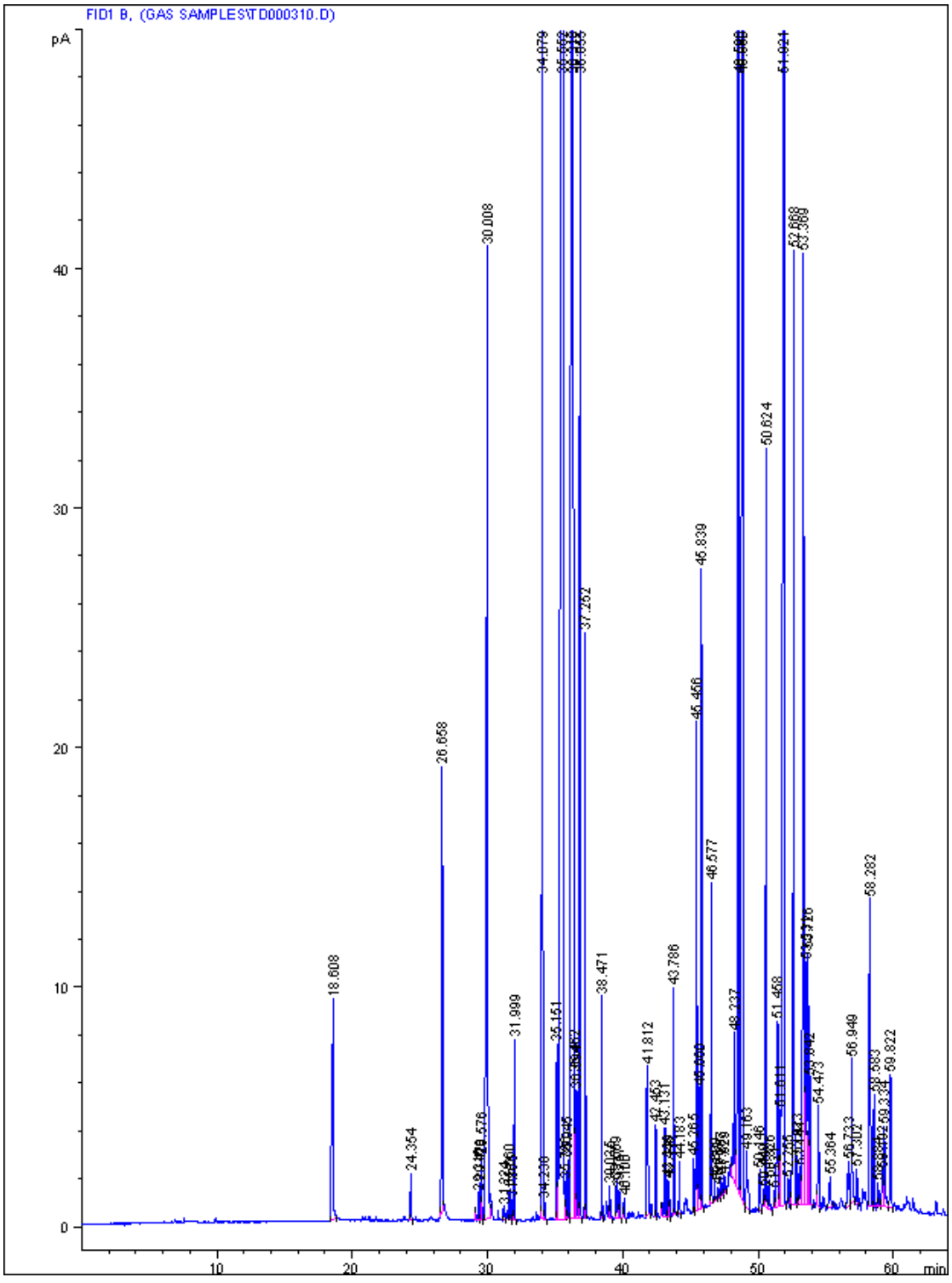

FIGURE B.10: FID chromatogram of *E. globulus* volatiles at 20.2 psi with 17.3:1 split ratio. Run 310

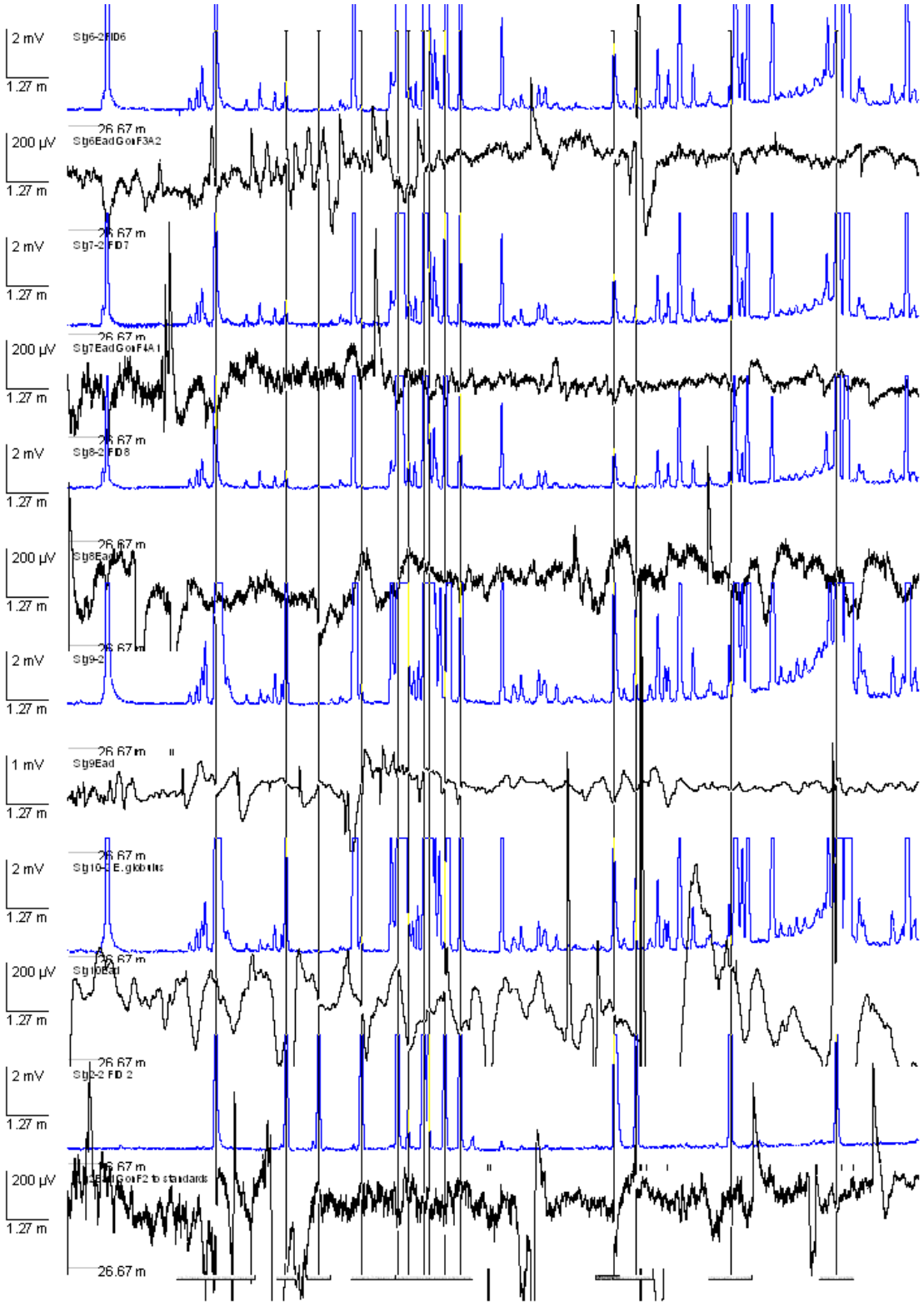

FIGURE B.11: GC-EAD traces for *E. globulus* volatiles. Bottom: EAG responses to standard compounds. The vertical lines correspond with standard retention times and should correspond exactly with the peaks in the sample runs. If they do not those compounds are simply not present or below the detection limit. All standard compounds except camphene, b-pinene, 3-carene and m-cymene were present in the *E. globulus* volatile profile.

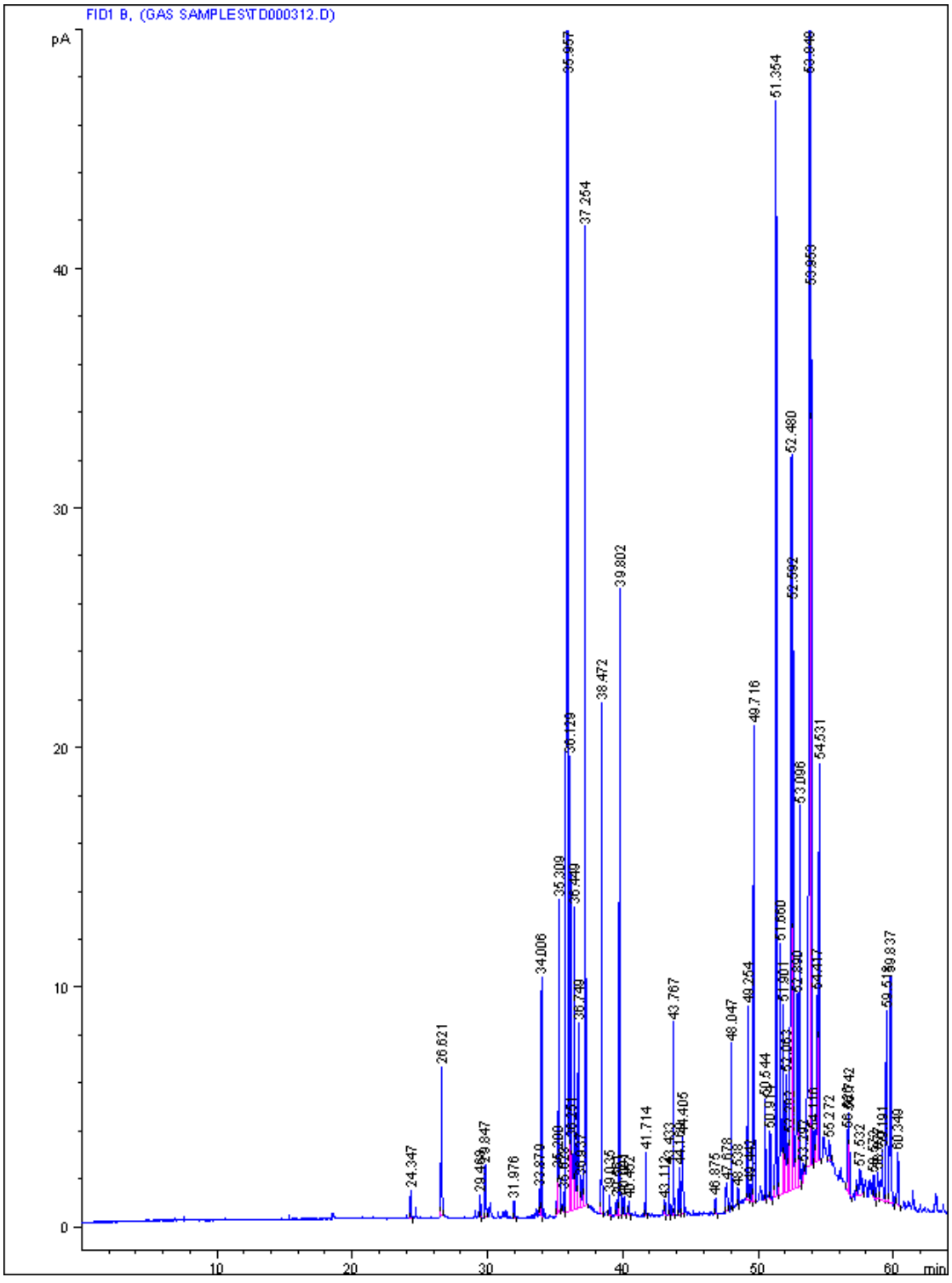

FIGURE B.12: FID chromatogram of *E. citriodora* volatiles at 20.2 psi with 17.3:1 split ratio. Run 312

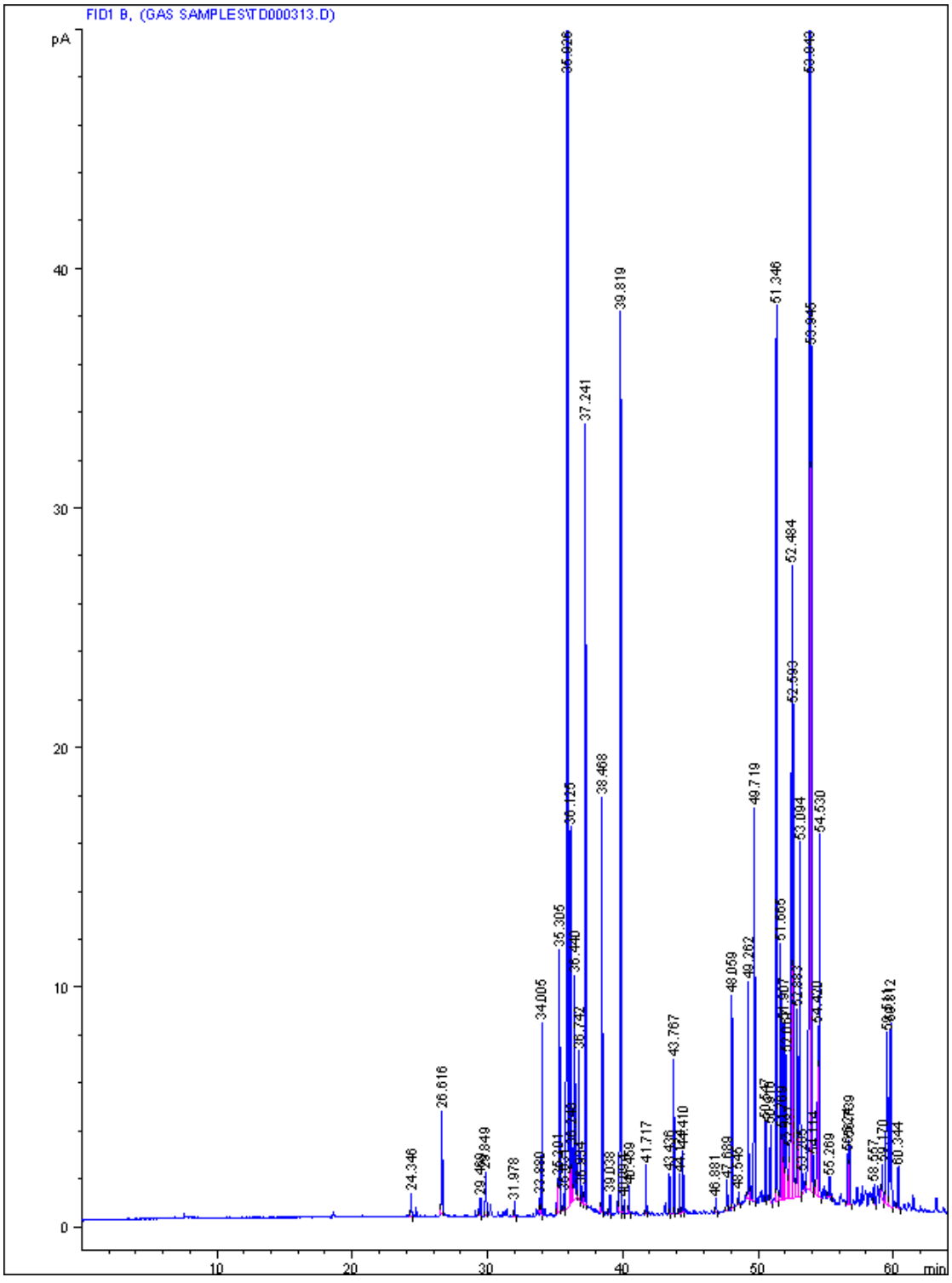

FIGURE B.13: FID chromatogram of *E. citriodora* volatiles at 20.2 psi with 17.3:1 split ratio. Run 313

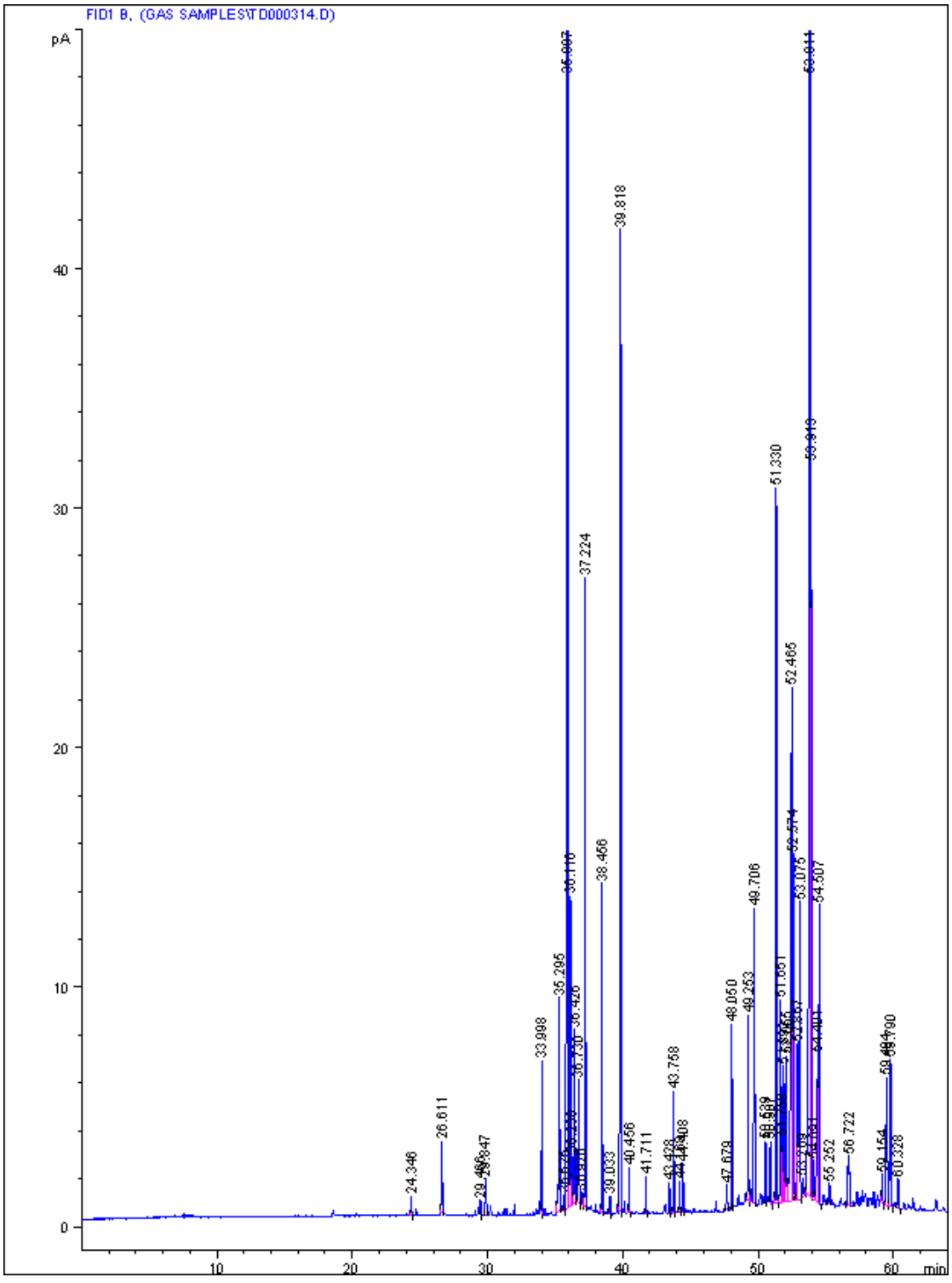

FIGURE B.14: FID chromatogram of *E. citriodora* volatiles at 20.2 psi with 17.3:1 split ratio. Run 314

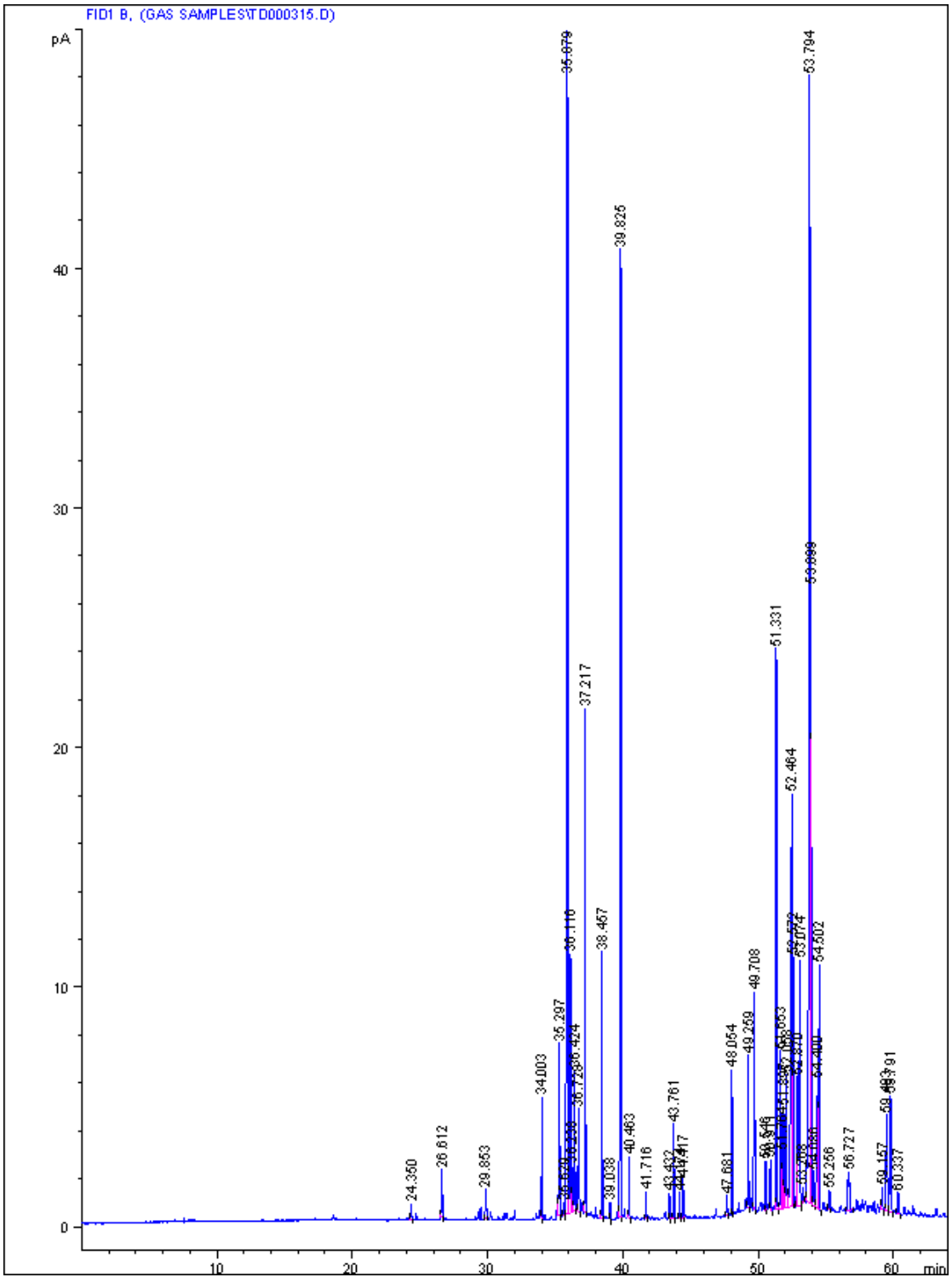

FIGURE B.15: FID chromatogram of *E. citriodora* volatiles at 20.2 psi with 17.3:1 split ratio. Run 315

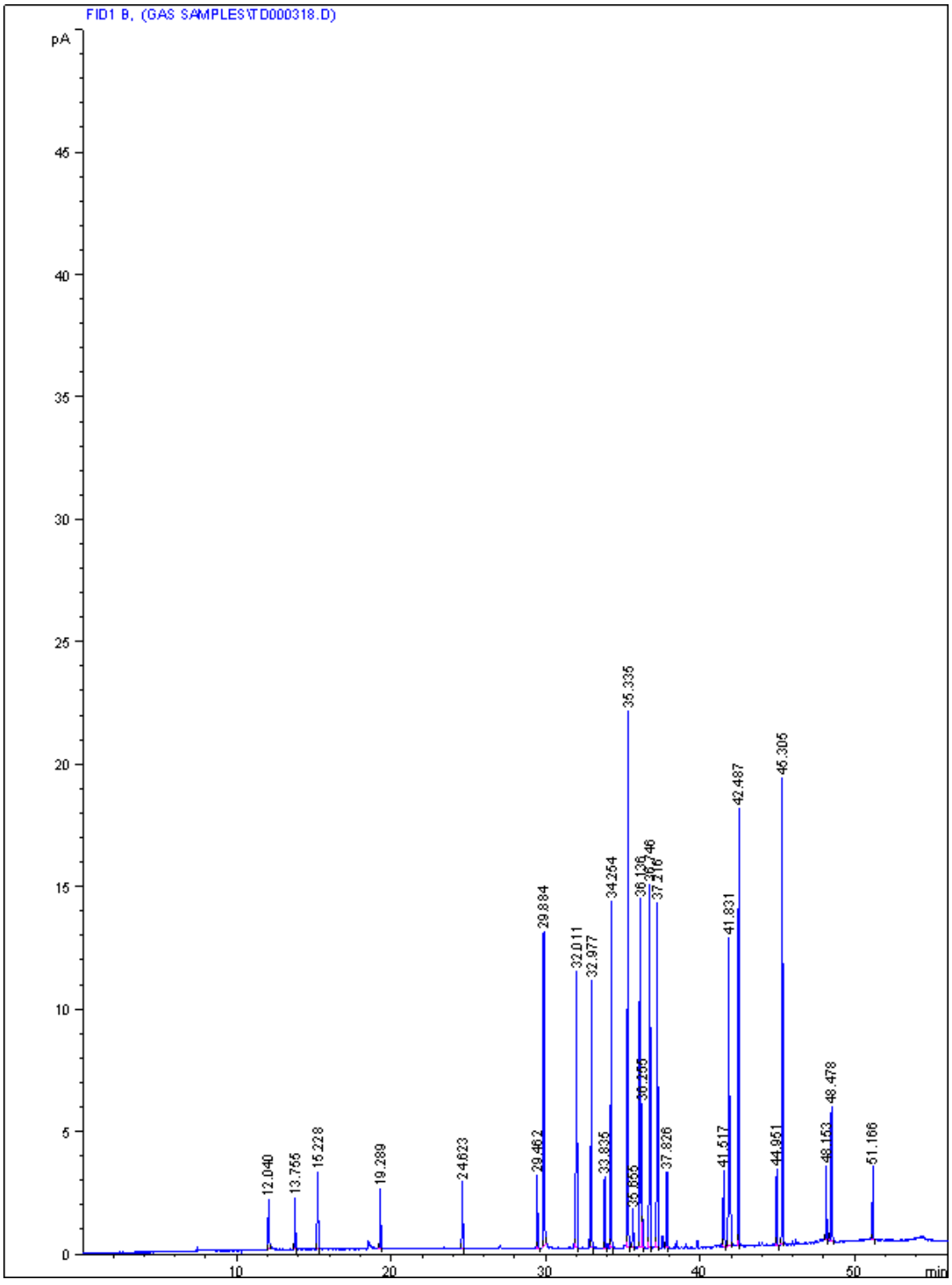

FIGURE B.16: Standard compounds (170 ng) and n-alkanes c5-c15 (42 ng): 23Sep2009 at 20.2 psi on the GC-FID

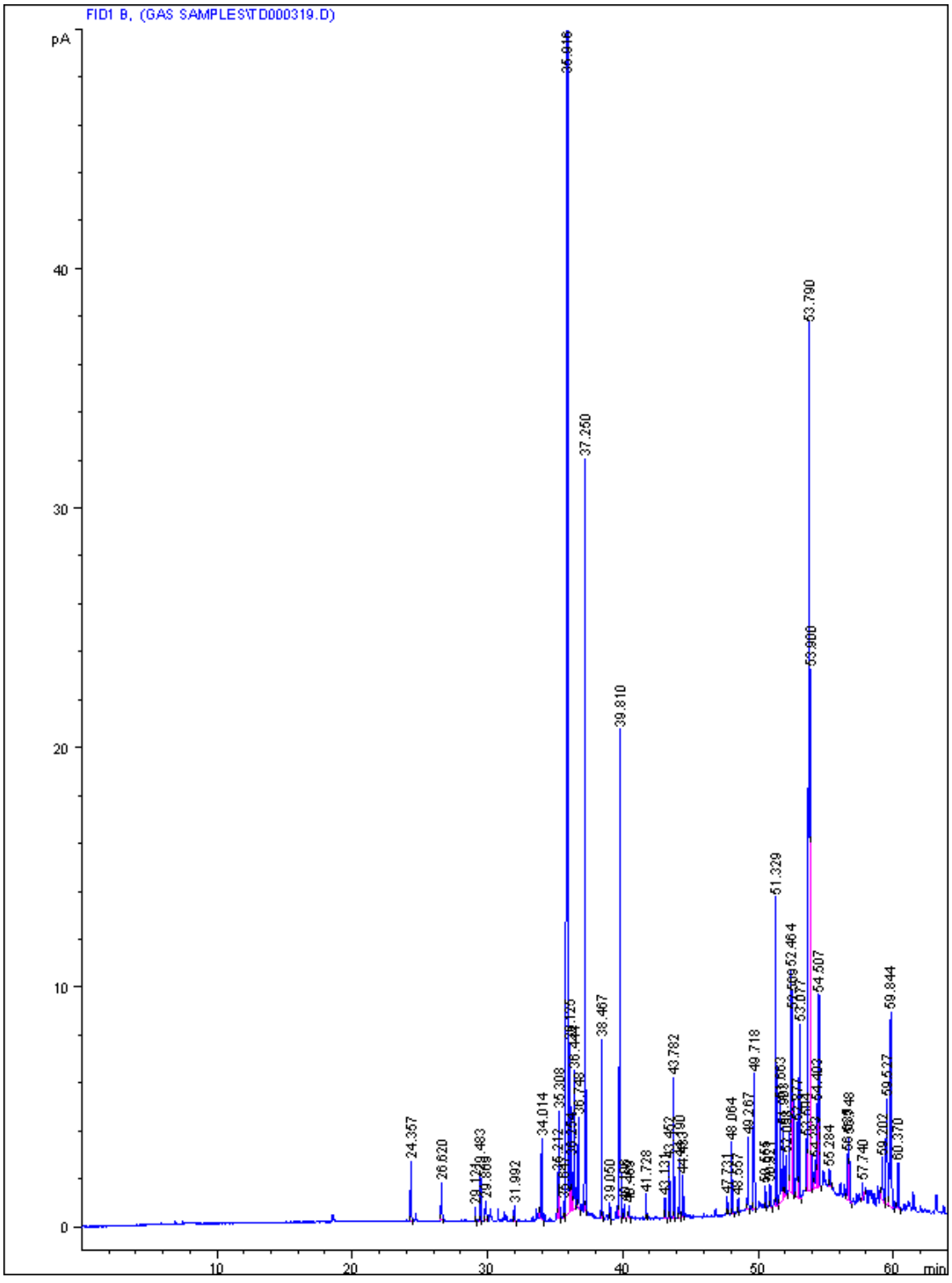

FIGURE B.17: FID chromatogram of *E. citriodora* volatiles at 20.2 psi with 17.3:1 split ratio. Run 319

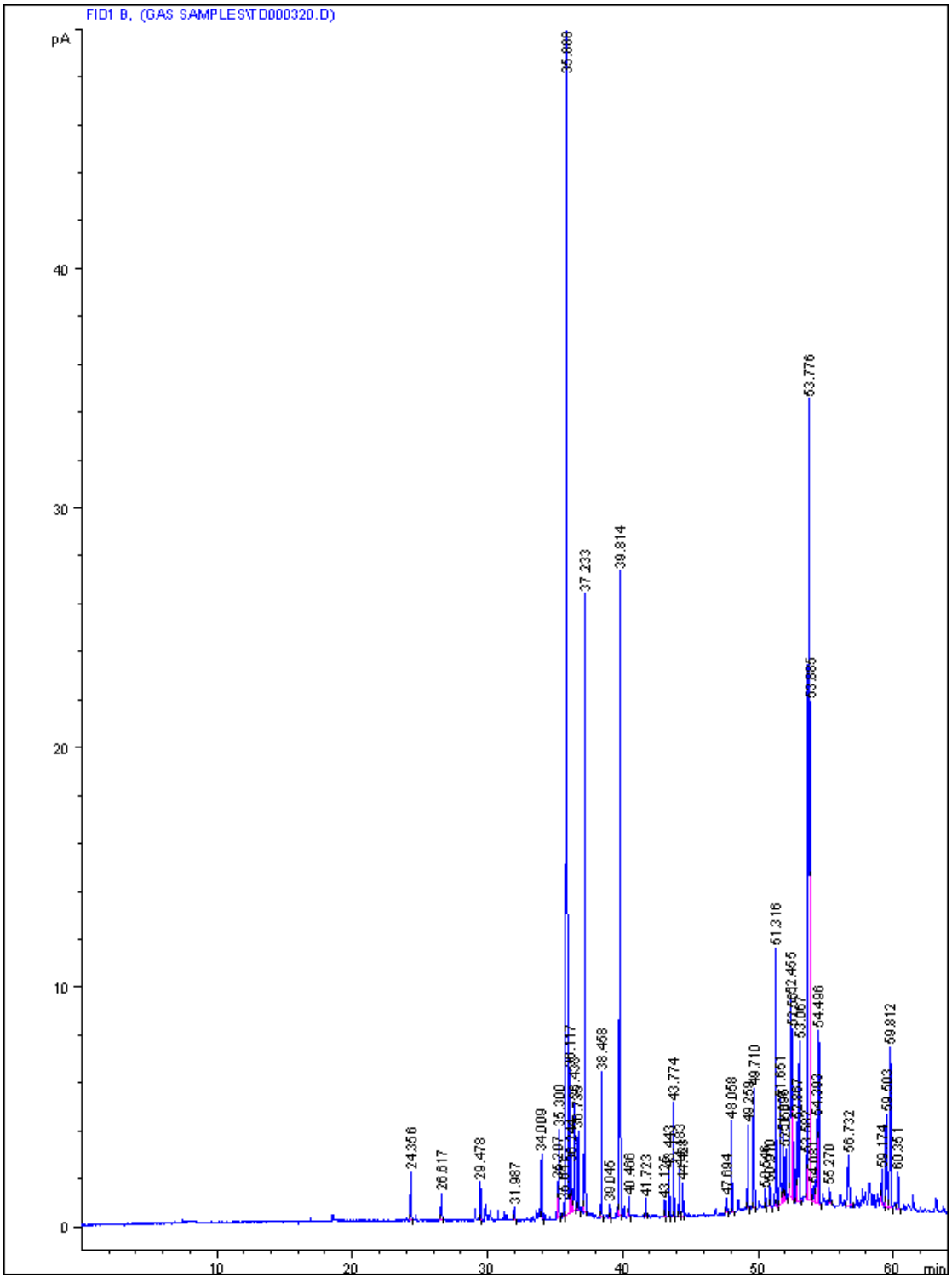

FIGURE B.18: FID chromatogram of *E. citriodora* volatiles at 20.2 psi with 17.3:1 split ratio. Run 320

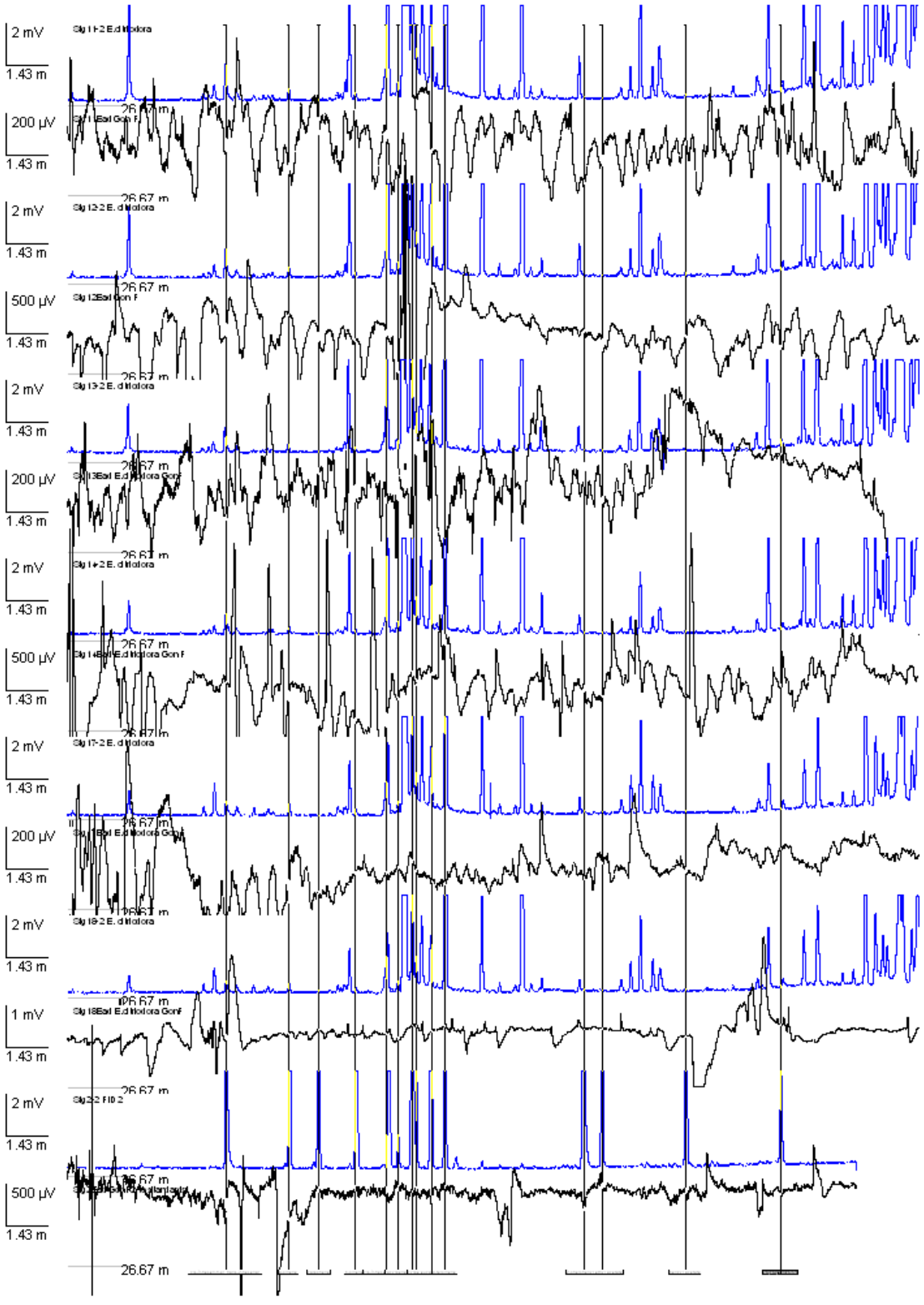

FIGURE B.19: GC-EAD traces for *E. citriodora* volatiles. Bottom: EAG responses to standard compounds. The vertical lines correspond with standard retention times and should correspond exactly with the peaks in the sample runs. If they do not those compounds are simply not present or below the detection limit.

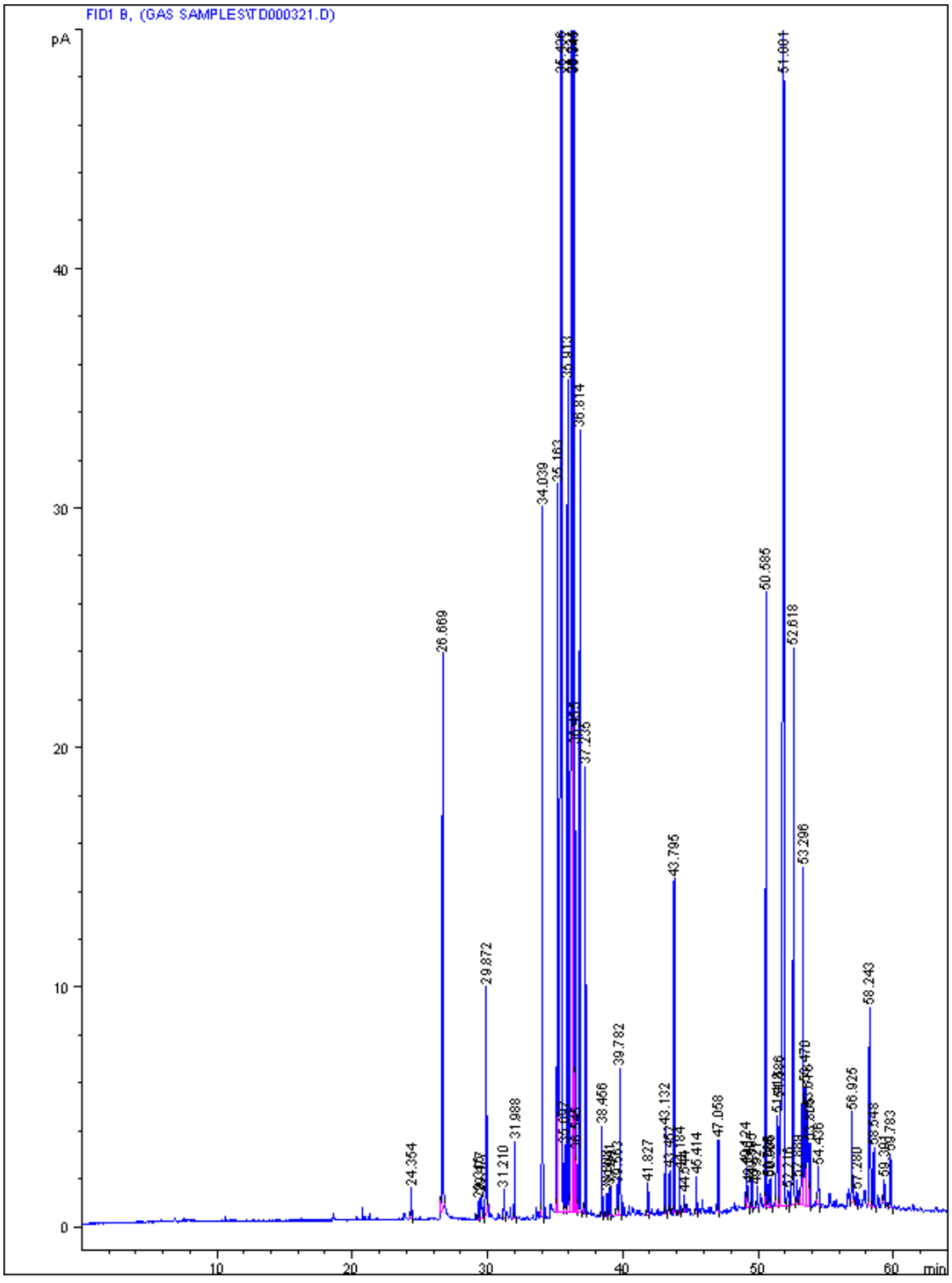

FIGURE B.20: FID chromatogram of *E. viminalis* volatiles at 20.2 psi with 17.3:1 split ratio. Run 321

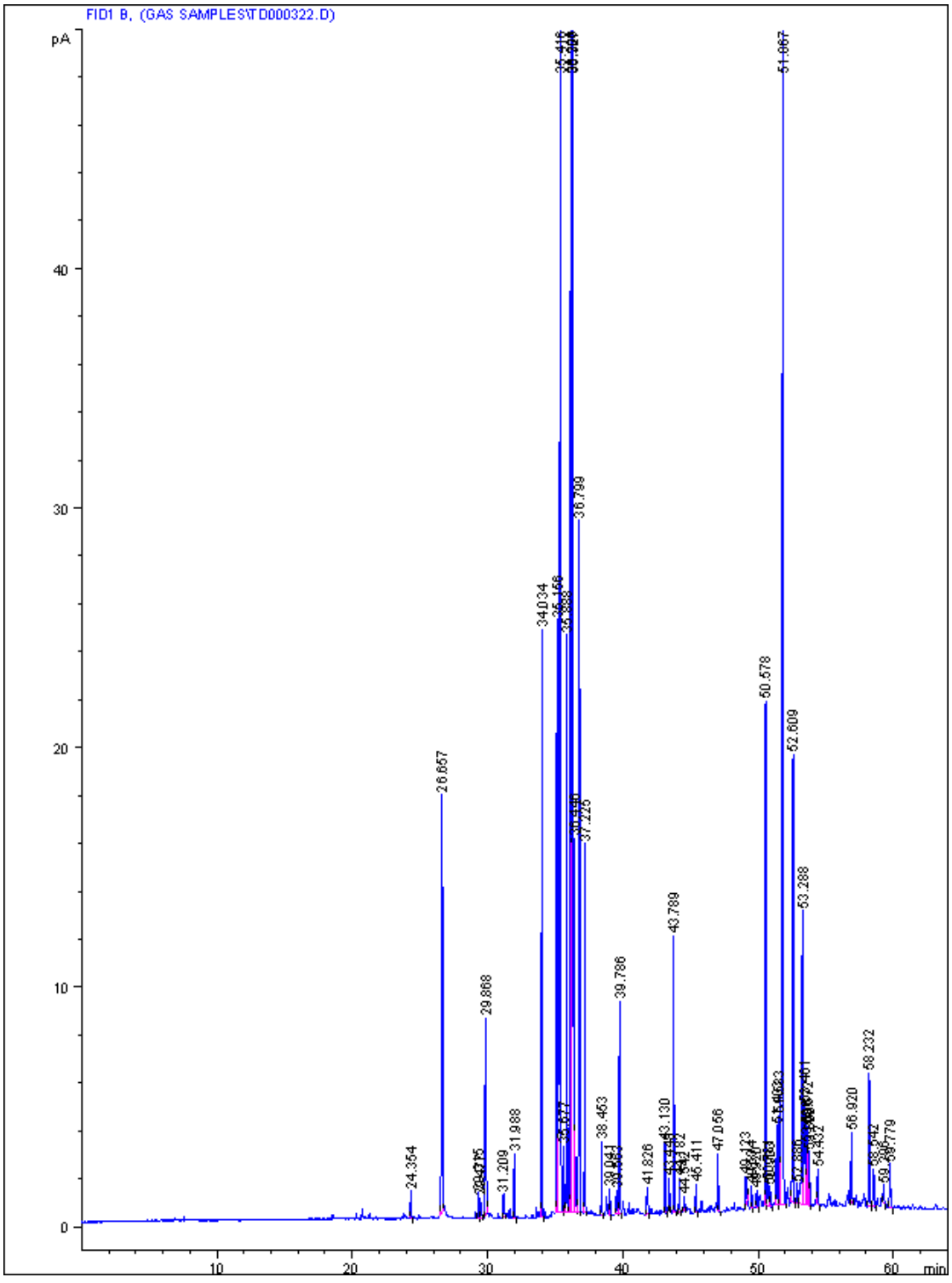

FIGURE B.21: FID chromatogram of *E. viminalis* volatiles at 20.2 psi with 17.3:1 split ratio. Run 322

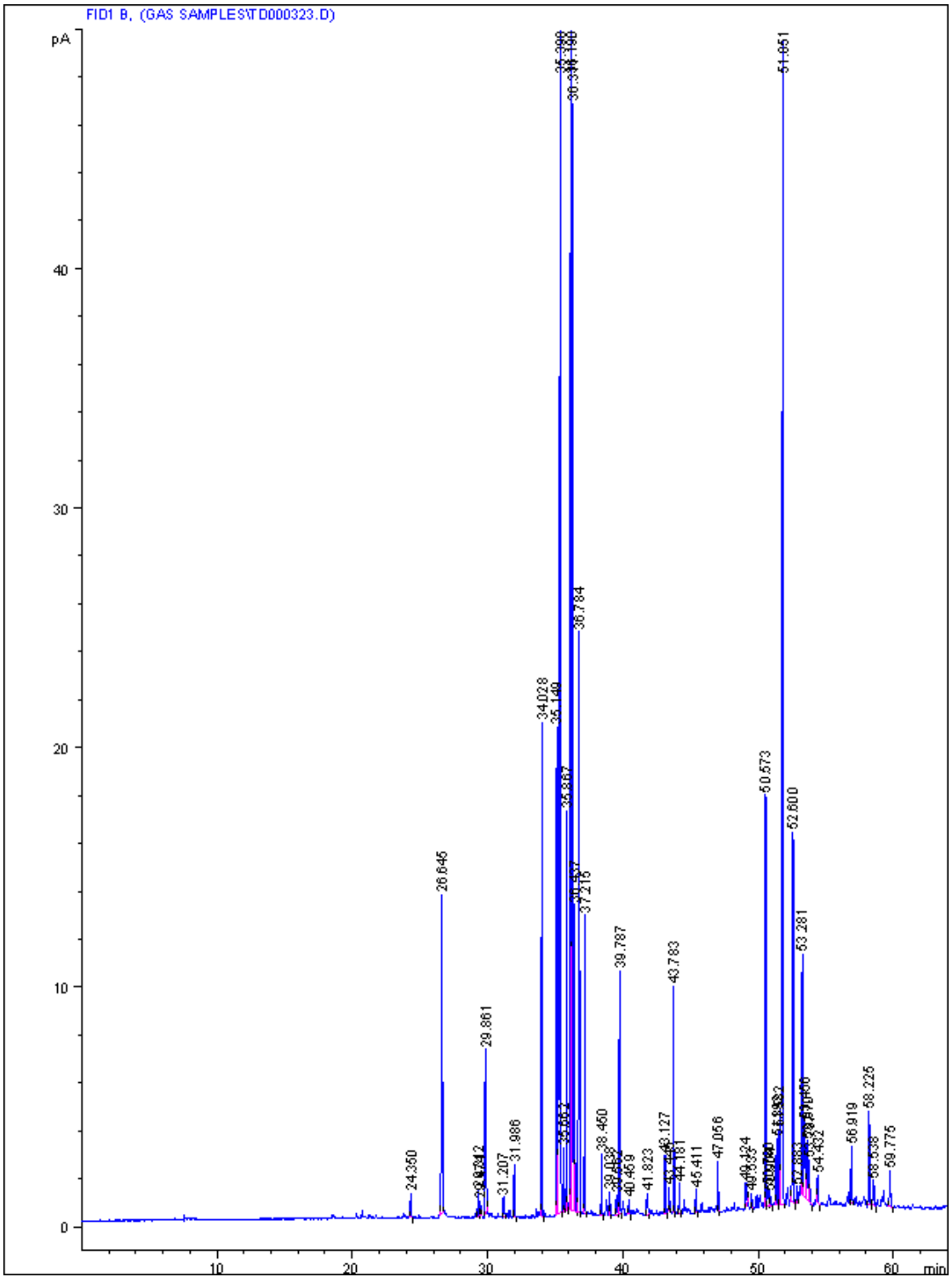

FIGURE B.22: FID chromatogram of *E. viminalis* volatiles at 20.2 psi with 17.3:1 split ratio. Run 323

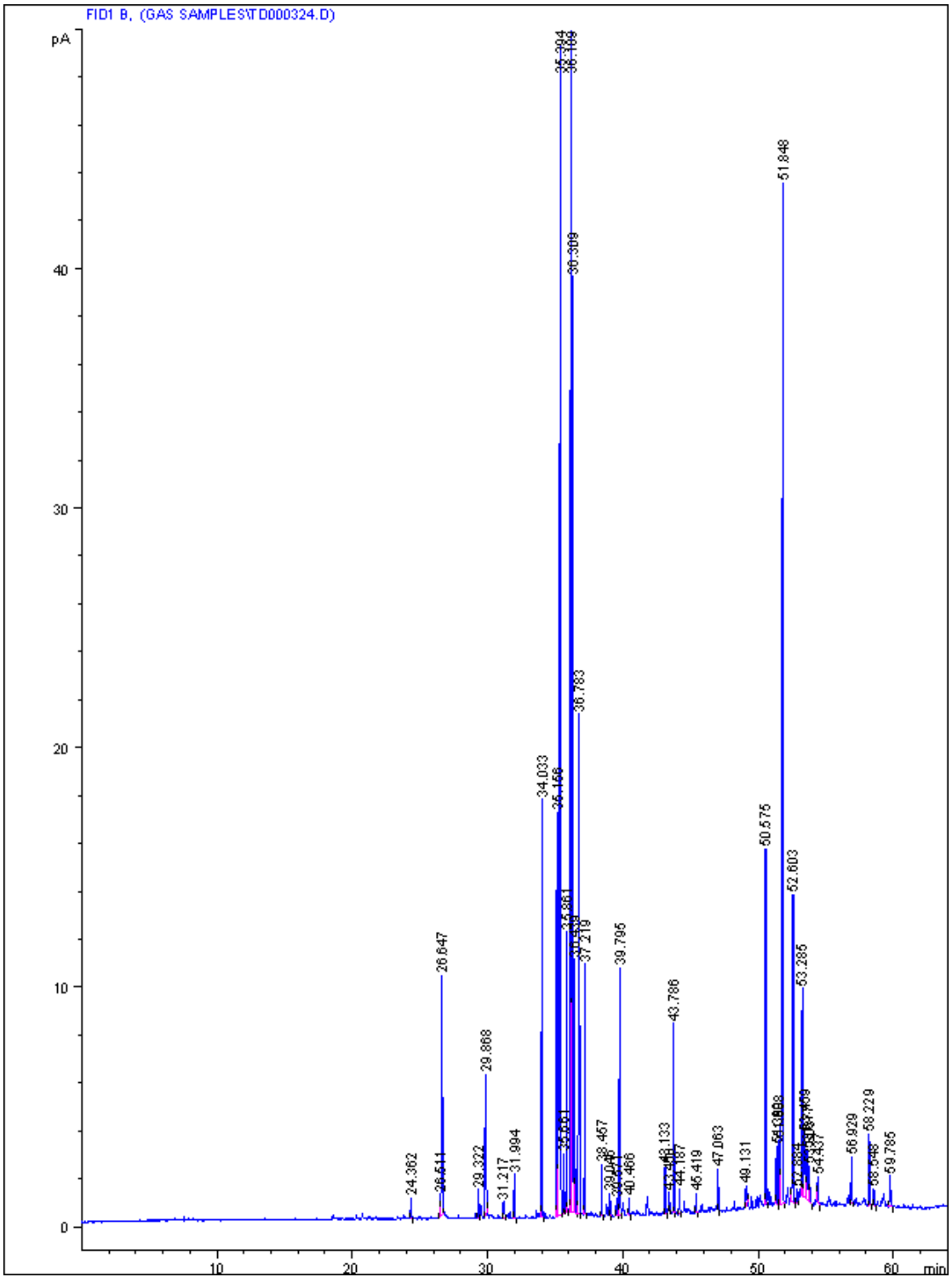

FIGURE B.23: FID chromatogram of *E. viminalis* volatiles at 20.2 psi with 17.3:1 split ratio. Run 324

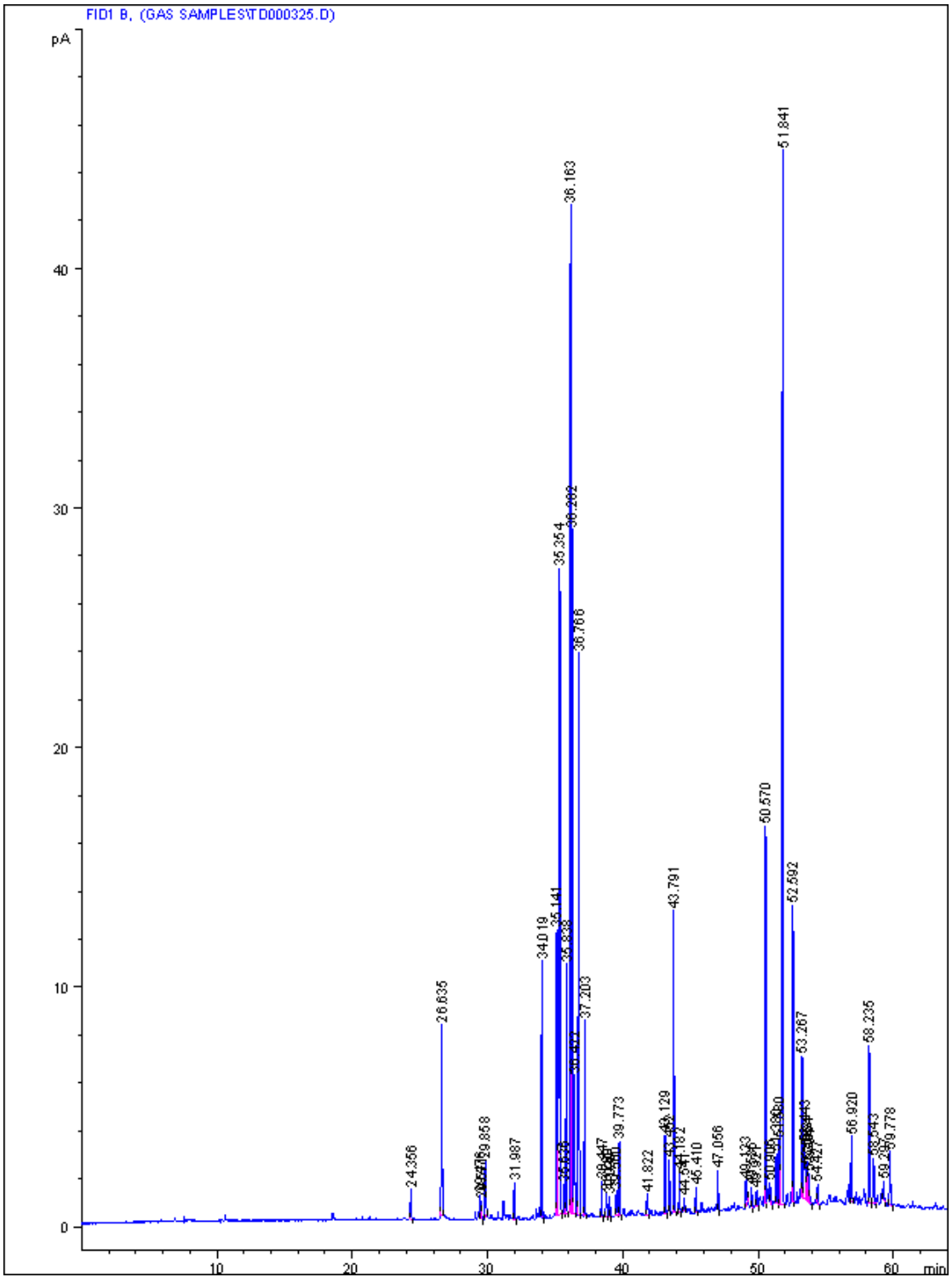

FIGURE B.24: FID chromatogram of *E. viminalis* volatiles at 20.2 psi with 17.3:1 split ratio. Run 325

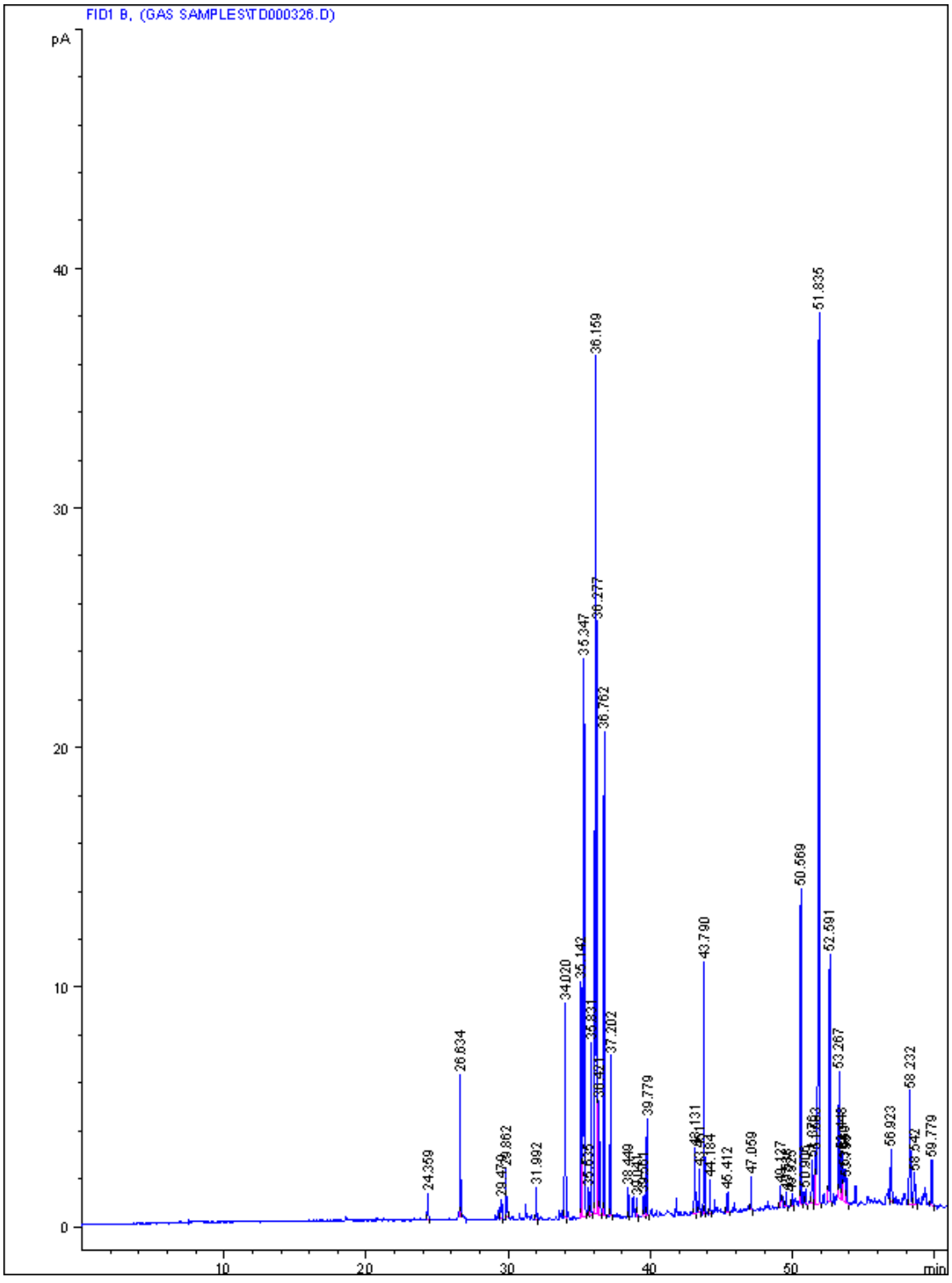

FIGURE B.25: FID chromatogram of *E. viminalis* volatiles at 20.2 psi with 17.3:1 split ratio. Run 326

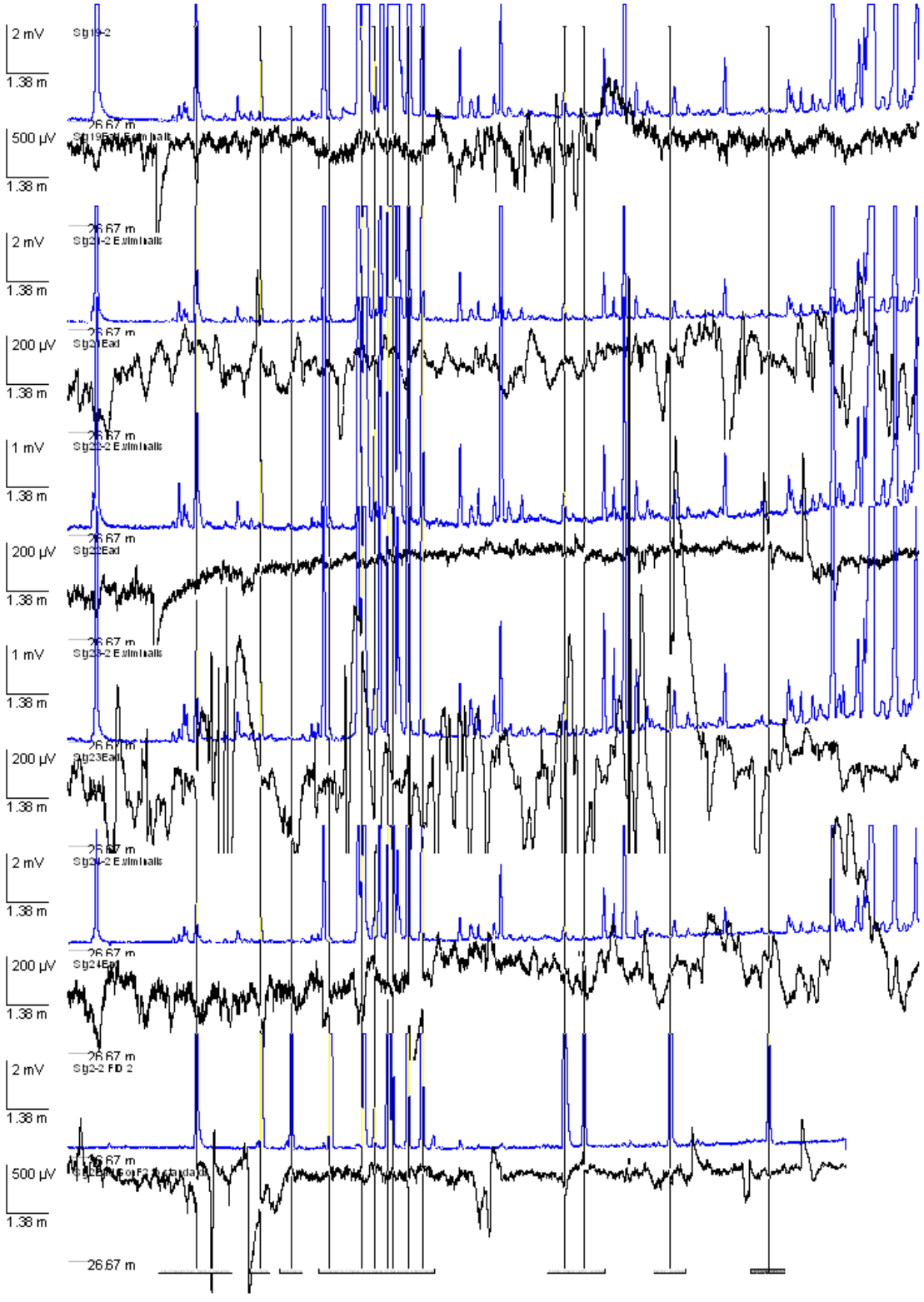

FIGURE B.26: GC-EAD traces for *E. viminalis* volatiles. Bottom: EAG responses to standard compounds. The vertical lines correspond with standard retention times and should correspond exactly with the peaks in the sample runs. If they do not those compounds are simply not present or below the detection limit.

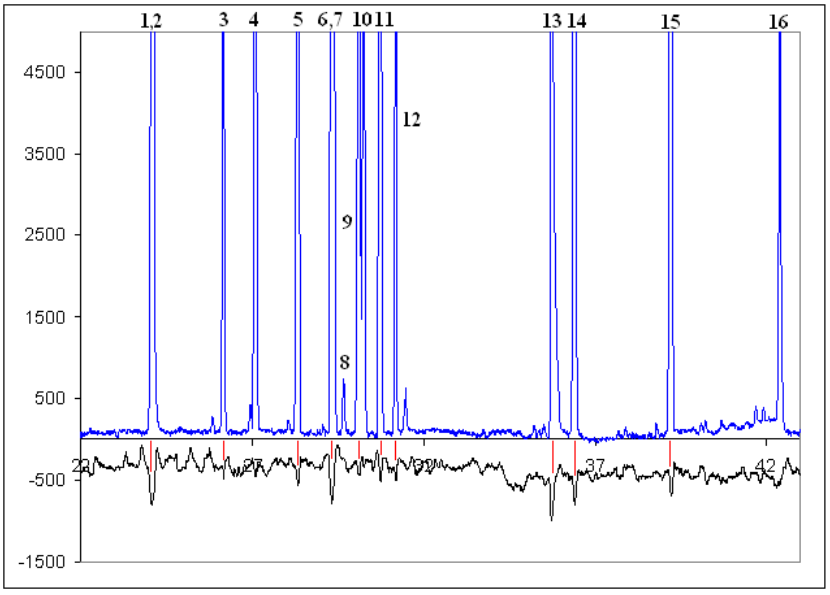

FIGURE B.27: GC-EAD trace for standard compounds after liquid injection at 20.0 psi (150 ng). Peak numbers refer to table B 1-4.

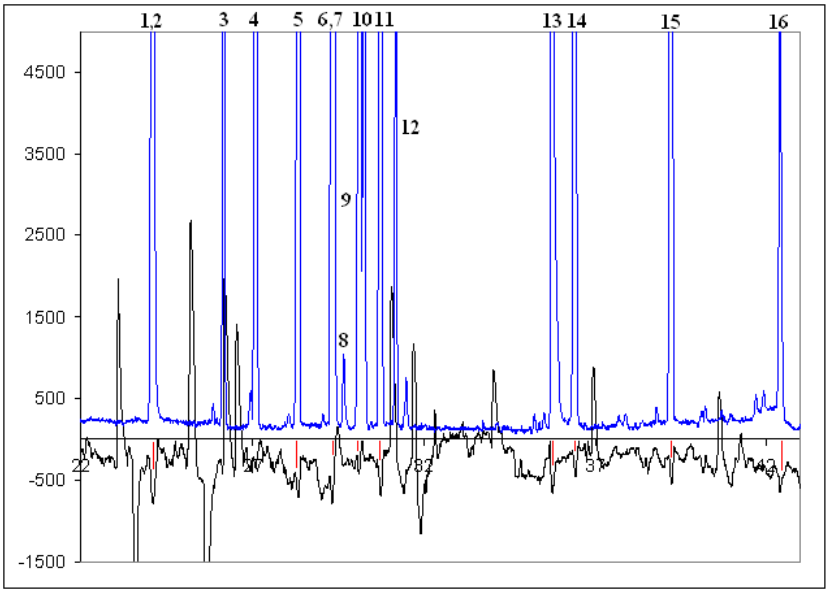

FIGURE B.28: GC-EAD trace for standard compounds after liquid injection at 20.0 psi (150 ng). Peak numbers refer to table B 1-4.

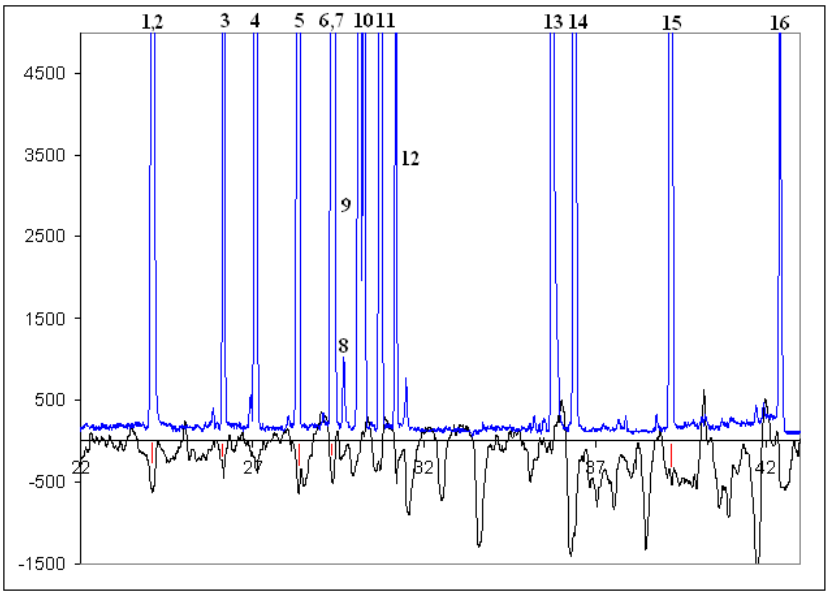

FIGURE B.29: GC-EAD trace for standard compounds after liquid injection at 20.0 psi (150 ng). Peak numbers refer to table B 1-4.

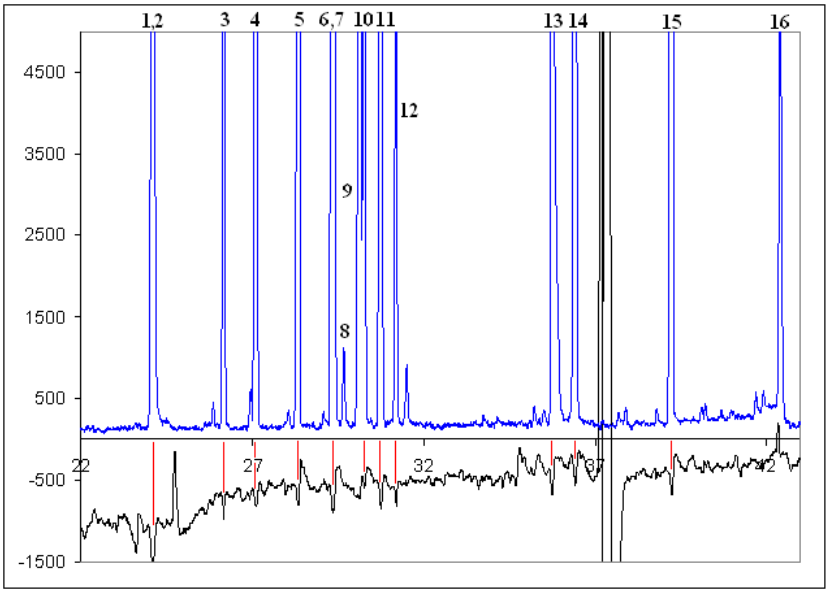

FIGURE B.30: GC-EAD trace for standard compounds after liquid injection at 20.0 psi (150 ng). Peak numbers refer to table B 1-4.

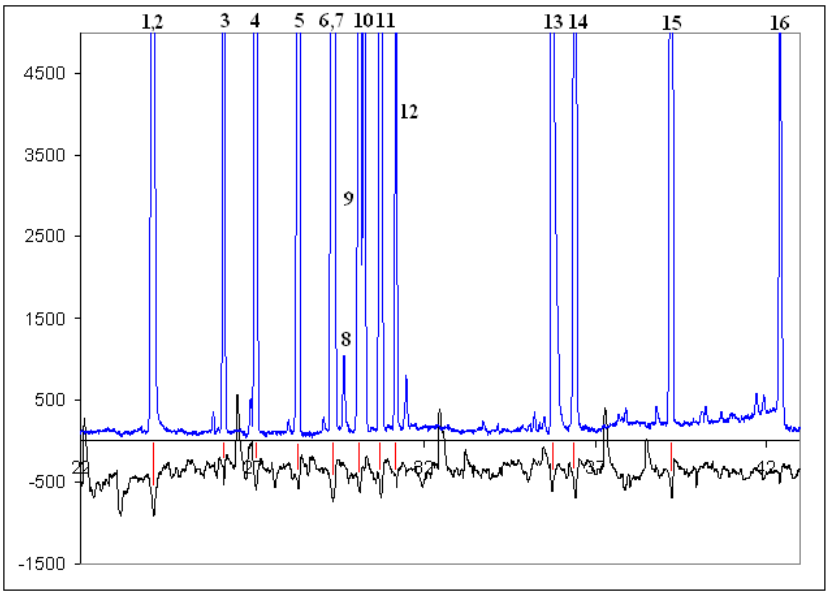

FIGURE B.31: GC-EAD trace for standard compounds after liquid injection at 20.0 psi (150 ng). Peak numbers refer to table B 1-4.

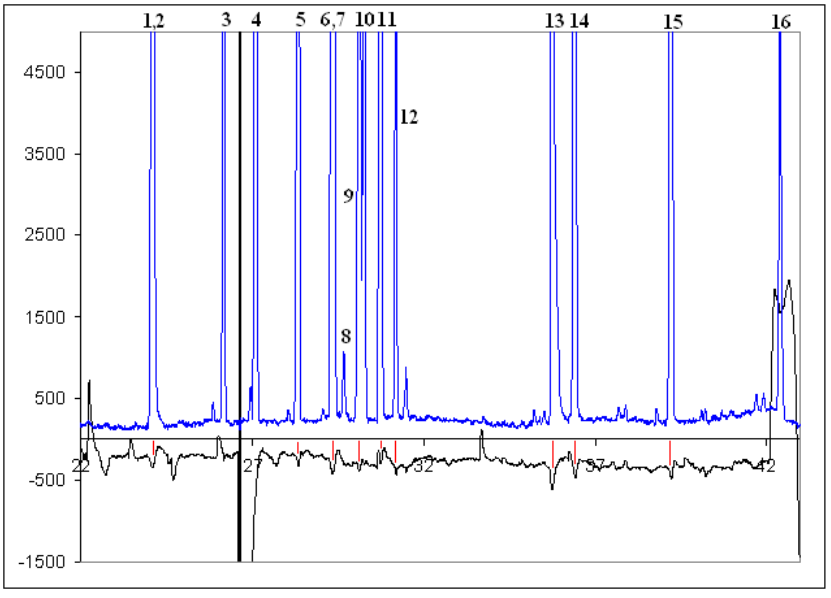

FIGURE B.32: GC-EAD trace for standard compounds after liquid injection at 20.0 psi (150 ng). Peak numbers refer to table B 1-4.

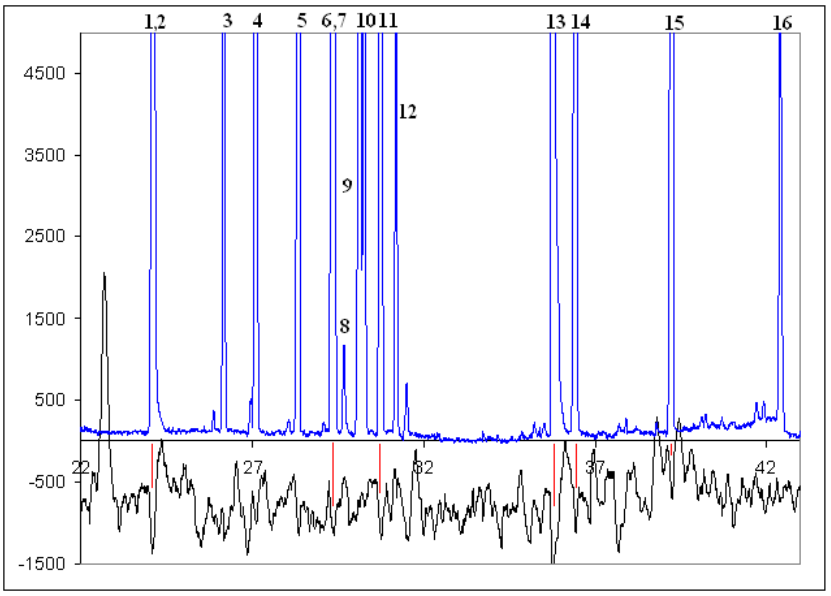

FIGURE B.33: GC-EAD trace for standard compounds after liquid injection at 20.0 psi (150 ng). Peak numbers refer to table B 1-4.

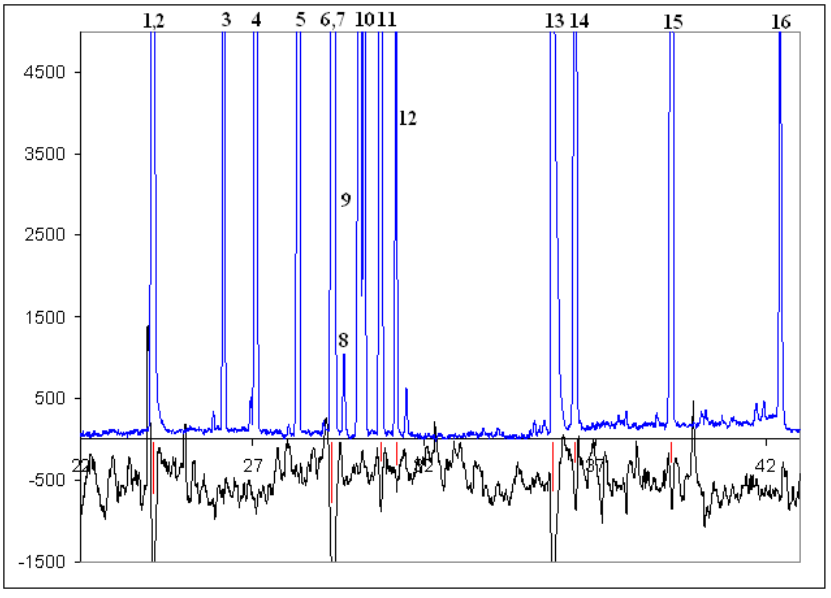

FIGURE B.34: GC-EAD trace for standard compounds after liquid injection at 20.0 psi (150 ng). Peak numbers refer to table B 1-4.

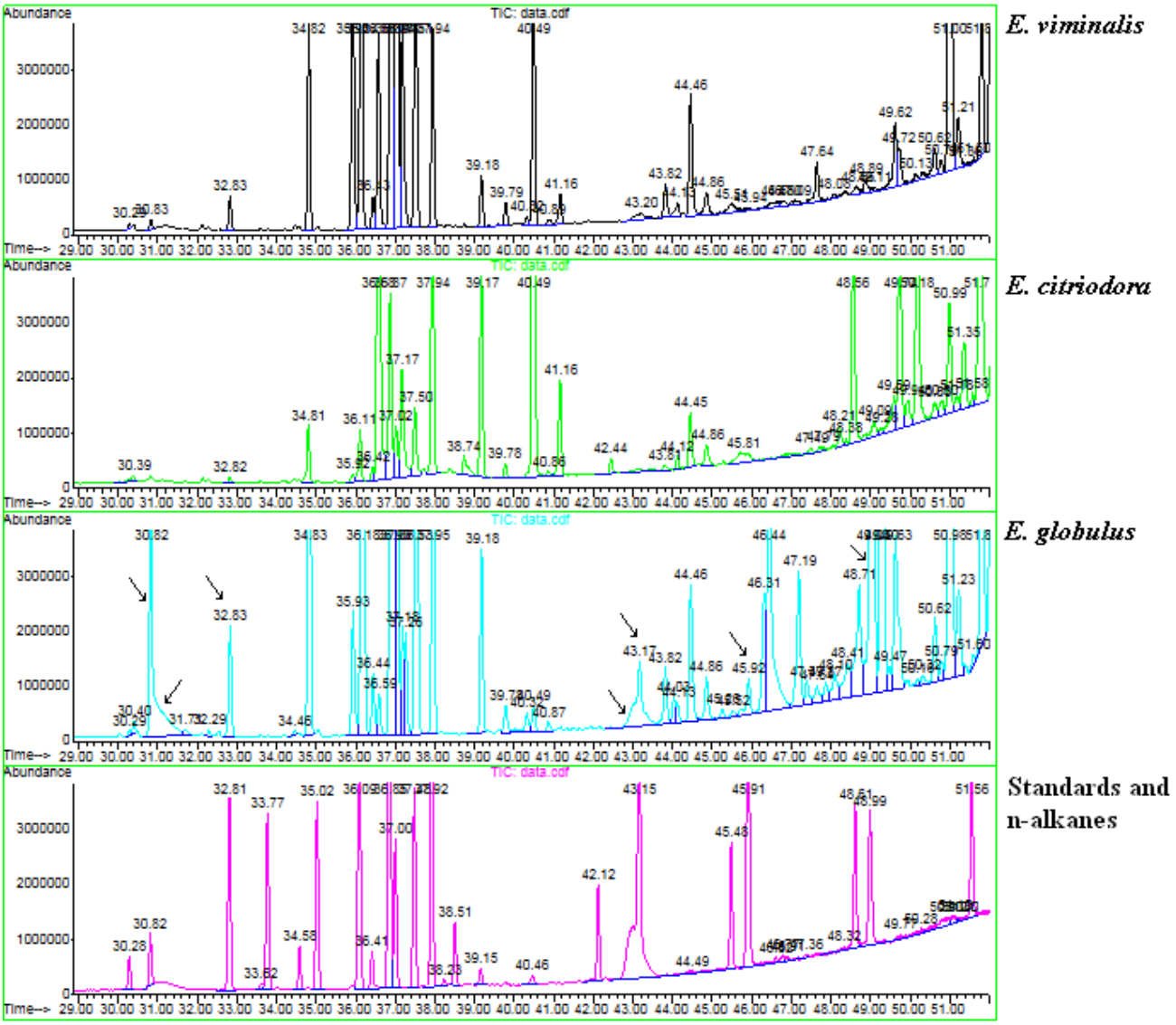

FIGURE B.35: A comparison between the GC-MS total ion chromatograms for *E. globulus* (Run 9OCTR7 and 8), *E. vimnalis* (Run 9OCTR5 and 6) and *E. citriodora* (Run 9OCTR3 and 4) compared to the standard mixture and n-alkanes. Arrows indicate the major differences for antennally active peaks for the three chromatographic profiles.

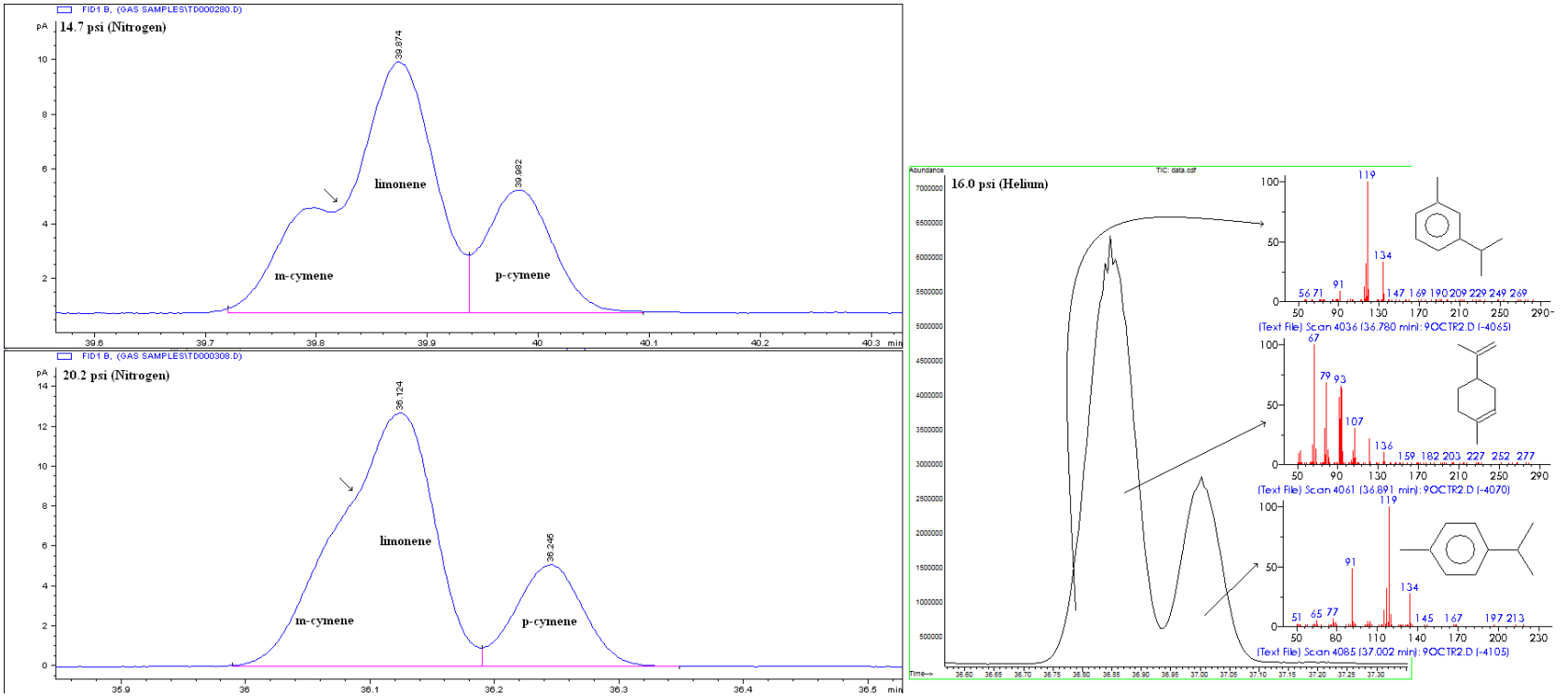

FIGURE B.36: The effect of the resolution difference between the GC-FID and GC-MS. Left: The standards run on the GC-FID system at 14.7 psi and 20.2 psi. Note the loss in resolution at a higher linear flow rate indicated by the arrows. Right: The same peaks on the GC-MS with their mass spectra at 16.0 psi. Note that here one can not discriminate between the m-cymene and lymonene peaks.

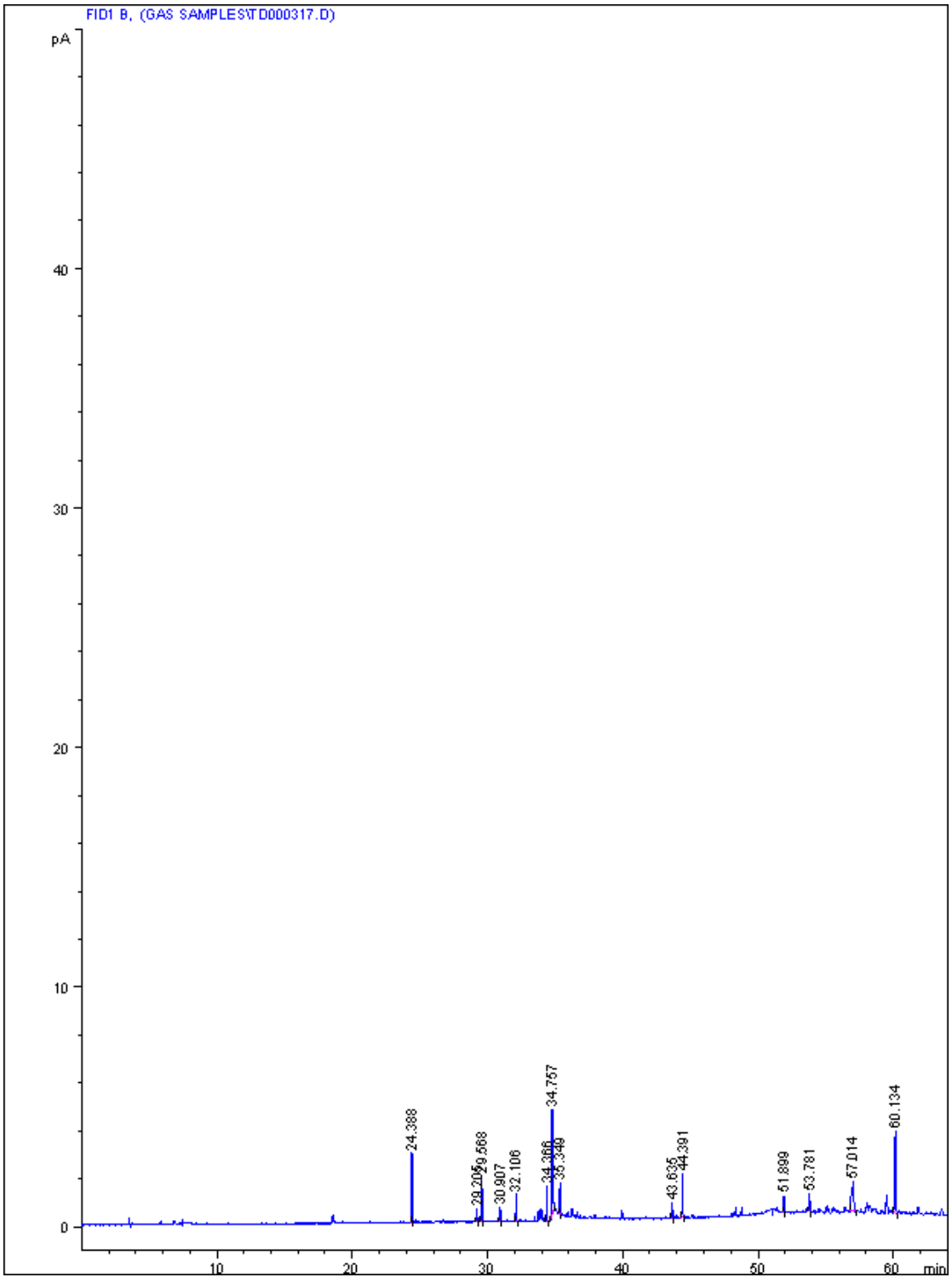

FIGURE B.37: Sample blank (Run: 317) with a 17.3:1 split ratio at 20.2 psi on the GC-FID system.

Appendix C

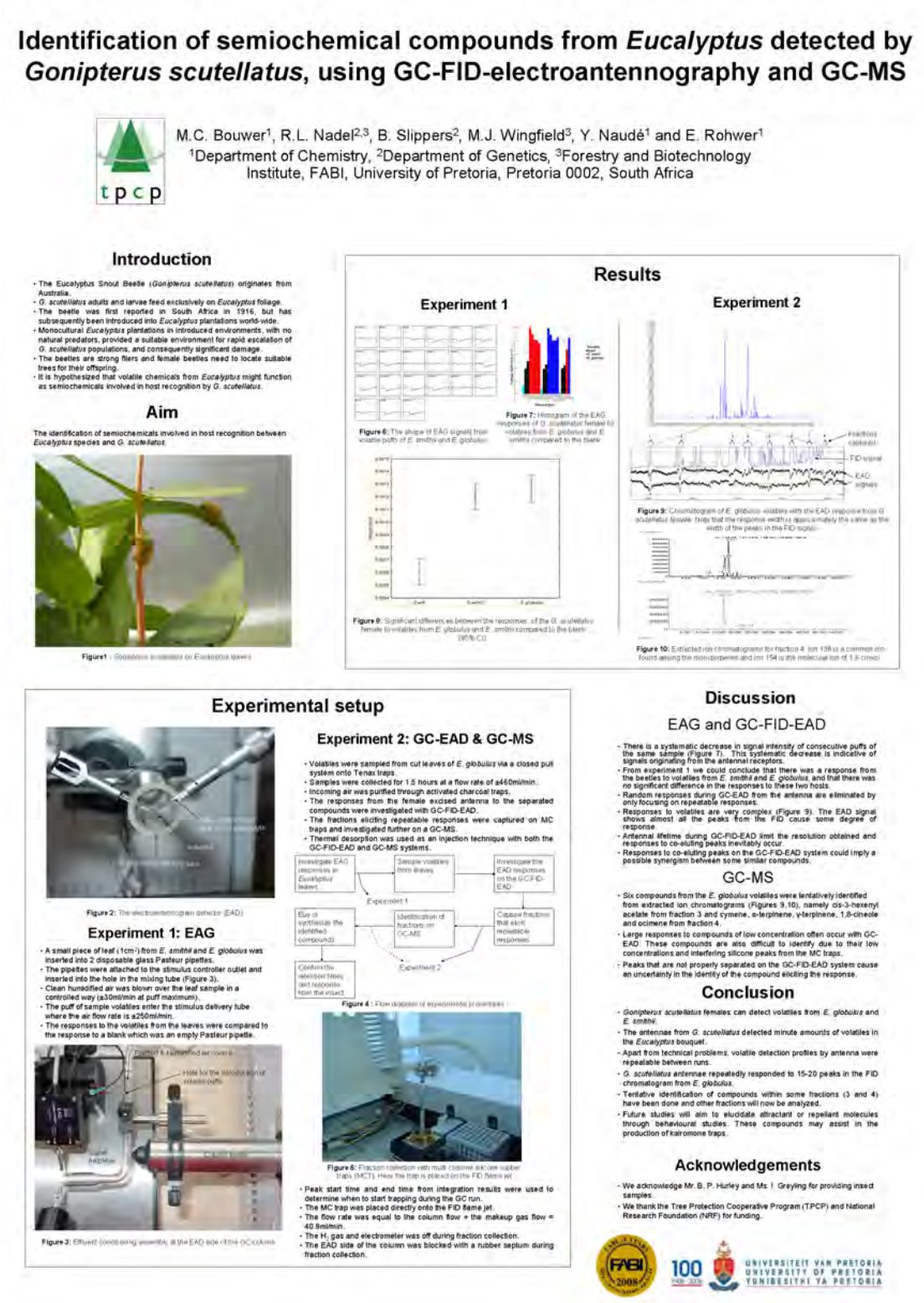

FIGURE C.1: Poster presented at CromSAAMS. In partial fulfillment of MSc in chemistry.

Bibliography

Agelopoulos, N.G. and Picket, J.A. (1998). Headspace analysis in chemical ecology, effects of different sampling methods on ratios of volatile compounds present in headspace samples. *Journal of Chemical Ecology*, vol. 24, pp. 1161–1172.

Angioy, A.M., Desogus, A., Barbarossa, I.T., Anderson, P. and Hansson, B.S. (2003). Extreme Sensitivity in an Olfactory System. *Chemical Senses*, vol. 28, pp. 279–284.

Augusto, F., Lopes, A.L. and Zini, C.A. (2003). Sampling and sample preparation for the analysis of aromas and fragrances. *Trends in Analytical Chemistry*, vol. 22, pp. 160–169.

Barata, E.N., Pickett, J.A., Wadhams, L.J., Woodcock, C.M. and Mustaparta, H. (2000). Identification of host and nonhost semiochemicals of the *Eucalyptus* woodborer *Phoracantha semipunctata* by gas chromatography-electroantennography. *Journal of Chemical Ecology*, vol. 26, pp. 1877–1895.

Baya, M.P. and Siskos, P.A. (1996). Evaluation of anasorb CMS and comparison with Tenax TA for the sampling of volatile organic compounds in indoor and outdoor air by breakthrough measurements. *Analyst*, vol. 121, pp. 303–307.

Bedard, W.D., Wood, D.L., Tilden, P.E., Lindahl, K.Q., Silverstein, R.M. and Rodin, J.O. (1980). Field responses of the western pine beetle and one of its predators to host- and beetle-produced compounds. *Journal of Chemical Ecology*, vol. 6, pp. 625–641.

Bichao, H., Borg-Karlson, A.-K., Wibe, A., Araújo, J. and Mustaparta, H. (2005). Molecular receptive ranges of olfactory receptor neurones responding selectively to terpenoids, aliphatic green leaf volatiles and aromatic compounds, in the strawberry blossom weevil *Anthonomus rubi*. *Chemoecology*, vol. 15, pp. 211–226. Available at: http://www.springerlink.com/content/7t0x1551u63k5u40

Bjostad, L.B. (1998). *Methods in Chemical Ecology*. Kluwer Academic Publishers.

Blight, M.M., Pickett, J.A., Wadhams, L.J. and Woodcock, C.M. (1995). Antennal perception of oilseed rape, *Brassica napus* (Brassicaceae), volatiles by the cabbage

seed weevil *Ceutorhynchus assimilis* (Coleoptera, Curculionidae). *Journal of Chemical Ecology*, vol. 21, pp. 1649–1664.
Available at: http://www.springerlink.com/content/u44406w339560554

Boeckh, J. (1984). Neurophysiological aspects of insect olfaction in Insect communication. *Royal Entomological Society of London*, pp. 83–103.

Boland, D.J., Brophy, J., Flynn, T. and Lassak, E. (1982). Volatile leaf oils of *Eucalyptus delegatensis* seedlings. *Phytochemisry*, vol. 21, pp. 2467–2469.

Brooker, I. and Kleinig, D. (1996). *Eucalyptus: An illustrated guide to identification.* Reed Books.

Brooker, M.I.H. (2000). A new classification of the genus *Eucalyptus* L'Hér. (Myrtaceae). *Australian Systematic Botany*, vol. 13, pp. 79–148.

Brown, W.L. (1968). An hypothesis concerning the function of the metapleural glands in ants. *Amer. Natur.*, vol. 102, pp. 188–191.

Brown, W.L., Eisner, T. and Whittaker (1970). Allomones and kairomones: Transspecific chemical messengers. *Bioscience.*, vol. 20, pp. 21–22.

Calogirou, A., Larsen, B. and Kotzias, D. (1999). Gas-phase terpene oxidation products: a review. *Atmospheric Environment*, vol. 33, pp. 1423–1439.

Carbone, S.S. and Fernández, F. (2004). Testing of selected insecticides to assess the viability of the integrated pest management of the eucalyptus snout beetle gonipterus scutellatus in north-west spain. *JEN.*, vol. 128, pp. 620–627.

Carbone, S.S. and Rivera, A.C. (1998). Sperm competition, cryptic female choice and prolonged mating in the eucalyptus snout-beetle, gonipterus scutellatus (coleoptera, curculionidae). *Entologia*, vol. 6, pp. 33–40.

Carbone, S.S. and Rivera, A.C. (2003). Egg load and adaptive superparasitism of the *Eucalyptus* snout beetle *Gonipterus scutellatus. The Netherlands Entomological Society.*, vol. 106, pp. 127–134.

Clark, A.F. (1932). The parasiodal control of *Gonipterus scutellatus* gyll. *NZ J. Sci. Tech.*, vol. 19, pp. 750–761.

Clarke, A.R., Paterson, S. and p. Pennington (1998). Gonipterus scutellatus oviposition on seven naturally co-occurring eucalyptus species. *For. Ecol. Manage.*, vol. 110, pp. 89–99.

Coeur, C., Jacob, V., Denis, I. and Foster, R. (1997). Decomposition of α-pinene and sabinene on solid sorbents, Tenax TA and Carboxen. *Journal of Chromatography A*, vol. 786, pp. 185–187.

Comes, P., Gonzalez-Flesca, N., Ménard, T. and Grimalt, J.O. (1993). Langmuir-derived equasions for the prediction of solid adsorption breakthrough volumes of volatile organic compounds in atmospheric emission effluents. *Analytical Chemistry*, vol. 65, pp. 1048–1053.

Cooke, K.M., Hassoun, S.H., Saunders, S.M. and Pilling, M. (2001). Identification and quantification of Volatile organic compounds found in a *Eucalyptus* forest during FIELDVOC 94 in Portugal. *Chemosphere-Global Change Science*, vol. 3, pp. 249–257.

Cunningham, S.A., Floyd, R.B. and Weir, T.A. (2005). Do *Eucalyptus* plantations host an insect community similar to remnant *Eucalyptus* forest? *Austral Ecology*, vol. 30, p. 103117.

DAlessandro, M. and Turlings, T.C.J. (2006). Advances and challenges in the identification of volatiles that mediate interactions among plants and arthropods. *The Analyst*, vol. 131, pp. 24–32.

Dethier, V.G. (1982). Mechanism of host-plant recognition. *Entomologia Experimentalis et Aplicata*, vol. 31, pp. 49–56.

Dettmer, K. and Engewald, W. (2002). Adsorbent materials commonly used in air analysis for adsorptive enrichment and thermal desorption of volatile organic compounds. *Analytical and Bioanalytical Chemistry*, vol. 373, pp. 490–500.

Dicke, M. (2000). Chemical ecology of host-plant selection by herbivorous arthropods, a multitrophic perspective. *Biochemical Systematics and Ecology.*, vol. 28, pp. 601–617.

Donaldson, J.R., Stevens, M.T., Barnhill, H.R. and Lindroth, R.L. (2006). Age-related shifts in leaf chemistry of clonal aspen (*Populus tremuloides*). *Journal of Chemical Ecology*, vol. 32, pp. 1415–1429.

Dudareva, N., Negre, F., Nagegowda, D.A. and Orlova, I. (2004). Biochemistry of plant volatiles. *Plant Physiology*, vol. 135, pp. 1893–1902.

Dudareva, N., Negre, F., Nagegowda, D.A. and Orlova, I. (2006). Plant volatiles: Recent advances and future perspectives. *Critical Reviews in Plant Sciences.*, vol. 25, pp. 417–440.

Dungey, H.S. and Potts, B.M. (2003). Eucalypt hybrid susceptibility to *Gonipterus scutellatus* (Coleoptera: Curculionidae). *Austral Ecology*, vol. 28, pp. 70–74.

DWAF (2007-2008). South African Forestry Facts. *Department of Water Affairs and Forestry*.

Eldrige, K., Davidson, J., Harwood, C. and Wyk, G. (1993). *Eucalypt domestication and breeding*. Clarendon Press.

Engelberth, J., Alborn, H.T., Schmelz, E.A. and Tumlinson, J.H. (2004). Airborne signals prime plants against herbivore attack. *Plant Biology.*, vol. 101, pp. 1781–1785.

European and protection Organization (EPPO), M.P. (2005). Data sheets on quarantine pests. *OEPP/EPPO Bulletin*, vol. 35, pp. 368–370.

Fraser, A.M., Mechaber, W.L. and Hildebrand, J.G. (2003 May). Electroantennographic and behavioural resposes of the Sphinx moth *Manduca sexta* to host plant headspace volatiles. *Journal of Chemical Ecology*, vol. 29, pp. 1813–1833.

Frigge, K., Rabel, W. and Wieck, A. (1987). Adsorptionsmittel zur anreicherung von organischen luftinhaltsstoffen. *Fresenius Journal of Analytical Chemistry*, vol. 327, pp. 261–278.

Gailliard, T. and Matthew, J. (1976). Lipoxygenase-mediated cleavage of fatty acids to carbonyl fragments in tomato fruits. *Phytochemistry.*, vol. 16, pp. 339–343.

Gras, E.K., Read, J., Mach, C.T., Sanson, G.D. and Clissold, F.J. (2005). Herbivore damage, resource richness and putative defences in juvinyl *versus* adult *Eucalyptus* leaves. *Australian Journal of Botany*, vol. 53, pp. 33–44.

Guenther, A.B. (1991). Isoprene and monoterpene emission rate variability: Observations with *Eucalyptus* and emision rate algorithm development. *Journal of Geophysical Research*, vol. 96, pp. 10799–10808.

Hanks, L.M., Millar, J.G., Paine, T.D. and Campbell, C.D. (2000). Classical biological control of the australian weevil *Gonipterus scutellatus* (Coleoptera: Curculionidae) in California. *Environmental Entomology*, vol. 29, pp. 369–375.

Hansson, B., Larsson, M. and Leal, W. (1999). Green leaf volatile-detecting olfactory receptor neurons display very high sensitivity and specificity in the scarab beetle. *Physiological Entomology*, vol. 24, pp. 121–126.

Harper, M. (1993). Evaluation of solid sorbent sampling methods by breakthrough volume studies. *Annalysis of Occupational Hygene*, vol. 37, pp. 65–88.

Harper, M. (2000). Sorbent trapping of volatile organic compounds from air. *Journal of Chromatography A*, vol. 885, pp. 129–151.

Heath, R.R. and Duben, B.D. (1998). *Analytical and Preparative Gas Chromatography In: Methods in Chemical Ecology.* Kluwer Academic Publishers.

Hurley, B. (Personal communication). *Forestry and Agricultural Biotechnology Institute, University of Pretoria, South Africa.*

Kesselmeier, J. and Staudt, M. (1998). Biogenic volatile organic compounds (voc): An overview on the emission, physiology and ecology. *Journal of Atmospheric Chemistry*, vol. 33, pp. 23–88.

Kessler, A. and Baldwin, I.T. (2001). Defensive function of herbivore induced plant volatile emissions in nature. *Science*, vol. 291, pp. 2141–2144.

Lanfranco, D. and Dungey, H.S. (2001). Insect damage in eucalyptus: A review of plantations in Chile. *Austral Ecology.*, vol. 26, pp. 477–481.

Larsson, M.C., Leal, W.S. and Hansson, B.S. (2001). Olfactory receptor neurons detecting plant odours and male volatiles in anomala cuprea beetles (coleoptera: Scarabaeidae). *Journal of Insect Physiology.*, vol. 27, pp. 1065–1027.

Li, H. and Madden, J.L. (1995). Analysis of leaf oils from a *Eucalyptus* species trial. *Biochemical Systematics and Ecology.*, vol. 23, pp. 167–177.

Light, D.M., Flath, R.A., Buttery, R.G., Zalom, F.G., Rice, R.E., Dickens, J.C. and Jang, E.B. (1993). Host-plant green-leaf volatiles synergize the synthetic sex pheromones of the corn earworm and codling moth (Lepidoptera). *Chemoecology.*, vol. 4, pp. 145–152.

Loch, A.D. (2005). Mortality and recovery of Eucalypt beetle pest and beneficial arthropod populations after commercial application of the insecticide alpha-cypermethrin. *Forest Ecology and Management.*, vol. 217, pp. 255–265.

Loch, A.D. (2006). Phenology of the *Eucalyptus* weevil, *Gonipterus scutellatus* Gyllenhall (Coleoptera: Curculionidae), and chrysomelid beetles in *Eucalyptus globulus* plantations in south-western Australia. *Agricultural and Forest Entomology.*, vol. 8, pp. 155–165.

Loch, A.D. (2008). Parasitism of the *Eucalyptus* weevil, *Gonipterus scutellatus* Gyllenhal, by the egg parasitoid *Anaphes nitens* Girault, in *Eucalyptus globulus* plantations in south-western Australia. *Biological Control.*, vol. 47, pp. 1–7.

Loch, A.D. and Floyd, R.B. (2001). Insect pests of the Tasmanian blue gum, *Eucalyptus globulus*, in south-western Australia: History, current perspectives and future prospects. *Austral Ecology.*, vol. 26, pp. 458–466.

Lucia, A., Audino, P.G., Seccacini, E., Licastro, S., Zerba, E. and Masuh, H. (2007). Larvicidal effect of *Eucalyptus grandis* essential oil and turpentine and their major components on *Aedes aegypti* larvae. *Journal of the American Mosquito Control Association.*, vol. 23, pp. 299–303.

Malausa, J.C., Rabasse, J. and Kreter, P. (2008). Les insects entomophages dintrt agricole acclimates en France mtropolitaine depuis le dbut du 20me sicle. *EPPO Bulletin.*, vol. 38, pp. 136–146.

Mally, C.W. (1924). The *Eucalyptus* snout beetle *Gonipterus scutellatus* Gyll.). *Journal of the Department of Agriculture South Africa*, pp. 3–31.

Malo, E.A., Rnou, M. and Guerrero, A. (2000). Analytical studies of *Spodoptera littoralis* sex pheromone components by electroantennography and coupled gas chromatography-electroantennographic detection. *Talanta*, vol. 52, pp. 525–532.

Matsui, K., Ujita, C., Fujimoto, S., Wilkinson, J., Hiatt, B., Knauf, V., Kajiwara, T. and Feussner, I. (2000). Fatty acid 9- and 13-hydroperoxide lyases from cucumber. *FEBS Letters.*, vol. 481, pp. 183–188.

McCaffrey, C.A. and MacLachlan, J. (1994). Adsorbent tube evaluation for the preconcentration of volatile organic compounds in air for analysis by Gas chromatography-mass spectrometry. *Analyst*, vol. 119, pp. 897–902.

Metcalf, R.L. and Metcalf, E.R. (1992). *Plant kairomones in insect ecology and control.* Chapman and Hall.

Millar, J.G. and Sims, J.J. (1998). *Preparation, Cleanup, and Preliminary Fractionation of Extracts In: Methods in Chemical Ecology*, vol. 1. Kluver Academic Publishers.

Miller, J.R. and Stickler, K.L. (1984). *Finding and accepting host plants.* Chapman and Hall Ltd.

Moorhouse, J.E., Yeadon, R., Beevor, P.S. and Nesbitt, B. (1969). Method for use in studies of insect chemical communication. *Nature*, vol. 223, pp. 1174–1175.

Nagai, T. (1981). Electroantennogram response gradient on the antenna of the European corn borer, *Ostrinia nubilalis*. *Insect Physiology*, vol. 27, pp. 889–894.

Nunes, T.V. and Pio, C.A. (2001). Emision of volatile organic compounds from Portuguese *Eucalyptus* forests. *Chemosphere-Global Change Science.*, vol. 3, pp. 239–248.

Paré, P.W. and Tumlinson, J.H. (1999). Plant volatiles as a defense against insect herbivores. *Plant Physiology.*, vol. 121, pp. 325–331.

Peters, R.J.B., Duivenbode, J.A.D.V.R.V., Duyzer, J.H. and Verhagen, H.L.M. (1994). The determination of terpenes in forest air. *Atmospheric Environment*, vol. 28, pp. 2413–2419. ISSN 1352-2310.

Pio, C.A., Nunes, T.V., Castro, L.M. and Lopes, D.A. (2001). Volatile and particulate organic compounds in the ambient air of a eucalyptus forest in portugal during the FIELDVOC94 campaign. *Chemosphere-Global Change Science.*, vol. 3, pp. 283–293.

Poynton, R.J. (1979). *Tree planting in Southern Africa*, vol. 2. Department of Forestry.

Price, P.W., Bouton, C., Gross, P., McPheron, B.A., Thompson, J.N. and Weis, A.E. (1980). Interactions among three trophic levels: Influence of plants on interactions between insect herbivores and natural enemies. *Annual Review of Ecology and Systematics,*, vol. 11, pp. 41–65.

Raguso, R.A. and Pellmyr, O. (1998). Dynamic headspace analysis of floral volatiles: A comparison of methods. *Oikos*, vol. 81, pp. 238–254.
Available at: http://www.jstor.org/stable/3547045

Richardson, K.F. and Meakins, R.H. (1984). Inter- and intra-specific variation in the susceptibility of eucalypts to the snout beetle *Gonipterus scutellatus* Gyll. (Coleoptera: Curculionidae). *South Afrikaanse Bosboutydskrif*, vol. 139, pp. 21–31.

Rivera, A.C. and Carbone, S.S. (2000). The effect of tree species of *Eucalyptus* on the growth and fecundity of the *Eucalyptus* snout beetle (*Gonipterus scutellatus*). *Forestry.*, vol. 73, pp. 21–29.

Rivera, A.C., Carbone, S.S. and Andrés, J.A. (1999). Life cycle and biological control of the *Eucalyptus* snout beetle (Coleoptera, Curculionidae) by *Anaphes nitens* (Hymenoptera, Mymaridae) in north-west Spain. *Agricultural and Forest Entomology.*, vol. 1, pp. 103–109.

Ruther, J. (2000). Retention index database for identification of general green leaf volatiles in plants by coupled capillary gass chromatography-mass spectrometry. *Journal of Chromatography A*, vol. 890, pp. 313–319.

Ruther, J., Reinecke, A. and Hilker, M. (2002). Plant volatiles in sexual communication of *Melolontha hippocastani*: response towards time dependant bouquets and novel function of (Z)-3-hexen-1-ol as a sexual kairomone. *Ecological Entomology*, vol. 27, pp. 76–83.

Sandra, P. (1989*a*). Fundamentals part 1. *Journal of High Resolution Chromatography*, vol. 12, pp. 82–86.

Sandra, P. (1989*b*). Fundamentals part 2. *Journal of High Resolution Chromatography*, vol. 12, pp. 273–277.

Schneider (1957). Electrophysiological investigation on the antennal receptors of the silk moth during chemical and mechanical stimulation. *Experientia*, vol. 13, pp. 89–91.

Slippers, B. (Personal communication). *Forestry and Agricultural Biotechnology Institute, University of Pretoria, South Africa.*

Slone, D.H. and Sullivan, B.T. (2007). An automated approach to detecting signals in electroantennogram data. *Journal of Chemical Ecology*, vol. 33, pp. 1748–1762.

Struble, D.L. and Arn, H. (1984). *Combined Gas Chromatography and Electroantennogram Recording of Insect Olfactory Responses In: Techniques in Pheromone Research.* Springer-Verlag.

Sullivan, B.T. (Private communication). *USDA Forest Service, Southern Research Station, Forest Insect Research, 2500 Shreveport Hwy.,Pineville, LA 71360, USA.*

Syed, Z. and Guerin, P. (2004). Tsetse flies are attracted to the invasive plant *Latana camara*. *Journal of Insect Physiology.*, vol. 50, pp. 43–50.

Takeoka, G.R., Flath, R.A., Guentert, M. and Jennings, W. (1988). Nectarine volatiles: vacuum steam distillation versus headspace sampling. *Journal of Agricultural and Food Chemistry*, vol. 36, pp. 553–560.

Tholl, D., Boland, W., Hansel, A., Loreto, F., Rose, U. and Schnitzler, J. (2006). Practical approaches to plant volatile analysis. *The Plant Journal*, vol. 45, pp. 540–560.

Tol, R.W.H.M. and Visser, J.H. (2002). Olfactory antennal responses of the vine weevil otiorhynchus sulcatus to plant volatiles. *Entomologia Experimentalis et Aplicata*, vol. 102, pp. 49–64.

Tooke, F.G.C. (1953). *The eucalyptus snout-beetle, Gonipterus scutellatus Gyll: a study of its ecology and control by biological means. Entomology Memoirs, Department of Agriculture, Union of South Africa.* The Government Printer Pretoria.

Van den Berg, J., Torto, B., Pickett, J.A., Smart, L.E. and Woodcock, L.J.W..C.M. (2008). Influence of visual and olfactory cues on field trapping of the pollen beetle, *Astylus atromaculatus* (Col.: Melyridae). *Journal of Applied Entomology*, vol. 132, pp. 490–496.

Visser, J. (1986). Host odor perception in phytophagous insects. *Annual Review of Entomology.*, vol. 31, pp. 121–144.

Wadhams, L.J. (1984). *The coupled gas chromatography-single cell recording technique. In: Techniques in pheromone research.* Springer-Verlag.

Webster, F.X., Millar, J.C. and Kiemle, D.J. (1998). *Mass Spectrometry In: Methods in Chemical Ecology*, vol. 1. Kluver Academic Publishers.

Weissbecker, B., Loon, J.J.A.V. and Dike, M. (1999). Electroantennogram responses of a predator, *Perillus bioculatus*, and its prey, *Leptinotarsa decemlineata*, to plant volatiles. *Journal of Chemical Ecology.*, vol. 25, pp. 2313–2325.

Wibe, A., Borg-Karlson, A.-K., Norin, T. and Mustaparta, H. (1997 May). Identification of plant volatiles activating single receptor neurons in the pine weevil (*Hylobius abietis*). *Journal of Comparative Physiology A: Neuroethology, Sensory, Neural, and Behavioral Physiology*, vol. 180, pp. 585–595. ISSN 0340-7594 (Print) 1432-1351.

Williams, J.R., A., M.L. and Hermelin, P.R. (1951). The Biological Control of *Gonipterus scutellatus* Gyll. in Mauritius. *Bulletin of Entomological Research*, vol. 42, pp. 23–28.

Withers, T.M. (2001). Colonization of eucalypts in New Zealand by australian insects. *Austral Ecology*, vol. 26, pp. 467–476.

Yan, Z. and Wang, C. (2005). Wound-induced green leaf volatiles cause the release of acetylated derivatives and a terpenoid in maize. *Phytochemistry.*, vol. 67, pp. 34–42.

Yang, Y., Choi, H., Choi, W., Clark, J.M. and Ahn, Y. (2004). Ovicidal and Adulticidal activity of *Eucalyptus globulus* leaf oil terpenoids against *Pediculus humanus capitis* (Anoplura: Pediculidae). *Journal of Agricultural and Food Chemistry.*, vol. 52, pp. 2507–2511.

Yassaa, N., Meklati, B.Y. and Cecinato, A. (2000). Evaluation of monoterpenic volatile organic compounds in ambient air around *Eucalyptus globulus, Pinus halepensis* and *Cedrus atlantica* trees growing in Algiers city area by chiral and achiral capillary gas chromatography. *Atmospheric Environment.*, vol. 34, pp. 2890–2816.